Modeling Retention Volumes, Isotherms and Plate Heights for Whey Proteins in Anion-Exchange Chromatography

Pedersen, Linda

Publication date:
2003

Document Version
Early version, also known as pre-print

Modeling Retention Volumes, Isotherms and Plate Heights for Whey Proteins in Anion-exchange Chromatography

by

Linda Pedersen

Ph.D. Thesis

IVC-SEP, Department of Chemical Engineering, Technical University of Denmark

ISBN 87-90142-88-8
Printed by BookPartner, Nørhaven Digital, Copenhagen, Denmark

PREFACE

This thesis is submitted in partial fulfillment of the requirements for admission to the candidacy for the degree of philosophy, Ph.D., at the Technical University of Denmark.

I want to thank my supervisor Jørgen Mollerup, IVC-SEP, KT, DTU for his contributions to the scientific work constituting this thesis. His excellent theoretical insight has resulted in a lot of good ideas and proposals for the experimental work and contents of this thesis.

Lyngby, December 2002

Linda Pedersen

ABSTRACT

This thesis is divided into 2 parts. Part 1 deals with the work and study I have done at IVC-SEP, KT, DTU, and part 2 deals with the work I have done at Amersham Biosciences, Sweden.

PART 1

In this work the whey proteins BSA, α-lactalbumin, β-lactoglobulin A and B and the media Source 30Q, Q-Sepharose XL, Ceramic Q-HyperD F and Fractogel EMD TMAE 650(s) have been used. Most work has been done with BSA and Source 30Q. The ion-exchange capacity has been determined for all four media by in-column acid-base titration and by breakthrough experiments with nitrate. For the Source 30Q media batch experiments for determination of the ion-exchange capacity have been made, but the reproducibility of these experiments is very poor, so that in-column determination with nitrate is recommended.

Retention volumes in the linear range of the isotherm have been measured by all four proteins on all four media both by isocratic and linear gradient elution. The retention volumes measured by isocratic elution have been correlated by the Steric Mass Action formalism. The results show that the Steric Mass Action formalism correlates the isocratic retention volumes very well, and that it can correlate the linear gradient retention volumes with the parameters determined from the correlation of the isocratic retention volumes. From the retention volumes some theoretical considerations concerning separation of the four proteins are made. The best separation of the four proteins can be achieved at a pH of 6 on Source 30Q.

Capacity measurements were made with BSA on Source 30Q at a pH of 7 and 8 and the Steric Mass Action formalism was used to construct the isotherms. The isotherms could not be correlated by one shielding factor common to both pH values, but only with one shielding factor for each pH value.

Reduced plate heights have been determined from the isocratic elutions and correlated with the van Deemter equation and the parallel diffusion model. Due to impurities the variances of the peaks at high equilibrium ratios tend to be ambiguous and reduced plate height data cannot be obtained. Where reduced plate heights are available at both weak and strong retention the data shows that pore diffusion controls at weak retention and solid diffusion controls at strong retention. In between none of the mechanisms are in control, but work in parallel.

The van Deemter equation has also been used to derive some rule of thumb guidelines for scaling. The scaling is done by the concept of times scales. The time scales are kept identical for all the columns by scaling the flow rate, the gradient length and the load to the column volume. The results show that it is possible to increase both the column length and the diameter and still achieve the same or even better performance of the column.

PART 2

In this work a prototype media and the Superdex 30 prep grade have been used. Most of the experiments have been carried out with FineLINE 70 columns.

The reversed flow technique was used for bed characterization in order to eliminate the contributions to band broadening due to macroscopic factors. The experiments with the prototype media showed that the axial packing technique used for the FineLINE 70 column gives homogeneously packed beds at packing pressures of 7 to 21 bars. The porosities are constant up to a packing pressure around 15 bars and then decrease due to compressibility. The reversed flow experiments also showed some unexpected irreversible effects in the system. The irreversible effects made it difficult to draw any conclusions regarding optimum packing pressure.
It was not possible to find the cause of the irreversible effects. They were neither constant nor related to the packing pressure. Two other problems with the prototype media were formation of gas bubbles in the column and bed compression.
Due to the problems with the prototype media experiments with the Superdex 30 prep grade were made. The experiments showed that the irreversible effects were not related to the prototype media, because they were also present in the experiments with the Superdex 30 prep grade. For the Superdex 30 prep grade media injections were performed both at the top and the bottom of the column. These experiments showed that the irreversible effects depend on where the injections are made. This indicates that a connection exists between the flow distributors and the irreversible effects.
To decide if the reversed flow technique is suited for bed characterization more experiments have to be made. The cause of the irreversible effects has to be established.

RESUMÉ

Denne afhandling er delt i to. Del 1 omhandler det arbejde og studie jeg har udført i IVC-SEP, KT, DTU, og del 2 omhandler det arbejde, jeg har udført hos Amersham Biosciences, Sverige.

DEL 1

I dette arbejde har valleproteinerne BSA, α-lactalbumin, β-lactoglobulin A og B og gelerne Source 30Q, Q-Sepharose XL, Ceramic Q-HyperD F og Fractogel EMD TMAE 650(s) været anvendt. Størstedelen af arbejdet er udført med BSA og Source 30Q. Ionbytningskapaciteten er blevet bestemt for alle fire geler ved syre-base titrering i kolonnen og ved gennembrudskurver med nitrat. Batchforsøg til bestemmelse af ionbytningskapaciteten er blevet udført med Source 30Q, men reproducerbarheden er meget dårlig, og derfor anbefales bestemmelse ved gennembrudskurver med nitrat.

Der er målt retentionsvoluminer i det lineære område af isotermen med alle fire proteiner på alle fire geler ved både isokratisk og linear gradient eluering. De retentionsvoluminer, som er målt ved isokratisk eluering, er korreleret med massevirkningsloven. Resultaterne viser, at massevirkningsloven er i stand til at korrelere de isokratiske retentionsvoluminer, samt at den kan korrelere retentionsvoluminerne fra gradient elueringerne med de parametre, der er bestemt fra modelleringen af de isokratiske retentionsvoluminer. Ud fra retentionsvoluminerne er der foretaget nogle teoretiske overvejelser vedrørende separation af de fire proteiner. Den bedste separation kan opnås ved pH 6 på Source 30Q.

Der er foretaget kapacitetsmålinger med BSA på Source 30Q ved pH 7 og 8, og massevirkningsloven er anvendt til at konstruere isotermerne. Isotermerne kunne ikke korreleres med en fælles skærmningsfaktor for begge pH værdier, men kun med en skærmningsfaktor for hver af de to pH værdier.

Fra de isokratiske elueringer er de reducerede højder af en overføringsenhed bestemt og korreleret med van Deemter ligningen og modellen for paralleldiffusion. På grund af urenheder kan variansen af toppene ved højt ligevægtsforhold være tvetydig, og det er derfor ikke muligt at bestemme højden af en overføringsenhed. Når de reducerede højder af en overføringsenhed er tilgængelige ved både lavt og højt ligevægtsforhold, kan det af disse data ses, at porediffusion dominerer ved lave ligevægtsforhold og fastfasediffusion dominerer ved høje ligevægtsforhold. I det mellemliggende område dominerer ingen af de to mekanismer, og diffusionen foregår ved, at de virker parallelt.

van Deemter ligningen er også blevet anvendt til at udlede tommelfingerregler for skalering. Skaleringen er foretaget ud fra konceptet om tidskonstanter. Tidsskalaerne er holdt konstante for alle kolonnerne ved at skalere strømningshastigheden, gradientlængden og voluminet af den injicerede prøve med kolonnevoluminet. Resultaterne viser, at der kan opnås samme eller bedre effektivitet af kolonnen, selvom både kolonnediameteren og -længden øges.

DEL 2

I dette arbejde har der været anvendt en prototype gel og Superdex 30 prep grade gelen, og de fleste af eksperimenterne er udført i FineLINE 70 kolonner.

Den omvendte strømningsteknik blev anvendt til karakterisering af kromatografiske matricer for at eliminere de makroskopiske faktorers bidrag til topspredningen. Eksperimenterne med prototype gelen viste, at den aksiale pakningsteknik, som anvendes ved pakning af FineLINE 70 kolonnerne, giver homogent pakkede matricer ved pakningstryk på 7 til 21 bar. Porøsiteterne er konstante op til et pakningstryk på ca. 15 bar, hvorefter de falder som følge af komprimering. Forsøgene med omvendt strømningsteknik viste nogle uventede irreversible påvirkninger i systemet, som gjorde det meget svært at komme med en konklusion om optimalt pakningstryk.
Det var ikke muligt at finde årsagen til de irreversible påvirkninger. De var ikke konstante og afhang heller ikke af pakningstrykket. To andre problemer med prototype gelen var dannelse af gasbobler i kolonnen og komprimering af matricen.
Som følge af problemerne med prototype gelen blev der lavet nogle eksperimenter med Superdex 30 prep grade. Disse eksperimenter viste, at de irreversible påvirkninger ikke skyldtes prototype gelen, da de også var til stede i eksperimenterne med Superdex 30 prep grade. For Superdex 30 prep grade gelen er der både foretaget injektioner i toppen og bunden af kolonnen. Disse eksperimenter viste, at de irreversible påvirkninger afhænger af, hvor injektionerne foretages. Dette indikerer, at der er en forbindelse mellem strømningsfordelerne og de irreversible påvirkninger.
For at afgøre om den omvendte strømningsteknik er egnet til karakterisering af matricer er det nødvendigt med flere forsøg. Årsagen til de irreversible påvirkninger skal findes.

TABLE OF CONTENTS

PART 1

PART 2

SYMBOLS (PART 1)

A	Equilibrium ratio	
A_{above}	Area above breakthrough curve	[abs. 280 nm · s]
A_{below}	Area below breakthrough curve	[abs. 280 nm · s]
A_H	Constant in the simple van Deemter equation	[cm]
A_{peak}	Peak area	[abs. 280 nm · s]
a_p	Surface area to volume ratio	[cm^{-1}]
B	Lumped equilibrium parameter	
B_H	Constant in the simple van Deemter equation	[cm]
C_H	Constant in the simple van Deemter equation	[cm]
c_0	Protein concentration at the interface	[M]
c_{BSA}	BSA concentration in mobile phase	[g/l] or [M]
c_{Cl^-}	Chloride ion concentration	[M]
$c_{Cl^-,A}$	Chloride ion concentration in buffer A	[M]
$c_{Cl^-,B}$	Chloride ion concentration in buffer B	[M]
$c_{Cl^-,AB}$	Chloride ion concentration in buffer prepared from buffer A and B	[M]
c_{HCl}	HCl concentration	[M]
$c_{HCl,\ added}$	HCl concentration of added solution	[ml]
$c_{HCl,\ blank}$	HCl concentration for blank titration	[ml]
$c_{NaCl,\ before}$	NaCl concentration before pH adjustment	[M]
c^m_{NaCl}	Molal NaCl concentration	[mol/kg]
c_{NaNO_3}	$NaNO_3$ concentration in mobile phase	[M]
c_p	Protein concentration in mobile phase	[g/l] or [M]
c_{pore}	Protein concentration in pore phase	[mol/l pore volume]
c_s	Salt concentration in mobile phase	[M]
$c_{s,0}$	Salt concentration at the beginning of the gradient	[M]
$c_{s,1}$	Salt concentration at the end of the gradient	[M]
$c_{s,A}$	Salt concentration in buffer A	[M]
$c_{s,R}$	Salt concentration where the protein is eluted	[M]
D_{ax}	Axial dispersion coefficient	[cm^2/s]
D_m	Ordinary diffusion coefficient	[cm^2/s]
D_p	Pore diffusion coefficient	[cm^2/s]
D_s	Solid diffusion coefficient	[cm^2/s]
d_{col}	Column diameter	[cm]
d_p	Particle diameter	[μm]
E_D	Eddy diffusion coefficient	[cm^2/s]

G	Gradient parameter/slope	[M/ml]
H	Height equivalent to a theoretical plate (plate height)	[cm]
h	Reduced plate height	
J	Flux	[mol/s·l pore volume]
K_d	Exclusion factor	
$K_{d,BSA}$	Exclusion factor for BSA	
$K_{d,\alpha\text{-lactalbumin}}$	Exclusion factor for α-lactalbumin	
$K_{d,\beta\text{-lactoglobulins}}$	Exclusion factor β-lactoglobulin A and B	
K_m	Overall mass transfer coefficient	[cm/s]
k'	Retention factor	
k_f	Film mass transport coefficient	[cm/s]
k_p	Pore mass transfer coefficient	[cm/s]
k'_p	Protein retention factor	
$k'_{p,0}$	Protein retention factor at $c_{s,0}$	
k_s	Solid mass transfer coefficient	[cm/s]
k'_s	Salt retention factor	
l_{col}	Column length	[cm]
$l_{col,1}$	Length of column 1	[cm]
$l_{col,2}$	Length of column 2	[cm]
l_{d0}	Distance in the column corresponding to t_{d0}	[cm]
l_g	Gradient position in the column	[cm]
l_p	Protein position in the column	[cm]
m_{BSA}	Amount of BSA	[mg]
$m_{drained\ media}$	Mass of drained media	[g]
$m_{dry\ media}$	Mass of oven dried media	[g]
N	Plate number	
N_1	Plate number for column 1	
N_2	Plate number for column 2	
n_{NaCl}	Amount of NaCl	[mol]
p	Lumped parameter (Equation 7-12)	
Q	Volumetric flow rate	[ml/min]
q	Protein concentration in adsorbed state	[g/l column volume]
		or [mol/l pore volume]
q_0	Protein concentration at the interface	[mol/l pore volume]
q_{BSA}	BSA concentration in adsorbed state	[mol/l pore volume]
q_p^{max}	Protein saturation capacity	[mol/l pore volume]
q_p	Protein concentration in adsorbed state	[mol/l pore volume]
q_s	Salt concentration in adsorbed state available for exchange	[mol/l pore volume]

$\hat{q}_s$	Sterically hindered salt ion concentration	[mol/l pore volume]
$\bar{q}_s$	Total salt concentration in adsorbed state	[mol/l pore volume]
R	Gas constant	[J/K·mol]
R	Resolution (Equation 5-1)	
s	Average concentration in the column	[mol/ l pore volume]
T	Temperature	[K]
t	Time	[s]
t_0	Time constant for flow	[min]
$t_{0,1}$	Time constant for flow for column 1	[min]
$t_{0,2}$	Time constant for flow for column 2	[min]
t_{d0}	Dead time	[s]
t_R	Retention time	[min]
$t_{R,\ peak1}$	Retention time of peak 1	[min]
$t_{R,\ peak2}$	Retention time of peak 2	[min]
u_g	Linear velocity of the gradient	[cm/s]
$u'_{p,0}$	Linear velocity of the protein at $c_{s,0}$	[cm/s]
u_s	Linear velocity of the salt	[cm/s]
UV_1	UV signal at data point 1	[abs. 280 nm]
$UV_{baseline}$	UV signal at baseline	[abs. 280 nm]
UV_i	UV signal at data point i	[abs. 280 nm]
UV_n	UV signal at last data point	[abs. 280 nm]
V_1	Volume between injection and inlet to the bypass valve	[ml]
V_2	Volume between inlet to the bypass valve and column inlet	[ml]
V_3	Volume between column outlet and outlet of the bypass valve	[ml]
V_A	Volume of buffer A	[l]
V_{above}	Volume corresponding to area above breakthrough curve	[ml]
V_B	Volume of buffer B	[l]
V_{CD}	Volume between column outlet and detector	[ml]
V_{col}	Column volume	[ml]
$V_{connection\ link}$	Volume of connection link	[ml]
$V_{cor.}$	Corrected volume	[ml]
V_{d0}	Dead volume corresponding to t_{d0}	[cm]
V_{dead}	Dead volume	[ml]
V_{dead}	Dead volume	[ml]
$V_{empty\ col.}$	Empty column volume	[ml]
$V_{empty,\ waters}$	Volume of empty Waters column	[ml]
$V_{empty10}$	Volume of empty HR10 column	[ml]
$V_{empty10,\ incl.\ filters}$	Volume of empty HR10 column with filters	[ml]

$V_{empty16}$	Volume of empty HR16 column	[ml]
$V_{empty16,\ incl.\ filters}$	Volume of empty HR16 column with filters	[ml]
$V_{empty5,\ incl.\ filters}$	Volume of empty HR5 column with filters	[ml]
$V_{filters}$	Dead of volume filters	[ml]
V_g	Gradient volume	[ml]
$V_{HCl,\ blank}$	HCl volume for blank titration	[ml]
$V_{HCl,\ inflection\ point}$	HCl volume at inflection point	[ml]
V_{HCl}	HCl volume	[ml]
V_{ID}	Volume between injection and detector	[ml]
V_m	Volume the gradient travels before it reaches the detector	[ml]
V_{MC}	Volume between mixer and column inlet	[ml]
V_{MD}	Volume between mixer and detector	[ml]
V_{MI}	Volume between mixer and injection	[ml]
V_{NA}	Retention volume under non-adsorbed conditions	[ml]
$V_{NA,\ \alpha\text{-lactalbumin}}$	α-lactalbumin retention volume under non-adsorbed conditions	[ml]
$V_{NA,\ \beta\text{-lactoglobulins}}$	β-lactoglobulin A and B retention volume under non-adsorbed conditions	[ml]
$V_{NA,BSA}$	BSA retention volume under non-adsorbed conditions	[ml]
$V_{pos,1}$	Dead volume in position 1	[ml]
$V_{pos,2}$	Dead volume in position 2	[ml]
V_R	Retention volume	[ml]
$V_{R,0}$	Protein retention volume at $c_{s,0}$	[ml]
V_{R1}	Retention volume of peak 1	[ml]
V_{R2}	Retention volume of peak 2	[ml]
$V_{R,Gauss}$	Gaussian retention volume	[ml]
V_{Rg}	Retention volume at gradient elution	[ml]
V_{R,NO_3^-}	Nitrate retention volume	[ml]
$V_{R,s}$	Salt retention volume	[ml]
V_t	Total liquid volume	[ml]
V_{total}	Total volume	[ml]
V_{water}	Water volume	[ml]
v	Interstitial velocity	[cm/s]
v_0	Superficial velocity	[cm/s]
x	Dimensionless position in the column	
x_g	Dimensionless position of the gradient start in the column	
x_p	Dimensionless position of protein in the column	
z	Length coordinate in the column	[cm]
z_s	Charge of salt ion	
z_p	Binding charge of protein	

Greek Letters

α	Slope	[kg/mol]
α	Constant in the expression for the film mass transfer coefficient	
α_{BSA}	Slope of BSA calibration curve	[abs. 280 nm·l/g]
α_{NaNO_3}	Slope of $NaNO_3$ calibration curve	[abs. 280 nm·l/mol]
β	Constant in the expression for the film mass transfer coefficient	
Δc_s	Change in salt concentration	[M]
ΔG^0	Standard Gibbs energy change	[J/mol]
$\Delta G^0_{ads,BSA}$	Standard Gibbs energy change of BSA adsorption	[J/mol]
$\Delta G^0_{ads,Cl^-}$	Standard Gibbs energy change of Cl^- adsorption	[J/mol]
$\Delta G^0_{ads,p}$	Standard Gibbs energy change of protein adsorption	[J/mol]
$\Delta G^0_{ads,s}$	Standard Gibbs energy change of salt adsorption	[J/mol]
ΔG^0_{exc}	Standard Gibbs energy change of exchange reaction	[J/mol]
ΔG^0_p	Standard Gibbs energy change of the protein	[J/mol]
ΔG^0_s	Standard Gibbs energy change of the salt	[J/mol]
Δt	Change in time	[s]
$\Delta t_{R,12}$	The difference between the retention times of two peaks	[ml]
δ	Small distance in the column	[cm]
ε	Interstitial porosity	
ε_p	Particle porosity	
ε_t	Total porosity	
φ	Volume correction factor	
$\mu^0_{q_p}$	Standard chemical potential of the protein in the adsorbed state	[J/mol]
$\mu^0_{q_s}$	Standard chemical potential of the protein in the mobile phase	[J/mol]
$\mu^0_{q_s}$	Standard chemical potential of the salt in the adsorbed state	[J/mol]
$\mu^0_{c_s}$	Standard chemical potential of the salt in the mobile phase	[J/mol]
Λ	Ion-exchange capacity	[eqv./ml pore volume] or [eqv./g dry media]
$\Lambda_{NO_3^-}$	Ion-exchange capacity measured by $NaNO_3$	[eqv./ml pore volume] or [eqv./g dry media]

Λ_{OH^-}	Ion-exchange capacity measured by NaOH	[eqv./ml pore volume] or [eqv./g dry media]
λ	Constant related to the axial dispersion coefficient (Equation 7-12)	
λ	Ion-exchange capacity	[eqv.]
λ_{OH^-}	Ion-exchange capacity measured by NaOH	[eqv.]
$\lambda_{NO_3^-}$	Ion-exchange capacity measured by $NaNO_3$	[eqv.]
ν	Charge ratio	
σ	Shielding factor	
σ_1	Square root of the variance for peak 1	[ml]
σ_2	Square root of the variance for peak 2	[ml]
σ^2	Variance	[ml^2]
σ^2_{Gauss}	Gaussian variance	[ml^2]
τ	Distortion factor (EMG parameter)	[ml]

Abbreviations

EMG Exponential Modified Gauss

LDF Linear Driving Force

SMA Steric Mass Action

PART 1

1 INTRODUCTION

1.1 Overview

Chromatographic separations are widely used in the biopharmaceutical industry, because they can yield high-purity products and are relatively easy to develop and scale up from laboratory scale to production level. However, relatively easy to develop, the chromatographic separations are complex processes to optimize due to the many process parameters such as choice of media, salt, buffer, gradient, pH and temperature. To be able to use optimization tools in chromatography it is necessary to acquire a greater understanding of the chromatographic separation through laboratory investigations and modeling.

This study is part of a project where the scope is to develop a consistent set of chromatographic data for whey proteins, including isotherms, mass transport properties and scale-up studies and appropriate models for the anion exchangers Source 30Q, Q-Sepharose XL, Ceramic Q-HyperD F and Fractogel EMD TMAE 650(s).

When a consistent set of data has to be obtained, it is essential to start with the adsorption isotherm, because the equilibrium ratio is needed in the equations for determination of the mass transfer coefficients. Our criteria for a model for correlation of the isotherms were that it should be relatively simple and easy to use, applicable in the linear range and extendable to multicomponent systems in a consistent manner. The Langmuir isotherm is a simple and widely used correlation for adsorption behavior, but it is not applicable in the linear range, because the dependence of the distribution ratio on the salt concentration cannot be derived from the model. The Langmuir model was therefore rejected and the Steric Mass Action formalism developed by Brooks and Cramer [Brooks, 1992] was chosen. The SMA formalism is a three parameter model where the distribution ratio in the linear range determines two of the parameters, and the third parameter is determined from capacity measurements. For the SMA formalism the distribution ratio in the linear range can be derived from the model for the non-linear isotherm as a limit of the distribution ratio at zero protein concentration. The SMA formalism is also extendable to multicomponent systems in a consistent manner.

The model for the mass transfer behavior was chosen on the basis of the study by Ernst Hansen [Hansen, 2000]. He showed that the parallel diffusion model in combination with the linear driving force (LDF) approximation could satisfactorily describe the mass transfer under linear and non-

linear adsorbing conditions in three types of ion-exchange media. In this work the mass transfer has only been studied in the linear range of the isotherm.
In the parallel diffusion model intraparticle mass transport takes place by two mechanisms, pore and solid diffusion, working in parallel. In the pore diffusion model the mass transfer in the pores is described by hindered diffusion, and the driving force is the gradient in the pore phase concentration. The driving force in the solid diffusion model is the gradient in the concentration of solute adsorbed in the solid phase. When the LDF approximation is used it is assumed that the concentration gradients can be linerized.
In the linear range the overall mass transfer coefficient is determined by a correlation of the reduced plate heights with the van Deemter equation. The overall mass transport coefficient includes, beyond the expression for the intraparticle mass transfer, an expression for the external mass transfer. The external mass transfer is the mass transfer from the mobile phase to the particle surface, and the linear driving force is the difference between the solute concentration in the mobile phase and on the particle surface.
The reduced plate heights at strong retention are primarily determined by solid diffusion and at weak retention by pore diffusion. At intermediate retention the reduced plate heights are determined by the two models working in parallel, and the pore and solid diffusion models are thus limiting cases of the parallel diffusion model.

Scale-up in chromatography is essential because method development due to time and economic aspects is done at small columns and is then transferred to a large scale for production. Scale-up in chromatography is often done by keeping the column length constant and increasing the column diameter. The result is often a column where the diameter to length ratio is rather high, and it is difficult to obtain a proper flow distribution in the column.
The van Deemter equation can be used to derive some guidelines for scaling where the column length does not have to be kept constant. The maximum column length will only be limited by the pressure drop. The minimum column diameter is limited by the particle diameter of the media. The scaling is done by keeping the time scale constant when the column dimensions are changed. The identical time scales are achieved by scaling the flow rate, column length and load to the column volume.

1.2 The Media and Columns

In this work four different anion exchanger media have been used: Source 30Q, Q-Sepharose XL, Ceramic Q-HyperD F and Merck Fractogel EMD TMAE 650(s).

Manufacture	Media	d_p [μm]	Column	d_{col} [cm]	l_{col} [cm]	V_{col} [ml]
Amersham Biosciences	Source 30Q	28.7-32.8 (30 av.)	HR10/10	1.0	10.27	8.07
Amersham Biosciences	Q-Sepharose XL	45-165 (90 av.)	HR16/10	1.6	3.76	7.56
Biosepra	Ceramic Q-HyperD F	50 (av.)	HR10/10	1.0	9.62	7.56
Merck	Fractogel EMD TMAE 650(s)	20-40	Prepacked	1.0	5.00	3.93

Table 1-1: The columns used for experiments in the linear range.

Source 30Q is a strong anion exchanger and is based on monodisperse, hydrophilized and rigid polystyrene/divinyl benzene beads with controlled pore structure [Pharmacia Biotech, 2002, data file 18-1107-12]. The anion-exchanger is produced by substitution of the base matrix by quaternary amino groups. Source 30Q is a high-performance media for fast and high-resolution separations of biomolecules.

Q-Sepharose XL is a strong anion exchanger and is based on a highly cross-linked, bead-formed 6% agarose matrix. Long flexible chains of dextran with bound quaternary amino groups are covalently coupled to the matrix [Pharmacia Biotech, 2002, data file 18-1123-82]. The intra-chain cross-linking makes the matrix highly rigid. Q-Sepharose XL is a high-capacity media for capture of biomolecules directly from clarified feedstocks.

Ceramic Q-HyperD F is a strong anion exchanger and is based on a rigid porous bead, which is coated and permeated with a functionalized hydrogel [BioSepra, 2002]. This design combines the characteristic soft high-capacity hydrogel with the dimensional stability of a rigid ceramic bead. The functional group in the Q-HyperD F is also a quaternary amino group. Q-HyperD F is a high-capacity media and very useful in capture steps and general downstream processing.

Fractogel EMD TMAE 650(s) is a strong anion exchanger and is based on a polymeric resin of a synthetic methacrylate [Merck, 2002]. The pores are formed from intertwined polymer agglomerates. Long linear polymer chains (tentacles) carry the functional ligands, the quaternary amino groups. The ligands are covalently bound to the hydroxyl groups of the backbone structure. Due to the tentacles the target molecule is adsorbed very tightly and the Fractogel EMD TMAE 650(s) media is very useful in capture steps and downstream processing.

Common to the four anion exchangers is the functional group, the quaternary amino group, and the large pH stability range (2-12 for Source 30Q and Ceramic Q-HyperD F, 1-13 for Fractogel EMD TMAE 650(s) and 3-13 for Q-Sepharose XL). They are chemically very stable and can be used at high linear flow rates up to 800-1000 cm/h, except Q-Sepharose XL, which has a maximum flow rate of 500 cm/h.

The Source 30Q media has been used in several other columns. Some of them are used for scale-up experiments and some for capacity measurements. The different Source 30Q columns used in this work are listed in the table below.

Column	d_{col} [cm]	l_{col} [cm]	V_{col} [ml]	Used for
HR16/10	1.6	0.23	0.46	Capacity measurements
HR5/10	0.5	4.99	0.98	Scale-up experiments
HR10/5	1.0	1.72	1.35	Capacity measurements
HR16/10	1.6	4.67	9.39	Scale-up experiments
HR16/10	1.6	5.85	11.76	Capacity measurements
HR16/10	1.6	6.50	13.07	Capacity measurements
HR16/10	1.6	6.75	13.57	Capacity measurements
Waters	2.0	17.7	55.61	Scale-up experiments

Table 1-2: Different Source 30Q columns used in this work.

1.3 The Proteins

The proteins in milk are divided into two groups, the caseins and the whey proteins. The caseins represent about 80% of the proteins in milk, and the whey proteins the remaining 20%.
Whey proteins are the proteins appearing in the supernatant of milk after precipitation at a pH of 4.6. The whey proteins are mainly: β-lactoglobulin A and B, α-lactalbumin, bovine serum albumin (BSA), immunoglobulins, lactoferrin and lactoperoxidase. These proteins are globular and more water soluble than the caseins.
In the table below, the concentration, molecular weight and isoelectric point of the whey proteins are given. The concentrations are approximate concentrations, because they vary a little, especially among breeds.

Protein	Concentration [g/l milk]	Mw [kD]	pI
β-lactoglobulins	3.2	18.4	5.2-5.4
α-lactalbumin	1.2	14.2	4.7-5.1
Immunoglobulins	0.8	150-1000	5.8-7.3
BSA	0.4	65-69	4.9-5.1
Lactoferrin	0.2	93	8.0
Lactoperoxidase	0.03	78-80	9.6

Table 1-3: The whey proteins.

In this work four of the whey proteins are used: β-lactoglobulin A and B, α-lactalbumin and BSA, and a value of 65 kD is used for the molecular weight of BSA.

β-lactoglobulin A and B are very similar. Only amino acid numbers 64 and 118 in the amino acid sequence of the two proteins are different. In β-lactoglobulin A amino acid number 64 is aspartic acid and amino acid 118 is valine. In β-lactoglobulin B amino acid 64 is glycine and amino acid 118 is alanine [Vejledning til øvelser i proteinkemi, 2001]. Valine and alanine are hydrophilic amino acids. Aspartic acid is negatively charged and glycine is neutral. This difference between aspartic acid and glycine makes β-lactoglobulin A a little more charged than β-lactoglobulin B.

2 THE STERIC MASS ACTION MODEL

The Steric Mass Action (SMA) formalism is developed by Brooks and Cramer [Brooks, 1992]. It is a three parameter model for description of non-linear adsorption in ion-exchange systems. The SMA model is the first model to take the steric hindrance of the salt counterions into account. When a macromolecule (e.g. a protein) binds to the stationary phase, the size of the macromolecule leads to a cover of more sites than dictated by its characteristic size.

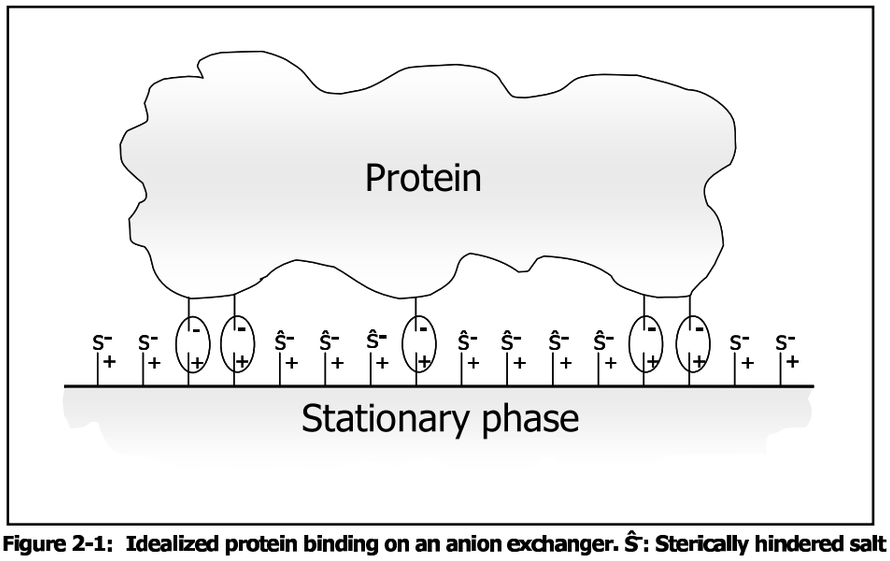

Figure 2-1: Idealized protein binding on an anion exchanger. $\hat{S}^-$: Sterically hindered salt counterions; S^-: Non-sterically hindered salt counterions.

The protein is adsorbed to the stationary phase on a number of exchange sites given by an effective charge. The effective charge is most often less than the net charge of the protein because not all charges on the protein surface can be attached to the ligands. In Figure 2-1 the protein is adsorbed to five exchange sites but covers additional seven exchange sites. The stoichiometric exchange of the protein and the exchangeable salt counterions can be represented by

$$z_s c_p + z_p q_s \Leftrightarrow z_s q_p + z_p c_s \qquad \textbf{(2-1)}$$

c is the concentration in the mobile phase and q is the concentration in the adsorbed state in the stationary phase. The subscripts p and s refer to the protein and the salt.

By defining ν as the ratio of the binding charge of the protein z_p and the charge of the salt counterion z_s: $\nu = \frac{z_p}{z_s}$, Equation 2-1 can be represented as

$$c_p + \nu q_s \Leftrightarrow q_p + \nu c_s \qquad \textbf{(2-2)}$$

q_s is the concentration of adsorbed salt ions available for exchange with the protein. z_p and thus ν depend on the pH, the protein and the ion-exchange media.

It is assumed that the solution and the adsorbed phases are thermodynamically ideal [Brooks, 1992]. This allows the use of concentrations instead of activities, and the equilibrium constant K for the ion-exchange reaction is then defined as

$$K = \left(\frac{q_p}{c_p}\right)\left(\frac{c_s}{q_s}\right)^{\nu} \qquad \textbf{(2-3)}$$

The total concentration of sterically hindered salt ions $\hat{q}_s$ unavailable for exchange is given by

$$\hat{q}_s = \sigma q_p \qquad \textbf{(2-4)}$$

where σ is the shielding factor of the protein. The shielding factor depends on the size and the conformation of the protein molecule.

After the exchange reaction the total concentration of salt ions $\bar{q}_s$ in the stationary phase is given by the expression

$$\bar{q}_s = q_s + \hat{q}_s = q_s + \sigma q_p \qquad \textbf{(2-5)}$$

Electroneutrality requires that the sum of the positive and the negative charges in the exchanger is zero. If the capacity (eqv/l pore volume) of the ion exchanger is Λ, electroneutrality requires that

$$\Lambda = z_s \bar{q}_s + z_p q_p = z_s q_s + (z_s \sigma + z_p) q_p \quad \Leftrightarrow \qquad \textbf{(2-6)}$$

$$\frac{1}{z_s}\Lambda = q_s + (\sigma + \nu) q_p \qquad \textbf{(2-7)}$$

Substitution of Equation 2-7 into Equation 2-3 gives

$$K = \left(\frac{q_p}{c_p}\right)\left(\frac{c_s}{\frac{1}{z_s}\Lambda - (\sigma + \nu) q_p}\right)^{\nu} = \left(\frac{q_p}{c_p}\right)\left(\frac{z_s c_s}{\Lambda - (\sigma + z_p) q_p}\right)^{\nu} \qquad \textbf{(2-8)}$$

By rearranging we obtain the following expression for the isotherm:

$$c_p = \left(\frac{q_p}{K}\right)\left(\frac{z_s c_s}{\Lambda - (\sigma + z_p)q_p}\right)^{\nu} \qquad \textbf{(2-9)}$$

In the linear range of the isotherm, where $c_p \rightarrow 0$ and $\Lambda \gg (\sigma+z_p)q_p$ because q_p is very small, the expression for the isotherm can be reduced to

$$c_p = \left(\frac{q_p}{K}\right)\left(\frac{z_s c_s}{\Lambda}\right)^{\nu} \qquad \textbf{(2-10)}$$

From Equation 2-7 it is seen that the isotherm under overload conditions, where $c_p \rightarrow \infty$ and $q_s \approx 0$, will approach:

$$q_p = q_p^{max} = \frac{\Lambda}{z_s(\sigma + \nu)} \qquad \textbf{(2-11)}$$

From Equation 2-11 it is observed that the saturation capacity q_p^{max} of an SMA isotherm is independent of the mobile phase counterion concentration. This is contrary to the Langmuir isotherm, where the saturation capacity depends on the mobile phase counterion concentration.

By use of standard thermodynamics, the equilibrium constant K can be calculated from the standard Gibbs energy changes [Gerstner, 1994]:

$$\Delta G^0_{exc} = -RT \ln K \qquad \textbf{(2-12)}$$

For the exchange reaction of Equation 2-2 the standard Gibbs energy change of exchange ΔG^0_{exc} is defined as

$$\Delta G^0_{exc} = \mu^0_{q_p} + \nu\mu^0_{c_s} - \mu^0_{c_p} - \nu\mu^0_{q_s} \qquad \textbf{(2-13)}$$

where μ_i^0 is the chemical potential of species i in its standard state. The Gibbs energy of adsorption of the protein ($\Delta G^0_{ads,p}$) and of the salt ions ($\Delta G^0_{ads,s}$) is defined as

$$\Delta G^0_p = \Delta G^0_{ads,p} = \mu^0_{q_p} - \mu^0_{c_p} \qquad \textbf{(2-14)}$$

$$\Delta G^0_s = -\Delta G^0_{ads,s} = \mu^0_{c_s} - \mu^0_{q_s} \qquad \textbf{(2-15)}$$

In the exchange reaction the protein is adsorbed and the salt is desorbed, so that $\Delta G^0_{ads,s}$ for the salt is negative. Inserting Equation (14) and (15) in Equation (13) gives:

$$\Delta G^0_{exc} = \Delta G^0_{ads,p} - \nu \Delta G^0_{ads,s} \qquad \textbf{(2-16)}$$

Substituting Equation (16) into Equation (12) and rearranging yield the following expression for the equilibrium constant for the exchange reaction:

$$K = \exp\left(\frac{-\Delta G^0_{ads,p}}{RT} + \nu \frac{\Delta G^0_{ads,s}}{RT} \right) \qquad \textbf{(2-17)}$$

$\Delta G^0_{ads,p}$ depends on the protein and the ion-exchange media, but it is assumed to be independent of pH. $\Delta G^0_{ads,s}$ depends on the ion-exchange media but is independent of the protein adsorbed.

The SMA model takes the steric hindrance of the salt counterions into account, but it assumes that the effects of co-ions can be neglected in the ion-exchange process [Brooks, 1992]. Furthermore, the SMA model ignores protein-protein interactions in solution, and protein-protein interactions while adsorbed [Gerstner, 1994]. The protein-protein interactions are most pronounced when the concentration is high, such as on the surface of the stationary phase and in complex protein mixtures, e.g. feedstocks in biotechnology.

The unknown parameters in the SMA model are ν, K and σ. From isocratic or gradient elution experiments in the linear range ν, $\Delta G^0_{ads,p}$, $\Delta G^0_{ads,s}$ and thus K can be determined. In this work the parameters ν, $\Delta G^0_{ads,p}$ and $\Delta G^0_{ads,s}$ are estimated from isocratic elution data. This is described in Chapter 4. The parameters determined from the isocratic elution experiments are used in the model for the retention volume at gradient elution. The experimental retention volumes from gradient elution are compared with the retention volumes predicted by the model, when the parameters determined from the isocratic elution experiments are used.
When ν and K have been determined the only unknown in the SMA model for the isotherm is the shielding factor σ. In Chapter 5 σ is determined from a few capacity measurements in the non-linear range.

3 DETERMINATION OF SYSTEM, COLUMN AND MEDIA CONSTANTS

Before any experiment planning and model use, it is necessary to characterize the system and the columns. Both the system and the columns contribute to the dead volumes and the band broadening, and in order to be able to eliminate these contributions, they have to be determined.
Before any use of the columns it is necessary to characterize the packed beds. In most models it is also necessary to know the bed constants such as retention volumes under non-binding conditions, porosities and ion-exchange capacity.
This chapter describes the methods used in this work for determination of system and column constants and gives the results obtained.

3.1 Dead Volumes of the BioCAD System

The dead volumes are caused by the tubes and valves in the BioCAD system. To be able to determine the dead volumes of the system, it is necessary to know how the different units in the system are connected. This section will therefore also give a short description of the BioCAD system.

3.1.1 The Construction and Dead Volumes of the BioCAD

Figure 3-1 shows a schematic representation of the BioCAD.

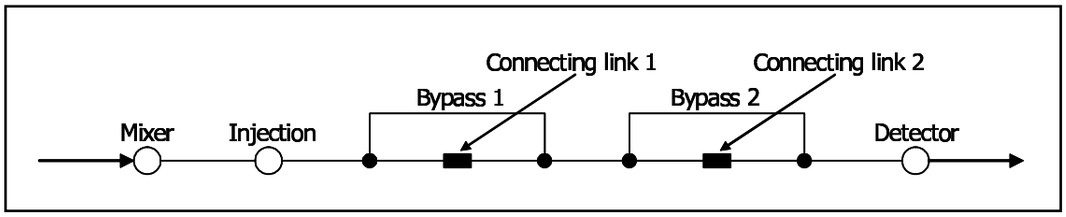

Figure 3-1: Schematic representation of the BioCAD system.

The dead volumes of the BioCAD system are determined without columns. The tubes to the column inlet and outlet are instead connected with connecting links. The buffer solution is first pumped to the mixer, then to the injection valve, column position 1, column position 2 and finally through the detector. If column position 1 is inline the flow path is: Mixer, injection valve, connecting link 1, bypass 2, and detector. If column position 2 is inline the flow path is: Mixer, injection valve, bypass 1, connecting link 2, and detector.

In Figures 3-2 and 3-3 the flow path and the dead volumes for position 1 and 2 respectively are indicated. The flow path is presented by a solid line. The symbols used for the different dead volumes are as follows:

V_{MD}: Volume between mixer and detector

V_{MC}: Volume between mixer and column inlet

V_{CD}: Volume between column outlet and detector

V_{MI}: Volume between mixer and injection

V_1: Volume between injection and inlet to the bypass valve

V_2: Volume between inlet to the bypass valve and column inlet

V_3: Volume between column outlet and outlet of the bypass valve

V_{ID}: Volume between injection and detector

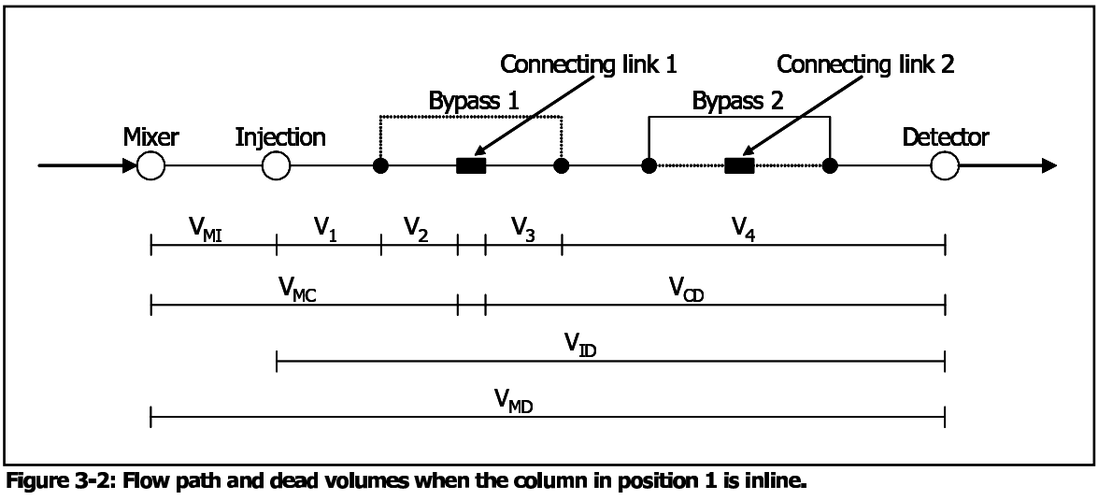

Figure 3-2: Flow path and dead volumes when the column in position 1 is inline.

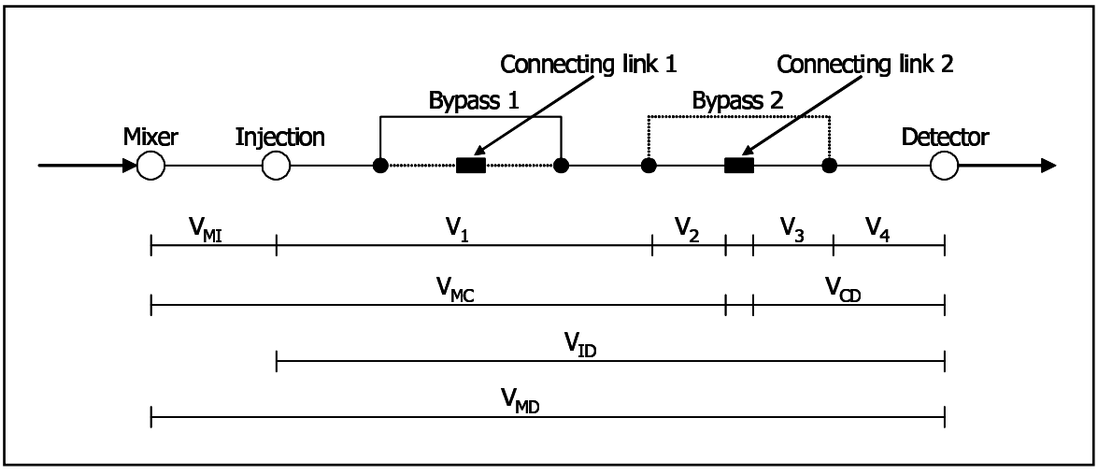

Figure 3-3: Flow path and dead volumes when the column in position 2 is inline.

3.1.2 Determination of the Dead Volumes

All the dead volumes except V_{ID} are determined by displacement experiments with water and $NaNO_3$. The volume V_{MD} is additionally determined by displacement experiments with NaCl and BSA as well. From the displacement experiments the volumes are determined from the area above or

below the curve. V_{ID} is determined by pulse injections of $NaNO_3$ with both NaCl and $NaNO_3$ as the mobile phase.

The first experiments for determination of V_{MD}, V_{MC} and V_{CD} were run manually and only a section of the entire run was saved in a file. This causes some uncertainty, because if the saved section does not include the entire displacement the calculated volumes will be too small. If the saved section includes a little more than the displacement, the calculated volumes will be too high. These experiments are therefore not included in the calculations of V_{MD}, V_{MC} and V_{CD} but they are given in Appendix B.I. The volume of V_2+V_3 including the connection link is determined from the peak area, for which reason it is not important if the experiments are run manually or by a method. In the following, the methods for determination of the different dead volumes will be described. All the dead volumes are determined at a flow rate of 1.01 ml/min except the volume V_{MD}, which is determined by NaCl and BSA at 2.94 ml/min.

The experimental data and calculations for determination of the dead volumes are given in Appendix B.I.

3.1.2.1 Volume between mixer and detector, V_{MD}

1) The entire system from the mixer to the UV detector is filled with water.
2) The method consisting of only one step is started. In the method nitrate is run through the system, and data is collected from the beginning to the end of the method.
3) The next method is started. In this method water is run through the system in order to displace the nitrate, and data is collected from the beginning to the end of the method.
4) More measurements are made by repeating steps 2 and 3.

The experiments with NaCl and BSA correspond to the experiments with $NaNO_3$ and water.

The displacement corresponds to breakthrough curves and the volume between the mixer and the detector is determined from the area above and below the curve.

The area below the curve, A_{below}, is determined by numerical integration:

$$A_{below} = \left(0.5\left(UV_1 - UV_{baseline}\right) + 0.5\left(UV_n - UV_{baseline}\right) + \sum_{i=2}^{n-1}\left(UV_i - UV_{baseline}\right) \right)\Delta t \qquad [\text{abs.}\ 280\,\text{nm}\cdot\text{s}]$$

(3-1)

where UV_1 is the UV signal at the first data point, UV_n is the UV signal at the last data point, n is the number of data points and Δt is the time between two data points. The area is converted to the unit abs. 280 nm·ml:

$$A_{below}\ [\text{abs. } 280\,\text{nm}\cdot\text{ml}] = \frac{A_{below}\ [\text{abs. } 280\,\text{nm}\cdot\text{s}]\,Q\ [\text{ml/min}]}{60\ \text{s/min}} \qquad \textbf{(3-2)}$$

The volume corresponding to the area below the curve, depending on whether nitrate or BSA is used, is now calculated as

$$V_{below} = \frac{A_{below}\ [\text{abs. } 280\,\text{nm}\cdot\text{ml}]}{\alpha_{NaNO_3}\, c_{NaNO_3}} \qquad \textbf{(3-3)}$$

$$V_{below} = \frac{A_{below}\ [\text{abs. } 280\,\text{nm}\cdot\text{ml}]}{\alpha_{BSA}\, c_{BSA}} \qquad \textbf{(3-4)}$$

α_{NaNO_3} and α_{BSA} are the slopes of the calibration curves for $NaNO_3$ and BSA.

When $NaNO_3$ or BSA is displaced by water or NaCl the volume below the curve is equal to the volume from the mixer to the detector, $V_{MD} = V_{below}$.

When it is the other way around, where water or NaCl is displaced by $NaNO_3$ or BSA, the volume from the mixer to the detector is equal to the volume corresponding to the area above the curve and is determined as

$$V_{MD} = V_{above} = V_{total} - V_{below} \qquad \textbf{(3-5)}$$

The experimental data is given in Appendix B.I.

3.1.2.2 Volume between mixer and column, V_{MC}

1) The entire system is filled with water.
2) The tube to the column inlet and the connection link are disconnected.
3) Nitrate is run through the system. The nitrate will leave the system at the column inlet tube, because of the disconnection.
4) The volume from the mixer to the column inlet is now filled with nitrate, and the column inlet tube and the connection link are connected again.
5) A method where water is run through the system is started, and data is collected. The water will displace the nitrate and the resulting curve is a peak.

The volume V_{MC} is calculated from the area of the nitrate peak:

$$A_{peak} = \left(0.5\,(UV_1 - UV_{baseline}) + 0.5\,(UV_n - UV_{baseline}) + \sum_{i=2}^{n-1}(UV_i - UV_{baseline})\right)\Delta t \qquad [\text{abs. } 280\,\text{nm}\cdot\text{s}]$$

(3-6)

$$A_{peak}\ [\text{abs. } 280\,\text{nm} \cdot \text{ml}] = \frac{A_{peak}\ [\text{abs. } 280\,\text{nm} \cdot \text{s}]\ Q\ [\text{ml/min}]}{60\ \text{s/min}} \qquad \textbf{(3-7)}$$

$$V_{MC} = \frac{A_{peak}\ [\text{abs. } 280\,\text{nm} \cdot \text{ml}]}{\alpha_{NaNO_3} c_{NaNO_3}} \qquad \textbf{(3-8)}$$

The experimental data is given in Appendix B.I.

3.1.2.3 Volume between column and detector, V_{CD}

The determination of the volume between the column and the detector is similar to the determination of the volume between the mixer and the column.

1) The entire system is filled with water.
2) The tube to the column outlet and the connection link are disconnected.
3) Nitrate is run through the system. The nitrate will leave the system at the connection link, because of the disconnection.
4) The system from the mixer to the column inlet tube (incl. the connection link) is filled with nitrate, and the connection link and the column outlet tube are connected again.
5) A method where nitrate is run through the system is now started, and data is collected. The nitrate will displace the water in the volume V_{CD}.
6) The system is now completely filled with nitrate. In the next method the volume from the mixer to the column inlet tube (incl. the connection link) is filled with water, before the tube and the connection link are connected again, and the nitrate is displaced by water.

The resulting curve is a breakthrough curve and not a peak. The volume from the column to the detector is therefore determined in the same way as the volume from the mixer to the detector.

The experimental data is given in Appendix B.I.

3.1.2.4 Volume between inlet and outlet of the bypass valve including the connection link, $V_2+V_3+V_{connection\ link}$

1) The system is filled with nitrate.
2) The method is started. In the method water is run through the system in bypass position. (After this step the volume $V_2 + V_3 + V_{connection\ link}$ is filled with nitrate and the remaining part of the system is filled with water).
3) The position is now changed from bypass to inline, and the data collection is started. The nitrate in the volume $V_2 + V_3 + V_{connection\ link}$ is displaced by water, and the volume is calculated from the area of the nitrate peak.

4) In the next method nitrate is run through the system in bypass position. The volume $V_2 + V_3 + V_{connection\ link}$ is now filled with water and the rest of the system with nitrate. When the position is changed from bypass to inline, the nitrate will displace the water, and the volume $V_2 + V_3 + V_{connection\ link}$ is calculated from the area of the (negative) water peak.

The volume $V_2 + V_3 + V_{connection\ link}$ is calculated in the same way as the volume V_{MC}.

The experimental data is given in Appendix B.I.

3.1.2.5 Volume between injection and detector, V_{ID}

The volume from the injection to the detector is determined by pulse injections of 25 µl nitrate. Both water and nitrate are used as mobile phase. When water is the mobile phase the concentration of the nitrate sample solution is 0.75 M, and when nitrate is the mobile phase the concentration of the nitrate sample solution is 0.5 M.

1) The entire system is filled with the mobile phase in use.
   Two slightly different methods are used. The only difference between the two methods is the time for injection.

2A) The injection is performed and the data collection is started.

2B) 2 ml of mobile phase is run through the system before the injection is performed. At the time for injection the data collection is started.

The volume from the injection to the detector is equal to the retention volume of the nitrate peak. The nitrate peak is fitted with the EMG function (EMG = Exponential Modified Gauss), and the retention volume is determined as

$$V_{R,nitrate} = V_{ID} = V_{R,Gauss} + \tau \qquad \textbf{(3-9)}$$

$V_{R,Gauss}$ is the Gaussian retention volume and τ is the distortion.

The experimental data is given in Appendix B.I.

3.2 Dead Volume of the Empty Columns

The dead volume of the columns is due to the tubes, filters, top and bottom assemblies in the columns. To get only the performance of the bed it is necessary to be able to eliminate contributions from both the system and the column. The determination of the column dead volume is very similar to the determination of the system dead volumes, but now the column is in place instead of the connection link.

When the dead volume of the empty column is determined the top and bottom assemblies are placed so close together in the column that they touch. When the dead volume is determined with filters, two filters are placed between the top and the bottom assemblies and the assemblies are mounted as close together as possible. The dead volumes have to be determined by a variable assembly (top assemblies) in both ends of the column; otherwise it will not be possible to bring the assemblies to touch and eliminate any additional dead volume in the column.
The dead volume of the empty columns is determined from pulse injections of $NaNO_3$ or BSA with $NaNO_3$ or NaCl as the mobile phase. The retention volume of the peak will be equal to the volume from the injection to the detector including the empty column. By subtraction of the dead volume from injection to detector the dead volume of the empty column is obtained.
The dead volumes of the empty columns have been determined for the HR10 and HR16 columns from Amersham Pharmacia. The Fractogel EMD TMAE 650(s) column is a prepacked column for which reason it has not been possible to determine the dead volume of the empty column. The column is very similar to the HR10 column and the dead volume has therefore been assessed to the value for the HR10 column with 2 variable assemblies.
An HR5 column with one variable assembly has also been used, but no measurements have been made on an empty column. The dead volume of the HR5 column has been estimated from the dead volumes of the similar HR10 and HR16 columns.
It was very difficult to determine the dead volume of the Waters column (used for scale-up), because the top and bottom assemblies had to be held together by hand during the experiments. It was very difficult to keep the assemblies close together during the entire experiment, but by repeating the experiments it was possible to estimate a value for the dead volume.

The experimental data and calculations for determination of the dead volumes of the empty columns are given in Appendix B.II

3.3 Retention Volumes under Non-adsorbed Conditions

The retention volumes under non-binding conditions, V_{NA}, were determined from pulse injections of the protein in a buffer of 1.0 or 2.0 M NaCl. No difference between the retention volumes determined in 1.0 or 2.0 M NaCl was observed. The determinations in the 2.0 M NaCl buffer were made to assure that no protein was adsorbed when the 1.0 M NaCl buffer was used.
The retention volumes under non-binding conditions are needed for calculation of K_d and for modeling the retention volumes at gradient elution.

The experimental data for determination of the retention volumes under non-adsorbed conditions is given in Appendix B.III.

3.4 Porosities

The interstitial or bed porosity ε is the volume between the particles, and the intrapartide porosity ε_p is the fractional void volume in the particles. The fractional void volume in a particle available for a molecule is $\varepsilon_p K_d$, where K_d is an exclusion factor which per definition is 1 for salt and less than 1 for large molecules like proteins. The total porosity ε_t is determined by a salt to assure that $K_d = 1$. For larger molecules the apparent total porosity becomes smaller, and for a totally excluded molecule ($K_d = 0$) it equals the interstitial porosity.
The porosities are related by

$$\varepsilon_t = \varepsilon + (1-\varepsilon)\varepsilon_p \qquad \textbf{(3-10)}$$

The total porosity is determined by a small pulse injection of 0.75 M $NaNO_3$ in a 1.0 M $NaNO_3$ buffer. The measured retention volume is corrected by the dead volume to obtain the total liquid volume

$$V_t = V_R - V_{dead} = V_R - (V_{empty\ col.} + V_{pos.} + V_{filters}) \qquad \textbf{(3-11)}$$

As mentioned earlier $V_{empty\ col.}$ and $V_{filters}$ are not known for all the columns. For these columns the assessed values are used.
The total porosity is calculated from the total liquid volume as

$$\varepsilon_t = \frac{V_t}{V_{col}} \qquad \textbf{(3-12)}$$

The interstitial particle porosity is very difficult to determine for anion exchangers because many of the compounds generally used for this purpose for other media (cation exchangers, RPC media, HIC etc.) stick to the anion exchanger. Therefore, it was decided to assess a reasonable value for ε, similar to those obtained from cation-exchange media or published data, and calculate ε_p from the total porosity for the salt:

$$\varepsilon_p = \frac{\varepsilon_t - \varepsilon}{(1-\varepsilon)} \qquad \textbf{(3-13)}$$

The exclusion factor K_d is determined from the retention volume of the protein in a 1.0 or 2.0 M NaCl buffer:

$$K_d = \frac{\frac{V_{NA}}{V_{col}} - \varepsilon}{(1-\varepsilon)\varepsilon_p} \qquad \textbf{(3-14)}$$

The experimental data for determination of the total porosity is given in Appendix B.IV.

3.5 Ion-exchange Capacity

The ion-exchange capacity is a measure of the number of exchange sites for a specified amount of the ion exchanger. The ion-exchange capacity is measured with small ions to assure that the ions can penetrate all the pores and reach all the exchange sites.

In the literature the ion-exchange capacity is often measured by potentiometric titration [Helfferich, 1995; Bentrop et al., 1991; Soldatov, 1995 and 1998; Son et al., 2000; Suzuki et al., 1999; Zuyi et al., 1996] or back titration [Helfferich, 1995; Soldatov, 1998] but also in-column frontal analysis has been used [Bentrop et al., 1991].

The ion-exchange capacity of the Q-Sepharose XL, the Ceramic Q-HyperD F and the Fractogel EMD TMAE media has only been determined by in-column measurements.

The ion-exchange capacity of the Source 30Q media has been determined both by batch experiments and in-column experiments. In the column the ion-exchange capacity has been determined both by acid-base titration and by frontal analysis with nitrate. Three different kinds of batch experiments have been performed: Back titration, potentiometric titration and titration from a pH of 11.0 to a pH of 2.5 or 2.0.

3.5.1 In-column Determination

In the following, two methods used for determination of the ion-exchange capacity of packed columns are described. The first is an acid-base titration where the column is saturated with OH^--ions. The amount of OH^--ions needed for saturation of the column is determined by titration with HCl.

In the other method the column is saturated with NO_3^--ions. The amount of NO_3^--ions needed for saturation of the column is determined from the area of the peak where the adsorbed NO_3^--ions are eluted from the column.

The experimental data for determination of the ion-exchange capacity by in-column acid-base titration is given in Appendix B.V and the experimental data for the determination by nitrate is given in Appendix B.VI.

3.5.1.1 Acid-base titration

The column is equilibrated with 0.10 M NaOH, washed with milliQ water and finally the column is eluted with NaCl and the eluate is collected. The eluate is titrated with 0.100 M HCl with phenolphthalein as the indicator.

The length of the three steps has been varied to assure that the column is completely saturated with hydroxide, that all unbound hydroxide is washed out of the column before it is eluted with NaCl and that all the adsorbed hydroxide is eluted and collected for titration with HCl.

The ion-exchange capacity in mmol is calculated as

$$\lambda = V_{HCl}\, c_{HCl} \qquad \textbf{(3-15)}$$

where V_{HCl} is the volume and c_{HCl} is the concentration of HCl used for titration of the eluate.

The experimental data is given in Appendix B.V.

3.5.1.2 Breakthrough curves with nitrate

Two slightly different methods are used. In the first the column is equilibrated with 2.0 M NaCl. Then 1.0 M KNO_3 or $NaNO_3$ is run through the system in bypass position, before it is loaded into the column. Before elution the bypass and the column are washed with milliQ water. The nitrate is now eluted from the column with 2.0 M NaCl.

In the other method the column is equilibrated with 2.0 M NaCl, loaded with 1.0 M KNO_3 or $NaNO_3$, washed with water and finally the nitrate is eluted with 2.0 M NaCl.

No difference between the results obtained by KNO_3 and $NaNO_3$ was observed.

The length of the different steps has been varied to assure that the column is completely saturated with nitrate, all unbound nitrate is washed out of the column before elution with NaCl and all nitrate is eluted from the column.

The ion-exchange capacity in mmol is calculated from the area of the elution peak as

$$\lambda = \frac{A_{peak} \cdot Q}{60\,\mathrm{s/min} \cdot \alpha_{NaNO_3}} \qquad \textbf{(3-16)}$$

where A_{peak} is the area of the peak in UV 280 nm/s, Q is the flow rate in ml/min and α_{NaNO_3} is the slope of the calibration curve for nitrate. The area of the peak is determined by a fit of the peak by the EMG function or the Logistic Power peak function in PeakFit.

The experimental data is given in Appendix B.VI.

3.5.2 Determination of Ion-exchange Capacity by Batch Experiments

The pretreatment of the media for the different kinds of batch experiments is identical:

1) The media is placed in a glass filter funnel.
2) The media is washed 3 times with 20 to 25 ml of 2.0 M NaCl.
3) The media is washed 3 times with 20 to 25 ml water.
4) The media is equilibrated with 3 times 20 to 25 ml of 1.0 M NaOH.
5) The media is washed with water until the pH of the washing water is neutral.
6) The media is now drained for 20 min. in the glass filter funnel.
7) From the filter cake samples for the specified batch experiment and for drying in the oven are taken without breaking the entire filter cake. Three samples are taken for drying in the oven. The first is taken before any samples for the experiments are taken. The next is taken when half of the samples for the experiments has been taken and the last when all the samples for the experiments have been taken. The samples for the experiments are dissolved in different solutions depending on the type of batch experiment.

The experimental data for batch determination of the ion-exchange capacity is given in Appendix B.VII (back titration) and B.VIII (acid-base titration).

3.5.2.1 Determination of amount of media, drying in a filter funnel and in the oven

The media was drained in a glass filter funnel in order to remove the water around the particles. But it was observed that it was not possible to drain the media to a constant weight. Even if the amount of media and the draining time were kept constant, the water content in the media after draining was not constant. In order to determine the water content in the media after draining, samples were taken for drying in the oven at 100 °C. In order to avoid a considerable evaporation of water from the filter cake during the collection of samples, the filter cake was not broken. A little amount of the filter cake was taken for each sample. Three samples from each filter cake were taken for drying in the oven. The samples were not taken at the same time in order to see, if there was any evaporation of water from the filter cake during the collection of samples. The samples were also taken at different spots of the filter cake in order to see, if there was any difference in the water content due to the placement in the glass filter funnel.

The water content in each of the three samples that have been dried in the oven is determined as

$$\%\text{water} = \frac{m_{\text{drained media}} - m_{\text{dry media}}}{m_{\text{drained media}}} \qquad \textbf{(3-17)}$$

The water content of the drained media used for batch experiments is determined as the mean of the water content in the three oven-dried samples.

3.5.2.2 Potentiometric titration

The samples for potentiometric titration are dissolved in 1.0 M or 0.01 M NaCl. The samples are titrated with 0.100 M HCl, by adding a few drops of HCl at a time with an auto burette. After every addition of HCl the pH and the total amount of HCl added are noted when the pH is stable. HCl is added until the pH is around 2.1.

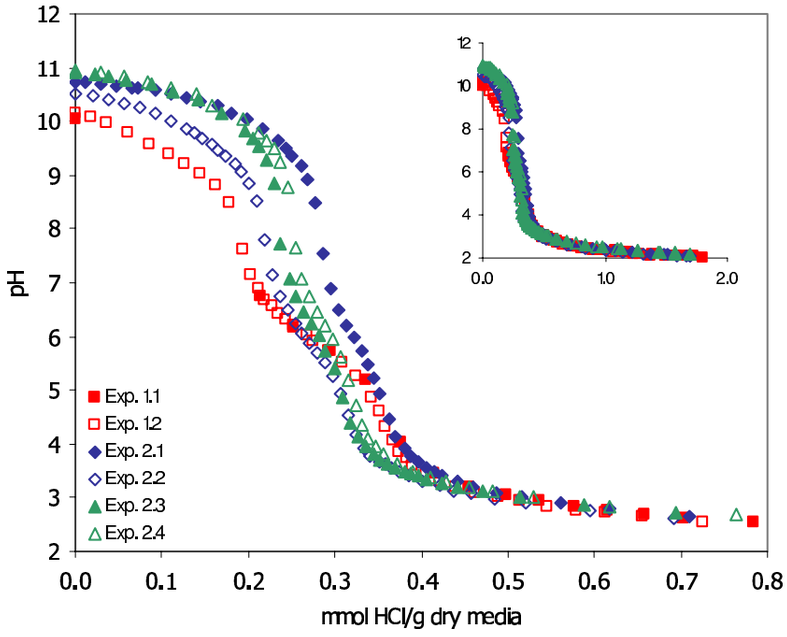

Figure 3-4: Potentiometric titration of Source 30Q. (The small figure in the upper right corner shows the entire titration curves and the big figure shows a section of the curves around the inflection point).

The 6 samples Exp. 1.1 to Exp. 2.4 for the potentiometric titration are as follows: Exp. 1.1 and Exp. 1.2 are taken from the same drained filter cake 1.0 M NaCl is added to both samples before titration. Exp. 2.1 to Exp. 2.4 are taken from another drained filter cake. 1.0 M NaCl is added to Exp. 2.1 and Exp. 2.2 and to Exp. 2.3 and Exp. 2.4 0.1 M NaCl is added before titration.

The capacity is determined as the inflection point. The titration curve is differentiated by numerical differentiation and the resulting peak(s) is fitted by the EMG function in PeakFit. The first moment of the peak corresponds to the inflection point of the titration curve in V_{HCl}, and the capacity is determined as

$$\lambda = V_{HCl,\ \text{inflection point}} \cdot c_{HCl} \qquad \textbf{(3-18)}$$

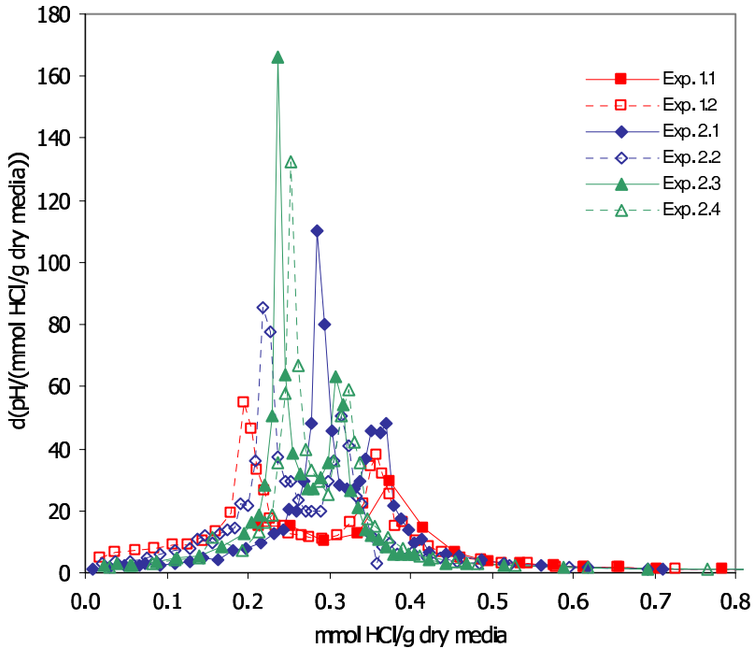

Figure 3-5: The slope of the titration curves for Source 30Q.

From Figures 3-4 and 3-5 it is observed that there are 2 inflection points on each titration curve. The question is now: Should the capacity be determined from the first or the second inflection point or from a mean of the two inflection points? It is hard to tell because the charged group in Source 30Q is a quaternary amino group, which only gives one inflection point. What causes the two inflection points is not known and therefore it is not possible to decide which inflection point to use for determination of the ion-exchange capacity.

3.5.2.3 Back titration

To the samples for titration 50 ml of 0.100, 0.050 or 0.010 M HCl are added, and they are left for 1 day. 20 – 30 ml of the sample solution are centrifuged and two times 10 ml of the solution are taken for titration with 0.100 M NaOH.

The titration is performed with an auto burette and the capacity in mmol is calculated as

$$\begin{aligned}\lambda &= V_{HCl}\,c_{HCl} - V_{NaOH}\,c_{NaOH} = 5\cdot\left(10\,\text{ml}\cdot 0.100\,\text{M} - V_{NaOH}\cdot 0.100\,\text{M}\right)\\ &= 5.0\,\text{mmol} - V_{NaOH}\cdot 0.500\,\text{M}\end{aligned} \qquad \textbf{(3-19)}$$

The experimental data is given in Appendix B.VII.

3.5.2.4 Acid-base titration

To the samples for titration 100 ml of 1.0 or 0.10 M NaCl are added. Some of the samples are titrated immediately and some are titrated after 1 or 3 days. All the titrations are performed with auto burettes.

The samples are first titrated to a pH of 11.00 with 0.100 M NaOH and then to a pH of 2.00 with 0.100 M HCl. Some blank titrations are also performed where 100 ml of the 1.00 M NaCl solution are titrated to a pH of 11.00 with 0.100 M NaOH and then to a pH of 2.00 with 0.100 M HCl. The blank titrations are performed on the same solutions as the ones added to the media. The blank titrations are performed on the same day as the titrations of the media containing samples.

The capacity in mmol is calculated as

$$\lambda = V_{HCl}\, c_{HCl} - V_{HCl,Blank}\, c_{HCl,Blank} = (V_{HCl} - V_{HCl,Blank}) \cdot 0.100\,M \qquad \textbf{(3-20)}$$

The experimental data is given in Appendix B.VIII.

3.6 Results and Discussion

3.6.1 System Dead Volumes

The experimental data is given in Appendix B.I.

$V_{connection\ link}$ = 0.04 ml

		Position 1	Position 2
V_{MD}	[ml]	5.38	5.33
V_{MC}	[ml]	4.67	4.80
V_{CD}	[ml]	0.43	0.51
V_{ID}	[ml]	0.31	0.40
$V_2 + V_3 + V_{connection\ link}$	[ml]	0.11	0.16

Table 3-1: BioCAD system dead volumes.

Many of the system dead volumes are very small and therefore difficult to determine without some uncertainty. The dead volumes in position 2 are a little higher than the dead volumes in position 1 except for the volume V_{MD}. That the volume V_{MC} is larger for position 2 than for position 1 is logic, because the flow path from the mixer to the column is longer for position 2 than for position 1. That the volume V_{CD} is larger for position 2 than for position 1 is not logic, because the flow path from the column to the detector is longer for position 1 than for position 2. This indicates some uncertainty in the determination of the volume V_{CD}. The volume V_{MD} is equal to $V_{MI} + V_{ID}$, where V_{MI} is the volume from the mixer to the injection. V_{MI} is a constant and independent of whether position 1 or 2 are inline, thus the largest volumes of V_{MD} and V_{ID} should be observed for the same

position. This is not the case, because V_{MD} for position 1 is larger than for position 2, but V_{ID} is larger for position 2 than for position 1. From this it follows that some inconsistency in the volumes V_{MD} and V_{ID} are present.
If the volumes are determined correctly the volume V_{MD} is equal to $V_{MC} + V_{connection\ link} + V_{CD}$

- Position 1: $V_{MC} + V_{connection\ link} + V_{CD}$ = 5.14 ml
- Position 2: $V_{MC} + V_{connection\ link} + V_{CD}$ = 5.35 ml

This indicates that the measured volume V_{MD} for position 1 is a little too high, but the difference between V_{MD} measured and V_{MD} calculated from the three other measurements is less than 5%, so the agreement between the measurements is reasonable.
The agreement between the determined dead volumes for position 2 is very good. The difference between V_{MD} measured and V_{MD} calculated from the three other measurements is less than 0.5%. Determination of dead volume by displacement experiments with nitrate and water is shown to be a fast, cheap and reliable method.

3.6.2 Dead Volumes of the Empty Columns

The experimental data is given in Appendix B.II.

One variable assembly:

- $V_{empty16}$ = 0.425 ml
- $V_{empty16,\ incl.\ filters}$ = 0.546 ml
- $V_{empty10}$ = 0.194 ml
- $V_{empty10,\ incl.\ filters}$ = 0.237 ml
- $V_{empty5,\ incl.\ filters}$ = 0.150 ml
- $V_{empty,\ waters}$ =1.0 ml

Two variable assemblies:

- $V_{empty16}$ = 0.606 ml
- $V_{empty16,\ incl.\ filters}$ = 0.727 ml
- $V_{empty10}$ = 0.247 ml
- $V_{empty10,\ incl.\ filters}$ = 0.290 ml

The dead volumes for the columns HR16 and HR10 with two variable assemblies are measured, and the dead volumes with only one variable assembly are calculated from these volumes and the length of the tubes.

The uncertainty of the dead volume for the empty HR16 column with two variable assemblies has been determined to be ±0.02 ml (Appendix A.I), and there is no reason to believe that it should be higher for the HR10 column. The uncertainty of the columns when they are used with only one variable assembly is due to measuring the tube length a little higher, but not much because the cross-sections of the tubes are only 0.002 cm^2 and 0.005 cm^2, respectively. A reading of the tube length which is 1.0 cm too high or too low will only result in ±0.002 ml or ±0.005 ml in the volume of the empty columns.

The dead volume of the empty HR5 columns is estimated from the dead volumes of the HR10 and HR 16 columns and therefore associated with some uncertainty. The dead volume of the Waters column is also associated with some uncertainty due to the difficulty of keeping the top and bottom assemblies close together during the measurements, but the relatively large volume of the Waters column makes the uncertainty negligible.

3.6.3 Column and Media Constants

The experimental is are given in Appendices B.III to B.VI.

		Source 30Q	Q-Sepharose	Q-HyperD F	Fractogel
V_{col}	[ml]	8.07	7.56	7.56	3.93
ε_t		0.74	0.93	0.81	0.75
ε_p		0.57	0.91	0.68	0.58
ε		0.40	0.30	0.40	0.40
$V_{NA,BSA}$	[ml]	4.93	2.80	3.53	2.19
$V_{NA,\alpha\text{-lactalbumin}}$	[ml]	5.28	4.46	3.64	2.73
$V_{NA,\beta\text{-lactoglobulins}}$	[ml]	5.17	3.52	3.58	2.34
$K_{d,BSA}$		0.61	0.11	0.165	0.45
$K_{d,\alpha\text{-lactalbumin}}$		0.74	0.46	0.201	0.85
$K_{d,\beta\text{-lactoglobulins}}$		0.70	0.26	0.181	0.56
λ_{OH^-}	[mmol]	0.688	1.69	1.81	0.0685
Λ_{OH^-}	[mmol/ml pore vol.]	0.251	0.352	0.590	0.0503
$\lambda_{NO_3^-}$	[mmol]	0.843	2.15	2.38	0.112
$\Lambda_{NO_3^-}$	[mmol/ml pore vol.]	0.308	0.448	0.777	0.0825

Table 3-2: Media and column constants for the columns used in the experiments in the linear range.

Due to the earlier mentioned problems with determination of the interstitial porosity for anion exchangers (the compounds used for determination sticks to the anion-exchange media), the interstitial porosities are assessed and the intraparticle porosities are calculated from the total porosity and the interstitial porosity. Nash et al. used $\varepsilon = 0.4$ and $\varepsilon_p = 0.60 - 0.65$ for Source 30S and $\varepsilon = 0.35$ and $\varepsilon_p = 0.88$ for SP-Sepharose FF [Nash et al., 1998], which is similar in structure but not identical to Q-Sepharose XL. Gebauer et al. used the values $\varepsilon = 0.35$ and $\varepsilon_p = 0.95$ for S-Sepharose FF, which is also similar but not identical to the Q-Sepharose XL [Gebauer et al., 1997].

Fernandez et al. estimated the intraparticle porosity in Q-HyperD F to be 0.65 [Fernandez et al., 1996 (p169-183)]. No data published for Fractogel EMD TMAE 650(s), but it is similar to Source 30Q and the interstitial porosity is therefore assessed to have the same value as Source 30Q.

		Source 30Q				
V_{col}	[ml]	0.46	0.98	1.35	9.39	55.61
ε_t		0.79	0.76	0.74	0.77	0.74
ε_p		0.57	0.57	0.57	0.57	0.57
ε		0.52	0.44	0.40	0.47	0.40
$V_{NA,BSA}$	[ml]	0.34	0.59	0.82	6.44	34.02
$K_{d,BSA}$		0.78	0.50	0.62	0.71	0.61
λ_{OH^-}	[mmol]	0.037	----	0.105	0.865	5.287
Λ_{OH^-}	[mmol/ml pore vol.]	0.291	----	0.226	0.303	0.277
$\lambda_{NO_3^-}$	[mmol]	0.049	0.091	0.114	----	----
$\Lambda_{NO_3^-}$	[mmol/ml pore vol.]	0.392	0.290	0.246	----	----

Table 3-3: Media and column constants for the Source 30Q columns used for scale-up and capacity measurements with BSA.

		Source 30Q		
V_{col}	[ml]	13.57	13.07	11.76
ε_t		0.77	0.76	0.77
ε_p		0.57	0.57	0.57
ε		0.45	0.44	0.46
$V_{NA,BSA}$	[ml]	8.47	8.01	----
$K_{d,BSA}$		0.54	0.55	----
λ_{OH^-}	[mmol]	1.008	0.951	1.131
Λ_{OH^-}	[mmol/ml pore vol.]	0.239	0.226	0.315
$\lambda_{NO_3^-}$	[mmol]	1.140	1.067	1.100
$\Lambda_{NO_3^-}$	[mmol/ml pore vol.]	0.270	0.254	0.306

Table 3-4: Media and column constants for the Source 30Q columns used for examination of the ion-exchange capacity.

The intraparticle porosity is a media constant, and for the Source 30Q column used for experiments in the linear range and for the columns with V_{col} =1.35 ml and V_{col} =55.61 ml, it was calculated to have the value 0.57 with ε = 0.40. The column used in the linear range and the column with V_{col} =1.35 ml are the two columns used in most experiments, and the column with V_{col} =55.61 ml is the largest column and the column with the smallest uncertainty of the column volume. The intraparticle porosity has therefore been assessed at 0.57 for all the other Source 30Q columns used in this work. The bed porosity is then calculated from the total porosity and the intraparticle porosity. For some of the columns this results in some rather high bed porosities. This is mostly due to the uncertainty of the column volume and the total porosities.

The exclusion factor is also a media constant, so that $K_{d,BSA}$ should have been identical for all the Source 30Q columns. The values determined for $K_{d,BSA}$ are in the range 0.50 to 0.78. The highest value is also the value with the highest uncertainty, because it is determined with the smallest column. An uncertainty of ±0.02 ml in the column volume results in very high uncertainties in the porosities and the K_d value.

The values used in the model calculations are the values for the columns with V_{col} = 1.35 ml and 8.07 ml. These values are very close to each other and within the experimental uncertainty. Furthermore, the values are very close to those determined for the largest column (V_{col} = 55.61 ml) where the uncertainty of the column volume and the porosities is smallest.

To see if a tendency can be found in the values for the other columns the calculations in Table 3-5 were made.

V_{col} [ml]	ε_t	$V_{NA,BSA}/V_{col}$	λ_{OH^-}/V_{col} [mmol/ml]	$\lambda_{NO_3^-}/V_{col}$ [mmol/ml]	$V_t/V_{NA,BSA}$	$\lambda_{NO_3^-}/\lambda_{OH^-}$
0.46	0.804	0.739	0.080	0.107	1.088	1.324
0.98	0.755	0.602	---	0.093	1.254	---
1.35	0.741	0.607	0.078	0.084	1.220	1.086
8.07	0.743	0.611	0.085	0.104	1.217	1.225
9.39	0.770	0.643	0.092	---	1.197	---
11.76	0.770	---	0.096	0.094	---	0.973
13.07	0.757	0.613	0.073	0.082	1.236	1.122
13.57	0.766	0.624	0.074	0.084	1.227	1.131
55.61	0.743	0.612	0.095	---	1.215	---

Table 3-5: Some relations between media and column constants for the Source 30Q columns.

With the values for the column with V_{col} = 8.07 ml as reference values, the ε_t and $V_{NA,BSA}/V_{col}$ values for the columns with V_{col} = 0.46, 9.39, 11.76, 13.07, 13.57 are higher indicating that the column volumes of these columns are too low. A look at the ratios between the capacities and the column volumes reveals the opposite tendency for the columns with a volume of 13.07 and 13.57 ml. The ratios are smaller than for the reference column, which indicates that the column volumes are too high. The values determined for the ratio $V_t/V_{NA,BSA}$ are close to the value determined for the reference column, except for the two smallest columns.

The values in Table 3-5 show that it is not possible to achieve identical determinations of the media constants for all the columns just by adjusting a single parameter e.g. the column volume. The difference in media constants determined is caused by uncertainties in the determination of the column volume, retention volumes and capacities. Even though many of the uncertainties are rather small they may sum up and result in a considerable deviation between the values determined at different columns, as it is observed for the $K_{d,BSA}$ values.

The ion-exchange capacity of the columns has been determined both by an acid-base titration (λ_{OH^-}) and by breakthrough experiments with nitrate (λ_{NO3^-}). The capacities determined by nitrate are higher than the capacities determined by hydroxide, even though they should be identical. Some measurements on very small columns (V_{col} < 0.5 ml) have also been made and for such small columns it is not possible to reproduce the measurements by acid-base titration, but it works very well for the breakthrough measurements by nitrate. Furthermore, the nitrate measurement is very fast and easy to perform. Therefore it was decided to use the capacities determined by nitrate.

The capacity is a media constant and the determinations for the Source 30Q media lay in the range 0.246 – 0.392 mmol/ml pore volume. The highest value 0.392 ml is determined for the smallest column and is assessed with the highest uncertainty because even small uncertainties in the column volume and the porosities will result in a high uncertainty of the capacity. The ion-exchange capacity for the Source 30Q media is assessed to have the value 0.308 mmol/ml pore volume, because this value is measured for the column used in the linear range and most experiments are made on this column. The uncertainty about the ion-exchange capacity is rather high because, for the three Source 30Q columns with column volumes in the range 11.76 ml to 13.57 ml, the smallest capacity measured differs 17.5% from the assessed value of 0.308 mmol/ml pore volume.

3.6.4 Investigation of Ion-exchange Capacity for Source 30Q by Batch Experiments

The experimental data is given in Appendices B.VII and B.VIII.

Back titration: $c_{HCl,added}$ = 0.010 M; Λ = 0.57 mmol/g dry media
$c_{HCl,added}$ = 0.050 M; Λ = 0.50 mmol/g dry media
$c_{HCl,added}$ = 0.100 M; Λ = 0.67 mmol/g dry media

The values measured for the samples to which 0.010 M and 0.050 M HCl were addedare lower than the values measured for the samples to which 0.100 M HCl was added. This could be because equilibrium is not reached when 0.010 M or 0.050 M HCl was added.

Acid-base titration from a pH of 11.0 to a pH of 2.50:
$c_{HCl,added}$ = 0.100 M; Λ = 0.220 mmol/g dry media
$c_{HCl,added}$ = 1.00 M; Λ = 0.176 mmol/g dry media

Acid-base titration from a pH of 11.0 to a pH of 2.00:
$c_{HCladded}$ = 0.100 M; Λ = 0.176 mmol/g dry media
$c_{HCl,added}$ = 1.00 M; Λ = 0.185 mmol/g dry media

There seems to be no difference between the values measured for the samples to which 0.100 M and 1.00 M HCl were added. Neither do the results seem to depend on whether the samples are titrated down to a pH of 2.50 or 2.00. One of the values (0.220 mmol/g dry media) differs considerably from the other three and it does not seem to be a reliable method.
The capacities measured by back titration are much higher than the capacities measured by acid-base titration. This could be due to the side process: non-exchange sorption of the acid due to their self-association in the solid phase of ion exchanger [Soldatov, 1998]. Even though this is most pronounced for the weak base groups and not the quaternary ammonium group present in the Source 30Q.

After the in-column determinations of the ion-exchange capacity the Source 30Q column with V_{col} = 11.76 ml was unpacked and the media was used for determinations of the ion-exchange capacity by batch experiments.

Titration on the same day the samples were prepared:

from a pH of 11.0 to a pH of 2.50 and $c_{HCl,added}$ = 1.0 M; Λ = 0.261 mmol/g dry media
from a pH of 11.0 to a pH of 2.00 and $c_{HCl,added}$ = 1.0 M; Λ = 0.310 mmol/g dry media

Titrations three days after the samples were prepared:

from a pH of 11.0 to a pH of 2.50 and $c_{HCl,added}$ = 1.0 M; Λ = 0.242 mmol/g dry media
from a pH of 11.0 to a pH of 2.00 and $c_{HCl,added}$ = 1.0 M; Λ = 0.278 mmol/g dry media

Equilibrium is reached after a few hours because the capacities measured on the day of preparation is not lower than the capacities measured after three days. That they on the contrary are higher must be due to experimental uncertainties. The rather large difference could also be a simple expression for a very bad reproducibility, because the same solution and media from the same column were used.
The values measured for the samples titrated down to a pH of 2.0 are higher than the values measured for the samples titrated down to a pH of 2.5. This indicates that the media is not completely saturated at a pH of 2.5, but more experiments need to be done before any conclusion can be drawn, because the other acid-base experiments do not show this tendency.

The amount of media in the column was determined and this makes it possible to compare the ion-exchange capacities determined by in-column and batch experiments.

Weight of the media from the 11.76 ml column:
$m_{drained\ media}$ = 8.38 g
$m_{dry\ media}$ = 3.43 g

Capacity measured in-column by acid base titration:
λ_{OH^-} = 1.131 mmol
This corresponds to a capacity of 0.330 mmol/g dry media

Capacity measured in-column by acid-base titration:
λ_{NO3^-} = 1.100 mmol
This corresponds to a capacity of 0.321 mmol/g dry media

For this column the capacities determined by hydroxide and nitrate are very close and lie within the experimental uncertainty, but for some of the other columns much larger differences are revealed.

The ion-exchange capacity determined by batch experiments is lower than the capacities determined by in-column experiments. The media was regenerated before use, but maybe this regeneration was not good enough. Especially, the values determined by titration to a pH of 2.50 are lower than the values determined by in-column experiments. It is therefore recommended to titrate the samples down to a pH of 2.00, but more experiments are needed before any final conclusions can be drawn. To lower the uncertainty of the batch determinations a larger amount of media should be used in the experiments. It would also be interesting to try to use all the media from a column in a batch determination of the capacity, because then it will be possible to compare the capacities determined by the two methods without any conversion of the units. If the capacities in mmol are compared, the uncertainty due to the determination of the media amount is eliminated.

4 THE LINEAR RANGE: ISOCRATIC AND LINEAR GRADIENT ELUTION

4.1 Isocratic Elution

In chromatography the retention volume can be calculated from the velocity of the center of mass of the eluted peak. The velocity depends on the void fractions in the column, the porosity of the particles and the distribution ratio A. The retention volume at isocratic elution is given as

$$V_R = V_{col}\left(\varepsilon + (1-\varepsilon)\varepsilon_p K_d (1+A)\right) \qquad \textbf{(4-1)}$$

The retention volume of a non-adsorbed compound is

$$V_{NA} = V_{col}\left(\varepsilon + (1-\varepsilon)\varepsilon_p K_d\right) \qquad \textbf{(4-2)}$$

By inserting Equation 4-2 in Equation 4-1 the expression for the retention volume becomes

$$V_R = V_{NA} + V_{col}(1-\varepsilon)\varepsilon_p K_d A \qquad \textbf{(4-3)}$$

The distribution ratio A in the linear range is calculated from Equation 2-10 as

$$A = \frac{q_p}{c_p} = K\left(\frac{\Lambda}{z_s c_s}\right)^{\nu} \qquad \textbf{(4-4)}$$

where K is given by Equation 2-17. For simplicity the parameter $B = V_{col}(1-\varepsilon)\varepsilon_p K_d K$ is introduced and the expression for the retention volume now becomes

$$V_R = V_{NA} + B\left(\frac{\Lambda}{z_s c_s}\right)^{\nu} \qquad \textbf{(4-5)}$$

The unknown parameters in this expression are ν, $\Delta G^0_{ads,s}$ and $\Delta G^0_{ads,p}$ and they are determined by a fit to the experimentally determined retention volumes. One fit is made per media where one $\Delta G^0_{ads,s}$ common to all the proteins is determined, one $\Delta G^0_{ads,p}$ for each protein is determined and four ν values are determined per protein, one at each pH. The problem is solved by Marquardt's method for least squares in MATLAB.

4.2 Linear Gradient Elution

In linear gradient elution the salt counterion concentration is increased linearly during the elution step and the gradient parameter G is defined as

$$G = \left(\frac{c_{s,1} - c_{s,0}}{V_g} \right) \tag{4-6}$$

where V_g is the gradient volume and $c_{s,0}$ and $c_{s,1}$ are the initial and the final salt concentrations of the gradient.

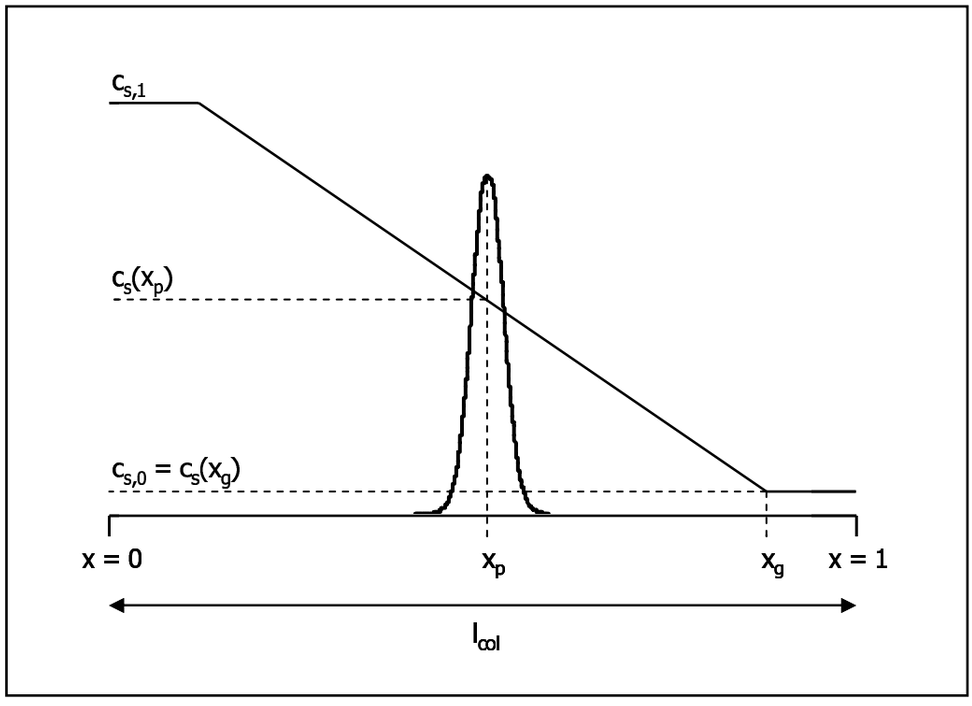

Figure 4-1: Linear gradient elution of a protein p in a column of the length l_{col}.

Figure 4-1 shows a linear gradient elution of a protein p in a column of the length l_{col}. The gradient starts in the dimensionless position x_g with a concentration of $c_{s,0}$ and ends at the concentration $c_{s,1}$. After the gradient the concentration is constant at $c_{s,1}$. x = 0 is the start of the column and x = 1 is the end of the column. x_p is the dimensionless position of the protein in the column and $c_s(x_p)$ is the salt concentration in that position. The salt concentration in the peak position is given as

$$c_s(x_p) = c_{s,0} - \frac{\partial c_s}{\partial x}(x_g - x_p) \tag{4-7}$$

where $x_g > x_p$ because the start of the gradient is in front of the protein.

The change in the salt concentration as a function of the position in the column is given as

$$\frac{\partial c_s}{\partial x} = \frac{\partial c_s}{\partial V}\frac{\partial V}{\partial x} = \frac{\Delta c_s V_t}{V_g} \qquad \textbf{(4-8)}$$

where $\Delta c_s = c_{s,1} - c_{s,0}$ and V_t is the total liquid volume in the column (the salt retention volume). The linear velocity of the gradient in the column, which is equal to the velocity of the salt in the column, is given as

$$u_s = u_g = \frac{l_g}{t} = \frac{x_g l_{col}}{t} \qquad \textbf{(4-9)}$$

Equation 4-8 and 4-9 are inserted in the equation for $c_s(x_p)$:

$$c_s(x_p) = c_{s,0} + \frac{\Delta c_s V_t}{V_g}\left(\frac{u_s t}{l_{col}} - x_p\right) \qquad \textbf{(4-10)}$$

The change in the salt concentration with time in the position x_p is

$$\frac{dc_s(x_p)}{dt} = \frac{\Delta c_s V_t}{V_g}\left(\frac{u_s}{l_{col}} - \frac{x_p}{t}\right) \qquad \textbf{(4-11)}$$

The velocity of the protein through the column is given as

$$\frac{dx_p}{dt} = \frac{u_p}{l_{col}} \qquad \textbf{(4-12)}$$

The change in the salt concentration with change in the position of the protein is

$$\frac{dc_s}{dx_p} = \frac{dc_s(x_p)/dt}{dx_p/dt} = \frac{\frac{\Delta c_s V_t}{V_g}\left(\frac{u_s}{l_{col}} - \frac{x_p}{t}\right)}{\frac{u_p}{l_{col}}} = \frac{\Delta c_s V_t}{v_g}\left(\frac{u_s}{u_p} - \frac{x_p l_{col}}{t u_p}\right) = \frac{\Delta c_s V_t}{v_g}\left(\frac{u_s}{u_p} - 1\right) \qquad \textbf{(4-13)}$$

Now $G = \frac{\Delta c_s}{V_g}$ and $u_i = \frac{v}{1 + k'_i}$ are inserted in Equation 4-13:

$$\frac{dc_s}{dx_p} = GV_t\left(\frac{1+k'_p}{1+k'_s} - 1\right) \qquad \textbf{(4-14)}$$

$V_t = V_{R,s} = V_{col}\varepsilon(1+k'_s)$ because K_d = 1 for salt ions. This is Inserted this in Equation 4-14:

$$\frac{dc_s}{dx_p} = GV_{col}\varepsilon\left((1+k'_p) - (1+k'_s)\right) \qquad \textbf{(4-15)}$$

$V_R = V_{col}\varepsilon(1+k'_p)$ and $V_t = V_{col}\varepsilon(1+k'_s)$ are inserted:

$$\frac{dc_s}{dx_p} = G(V_R - V_t) \qquad \textbf{(4-16)}$$

By Insertion of the expression $V_R = V_{NA} + B\left(\frac{\Lambda}{z_s c_s}\right)^{\nu}$ for the retention volume the equation becomes

$$\frac{dc_s}{dx_p} = G\left(V_{NA} + B\left(\frac{\Lambda}{z_s c_s}\right)^{\nu} - V_t\right) \quad \Leftrightarrow$$

$$G\,dx_p = \frac{1}{V_{NA} + B\left(\frac{\Lambda}{z_s c_s}\right)^{\nu} - V_t}\,dc_s \quad \Leftrightarrow$$

$$\int_{x_{p0}}^{1} G\,dx_p = \int_{c_{s,0}}^{c_{s,R}} \frac{1}{V_{NA} + B\left(\frac{\Lambda}{z_s c_s}\right)^{\nu} - V_t}\,dc_s \qquad \textbf{(4-17)}$$

4.2.1 The Lower Boundary

At the beginning of the experiment c_s is equal to $c_{s,0}$ and the protein and the salt move with the constant velocities:

$$u_s = \frac{v}{1+k'_s} \qquad \textbf{(4-18)}$$

$$u_{p,0} = \frac{v}{1+k'_{p,0}} \qquad \textbf{(4-19)}$$

where $k'_{p,0} = k'_p(c_{s,0})$.

Because of the dead volumes in the system the gradient does not reach the column until after the dead time t_{d0}, at that time the protein has traveled the distance l_{d0}.

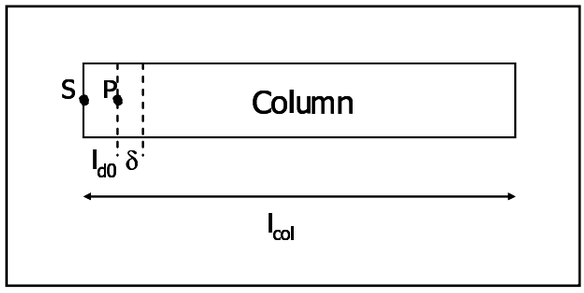

Figure 4-2: The position of the start of the gradient S and the protein P after the time t_{d0}.

The position of the start of the gradient and the protein after the time t_{d0} is

$$x_g = \frac{l_g}{l_{col}} = 0 \qquad \textbf{(4-20)}$$

$$x_p = \frac{l_p}{l_{col}} = \frac{l_{d0}}{l_{col}} \qquad \textbf{(4-21)}$$

After a certain time t the start of the gradient has caught up with the protein.

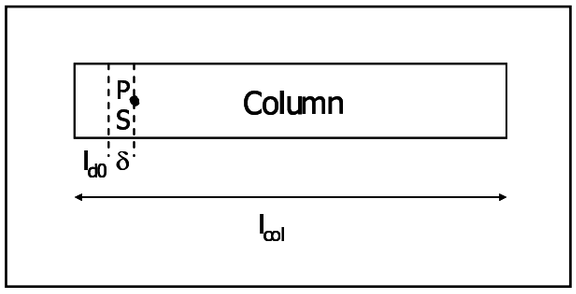

Figure 4-3: The position of the start of the gradient S and the protein P after the time t.

The position of the start of the gradient and the protein after the time t is

$$x_g = \frac{l_g}{l_{col}} = \frac{l_{d0} + \delta}{l_{col}} = x_p \qquad \textbf{(4-22)}$$

At the time $t-t_{d0}$ the protein has traveled the distance δ and the gradient has traveled the distance $l_{d0}+\delta$:

$$\left.\begin{aligned} u_s(t-t_{d0}) = l_{d0}+\delta \quad &\Leftrightarrow \quad (t-t_{d0}) = \frac{l_{d0}+\delta}{u_s} \\ u_{p,0}(t-t_{d0}) = \delta \quad &\Leftrightarrow \quad (t-t_{d0}) = \frac{\delta}{u_{p,0}} \end{aligned}\right\} \quad \Rightarrow \quad \frac{\delta}{u_{p,0}} = \frac{l_{d0}+\delta}{u_s} \quad \Leftrightarrow$$

$$u_{p0} = \frac{\delta u_s}{l_{d0}+\delta} \qquad \textbf{(4-23)}$$

By insertion of Equation 4-18 and 4-19 and rearrangement, the following expression for the distance δ is obtained:

$$\delta = \frac{l_{d0}(1+k'_s)}{(k'_{p,0}+k'_s)} \qquad \textbf{(4-24)}$$

The position of the protein after time t is

$$x_{p,0} = \frac{l_{d0}+\delta}{l_{col}} \qquad \textbf{(4-25)}$$

By insertion of $l_{d0} = u_{p,0}t_{d0} = \frac{vt_{d0}}{1+k'_{p,0}}$ and Equation 4-24 and rearrangement the expression for $x_{p,0}$ becomes

$$x_{p,0} = \frac{vt_{d0}}{l_{col}(k'_{p,0}-k'_s)} \qquad \textbf{(4-26)}$$

The difference between the retention volume of the protein and the retention volume of the salt at the salt concentration $c_{s,0}$ is

$$V_{R,0} - V_t = V_{col}\varepsilon(1+k'_{p,0}) - V_{col}\varepsilon(1+k'_s) = V_{col}\varepsilon(k'_{p,0}-k'_s) \quad \Leftrightarrow$$

$$k'_{p,0}-k'_s = \frac{V_{R,0}-V_t}{V_{col}\varepsilon} \qquad \textbf{(4-27)}$$

where $V_{R,0} = V_R(c_{s,0})$.

By insertion of Equation 4-27 in Equation 4-26, the equation for $x_{p,0}$ is given as

$$x_{p,0} = \frac{vt_{d0}V_{col}\varepsilon}{l_{col}(V_{R,0}-V_t)} \qquad \textbf{(4-28)}$$

$t_{d0} = \frac{V_{d0}}{Q}$ and $vV_{col}\varepsilon = l_{col}Q$ are inserted in Equation 4-28:

$$x_{p,0} = \frac{V_{d0}}{\left(V_{R,0} - V_t\right)} \qquad \textbf{(4-29)}$$

V_{d0} is the dead volume which in this case is the volume from the mixer to the column inlet: $V_{d0} = V_{MC}$.

4.2.2 The Upper Boundary

The protein is eluted at the salt concentration $c_{s,R}$ when the protein has traveled the distance l_{col} and the position of the protein is $x_p = 1$.

$$\int_{x_{p,0}}^{1} G dx_p = \int_{c_{s,0}}^{c_{s,R}} \frac{1}{V_{NA} + B\left(\frac{\Lambda}{z_s c_s}\right)^{\nu} - V_t} dc_s \qquad \textbf{(4-30)}$$

By making the assumption $B\left(\frac{\Lambda}{z_s c_s}\right)^{\nu}$ » $|V_{NA}-V_t|$, the equation is reduced to

$$\int_{x_{p,0}}^{1} G dx_p = \int_{c_{s,0}}^{c_{s,R}} \frac{(z_s c_s)^{\nu}}{B\Lambda^{\nu}} dc_s \qquad \Leftrightarrow$$

$$G\left(1 - x_{p,0}\right) = \frac{z_s\left(c_{s,R}^{\nu+1} - c_{s,0}^{\nu+1}\right)}{(1+\nu)B\Lambda^{\nu}} \qquad \Leftrightarrow$$

$$c_{s,R} = \left(\frac{1}{z_s} G\left(1 - x_{p,0}\right)(1+\nu)B\Lambda^{\nu} + c_{s,0}^{\nu+1}\right)^{\frac{1}{1+\nu}} \qquad \textbf{(4-31)}$$

There are two possibilities:

1) The protein is eluted on the gradient:
   $V_R < V_g + V_m$ and $c_{s,R} < c_{s,1}$
2) The protein is eluted after the gradient:
   $V_R \geq V_g + V_m$ and $c_{s,R} = c_{s,1}$

where V_m is the volume which the start of the gradient has to travel before it reaches the detector $V_m = V_{MD} + V_{R,NO_3^-} - V_{ID,pos.} - V_{connection\ link}$, where V_{R,NO_3^-} is the retention volume measured by nitrate not corrected for the dead volume: $V_{R,NO_3^-} = V_t + V_{dead}$.

4.2.2.1 Possibility 1

When the protein is eluted on the gradient the salt concentration at which the protein is eluted is given as

$$c_{s,R} = G(V_{Rg} - V_m) + c_{s,0} \qquad \textbf{(4-32)}$$

By insertion of Equation 4-31 and rearrangement, the following equation for the retention volume of the protein V_{Rg} is obtained:

$$V_{Rg} = \frac{1}{G}\left(\frac{1}{z_s} G(1 - x_{p,0})(1+\nu) B \Lambda^{\nu} + c_{s,0}^{\nu+1}\right)^{\frac{1}{1+\nu}} - \frac{c_{s,0}}{G} + V_m \qquad \textbf{(4-33)}$$

where $x_{p,0} = \frac{V_{MC}}{(V_{R,0} - V_t)}$

4.2.2.2 Possibility 2

The protein is eluted after the gradient at the salt concentration $c_{s,1}$. When the gradient ends the position of the protein, $x_{p,1}$, is given as

$$\int_{x_{p,0}}^{x_{p,1}} G\,dx_p = \int_{c_{s,0}}^{c_{s,1}} \frac{(z_s c_s)^{\nu}}{B\Lambda^{\nu}}\,dc_s \qquad \Leftrightarrow$$

$$G(x_{p,1} - x_{p,0}) = \frac{z_s\left(c_{s,1}^{\nu+1} - c_{s,0}^{\nu+1}\right)}{(1+\nu)B\Lambda^{\nu}} \qquad \Leftrightarrow$$

$$x_{p,1} = \frac{z_s\left(c_{s,1}^{\nu+1} - c_{s,0}^{\nu+1}\right)}{G(1+\nu)B\Lambda^{\nu}} + x_{p,0} \qquad \textbf{(4-34)}$$

The retention volume is given by the volume that has passed through the column when the gradient ends, $V_m + V_g$, and the volume from the end of the gradient to elution of the protein. From the end of the gradient to elution of the protein the salt concentration is constant at $c_{s,1}$ and the protein travels the distance from $x_{p,1}$ to $x_p = 1$:

$$V_{Rg} = V_m + V_g + (1 - x_{p,1})\left(V_{NA} + B\left(\frac{\Lambda}{z_s c_{s,1}}\right)^{\nu}\right) \qquad \textbf{(4-35)}$$

4.3 Experimental

4.3.1 Chemicals

Bovine serum albumin, BSA (A-6918) purity 98%, α-lactalbumin (L-5385) purity 85%, β-lactoglobulin A and B (L-0130) purity 90%, β-lactoglobulin A (L-7880) purity 90%, β-lactoglobulin B (L-8005) purity 90%, bis-tris propane (B-6755) were all from Sigma (St. Louise, MO, USA). The purity is according to the manufacturer. 5N NaCl (1.06404.1000) and 5N $NaNO_3$ (1.06537.1000) were from Merck (Darmstadt, Germany). HCl (LAB00440) and NaOH (Lab00334) were from Bie & Berntsen, Denmark. Standard solutions for the pH meter calibration, pH 10.012 ± 0.010 at 25 °C, 7.000 ± 0.010 at 25 °C and 4.005 ± 0.010 at 25 °C, were from Radiometer (Copenhagen, Denmark). The temperature sensitivity is very different for the three standard pH solutions, but the pH meter adjusts for this sensitivity if the temperature differs from 25 °C. The pH meter is calibrated every day, before any pH measurements are made.

4.3.2 Equipment

A BioCAD Chromatographic Workstation from Perceptive Biosystems (Cambridge, MA, USA). A pH meter (pHM 92) from Radiometer and 0.22 μm filters from Millipore.

One prepacked column Fractogel EMD TMAE 650(s) (Art No. 20338) from Merck and 3 columns packed in the laboratory were used. The 3 columns packed in the laboratory were packed in HR10/10 and HR16/10 columns from Pharmacia Biotech. The media used were: Source 30Q (lot No. 242339) and Q Sepharose XL (lot No. 245698) from Pharmacia Biotech and Ceramic Q-HyperD F (lot No. 8088) from Biosepra.

4.3.3 Solutions

Two stock solutions were prepared each at a pH of 6, 7, 8 and 9. The first solution, buffer A, was prepared by dissolving 20 mM bis-tris propane in MilliQ water (5.646 g/l water) and titrating the solution with 5N HCl, to the pH in question. The concentration of Cl^--counterions is calculated from the amount of 5N HCl added:

$$c_{Cl^-,A} = \frac{5N \cdot V_{HCl}}{V_{water} + V_{HCl}} \qquad \textbf{(4-36)}$$

The second solution, buffer B, was prepared by dissolving 5.646 g of Bis-Tris Propane and 58.44 g of NaCl per liter milliQ water and titrating the solution with 5N HCl to the same pH as the first solution. By the addition of NaCl to the water the volume is increased and the volume correction factor is calculated as

$$\varphi = \frac{1}{\left(1 - \alpha \cdot c^m_{NaCl}\right) \cdot \left(1 + c^m_{NaCl} \cdot Mw_{NaCl}\right)} \qquad \textbf{(4-37)}$$

where c^m_{NaCl} is the molal NaCl concentration (mol/kg). Mw_{NaCl} is the molecular weight of NaCl in kg/mol. The density of a NaCl-water solution is a linear function of the NaCl-concentration with a slope of α = 0.0351 kg/mol. For the calculation of the molal concentration it is assumed that the density of water is 1 kg/l.

The corrected volume of the solution is now calculated as

$$V_{cor.} = \frac{V_{water}}{\varphi} \qquad \textbf{(4-38)}$$

The molar concentration of NaCl, c_{NaCl}, before adjustment of the pH is:

$$c_{NaCl,\,before} = \frac{n_{NaCl}}{V_{cor.}} \qquad \textbf{(4-39)}$$

The actual concentration of Cl^--ions after pH adjustment with HCl is calculated as

$$c_{Cl^-,B} = \frac{c_{NaCl,before} \cdot V_{cor.} + c_{HCl} \cdot V_{HCl}}{V_{cor.} + V_{HCl}} \qquad \textbf{(4-40)}$$

All the other buffers were prepared by mixing of the two stock solutions, followed by titration with 5N HCl or 5N NaOH, to the same pH as in the 2 stock solutions. The concentration of Cl^--ions in the buffers prepared from the two stock solutions A and B after pH adjustment is calculated as

$$c_{Cl^-,AB} = \frac{V_A \cdot c_{Cl^-,A} + V_B \cdot c_{Cl^-,B} + V_{HCl} \cdot c_{HCl}}{V_A + V_B + V_{HCl}} \qquad \textbf{(4-41)}$$

Calculations of the uncertainty of the two stock solutions and buffers prepared from the stock solutions are given in Appendix A.V. The uncertainty about the Cl^--concentrations is very small. ±0.0002 M for buffer A and ±0.0020 M for buffer B. The uncertainty of the Cl^--concentration in the buffers prepared by mixing of buffer A and B depends on the volume of buffer A and B mixed. At a Cl^--concentration of 0.088 M the uncertainty is ±0.0013 M and at 0.525 M the uncertainty is ±0.0076 M.

Sample solutions were prepared by dissolving 3 g protein/l in an appropriate buffer solution. All solutions were filtered through 0.22 μm filters.

The pH meter was calibrated by standard solutions at a pH of 4.005 and 7.000 or 7.000 and 10.012, respectively.

4.3.4 Method

The elutions were performed on the BioCAD Chromatographic Workstation, and the peaks were detected at 280 nm. All the elutions were performed at room temperature (22 °C ±3). It is assumed that the small temperature variations have no influence on the retention volume, but it has not been investigated.

The column was first equilibrated with 40 ml buffer and the UV detector was zeroed. The column was loaded with 100 µl sample solution containing 3 g protein/l, and the data collection was started. For the gradient elutions the gradient is started simultaneously with the injection. During the elution step the salt concentration is increased linearly from $c_{s,0}$ to $c_{s,1}$ by use of the mixer in the BioCAD system. The gradient is started at the concentration 98% $c_{s,A}$ + 2% $c_{s,1}$ because the mixer does not mix linearly below 2%. A calibration of the mixer (Appendix A.II) shows that the 2% setting corresponds to 10.80%, so that the concentration at the beginning of the gradient is

$$c_{s,0} = 0.892\ c_{s,A} + 0.108\ c_{s,1} \qquad \textbf{(4-42)}$$

The calibration of the mixer also verifies that the mixing is linear in the range 10.80% (programmed 2%) to 100% (programmed 100%).
After the gradient the concentration is kept constant at $c_{s,1}$ for 20 - 40 ml before the column is regenerated with 1 M NaCl.

For the isocratic elutions the salt concentration is kept constant during the elution. After the elution the column is regenerated with 1 M NaCl to assure that all protein is desorbed from the column. From the retention volumes at gradient elution, it is possible to acquire an estimate of the retention volumes at isocratic elution. The amount of buffer necessary for an isocratic elution is determined as the retention volume calculated from the SMA model, with the parameters determined from the linear gradient elutions, with an addition of 10%.
The retention volume of the peaks at gradient elution is determined as the volume corresponding to the peak maximum.
The peaks from the isocratic elutions are fitted with the EMG function, except for the peaks where the peak shape makes it impossible to obtain a proper fit. The retention volume of these peaks is determined as the volume corresponding to the peak maximum, as for the peaks from gradient elution. For the peaks fitted with the EMG function the retention volume is determined as

$$V_R = V_{R,Gauss} + \tau - V_{dead} \qquad \textbf{(4-43)}$$

And the variance is determined as

$$\sigma^2 = \sigma^2_{Gauss} + \tau^2 \qquad \textbf{(4-44)}$$

All the experimental data from the isocratic elutions is given in Appendices C.I to C.XV. Where no σ_{Gauss} and τ values are given the retention volume is determined from the peak maximum. The experimental data from the linear gradient elutions is given in Appendices D.I to D.IV.
An estimate of the uncertainty of the retention volumes is given in Appendix A.I. This appendix also includes a calibration of the flow rate and uncertainty calculations to match.

4.4 Results

In figures 4-4 to 4-33, the experimental and correlated retention volumes are presented and the fitted parameters are given in tables. The parameters are determined from the correlations of the isocratic retention volumes, and these parameters are used to correlate the retention volumes at linear gradient elution.
The experimental data from the isocratic elution is given in Appendix C and the experimental data from the linear gradient elutions is given in Appendix D.
Q-Sepharose XL does not separate β-lactoglobulin A and B and most of the shown data is obtained by a mixture of the two proteins. Many of the data for β-lactoglobulin B is therefore identical to the data for β-lactoglobulin A. Only the isocratic data measured at low salt concentrations and the gradient data measured at the highest gradient volumes are obtained by pure β-lactoglobulin B.
In the figures the following symbols and colors are used: pH 6: ◊, pH 7: □, pH 8: ○ and pH 9:△.
The experimental data is represented by symbols and the models are represented by lines.

4.4.1 Source 30Q

The experimental data from the isocratic elutions is given in Appendices C.I to C.IV, and the experimental data from the gradient elutions is given in Appendix D.I.

The Gibbs energy change for the salt is independent of the protein and the pH, but depends on the media (and of course on the salt). For NaCl and Source 30Q the determined value is

$$\Delta G^0_{ads,Cl^-} / RT = 0.320$$

		Source 30Q			
		BSA	α-lactalbumin	β-lactoglobulin A	β-lactoglobulin B
	$\Delta G^0_{ads,p} / RT$	4.663	5.049	3.444	3.718
pH 6	ν	4.20	3.64	5.04	4.29
pH 7	ν	6.16	4.74	6.21	5.50
pH 8	ν	7.89	5.33	7.21	6.56
pH 9	ν	9.77	6.31	7.96	7.31

Table 4-1: The parameters fitted from the isocratic retention volumes for Source 30Q.

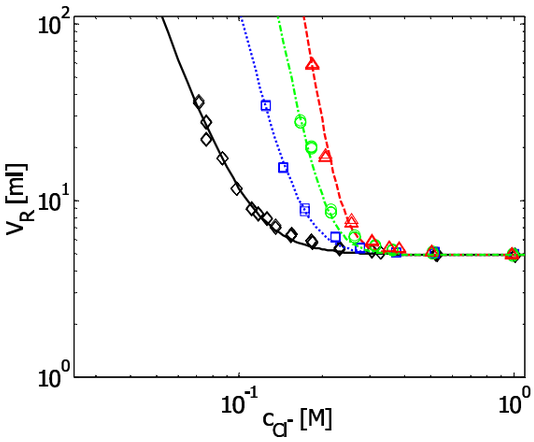

Figure 4-4: Isocratic elution of BSA on Source 30Q.

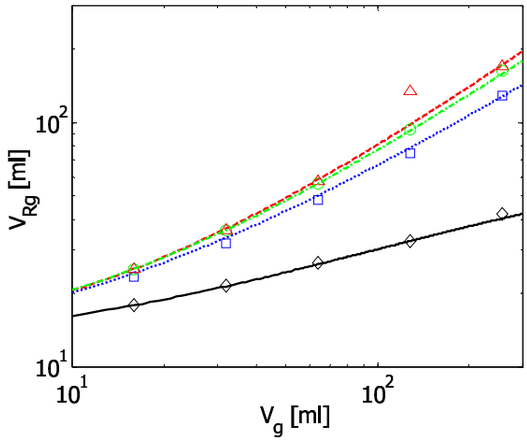

Figure 4-5: Linear gradient elution of BSA on Source 30Q.

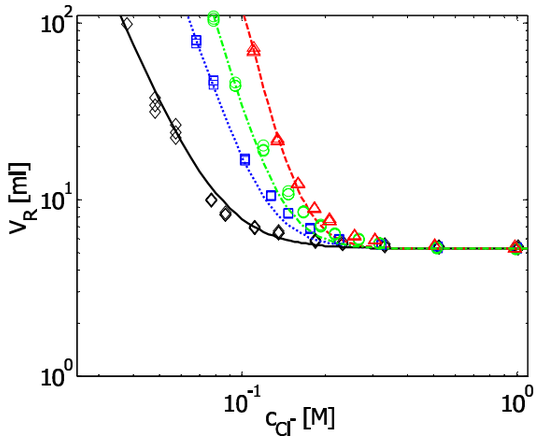

Figure 4-6: Isocratic elution of α-lactalbumin on Source 30Q.

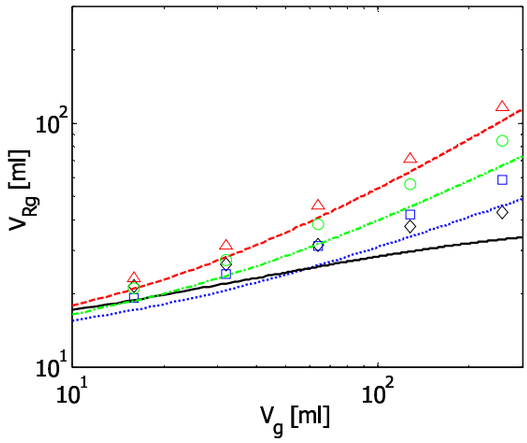

Figure 4-7: Linear gradient elution of α-lactalbumin on Source 30Q.

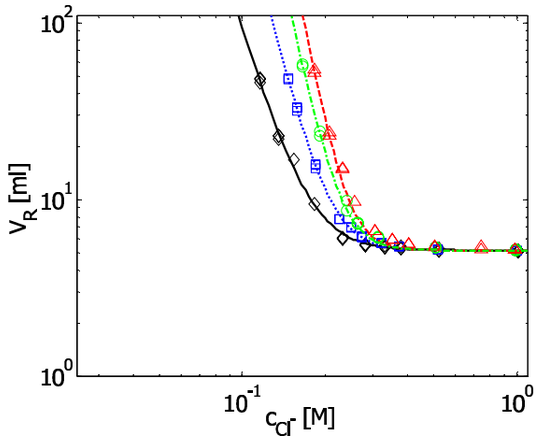

Figure 4-8: Isocratic elution of β-lactoglobulin A on Source 30Q.

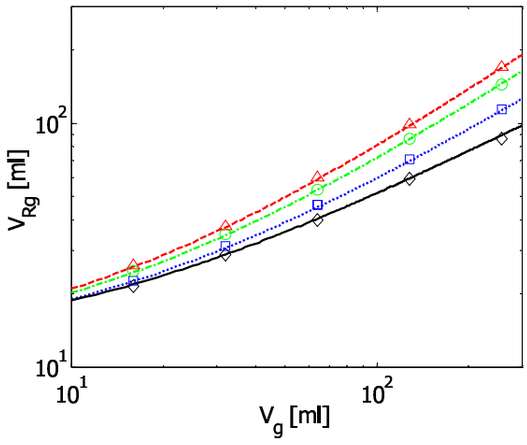

Figure 4-9: Linear gradient elution of β-lactoglobulin A on Source 30Q.

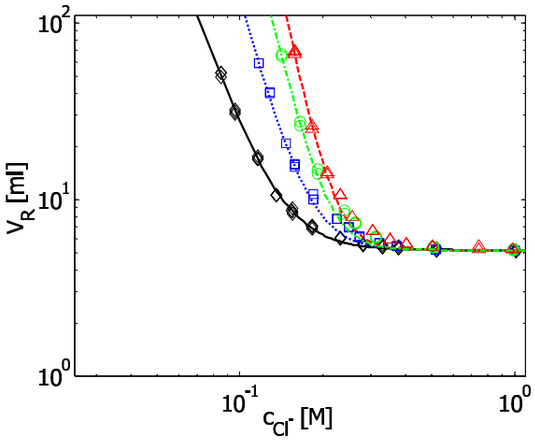

Figure 4-10: Isocratic elution of β-lactoglobulin B on Source 30Q.

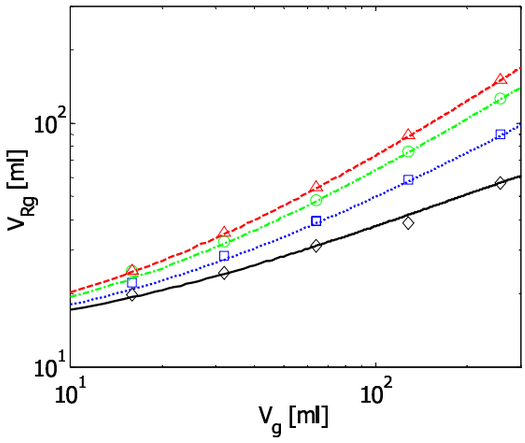

Figure 4-11: Linear gradient elution of β-lactoglobulin B on Source 30Q.

The model correlates very well the experimental data obtained for Source 30Q, except for the gradient elutions of α-lactalbumin. Some small differences are observed between the model and the experimental data for the isocratic elution, where the proteins start to bind to the column and the retention volume starts to increase. This deviation is most pronounced at a pH of 8 and 9 where the model is a little steeper than the experimental data.
The retention volumes obtained by gradient elution are very well correlated by the model with the parameters determined from the isocratic retention volumes. Except for α-lactalbumin where the model predictions at all pH values are lower than the experimental data.

A triple determination has been used for most of the experimental data obtained at isocratic elution and the repeatability is very good. The small deviations observed are mostly due to the different flow rates. The retention volumes increase a little with increasing flow rate, especially at the low Cl^--concentrations where the adsorption of the proteins is strong.

4.4.2 Q-Sepharose XL

The experimental data from the isocratic elutions is given in Appendices C.V to C.VII, and the experimental data from the gradient elutions is given in Appendix D.II.

Q-Sepharose XL cannot separate β-lactoglobulin A and B, so that the experiments were only made with β-lactoglobulin B.

The Gibbs energy change for NaCl and Q-Sepharose XL is

$$\Delta G^0_{ads,Cl^-} / RT = 0.363$$

		Q-Sepharose XL		
		BSA	α-lactalbumin	β-lactoglobulin B
	$\Delta G^0_{ads,p}$ /RT	3.635	2.504	1.696
pH 6	ν	5.01	2.76	3.69
pH 7	ν	6.62	3.69	4.99
pH 8	ν	8.00	4.13	5.27
pH 9	ν	8.83	4.74	5.55

Table 4-2: The parameters fitted from the isocratic retention volumes for Q-Sepharose XL.

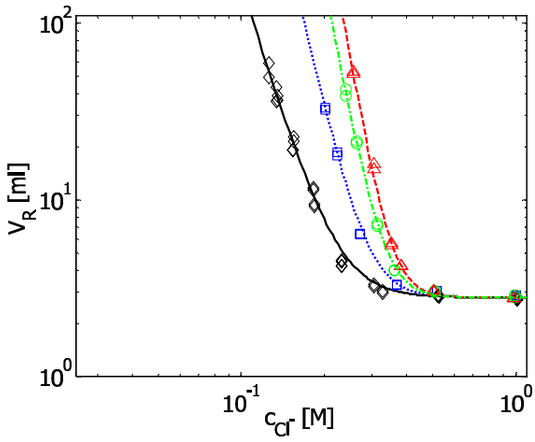

Figure 4-12: Isocratic elution of BSA on Q-Sepharose XL.

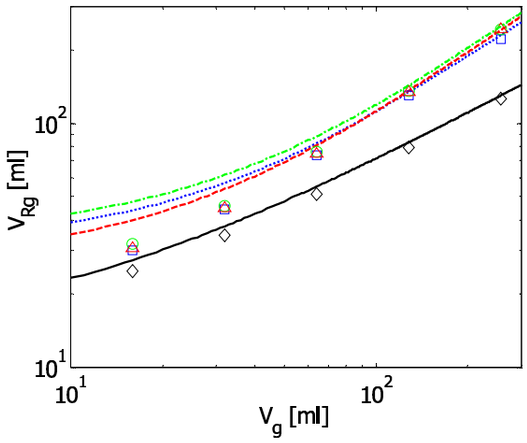

Figure 4-13: Linear gradient elution of BSA on Q-Sepharose XL.

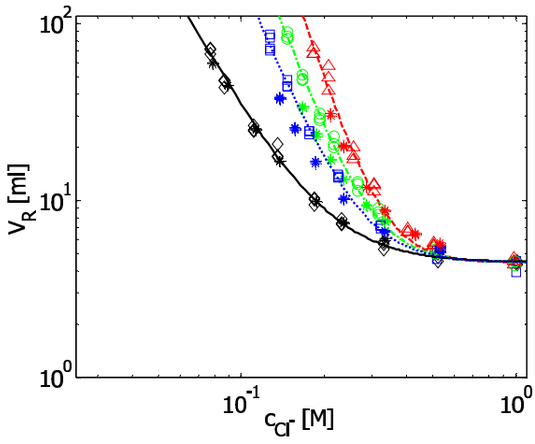

Figure 4-14: Isocratic elution of α-lactalbumin on Q-Sepharose XL.

(∗ Data by Søren Frederiksen, not incl. in the fit).

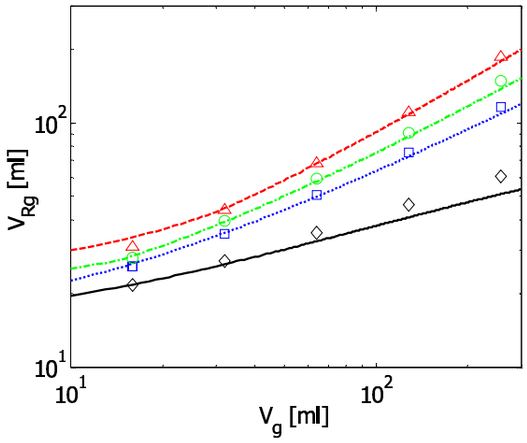

Figure 4-15: Linear gradient elution of α-lactalbumin on Q-Sepharose XL.

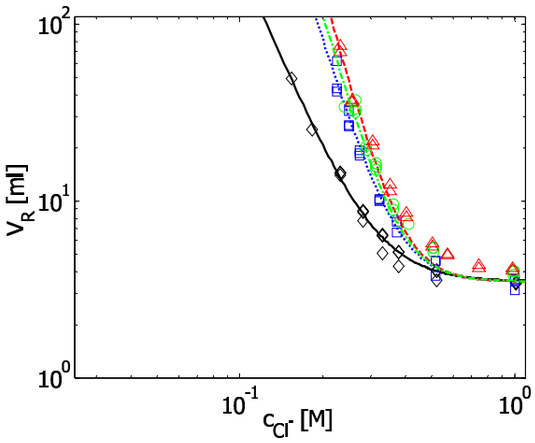

Figure 4-16: Isocratic elution of β-lactoglobulin B on Q-Sepharose XL.

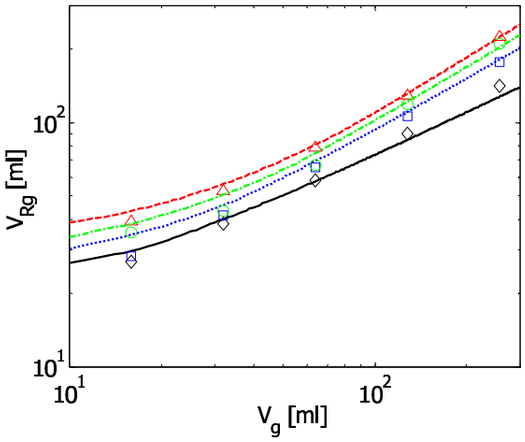

Figure 4-17: Linear gradient elution of β-lactoglobulin B on Q-Sepharose XL.

The model correlates reasonably well the experimental data obtained for Q-Sepharose XL, but not as well as for Source 30Q. For BSA and β-lactoglobulin B the model fails to correlate the experimental data at the smallest gradient volumes. The correlation of the isocratic retention volumes is good for BSA and α-lactalbumin. For β-lactoglobulin B some deviation between the model and the experimental data is observed at a pH of 8 and 9. This is probably due to the variations in the retention volumes at the Cl^-concentration of 1.0 M. It seems that some of the β-lactoglobulin B at a pH of 9 (and 8) adsorbs to the column even at this high concentration, and V_{NA} should probably have been determined at a higher Cl^--concentration.

The repeatability of the determination of the isocratic retention volumes is not as good as for the Source 30Q column. The difference between the flow rates used is also larger for Q-Sepharose XL than for Source 30Q. Thus, the difference between the retention volumes obtained at the smallest and the largest flow rate is more pronounced for Q-Sepharose XL than for Source 30Q. In Figure 4-14 experimental data obtained by Søren Frederiksen (given in appendix C.VI) is plotted. The retention volumes determined by S. Frederiksen are smaller than the retention volumes I have determined. This might be due to experimental uncertainty and a poor reproducibility, but might as well be due to the lower flow rates used by S. Frederiksen.

4.4.3 Ceramic Q-HyperD F

The experimental data from the isocratic elutions is given in Appendices C.VIII to C.XI, and the experimental data from the gradient elutions is given in Appendix D.III.

The Gibbs energy change for NaCl and Ceramic Q-HyperD F is

$$\Delta G^0_{ads,Cl^-} / RT = -0.249$$

		Ceramic Q-HyperD F			
		BSA	α-lactalbumin	β-lactoglobulin A	β-lactoglobulin B
	$\Delta G^0_{ads,p}/RT$	8.858	3.026	5.039	3.550
pH 6	ν	6.13	2.98	6.16	4.70
pH 7	ν	7.81	4.11	7.59	5.86
pH 8	ν	10.34	4.75	8.49	6.55
pH 9	ν	12.06	5.43	9.43	7.21

Table 4-3: The parameters fitted from the isocratic retention volumes for Ceramic Q-HyperD F.

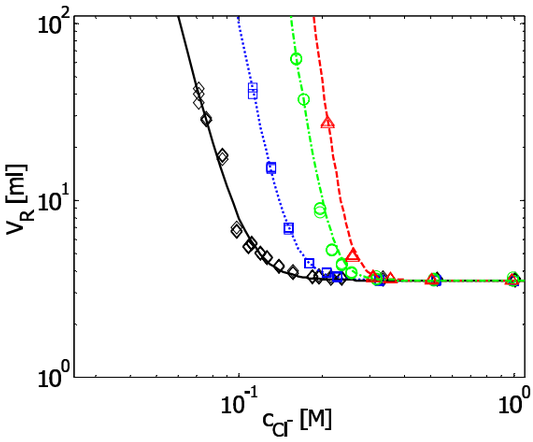

Figure 4-18: Isocratic elution of BSA on Ceramic Q-HyperD F.

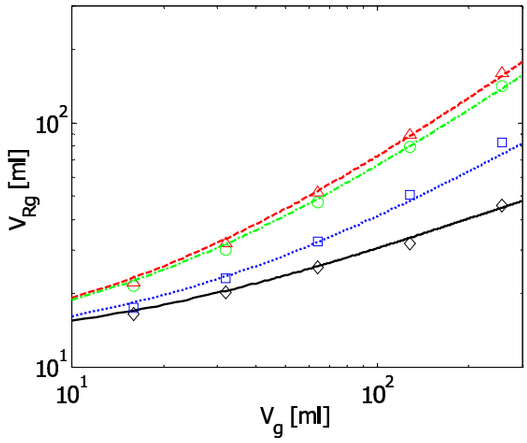

Figure 4-19: Linear gradient elution of BSA on Ceramic Q-HyperD F.

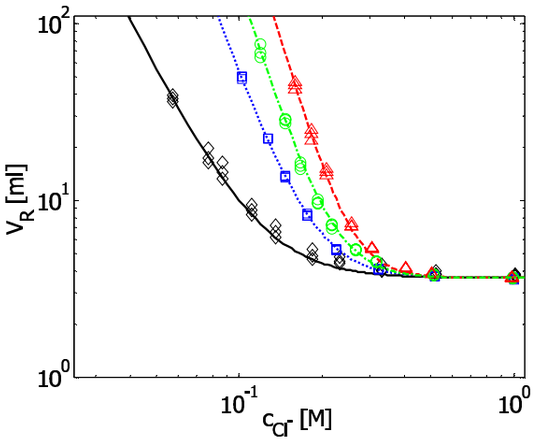

Figure 4-20: Isocratic elution of α-lactalbumin on Ceramic Q-HyperD F.

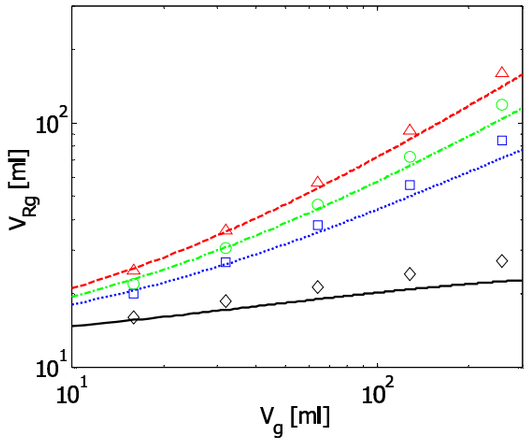

Figure 4-21: Linear gradient elution of α-lactalbumin on Ceramic Q-HyperD F.

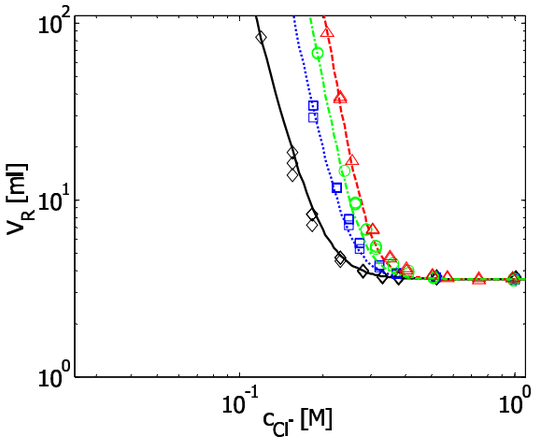

Figure 4-22: Isocratic elution of β-lactoglobulin A on Ceramic Q-HyperD F.

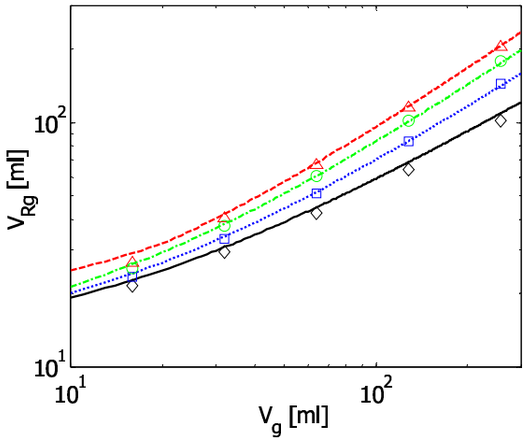

Figure 4-23: Linear gradient elution of β-lactoglobulin A on Ceramic Q-HyperD F.

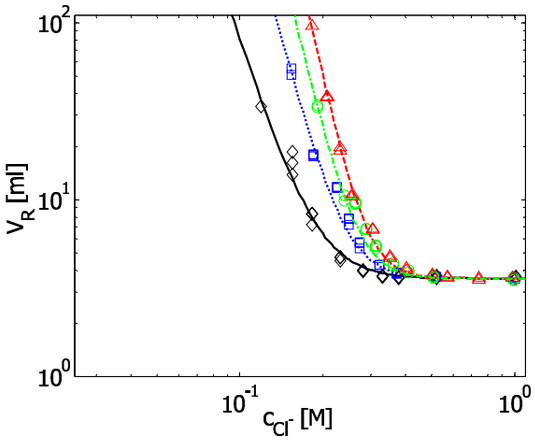

Figure 4-24: Isocratic elution of β-lactoglobulin B on Ceramic Q-HyperD F.

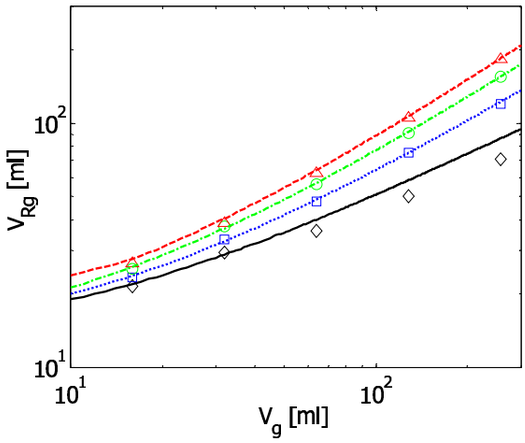

Figure 4-25: Linear gradient elution of β-lactoglobulin B on Ceramic Q-HyperD F.

The model correlates very well the retention volumes obtained by isocratic elution for Ceramic Q-HyperD F. For β-lactoglobulin A and B some small differences are observed between the model and the experimental data at a pH of 8 and 9 at the Cl^--concentrations where the proteins start to bind to the column.

The difference between the isocratic retention volumes obtained at the different flow rates is larger for Ceramic Q-HyperD F than for Source 30Q, even though the same linear flow rates are used.

As for Source 30Q a good correlation of the retention volumes from gradient elution is obtained by the model parameters determined from the correlation of the isocratic retention volumes, except for α-lactalbumin and β-lactoglobulin B at a pH of 6.

4.4.4 Fractogel EMD TMAE 650(s)

The experimental data from the isocratic elutions is given in Appendices C.XII to C.XV, and the experimental data from the gradient elutions is given in Appendix D.IV.

The Gibbs energy change for NaCl and Fractogel EMD TMAE 650(s) is

$\Delta G^0_{ads,Cl^-}/RT = 1.439$

		Fractogel EMD TMAE 650(s)			
		BSA	α-lactalbumin	β-lactoglobulin A	β-lactoglobulin B
	$\Delta G^0_{ads,p}/RT$	3.862	2.127	1.541	1.363
pH 6	ν	4.66	2.26	4.60	3.76
pH 7	ν	6.43	3.30	6.16	5.09
pH 8	ν	8.79	3.60	6.65	5.67
pH 9	ν	11.14	4.49	7.20	6.14

Table 4-4: The parameters fitted from the isocratic retention volumes for Fractogel EMD TMAE 650(s).

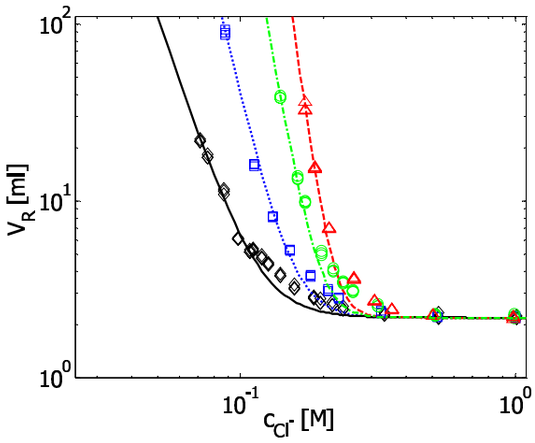

Figure 4-26: Isocratic elution of BSA on Fractogel EMD TMAE 650(s).

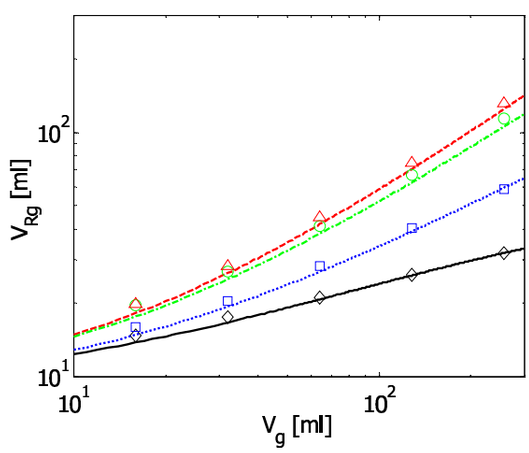

Figure 4-27: Linear gradient elution of BSA on Fractogel EMD TMAE 650(s).

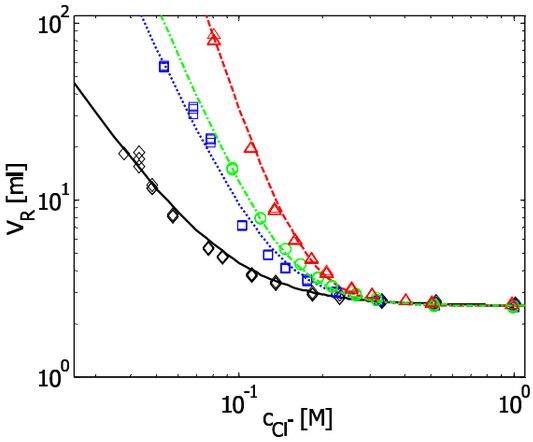

Figure 4-28: Isocratic elution of α-lactalbumin on Fractogel EMD TMAE 650(s).

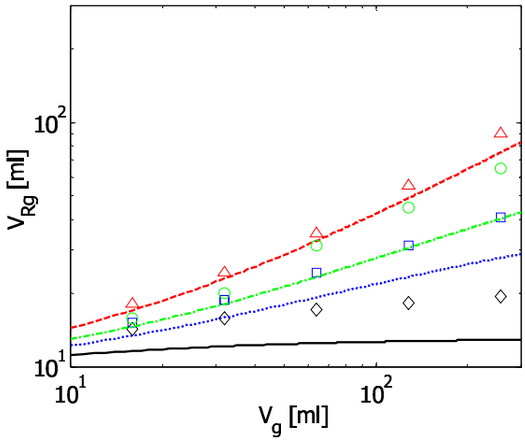

Figure 4-29: Linear gradient elution of α-lactalbumin on Fractogel EMD TMAE 650(s).

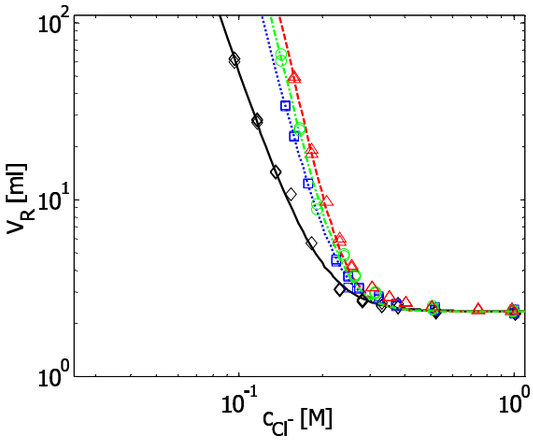

Figure 4-30: Isocratic elution of β-lactoglobulin A on Fractogel EMD TMAE 650(s).

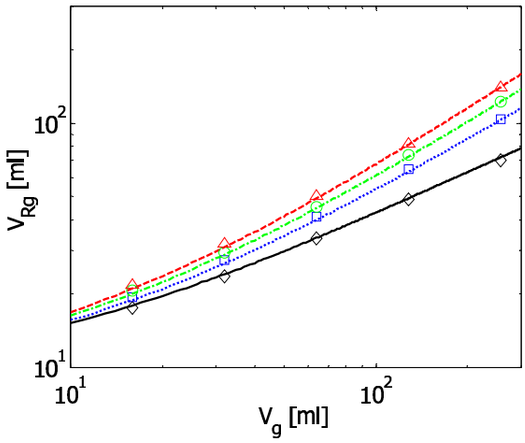

Figure 4-31: Linear gradient elution of β-lactoglobulin A on Fractogel EMD TMAE 650(s).

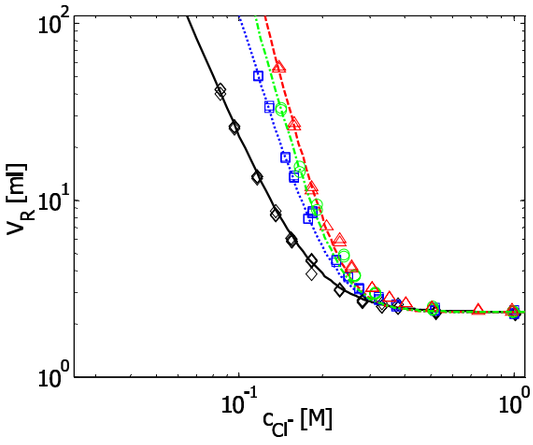

Figure 4-32: Isocratic elution of β-lactoglobulin B on Fractogel EMD TMAE 650(s).

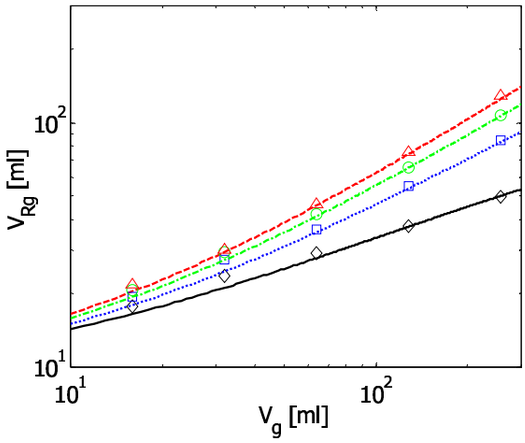

Figure 4-33: Linear gradient elution of β-lactoglobulin B on Fractogel EMD TMAE 650(s).

The correlation of the isocratic retention volumes is also very good for the Fractogel EMD TMAE 650(s) column, except for BSA (figure 4-26) where some differences between the model and the experimental data is observed at all four pH values where BSA starts to bind to the column.

The correlation of the retention volumes obtained by gradient elution is very good except for α-lactalbumin, where the model strongly underestimates the retention volumes.

4.5 Discussion

In general, the figures show that the models can correlate the measured isocratic retention data with sufficient accuracy, and most of the predicted gradient elution data is also in good agreement with the experimental data.

The assumption made in the derivation of the equation for the gradient retention volumes

For all four columns the prediction of the gradient data for α-lactalbumin is not as good as for the other proteins. To investigate if this is caused by the assumption $B\left(\frac{\Lambda}{z_s c_s}\right)^{\nu} \gg |V_{NA}-V_t|$, made in the derivation of the equation for the gradient retention volumes, some calculations were made. To determine which calculations to make the left side in the assumption was expressed as $B\left(\frac{\Lambda}{z_s c_s}\right)^{\nu} = V_{col}(1-\varepsilon)\varepsilon_p K_d A$, where all the parameters except the equilibrium ratio A are constant. To obtain the worst case scenario A has to be as small as possible. The smallest A is achieved at the highest Cl^--concentration, the concentration at which the protein is eluted. The highest Cl^--concentration is obtained for the steepest gradient, the lowest gradient volume. To minimize the amount of calculations the values of $B\left(\frac{\Lambda}{z_s c_s}\right)^{\nu}$ are only calculated for the gradient volumes of 8.0 ml and 256.0 ml. The calculations at 8.0 ml represent the worst case scenario and the calculations at 256.0 ml are made for comparison.

		Source 30Q			
		BSA	α-lactalbumin	β-lactoglobulin A	β-lactoglobulin B
$\|V_{NA}-V_t\|$		1.07	0.72	0.83	0.83
$B\left(\frac{\Lambda}{z_s c_s}\right)^{\nu}$	pH 6	2.39	2.21	2.74	2.05
	pH 7	3.40	0.67	1.93	1.16
	pH 8	1.91	0.56	1.74	0.98
	pH 9	1.72	0.60	1.55	1.58

Table 4-5: The parameters calculated for Source 30Q at V_g = 8.0 ml.

		Q-Sepharose XL		
		BSA	α-lactalbumin	β-lactoglobulin B
$\lvert V_{NA}-V_t \rvert$		4.27	2.61	3.55
$B\left(\frac{\Lambda}{z_s c_s}\right)^{\nu}$	pH 6	7.19	3.75	7.26
	pH 7	15.51	4.24	8.21
	pH 8	18.54	4.24	10.33
	pH 9	10.84	6.22	14.59

Table 4-6: The parameters calculated for Q-Sepharose XL at V_g = 8.0 ml.

		Ceramic Q-HyperD F			
		BSA	α-lactalbumin	β-lactoglobulin A	β-lactoglobulin B
$\lvert V_{NA}-V_t \rvert$		2.57	2.45	2.51	2.51
$B\left(\frac{\Lambda}{z_s c_s}\right)^{\nu}$	pH 6	2.33	2.35	3.82	3.26
	pH 7	2.39	3.12	2.81	2.73
	pH 8	3.19	3.53	2.96	2.84
	pH 9	3.15	3.15	3.71	3.21

Table 4-7: The parameters calculated for Ceramic Q-HyperD F at V_g = 8.0 ml.

		Fractogel EMD TMAE 650 (s)			
		BSA	α-lactalbumin	β-lactoglobulin A	β-lactoglobulin B
$\lvert V_{NA}-V_t \rvert$		0.75	0.40	0.60	0.60
$B\left(\frac{\Lambda}{z_s c_s}\right)^{\nu}$	pH 6	1.37	3.09	2.83	1.99
	pH 7	0.68	1.22	1.60	1.27
	pH 8	0.37	1.41	1.41	1.23
	pH 9	0.24	1.37	1.34	1.16

Table 4-8: The parameters calculated for Fractogel EMD TMAE 650 (s) at V_g = 8.0 ml.

		Source 30Q			
		BSA	α-lactalbumin	β-lactoglobulin A	β-lactoglobulin B
$\lvert V_{NA}-V_t \rvert$		1.07	0.72	0.83	0.83
$B\left(\frac{\Lambda}{z_s c_s}\right)^{\nu}$	pH 6	17.49	16.33	26.87	21.46
	pH 7	24.59	8.50	20.70	19.92
	pH 8	17.61	7.50	22.36	20.56
	pH 9	19.71	9.43	20.00	20.35

Table 4-9: The parameters calculated for Source 30Q at V_g = 256.0 ml.

		Q-Sepharose XL		
		BSA	α-lactalbumin	β-lactoglobulin B
$\lvert V_{NA}-V_t \rvert$		4.27	2.61	3.55
$B\left(\frac{\Lambda}{z_s c_s}\right)^{\nu}$	pH 6	36.46	19.28	30.67
	pH 7	44.22	26.98	41.19
	pH 8	38.44	26.97	32.11
	pH 9	25.39	29.98	37.71

Table 4-10: The parameters calculated for Q-Sepharose XL at V_g = 256.0 ml.

		Ceramic Q-HyperD F			
		BSA	α-lactalbumin	β-lactoglobulin A	β-lactoglobulin B
$\lvert V_{NA}-V_t \rvert$		2.57	2.45	2.51	2.51
$B\left(\frac{\Lambda}{z_s c_s}\right)^{\nu}$	pH 6	14.86	10.13	31.27	41.99
	pH 7	8.32	14.54	19.12	26.10
	pH 8	12.87	15.33	19.03	24.36
	pH 9	9.98	14.65	22.60	26.02

Table 4-11: The parameters calculated for Ceramic Q-HyperD F at V_g = 256.0 ml.

		Fractogel EMD TMAE 650 (s)			
		BSA	α-lactalbumin	β-lactoglobulin A	β-lactoglobulin B
$\lvert V_{NA}-V_t \rvert$		0.75	0.40	0.60	0.60
$B\left(\frac{\Lambda}{z_s c_s}\right)^{\nu}$	pH 6	16.10	8.03	25.32	22.54
	pH 7	15.31	8.84	20.32	20.44
	pH 8	9.76	6.77	20.41	20.82
	pH 9	7.83	10.87	20.80	18.52

Table 4-12: The parameters calculated for Fractogel EMD TMAE 650 (s) at V_g = 256.0 ml.

First of all it is observed that the values of $B\left(\frac{\Lambda}{z_s c_s}\right)^{\nu}$ are not much higher than the numerical values of V_{NA}-V_t for any of the columns or proteins. By taking into account that most of the gradient retention volumes are predicted very well, the difference seems to be big enough in most cases. If we look at the values for Source 30Q it is observed that the smallest difference between the values of $B\left(\frac{\Lambda}{z_s c_s}\right)^{\nu}$ and $\lvert V_{NA}-V_t \rvert$ is obtained by α-lactalbumin. At a pH of 7, 8 and 9 and a gradient volume of 8.0 ml the value of $\lvert V_{NA}-V_t \rvert$ is even higher than the value of $B\left(\frac{\Lambda}{z_s c_s}\right)^{\nu}$. For Source 30Q the prediction of the gradient retention volumes of α-lactalbumin is poor and the prediction for the other three proteins is very good. The poor correlation of the α-lactalbumin data

could therefore be due to the assumption, but if we look at the values for Q-HyperD F it seems unlikely. For Q-HyperD F the difference between $B\left(\frac{\Lambda}{z_s c_s}\right)^{\nu}$ and $|V_{NA}-V_t|$ at a gradient volume of 8.0 ml is smaller for BSA than for α-lactalbumin, but the BSA data is much better correlated than the α-lactalbumin data. It could be argued that the BSA and the α-lactalbumin data is equally well correlated at a gradient volume of 8.0 ml, but if we look at the data for a gradient volume of 256.0 ml the argument does not hold. At the gradient volume of 256.0 ml the BSA data is better correlated than the α-lactalbumin data, and the difference between $B\left(\frac{\Lambda}{z_s c_s}\right)^{\nu}$ and $|V_{NA}-V_t|$ is still smaller for BSA than for α-lactalbumin, except at a pH of 6.

For Q-Sepharose XL the difference between $B\left(\frac{\Lambda}{z_s c_s}\right)^{\nu}$ and $|V_{NA}-V_t|$ is larger for BSA than for α-lactalbumin at a gradient volume of 8.0 ml and 256.0 ml, but the α-lactalbumin data is correlated better than the BSA data, especially at the three lowest gradient volumes.

For Fractogel EMD TMAE 650(s) at a gradient volume of 8.0 ml the difference between $B\left(\frac{\Lambda}{z_s c_s}\right)^{\nu}$ and $|V_{NA}-V_t|$ is, in most cases, larger for α-lactalbumin than for the three other proteins, but the correlation of the data is much better for the three other proteins than for α-lactalbumin.

The assumption $B\left(\frac{\Lambda}{z_s c_s}\right)^{\nu} \gg |V_{NA}-V_t|$ made in the derivation of the equation for the retention volumes at gradient elution cannot explain the poor correlation of the α-lactalbumin data. A small deviation between the correlation and the experimental data is observed for most of the columns at the lowest gradient volume of 8.0 ml. This deviation is independent of the protein, and the largest deviation is observed for BSA on Q-Sepharose XL, where the difference between $B\left(\frac{\Lambda}{z_s c_s}\right)^{\nu}$ and $|V_{NA}-V_t|$ is the largest of all. Thus, it is unlikely that the deviation is caused by the assumption.

Even though $B\left(\frac{\Lambda}{z_s c_s}\right)^{\nu}$ is not much larger than $|V_{NA}-V_t|$ the assumption is reasonable, because the cases where the correlation of the experimental data is poor cannot be explained by the assumption. The worst correlation of experimental data at a gradient volume of 8.0 ml is obtained by BSA for Q-Sepharose XL, where the difference between $B\left(\frac{\Lambda}{z_s c_s}\right)^{\nu}$ and $|V_{NA}-V_t|$ is largest. Furthermore the model is not used for any parameter estimation. The retention volumes at gradient elution are correlated with the parameters estimated from the correlation of the isocratic retention volumes.

Calibration of the mixer

It was recognized that the α-lactalbumin data was measured later than the other data. It was measured about two months after the last of the other data. When this was discovered the mixer on the BioCAD was calibrated again, and it was observed that the mixer had changed (see Appendix A.II). The calibration was done after the measurements with α-lactoglobulin, so that it was not possible to decide whether the mixer had changed before or after the measurements with α-lactoglobulin. The change of the mixer resulted in a lower concentration at the beginning of the gradient and a little less steep gradient. The correlations for the new calibration of the mixer are shown in Figures 4-34 to 4-37, and the data is given in Appendix D.VI. The correlations for the old calibration of the mixer are shown in Figures 4-7, 4-15, 4-21 and 4-29.

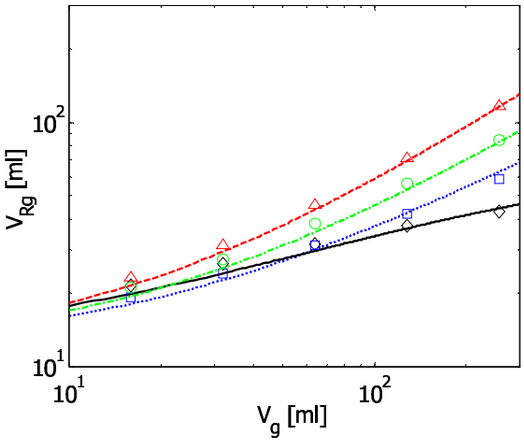

Figure 4-34: Linear gradient elution of α-lactalbumin on Source 30Q with the new calibration of the mixer.

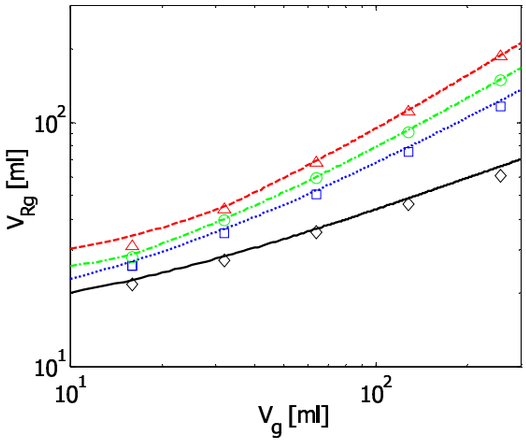

Figure 4-35: Linear gradient elution of α-lactalbumin on Q-Sepharose XL with the new calibration of the mixer.

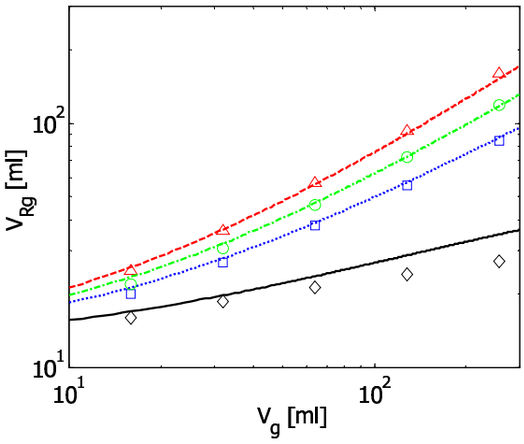

Figure 4-36: Linear gradient elution of α-lactalbumin on Ceramic Q-HyperD F with the new calibration of the mixer.

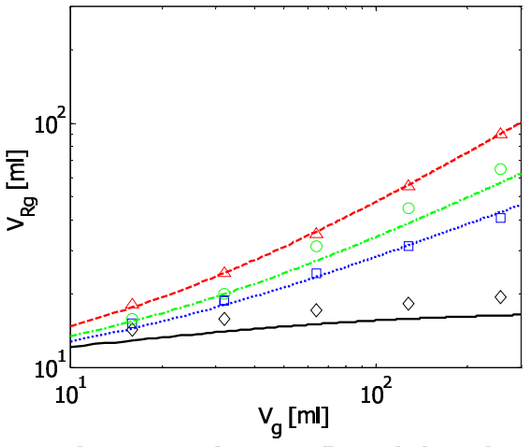

Figure 4-37: Linear gradient elution of α-lactalbumin on Fractogel EMD TMAE 650(s) with the new calibration of the mixer.

From Figures 4-34 to 4-37 it is seen that the correlation of the gradient data for α-lactalbumin is considerably improved when the new calibration of the mixer is used. The correlation of the data at a pH of 6 for Ceramic Q-HyperD F and Fractogel EMD TMAE 650(s) still shows some divergence from the experimental data, but the model correlates very well the data at the three other pH values. In general the data at a pH of 6 is the least well correlated. This could be due to the fact that the pH of 6 is close to the isoelectric point of the proteins.

Standard Gibbs energy changes

The estimated standard Gibbs energy changes for the salt are positive for all media except the Ceramic Q-HyperD F. This may be due to the fact that the Ceramic Q-HyperD F is a more hydrophilic media, because the hydrogel filled pores give rise to a high ligand charge density. The Fractogel EMD TMAE 650 (S) has the lowest ligand charge density and thus a more hydrophobic environment and consequently the largest standard Gibbs energy change for the salt. The estimated standard Gibbs energy changes for the proteins reflect a change in the protein conformation upon binding. A strong binding may bring about a larger conformational change than a weak binding may cause. But it may also reflect typical matrix characteristics as for example hydrophobic contributions. The difference in the values for the standard Gibbs energy changes of β-lactoglobulins on Q-HyperD F is unexpected when compared to the variations observed for the other media and is probably due to experimental uncertainty. The standard Gibbs energy change of α-lactalbumin on this media is lower than expected. For the other media the standard Gibbs energy changes of α-lactalbumin are generally 1.5 times higher than those of β-lactoglobulins.

Comparison with the literature

Gadam et al. made experiments with β-lactoglobulin A and B on the anion exchanger SAX, which is a strong anion exchanger with a quaternary amino group as the functional group [Gadam et al., 1993]. At a pH of 7.5 they found binding charges of 7.5 and 6.3 for β-lactoglobulin A and B, respectively. As determined in this work the binding charge of β-lactoglobulin A is higher than the binding charge of β-lactoglobulin B, and the values are close to the values determined by use of Source 30Q and Ceramic Q-HyperD F.

Bosma et al. made experiments with BSA on the anion exchanger Q-Sepharose FF, which is very similar to the Q-Sepharose XL anion exchanger. Bosma et al. determined the binding charge of BSA at a pH of 5.2 to 5.3 in an acetate buffer and found a value of 4.3 (25 °C), and in a Tris buffer at a pH of 7.5 and 7.8 to 7.9 they found the values 5.0 (5 °C) and 4.6 (37 °C) [Bosma et al., 1998]. Furthermore they found that the binding charge of BSA is independent of pH, which is quite opposite to what has been found in this work, where the binding charge of BSA indeed depends on pH. A binding charge of 4.3 at a pH of 5.2-5.3 seems reasonable compared to the values determined for BSA on Q-Sepharose XL in this work, but binding charges of 4.3 to 5.0 at a pH of

7.5 to 7.9 seem very low compared to the binding charges of 6.62 at a pH of 7 and 8.00 at a pH of 8 determined in this work.
Li et al. determined the binding charge of BSA on the weak anion exchanger Matrex PAE-1000 and found a value of 4.8 at a pH of 7 [Li et al., 1994]. This value is very low compared to the values (6.16 – 6.62) determined in this work by BSA at a pH of 7. The big difference could be due to the difference in the anion exchangers used. Li et al. used a weak anion exchanger and the four anion exchangers used in this work are strong anion exchangers.

Freitag et al. made experiments with α-lactalbumin and β-lactoglobulin on two strong anion exchangers and determined the binding charges at a pH of 8 [Freitag et al., 2000]. For α-lactalbumin they found binding charges of 5.81 and 5.62, and for β-lactoglobulin they found the values 7.68 and 7.38. As in this work the binding charge of α-lactalbumin is lower than that of β-lactoglobulin. Freitag et al. did not mention whether it is β-lactoglobulin A or B, but the binding charges Freitag et al. determined are very similar to the values determined in this work for α-lactalbumin and β-lactoglobulin A on Source 30Q.
Kundu et al. also determined the binding charge of α-lactalbumin and β-lactoglobulin on a strong anion exchanger with a quaternary amino group as the functional group [Kundu et al., 1997]. They determined the binding charges at a pH of 8 to be 4.5 for α-lactalbumin, 7.5 for β-lactoglobulin A and 6.3 for β-lactoglobulin B. The values are comparable to the values determined in this work. The binding charges of β-lactoglobulin A and B are very close to the values determined for Source 30Q, and the binding charges of α-lactalbumin are very close to the values determined for Ceramic Q-HyperD F.

Influence of the bed porosity

Because the bed porosity was assessed and not measured the influence of the porosity on the correlations was investigated. Fits were made where the bed porosities were changed by ±0.05 units. The change of the bed porosities had no visible effects on the correlations, so the figures are not shown. The values of the parameters $\Delta G^0_{ads,Cl^-}/RT$, $\Delta G^0_{ads,p}/RT$ and ν, fitted with the changed bed porosities, are given in Appendix C.XVI. The effect on the fitted parameters is very small. The largest effects are seen in the K_d values and the standard Gibbs energy for NaCl.
In general it can be concluded that the estimated standard Gibbs energy changes and the charge ratios ν are not sensitive to the choice of particle porosity, but the porosity must be chosen so that reasonable values for the exclusion factor for the proteins are obtained.

5 SEPARATION OF THE FOUR PROTEINS IN THE LINEAR RANGE

In the previous section it was observed that the SMA model was capable of correlating the retention volumes at isocratic and linear gradient elution. In this section the model will be used for some theoretical considerations regarding separation of the four proteins. An industrial separation will never take place in the linear range, but if the four proteins cannot be separated in the linear range, it will not be possible to separate them by preparative chromatography.

The possibility of separation of the four proteins by isocratic or linear gradient elution will be investigated by a comparison of the retention volumes at a constant pH. The considerations do not include the variance of the peaks, so that a separation that seems possible from a comparison of the retention volumes may turn out to be impossible, due to the variance of the peaks. The resolution R is for a Gaussian distribution given as

$$R = \frac{V_{R2} - V_{R1}}{2(\sigma_2 + \sigma_1)} \qquad \textbf{(5-1)}$$

where V_{R1} and σ_1 are the retention volume and the square root of the variance in ml for peak 1, and V_{R2} and σ_2 are the retention volume and the square root of the variance in ml for peak 2.

From Equation 5-1 it is obvious that even though the difference between the retention volumes of two peaks is large, the resolution may be poor if the peaks are very broad.

To be able to compare the retention volumes obtained at linear gradient elution the gradient has to start at the same Cl^--concentration, because the retention volume depends on the concentration at the beginning of the gradient $c_{s,0}$. This is illustrated in Figure 5-1.

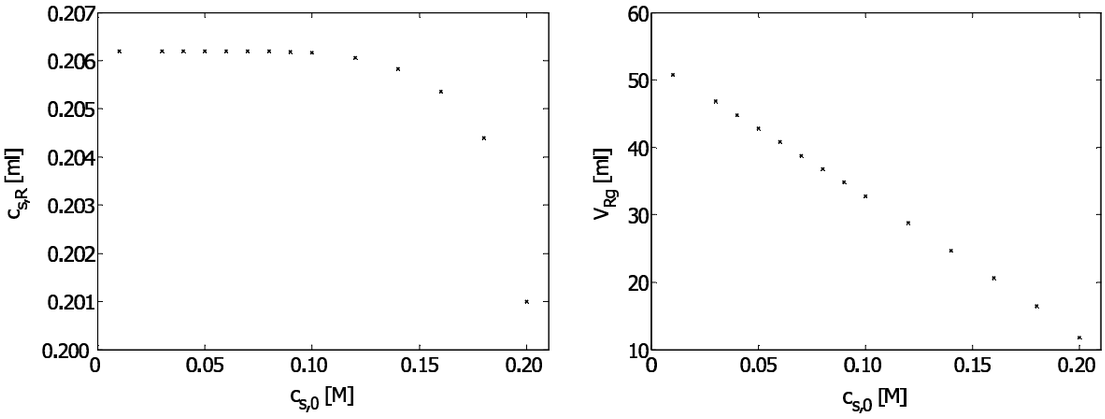

Figure 5-1: The concentration at which the protein is eluted (left) and the retention volume (right) as a function of the concentration at the beginning of the gradient for constant gradient parameter and volume.

In Figure 5-1 the gradient parameter G and the gradient volume V_g are kept constant and $c_{s,0}$ is increased. When $c_{s,0}$ is increased the concentration at the end of the gradient $c_{s,1}$ also has to be increased to achieve a constant gradient parameter. From the left plot in Figure 5-1 it is observed that the concentration at which the protein is eluted, $c_{s,R}$, is constant until $c_{s,0}$ reaches 0.100 M, where it starts to decrease. When the concentration at which the protein is eluted is constant and $c_{s,0}$ is increased, less solution has to be run through the column before the protein is eluted. This results in a decrease in the retention volume V_{Rg} when $c_{s,0}$ is increased as illustrated in the right plot in Figure 5-1.

The gradients used in this work are not started at exactly the same Cl^--concentration for all the proteins. Thus, the SMA model is used to calculate the retention volumes at gradient elution for identical conditions; the same Cl^--concentration at the beginning and end of the gradient and the same gradient volume. For Q-Sepharose XL the concentration at the end of the gradient $c_{s,1}$ is chosen to be higher than the ones used for the experimental work, to assure that the protein is eluted on and not after the gradient. The concentration at the beginning of the gradient $c_{s,0}$ is chosen to be as close to the original values as possible. For the three other columns both the $c_{s,0}$ and $c_{s,1}$ are chosen to be as close to the original values as possible. The concentrations $c_{s,0}$ and $c_{s,1}$ used for the calculations are listed in Appendix E.I. None of the experimental data may be obtained under these exact conditions, so that no experimental data but only the models are shown in the figures for the linear gradient elution.

The colors and lines used in the figures are common to both the isocratic and the gradient elutions and are as follows: BSA ····, α-lactalbumin –·– , β-lactoglobulin A — and β-lactoglobulin B – – –.
In the figures showing the isocratic elutions the following symbols are used for the experimental data: BSA +, α-lactalbumin ∗, β-lactoglobulin A ● and β-lactoglobulin B ×. The experimental data is given in appendix C. It is the same experimental data as those shown in the figures in Section 4.4.

The criteria for separations used in the following are as follows:

Isocratic elution: The difference in retention volume between the first and second eluted peak has to be at least 15 ml
The difference in retention volume between the second and third eluted peak has to be at least 30 ml
The difference in retention volume between the third and last eluted peak has to be at least 40 ml

Gradient elution: The difference in retention volume between the first and second eluted peak has to be at least 15 ml

The difference in retention volume between the second and third eluted peak has to be at least 20 ml

The difference in retention volume between the third and last eluted peak has to be at least 25 ml

Furthermore it is assumed that the presents of the other proteins will have no effect on the retention volumes.

5.1 Source 30Q

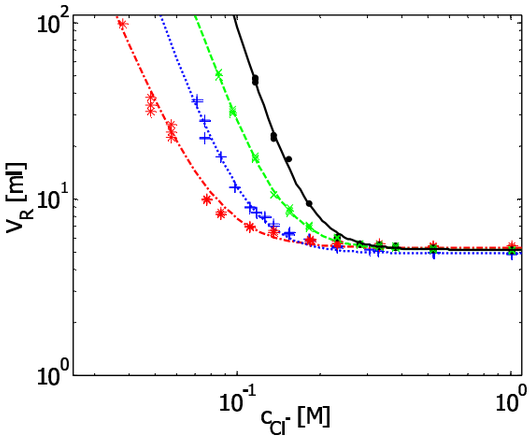

Figure 5-2: Isocratic elution of BSA, α-lactalbumin, β-lactoglobulin A and B on Source 30Q at a pH of 6.

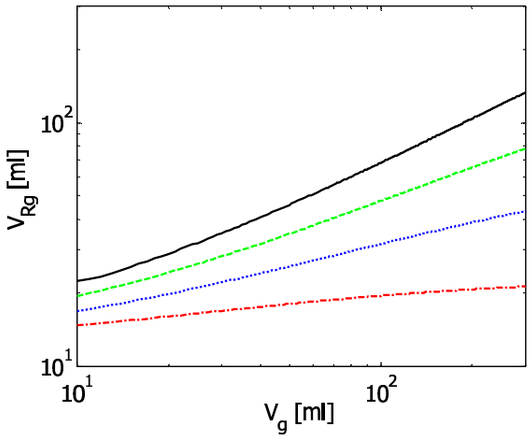

Figure 5-3: Linear gradient elution of BSA, α-lactalbumin, β-lactoglobulin A and B on Source 30Q at a pH of 6.

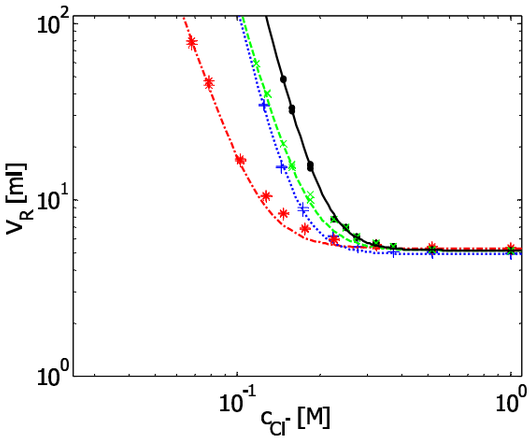

Figure 5-4: Isocratic elution of BSA, α-lactalbumin, β-lactoglobulin A and B on Source 30Q at a pH of 7.

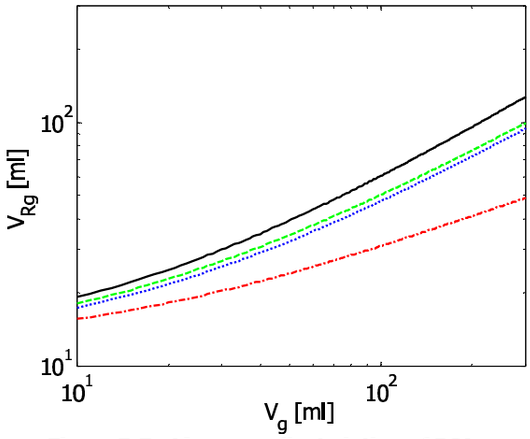

Figure 5-5: Linear gradient elution of BSA, α-lactalbumin, β-lactoglobulin A and B on Source 30Q at a pH of 7.

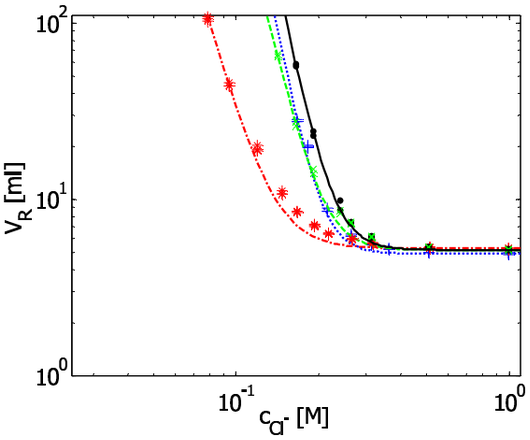

Figure 5-6: Isocratic elution of BSA, α-lactalbumin, β-lactoglobulin A and B on Source 30Q at a pH of 8.

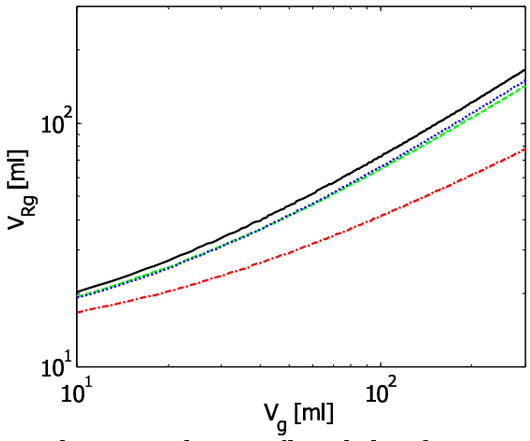

Figure 5-7: Linear gradient elution of BSA, α-lactalbumin, β-lactoglobulin A and B on Source 30Q at a pH of 8.

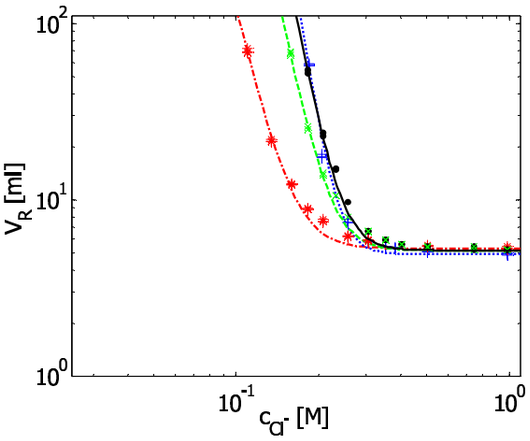

Figure 5-8: Isocratic elution of BSA, α-lactalbumin, β-lactoglobulin A and B on Source 30Q at a pH of 9.

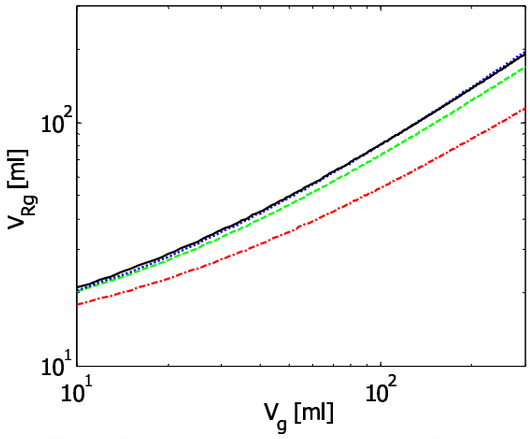

Figure 5-9: Linear gradient elution of BSA, α-lactalbumin, β-lactoglobulin A and B on Source 30Q at a pH of 9.

A separation of the four proteins on Source 30Q will only be possible at a pH of 6. In order to separate the four proteins by isocratic elution at a pH of 6 the Cl^--concentration has to be around 0.080 M. At Cl^--concentrations above 0.080 M the difference in retention volume between BSA and α-lactalbumin (first and second eluted peak) is smaller than 15 ml.

To separate the proteins by linear gradient elution from $c_{s,0}$ = 0.060 M to $c_{s,1}$ = 0.200 M the gradient volume has to be around at least 140 ml to fulfill the criteria for separation.

At a pH of 7 it is not possible to separate BSA and β-lactoglobulin B by either isocratic or linear gradient elution and at a pH of 8 and 9 it will only be possible to separate the proteins in two fractions; a fraction of α-lactalbumin and a fraction containing the remaining three proteins: BSA, β-lactoglobulin A and B.

5.2 Q-Sepharose XL

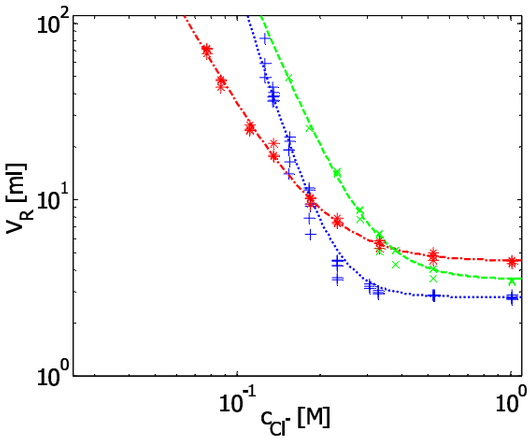

Figure 5-10: Isocratic elution of BSA, α-lactalbumin, β-lactoglobulin B on Q-Sepharose XL at a pH of 6.

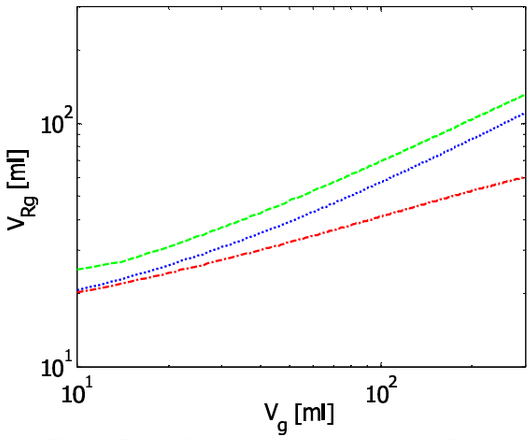

Figure 5-11: Linear gradient elution of BSA, α-lactalbumin, β-lactoglobulin B on Q-Sepharose XL at a pH of 6.

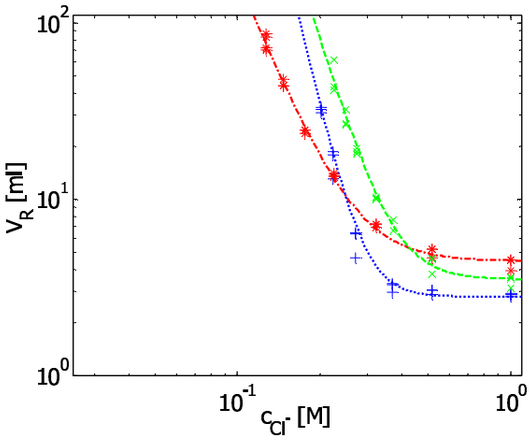

Figure 5-12: Isocratic elution of BSA, α-lactalbumin, β-lactoglobulin B on Q-Sepharose XL at a pH of 7.

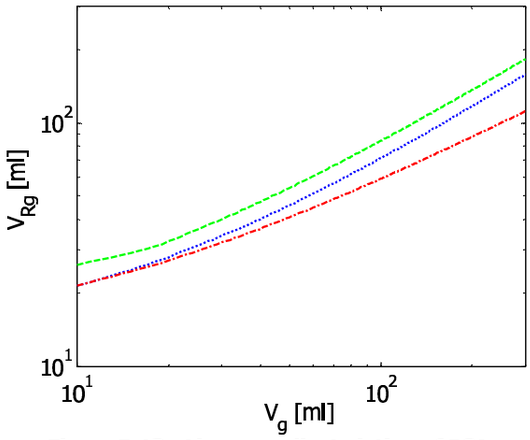

Figure 5-13: Linear gradient elution of BSA, α-lactalbumin, β-lactoglobulin B on Q-Sepharose XL at a pH of 7.

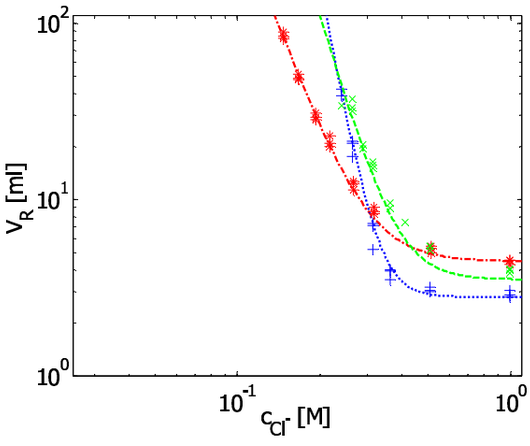

Figure 5-14: Isocratic elution of BSA, α-lactalbumin, β-lactoglobulin B on Q-Sepharose XL at a pH of 8.

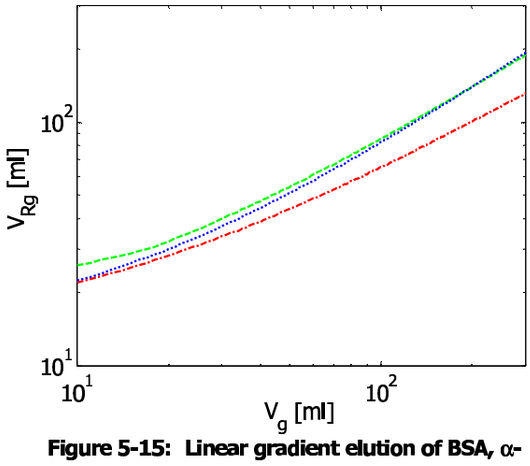

Figure 5-15: Linear gradient elution of BSA, α-lactalbumin, β-lactoglobulin B on Q-Sepharose XL at a pH of 8.

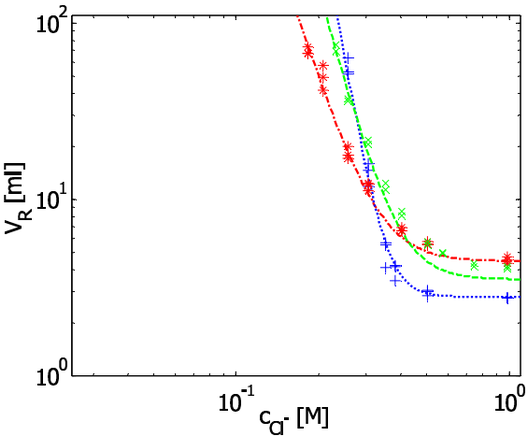

Figure 5-16: Isocratic elution of BSA, α-lactalbumin, β-lactoglobulin B on Q-Sepharose XL at a pH of 9.

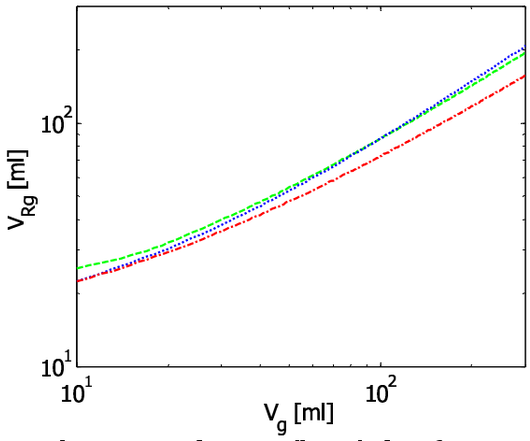

Figure 5-17: Linear gradient elution of BSA, α-lactalbumin, β-lactoglobulin B on Q-Sepharose XL at a pH of 9.

For Q-Sepharose XL the criteria for separation by isocratic elution are fulfilled at a pH of 6 and a Cl^--concentration around 0.130 M. At Cl^--concentrations much below or above 0.130 M it will not be possible to separate the three proteins BSA, α-lactalbumin and β-lactoglobulin B in one step by isocratic elution. At a pH of 6 and $c_{Cl^-} \approx 0.15 M$ the proteins can be separated into two fractions: one containing BSA and α-lactalbumin and one containing β-lactoglobulin B. At a pH of 6 and $c_{Cl^-} \approx 0.100 M$ the proteins can be separated into a fraction containing BSA and a fraction containing α-lactalbumin and β-lactoglobulin B. At a pH of 7 and $c_{Cl^-} \approx 0.21 M$ the proteins can also be separated into two fractions; one containing BSA and α-lactalbumin and one containing β-lactoglobulin B, and at $c_{Cl^-} \approx 0.18 M$ the proteins can be separated into one fraction containing BSA and one fraction containing α-lactalbumin and β-lactoglobulin B.

By isocratic elution at a pH of 8 and 9 it is only possible to separate the proteins into a fraction containing BSA and another containing α-lactalbumin and β-lactoglobulin B.

Also by gradient elution it is only possible to separate the three proteins at a pH of 6. To separate all three proteins by linear gradient elution from $c_{s,0}$ = 0.064 M to $c_{s,1}$ = 0.300 M, the gradient volume has to be around 200 ml. At this large gradient volume the retention volumes are around 85 ml for BSA and 105 ml for β-lactoglobulin B. The peaks obtained for Q-Sepharose XL are very broad at such high retention volumes and it is doubtful whether the separation will be possible in practice.

At a pH of 7, 8 and 9 it is only possible to separate the protein into two fractions: one containing BSA and another containing α-lactalbumin and β-lactoglobulin B.

5.3 Ceramic Q-HyperD F

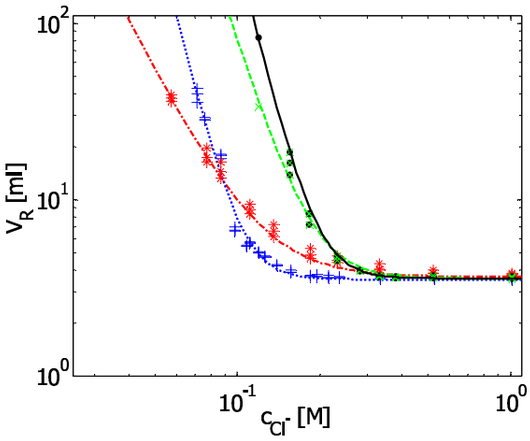

Figure 5-18: Isocratic elution of BSA, α-lactalbumin, β-lactoglobulin A and B on Ceramic Q-HyperD F at a pH of 6.

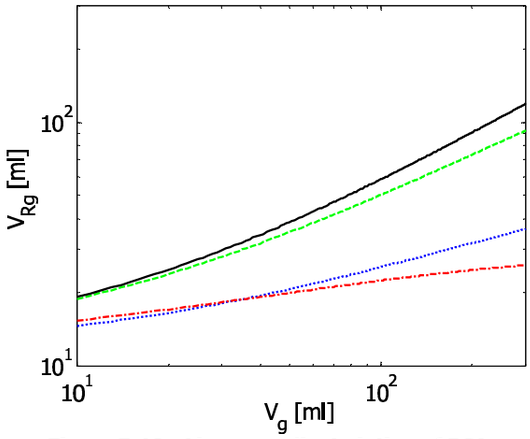

Figure 5-19: Linear gradient elution of BSA, α-lactalbumin, β-lactoglobulin A and B on Ceramic Q-HyperD F at a pH of 6.

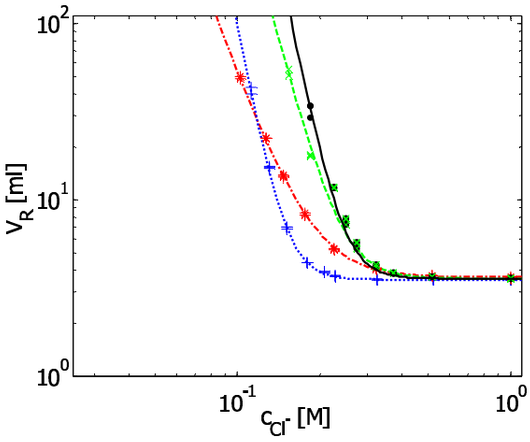

Figure 5-20: Isocratic elution of BSA, α-lactalbumin, β-lactoglobulin A and B on Ceramic Q-HyperD F at a pH of 7.

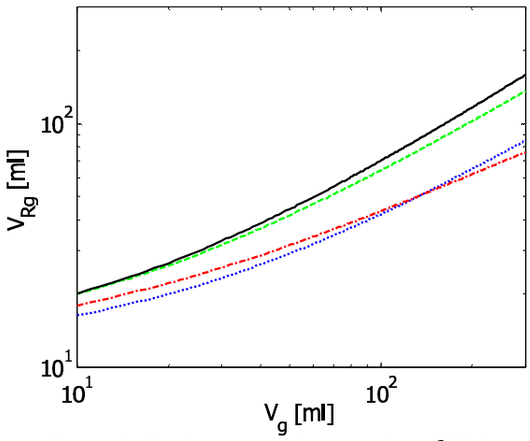

Figure 5-21: Linear gradient elution of BSA, α-lactalbumin, β-lactoglobulin A and B on Ceramic Q-HyperD F at a pH of 7.

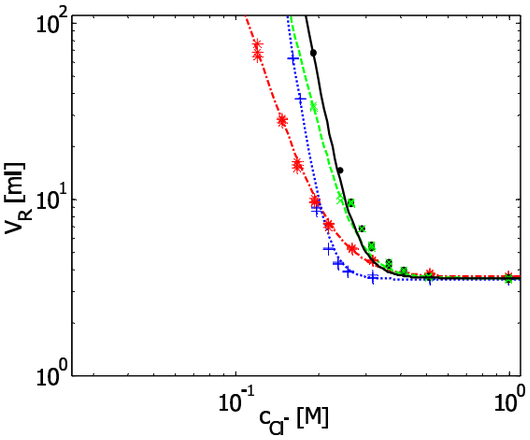

Figure 5-22: Isocratic elution of BSA, α-lactalbumin, β-lactoglobulin A and B on Ceramic Q-HyperD F at a pH of 8.

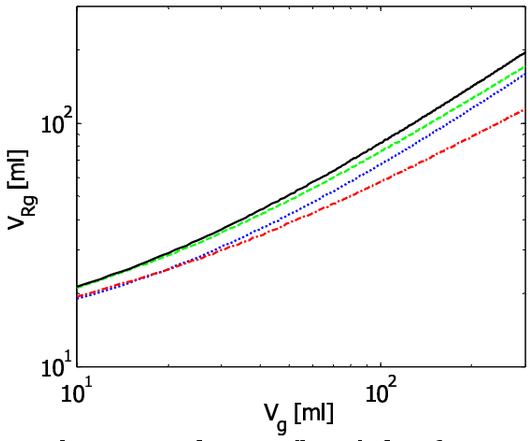

Figure 5-23: Linear gradient elution of BSA, α-lactalbumin, β-lactoglobulin A and B on Ceramic Q-HyperD F at a pH of 8.

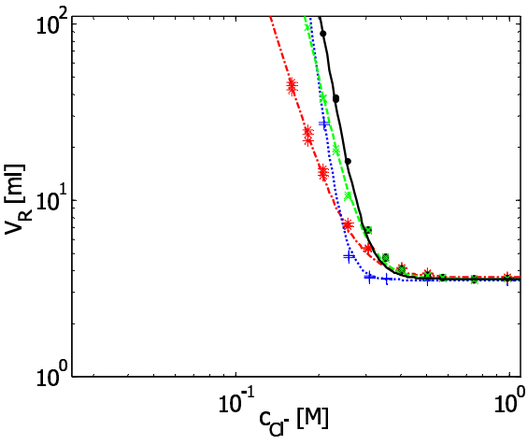

Figure 5-24: Isocratic elution of BSA, α-lactalbumin, β-lactoglobulin A and B on Ceramic Q-HyperD F at a pH of 9.

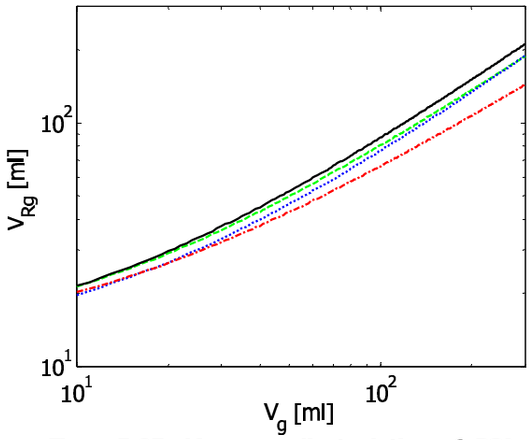

Figure 5-25: Linear gradient elution of BSA, α-lactalbumin, β-lactoglobulin A and B on Ceramic Q-HyperD F at a pH of 9.

For Ceramic Q-HyperD F it is not possible to separate all four proteins, because the retention volumes of BSA and α-lactalbumin and of β-lactoglobulin A and B are too close. To separate BSA and α-lactalbumin at a pH of 6 the Cl^--concentration has to be around 0.070 M and at this low concentration the proteins β-lactoglobulin A and B will never be eluted from the column. At gradient elution at a pH of 6 it is not possible to fulfill the separation criteria within a gradient volume of 250 ml. If the gradient volume is increased the difference between the retention volumes of BSA and α-lactalbumin and of β-lactoglobulin A and B will also increase, as well as the band broadening. The band broadening will be most pronounced for β-lactoglobulin A and B, because they have the largest retention volumes. The increased band broadening will make it impossible to separate β-lactoglobulin A and B at gradient volumes above 250 ml.

At a pH of 6 and 7 a mixture of the proteins can be separated into two fractions; one containing BSA and α-lactalbumin and another containing β-lactoglobulin A and B. At a pH of 8 only α-lactalbumin can be separated from the other three proteins, and at a pH of 9 it will be very difficult even to separate α-lactalbumin from the other proteins.

5.4 Fractogel EMD TMAE 650(s):

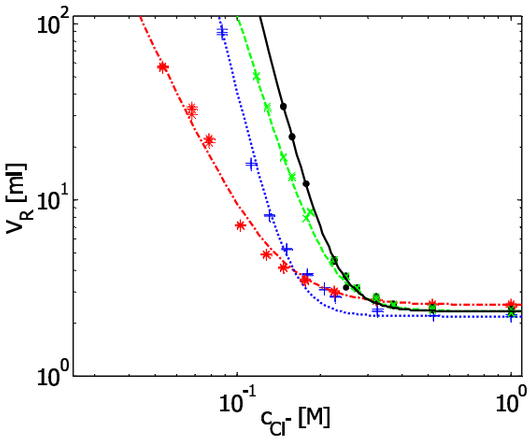

Figure 5-26: Isocratic elution of BSA, α-lactalbumin, β-lactoglobulin A and B on Fractogel EMD TMAE 650(s) at a pH of 6.

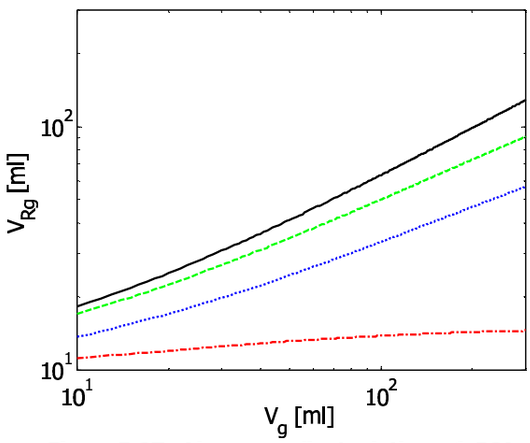

Figure 5-27: Linear gradient elution of BSA, α-lactalbumin, β-lactoglobulin A and B on Fractogel EMD TMAE 650(s) at a pH of 6.

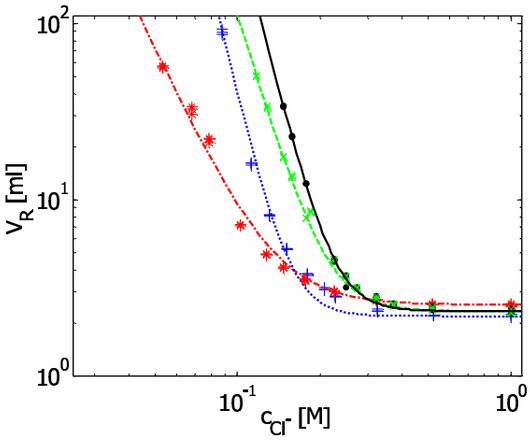

Figure 5-28: Isocratic elution of BSA, α-lactalbumin, β-lactoglobulin A and B on Fractogel EMD TMAE 650(s) at a pH of 7.

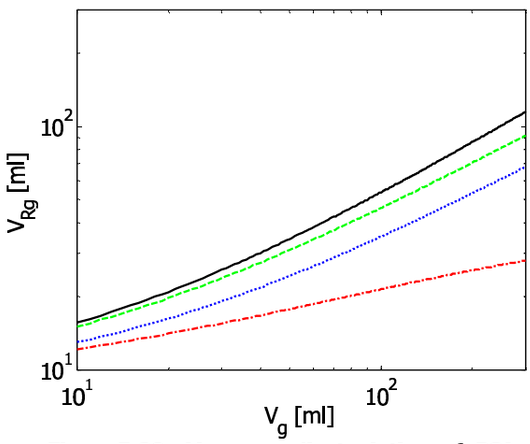

Figure 5-29: Linear gradient elution of BSA, α-lactalbumin, β-lactoglobulin A and B on Fractogel EMD TMAE 650(s) at a pH of 7.

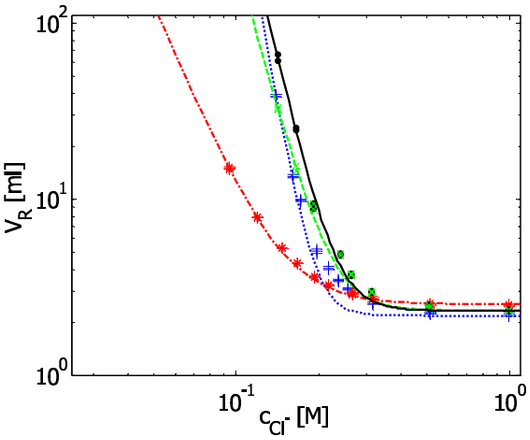

Figure 5-30: Isocratic elution of BSA, α-lactalbumin, β-lactoglobulin A and B on Fractogel EMD TMAE 650(s) at a pH of 8.

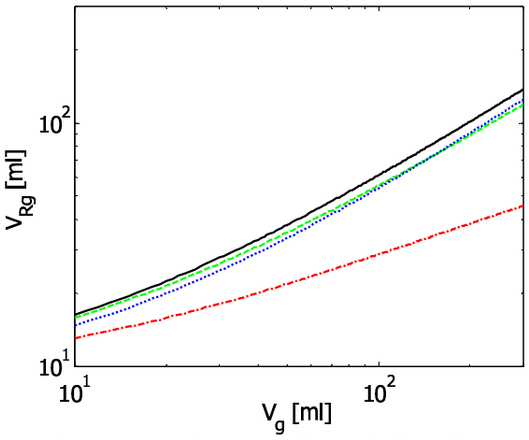

Figure 5-31: Linear gradient elution of BSA, α-lactalbumin, β-lactoglobulin A and B on Fractogel EMD TMAE 650(s) at a pH of 8.

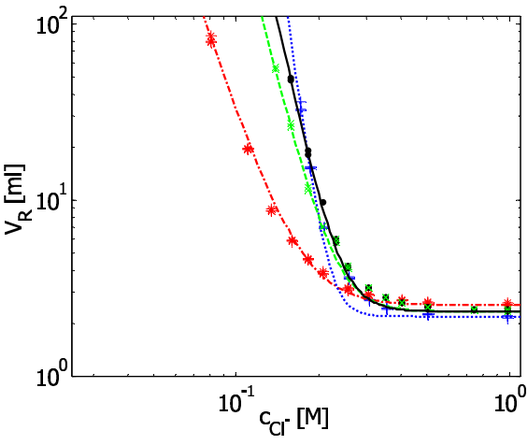

Figure 5-32: Isocratic elution of BSA, α-lactalbumin, β-lactoglobulin A and B on Fractogel EMD TMAE 650(s) at a pH of 9.

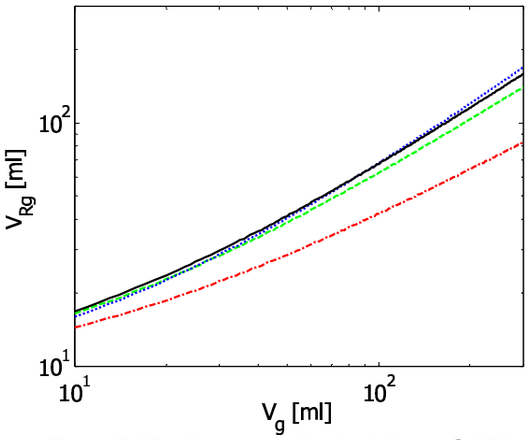

Figure 5-33: Linear gradient elution of BSA, α-lactalbumin, β-lactoglobulin A and B on Fractogel EMD TMAE 650(s) at a pH of 9.

A separation of all four proteins on Fractogel EMD TMAE 650(s) will only be possible at a pH of 6. To separate the proteins by isocratic elution at a pH of 6 the Cl^--concentration has to be around 0.105 M. A separation of the four proteins by linear gradient elution from $c_{s,0}$ = 0.045 M to $c_{s,1}$ = 0.200 M at a pH of 6 will require a gradient volume of at least 140 ml, in order to separate the proteins β-lactoglobulin A and B. At a pH of 7 it may be possible to separate the proteins into three fractions; BSA, α-lactalbumin and a fraction containing both β-lactoglobulin A and B. At a pH of 8 and 9 it will only be possible to separate α-lactalbumin from the remaining three proteins.

5.5 Discussion

At a pH of 6 the relative difference between the binding charges of the proteins is largest and the best separation of the proteins can, as expected, be achieved here. The best separation of the proteins can be obtained for Source 30Q.

For Q-HyperD F it is not possible to separate all four proteins by isocratic or gradient elution in one step. For Q-Sepharose XL it may be possible to separate the proteins BSA, α-lactalbumin and β-lactoglobulin B at a pH of 6 by gradient elution, but the separation strongly depends on the peak broadening, because the difference between the retention volumes is very small.

For Source 30Q and Fractogel EMD TMAE 650(s) it is possible to separate the proteins by both isocratic and gradient elution at a pH of 6. For practical use the separation by gradient elution will be preferred, because the separation time is shorter and the band broadening is less than by isocratic elution. The problem with isocratic elution is the retention volume of the last one or two eluted proteins. In order to separate all four proteins by isocratic elution, the Cl^--concentration has to be low. This results in large retention volumes, pronounced band broadening and very dilute fractions for the last one or two eluted proteins. At gradient elution it is possible to elute all four proteins within reasonable time and still achieve a good separation.

Another possibility is first to separate the least retained protein (α-lactalbumin) from the other three proteins by isocratic elution and then separate the remaining three proteins by linear gradient elution starting at the Cl^--concentration used for the isocratic elution.

6 THE ADSORPTION ISOTHERM

The expression for the isotherm was derived in Chapter 2. The isotherm at any load is calculable from Equation 2-8. Rearranging the equation leads to

$$c_p = \left(\frac{q_p}{K}\right)\left(\frac{z_s c_s}{\Lambda - (\sigma + z_p)q_p}\right)^{\nu} \qquad \textbf{(6-1)}$$

The equilibrium constant K and the charge ratio ν have been determined from the experiments in the linear range, the isocratic retention volumes. The only parameter left to be determined before the isotherms can be constructed is the shielding factor σ. σ is rather empirical by nature, but due to exclusion and repulsive effects only a fraction of the ligands will interact with the charged proteins [Guiochon, 1994].
The shielding factor can be determined from capacity measurements at a single protein concentration at a number of salt concentrations and the rest of the isotherm can be calculated by means of the model.

The shielding factor is determined by fitting Equation 6-1 to the experimental protein concentrations. Different correlations are made. In the first correlation only σ is fitted, and correlations are made where one σ is determined per salt concentration per pH value and where only one σ is determined per pH value. In the second only $\Delta G^0_{ads,Cl^-}$ is kept constant and $\Delta G^0_{ads,BSA}$, ν, and σ are determined from a fit to both the isocratic retention volumes and the capacity data at a pH of 7 and 8. Also in this case correlations are made where one σ is determined per salt concentration per pH value and where only one σ is determined per pH value.
The problems are solved by Marquardt's method for least squares in MATLAB.

6.1 Experimental

6.1.1 Solutions

Two stock solutions with nominal concentrations of 0 M and 1.0 M were prepared as for the pulse experiments in the linear range. The two stock solutions were titrated down to a pH of 6 with 5N HCl. Buffers with other concentrations were prepared by mixing of the two stock solutions, followed by titration with 5N NaOH up to the pH in question. The titration down to a pH of 6 assures that the concentration of Cl^--ions in the buffer solutions is independent of pH, because the concentration of Cl^--ions will be the same regardless of the buffers being titrated up to 7, 8 or 9 with 5N NaOH. After adjustment of pH the buffer solution is divided into two solutions A and B. To solution B BSA is added in a concentration of around 5 g/l. The exact BSA concentration is determined from the BSA calibration curve (Appendix A.IV).

6.1.2 Method

The breakthrough experiments were performed with the BioCAD Chromatographic Workstation, and effluent was detected at 280 nm. All the experiments were performed at room temperature (22 °C ±3). It has been assumed that the small temperature variations have no influence on the capacities, but it has not been investigated.

The steps in the method are described below and the corresponding chromatogram is shown in Figure 6-1.

Step 1: Equilibration of the column with 40 ml of buffer A (the solution without BSA). After 37 ml the UV detector was zeroed. (This step is not shown in the chromatogram in Figure 6-1).

Step 2: The column is set offline and the sample solution, which is either pure buffer B (the solution with a BSA concentration around 5 g/l) or a specified mixture of buffer A and B, is run through the bypass position. (This step is not shown in Figure 6-1).

Step 3: The column is set inline and the sample solution is loaded to the column.

Step 4: The column is set offline and the sample solution is run through the bypass position until a constant absorbance is reached. The actual, loaded BSA concentration is determined from this absorbance and the calibration curve:

$$c_{BSA} = \frac{Abs.280\,nm}{\alpha_{BSA}} \qquad \textbf{(6-2)}$$

Step 5: The column is still offline and the bypass is washed with water.

Step 6: The column is set inline and washed with water to remove the non-adsorbed BSA.

Step 7: The adsorbed BSA is eluted from the column with a linear gradient of NaCl.

Step 8: The column is regenerated with 1 M NaCl before the next breakthrough curve is run. (This step is not shown in Figure 6-1).

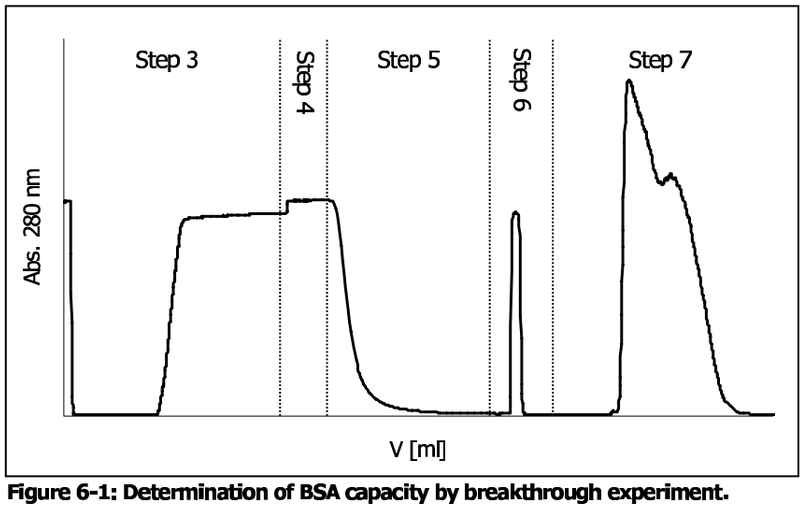

Figure 6-1: Determination of BSA capacity by breakthrough experiment.

The amount of BSA adsorbed to the column is determined from the area of the elution peak. The elution has to be performed so the top of the peak does not enter the non-linear range of the UV detector. This results in very broad and irregular peaks, which cannot be fitted with any peak function. The area of the peak is therefore determined by numerical integration in Excel. From the area of the peak and the BSA calibration curve, the amount in mg of BSA adsorbed is calculated as

$$m_{BSA} = \frac{AQ}{\alpha_{BSA}\ 60\,s/min} \qquad \textbf{(6-3)}$$

A is the area in Abs. 280nm·s, Q is the flow rate in ml/min and α_{BSA} = 0.3617 Abs. 280 nm·l/g is the slope of the calibration curve.

The concentration of BSA in mol per l accessible pore volume q_{BSA} is calculated as

$$q_{BSA} = \frac{m_{BSA}}{V_{col}K_d\varepsilon_p(1-\varepsilon)\,65000\,g/mol} \qquad \textbf{(6-4)}$$

The 65000 g/mol is the molecular weight of BSA.
For the fits, q_{BSA} and c_{BSA} are calculated in mol/l accessible pore volume and mol/l, respectively, but for clarity q_{BSA} and c_{BSA} are plotted in the unit g/l column volume (g/l CV) and g/l.

From the slope of the first linear part of the adsorption isotherm it is possible to calculate the retention volume at isocratic elution for the salt concentration in question. A very small value of q_p on the linear part of the isotherm is chosen and the corresponding mobile phase concentration c_p is calculated from Equation 6-1. The equilibrium ratio A is calculated as

$$A = \frac{dq_p}{dc_p} = \frac{q_p - 0}{c_p - 0} = \frac{q_p}{c_p} \qquad \textbf{(6-5)}$$

It is now possible to calculate the isocratic retention volume from Equation 4-3. In Figures 6-18 and 6-21 the retention volumes calculated from the slope of the first linear part of the adsorption isotherm are plotted.

6.2 Results and Discussion

The experimental data obtained at a pH of 7 is given in Appendix F.I and the experimental data obtained at a pH of 8 is given in Appendix F.II.

The $\Delta G^0_{ads,Cl^-}$, $\Delta G^0_{ads,p}$ and the ν values are independent of the salt counterion concentration. $\Delta G^0_{ads,Cl^-}$ depends on the salt and the ion exchanger. $\Delta G^0_{ads,p}$ depends on the protein and the ion exchanger and ν depends on the salt, the ion exchanger and the pH. The shielding factor is a geometric factor and depends on the size of the protein and the ion exchanger. According to the SMA formalism the shielding factor should be independent of the salt counterion concentration [Brooks, 1992]. In the following it will be investigated if it is possible to correlate the isotherms with a shielding factor that is independent of the Cl^--concentration.

Common to all the fits:

- At each Cl^--concentration only the capacities measured at the column with V_{col} = 1.35 ml at the highest BSA concentration (around 5 g/l) are used for the correlations
- In all the correlations, $\Delta G^0_{ads,Cl^-}$ is kept constant at the value determined from the correlations of the isocratic retention volumes, $\Delta G^0_{ads,Cl^-}/RT = 0.320$
- Symbols used in the figures:
  - ◊ Experimental data obtained at the column with V_{col} = 1.35 ml
  - ◊ Experimental data obtained at the column with V_{col} = 1.35 ml about a year before the data used for the fits
  - △ Experimental data obtained at the column with V_{col} = 0.46 ml
  - ○ Experimental data obtained at the column with V_{col} = 0.98 ml
  - — The model at $c_{Cl^-} = 0.037$ M
  - ···· The model at $c_{Cl^-} = 0.077$ M
  - -·- The model at $c_{Cl^-} = 0.117$ M
  - --- The model at $c_{Cl^-} = 0.157$ M

Correlation of the capacity data. Determination of four shielding factors at each pH value; one at each Cl⁻-concentration

In the first correlations eight shielding factors are determined; one at each Cl⁻-concentration at a pH of both 7 and 8. $\Delta G^0_{ads,BSA}$ and ν values are kept constant at the values determined from the isocratic retention volumes.

		BSA
	$\Delta G^0_{ads,BSA}$ / RT	4.663
pH 6	ν	4.20
pH 7	ν	6.16
pH 8	ν	7.89
pH 9	ν	9.77

Table 6-1: Parameters for BSA on Source 30Q determined from the correlation of the isocratic retention volumes.

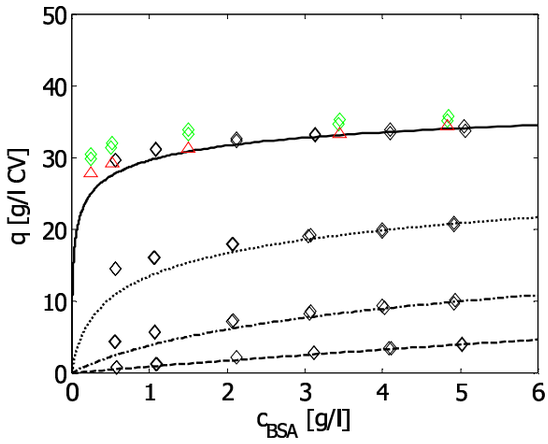

Figure 6-2: Adsorption isotherms for BSA on Source 30Q at a pH of 7. Four σ values fitted.

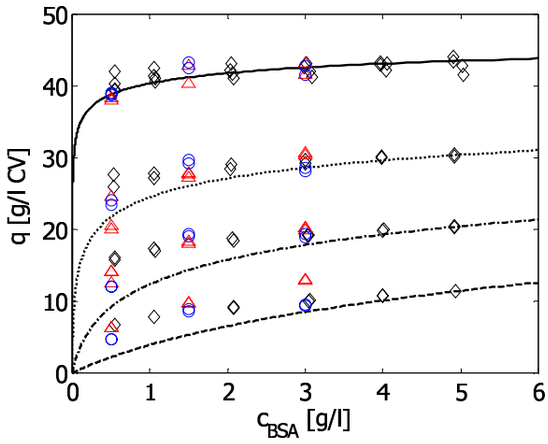

Figure 6-3: Adsorption isotherms for BSA on Source 30Q at a pH of 8. Four σ values fitted.

	σ at c_{Cl^-} = 0.037 M	σ at c_{Cl^-} = 0.077 M	σ at c_{Cl^-} = 0.117 M	σ at c_{Cl^-} = 0.157 M
pH 7	77.9	69.7	59.2	18.3
pH 8	65.3	61.9	49.5	28.2

Table 6-2: The shielding factors fitted when the parameters determined from the isocratic retention volumes are used in the correlations.

A comparison of Figures 6-2 and 6-3 shows that the model correlates the experimental data better at a pH of 7 than at a pH of 8, but at both pH values the model has a problem of correlating the data at the lowest BSA concentrations. From the figures it is also observed that the repeatability of the data is very good. Furthermore, a good reproducibility of the data is observed, because the agreement between the data obtained at different columns is good.

From table 6-2 it is seen that at a pH of both 7 and 8 the differences between the shielding factors at the three lowest Cl^--concentrations are relatively small. Only the shielding factors at $c_{Cl^-} = 0.157$ M are very different from the other shielding factors, so it may be possible to correlate the isotherms with a salt independent shielding factor. If the protein does not change size or conformation, when the pH is changed from 7 to 8, the shielding factor should also be independent of the pH, but first it was tried to correlate the data with only one shielding factor at each pH value.

Correlation of the capacity data. Determination of two shielding factors; one at each pH value

In this correlation two factors are determined; one at a pH of 7 and one at a pH of 8. $\Delta G^0_{ads,BSA}$ and ν values are kept constant at the values determined from the isocratic retention volumes.

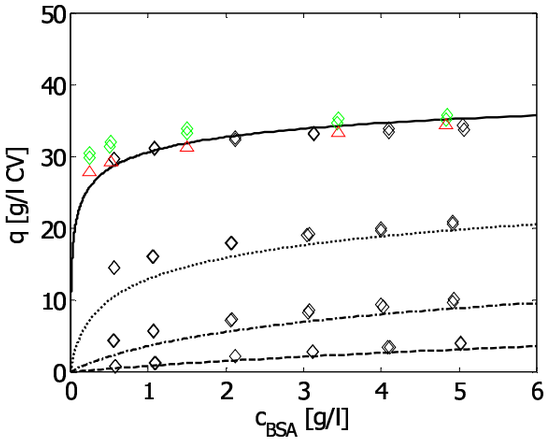

Figure 6-4: Adsorption isotherms for BSA on Source 30Q at a pH of 7. One σ value fitted.

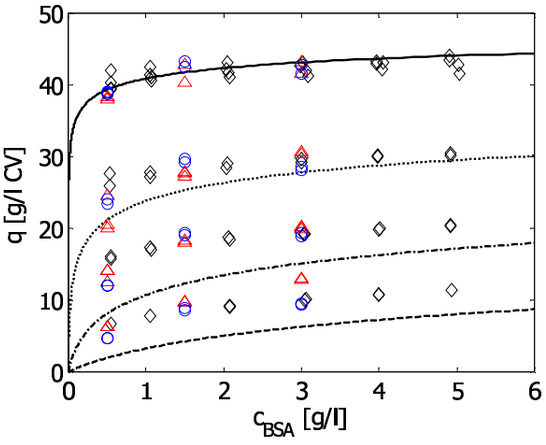

Figure 6-5: Adsorption isotherms for BSA on Source 30Q at a pH of 8. One σ value fitted.

The fitted shielding factors:

- pH 7: $\sigma = 74.9$
- pH 8: $\sigma = 64.3$

As expected the fits get worse when only one shielding factor is fitted at each pH. Especially at a pH of 8 the model completely fails to describe the data at the highest Cl^--concentrations. If the shielding factor is forced to a lower value, the model would fail to describe the data at the lowest Cl^--concentrations.

Correlation of the capacity data. Only one shielding factor is determined

$\Delta G^0_{ads,BSA}$ and ν values are still kept constant at the values determined from the isocratic retention volumes.

To see how the effect on the correlations would be if only one σ value was fitted, the σ determined from the fit at a pH of 7 is used to model the data at a pH of 8, and the σ determined from the fit at a pH of 8 is used to model the data at a pH of 7. It is also tried to use a mean value of shielding factors to model the data at a pH of both 7 and 8.

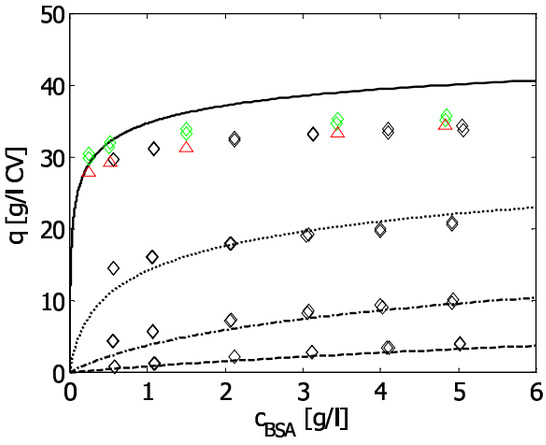

Figure 6-6: Adsorption isotherms for BSA on Source 30Q at a pH of 7. σ = 64.3.

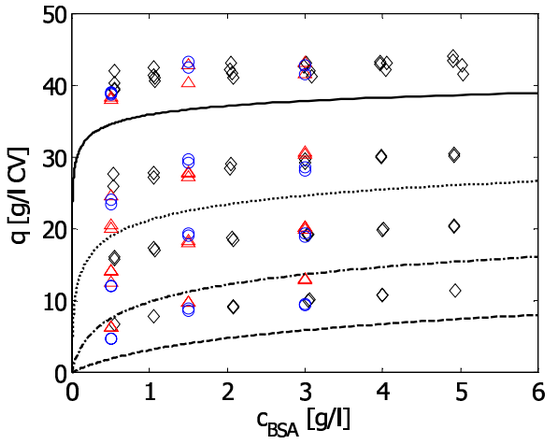

Figure 6-7: Adsorption isotherms for BSA on Source 30Q at a pH of 8. σ = 74.9.

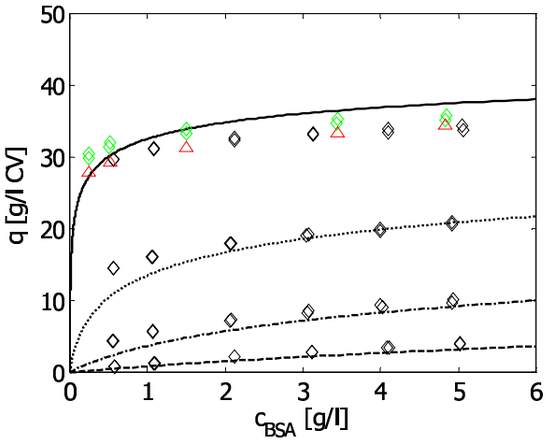

Figure 6-8: Adsorption isotherms for BSA on Source 30Q at a pH of 7. σ = 69.6.

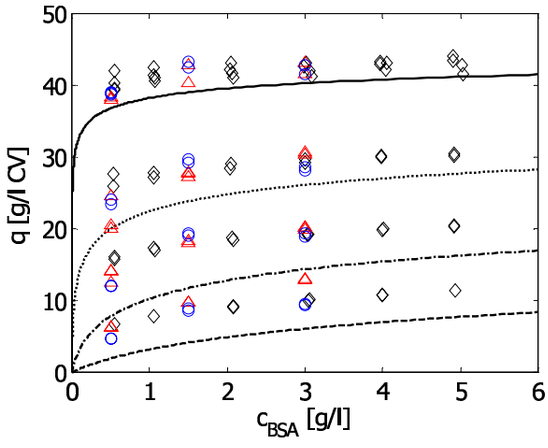

Figure 6-9: Adsorption isotherms for BSA on Source 30Q at a pH of 8. σ = 69.6.

From Figures 6-6 to 6-9 it is obvious that it is impossible to model the adsorption isotherms by one shielding factor common to a pH of both 7 and 8. Especially, the modeling of the data at a pH of 8 is very poor.

Simultaneous correlation of isocratic retention volumes and capacity data. Determination of four shielding factors at each pH value; one at each Cl⁻-concentration

The largest problem in correlation of the data is to get the initial slope of the isotherms steep enough. This part of the isotherm is determined from the experiments in the linear range. Thus, a simultaneous correlation of the isocratic retention volumes of BSA on Source 30Q and the capacity data at a pH of 7 and 8 is made. The standard Gibbs energy change for the Cl^--ions is kept constant at the value determined from the correlation of the retention volumes, because this value is common to all four proteins, but $\Delta G^0_{ads,BSA}/RT$, ν at a pH of 6, 7, 8 and 9 and the σ values are determined from the correlation. Two different correlations are made. In the first correlation eight σ values are determined, one at each Cl^--concentration at a pH of 7 and 8.

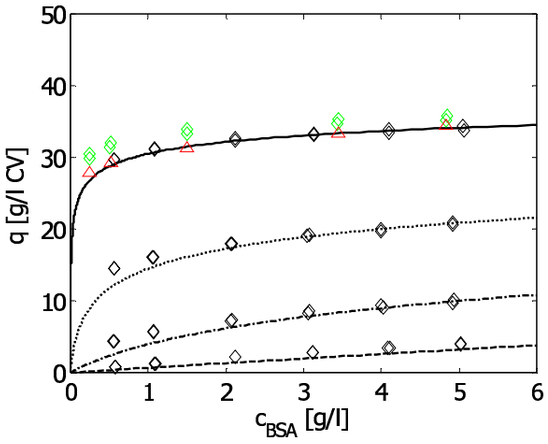

Figure 6-10: Adsorption isotherms for BSA on Source 30Q at a pH of 7. $\Delta G^0_{ads,BSA}/RT$, ν and four σ values fitted.

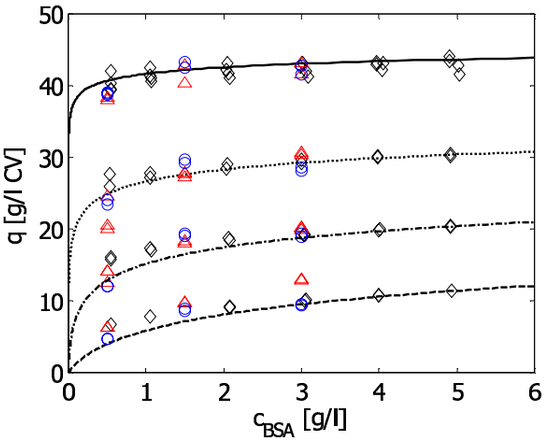

Figure 6-11: Adsorption isotherms for BSA on Source 30Q at a pH of 8. $\Delta G^0_{ads,BSA}/RT$, ν and four σ values fitted.

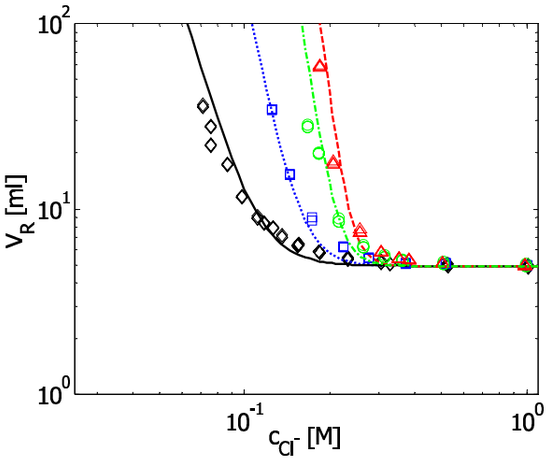

Figure 6-12: The isocratic retention volumes for BSA on Source 30Q, fitted simultaneously with capacity data. Symbols and colors: ◊ pH 6, □ pH 7, ○ pH 8, △ pH 9.

The fitted parameters:

$\Delta G^0_{ads,BSA}$ /RT = 6.238

pH 6: ν = 5.39

pH 9: ν = 12.46

	pH 7	pH 8
σ at c_{a^-} = 0.037 M	77.1	65.1
σ at c_{a^-} = 0.077 M	68.5	66.3
σ at c_{a^-} = 0.117 M	50.8	60.2
σ at c_{a^-} = 0.157 M	0.0	49.6
ν	7.43	10.53

Table 6-3: The shielding factors and ν values determined from the correlation of both the isocratic retention volumes and the capacity measurements.

If Figures 6-10 and 6-11 are compared with Figures 6-4 and 6-5, where only the shielding factors are fitted, it is observed that the correlations are improved when the standard Gibbs energy change and the binding charges of BSA are also fitted. The fitted $\Delta G^0_{ads,BSA}$ /RT and the ν values have increased compared to the values determined from the correlation of the isocratic retention volumes, but because the parameters are strongly correlated only minor effects on the correlation of the isocratic retention volumes (Figure 6-11) are observed. The largest influence on the model for the retention volumes is observed where BSA starts to bind to the column and the retention volume starts to increase, but the model still describes the experimental data reasonably well.

Simultaneous correlation of isocratic retention volumes and capacity data. Determination of two shielding factors; one at each pH value

At a pH of 7 and 8 the shielding factors are relatively close except for the ones at the highest Cl^--concentration, so that it was examined if it was possible to correlate the data with only one shielding factor at each pH, when the retention volumes and the capacity measurements were correlated at the same time.

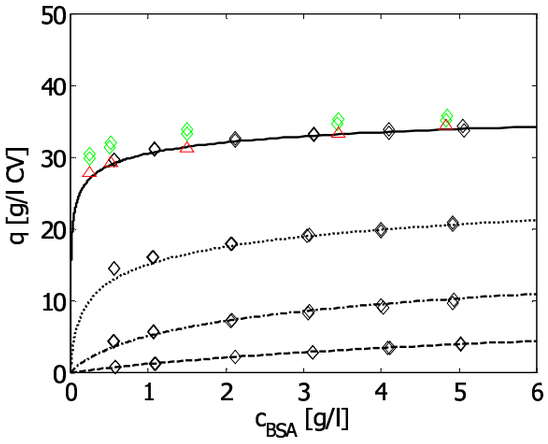

Figure 6-13: Adsorption isotherms for BSA on Source 30Q at a pH of 7. $\Delta G^0_{ads,BSA}/RT$, ν and one σ value fitted.

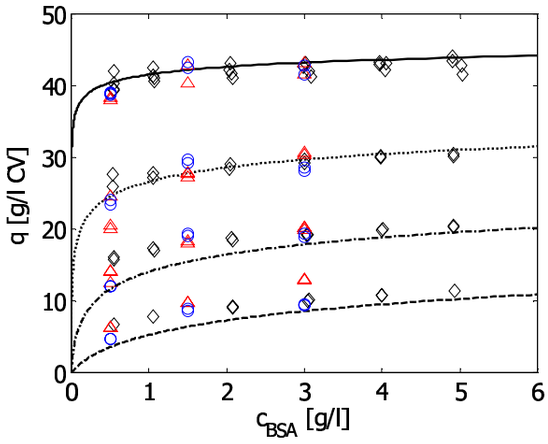

Figure 6-14: Adsorption isotherms for BSA on Source 30Q at a pH of 8. $\Delta G^0_{ads,BSA}/RT$, ν and one σ value fitted.

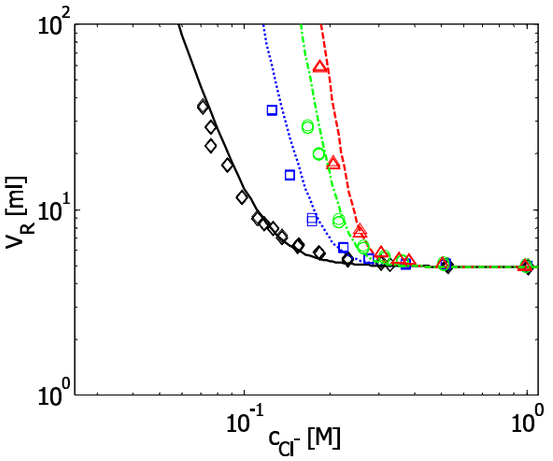

Figure 6-15: The isocratic retention volumes for BSA on Source 30Q, fitted simultaneously with the capacity data. Symbols and colors: ◊ pH 6, □ pH 7, ○ pH 8, △ pH 9.

The fitted parameters:

$\Delta G^0_{ads,BSA}/RT = 5.018$

pH 6: $\nu = 4.56$

pH 7: $\nu = 6.97$ and $\sigma = 81.5$

pH 8: $\nu = 9.17$ and $\sigma = 65.8$

pH 9: $\nu = 11.05$

From Figure 6-13 it is seen that the four isotherms at a pH of 7 are correlated very well with one shielding factor. The correlation is even improved compared to the correlation where four shielding factors, one per Cl^--concentration, are fitted. This is due to a lower value of $\Delta G^0_{ads,BSA}/RT$ and the ν's, but these lower values at the same time result in a deterioration of the model at a pH of 8 (Figure 6-13) compared to the correlation where four shielding factors are fitted. The isotherms at

the Cl^--concentrations 0.037 M and 0.077 are still very well correlated, and the correlations at the Cl^--concentrations 0.117 M and 0.157 are reasonably good.

The lowering of $\Delta G^0_{ads,BSA}/RT$ and the ν's brings them closer to the original values determined from the fit of the isocratic retention volumes, and the correlation of the retention volumes where BSA starts to bind is improved, but the correlation at the lowest Cl^--concentrations is not as good as in Figure 4-4. The slope of the curves is steeper.

Simultaneous correlation of isocratic retention volumes and capacity data. Change of Cl^--concentrations and determination of two shielding factors; one at each pH value

The difficulty of the correlation of the isotherms at low BSA and high Cl^--concentrations is due to the distribution ratio A being too low. The distribution ratio at the first part of the isotherms is determined from the experiments in the linear range, the correlation of the retention volumes. From Equation 4-4 it is seen that a way to increase the distribution ratio is to lower the salt concentration. In the next correlations it is investigated how much it is necessary to lower the Cl^--concentrations 0.117 M and 0.157 M in order to correlate the isotherms with one shielding factor at each pH. The retention volumes and the capacity measurements are still correlated together, but in the model for the isotherms at c_{Cl^-} = 0.117 M and 0.157 M the concentrations are decreased.

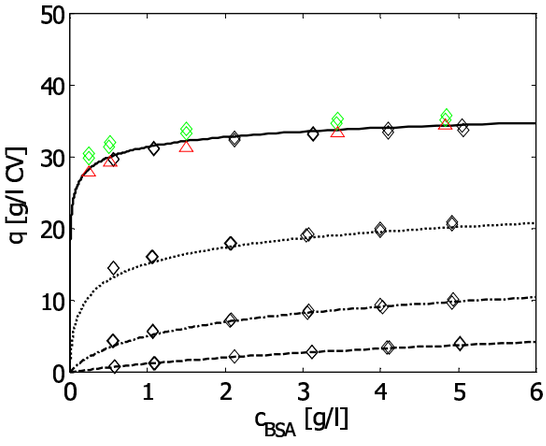

Figure 6-16: Adsorption isotherms for BSA on Source 30Q at a pH of 7. Fitted parameters: $\Delta G^0_{ads,BSA}/RT$, ν and one σ value. The Cl^--concentrations 0.117 M and 0.157 M are decreased to 0.114 M and 0.148 M, respectively.

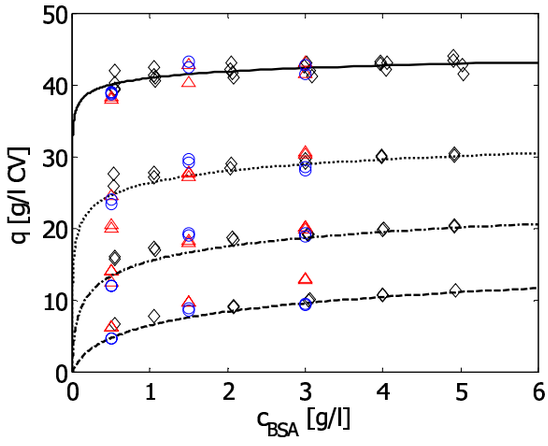

Figure 6-17: Adsorption isotherms for BSA on Source 30Q at a pH of 8. Fitted parameters: $\Delta G^0_{ads,BSA}/RT$, ν and one σ value. The Cl^--concentrations 0.117 M and 0.157 M are decreased to 0.111 M and 0.147 M, respectively.

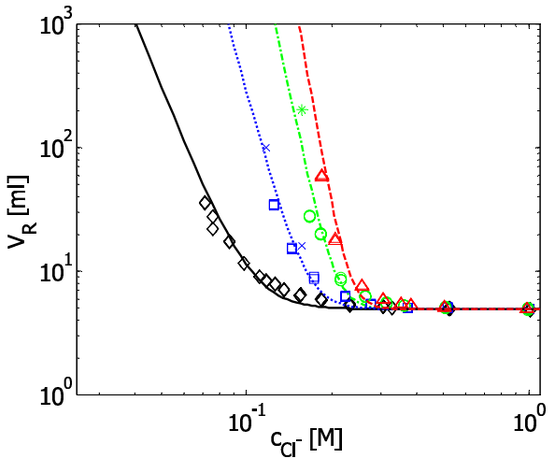

Figure 6-18: The isocratic retention volumes for BSA on Source 30Q, fitted simultaneously with the capacity data. Symbols and colors: ◊ pH 6, □ pH 7, ○ pH 8, △ pH 9. × retention volume calculated from the capacity data at a pH of 7 and the Cl^--concentrations 0.114 M and 0.148 M. ✳ retention volume calculated from the capacity data at a pH of 8 and the Cl^--concentration 0.147 M.

The fitted parameters:

$\Delta G^0_{ads,BSA} / RT = 6.714$

pH 6: $\nu = 5.57$

pH 7: $\nu = 8.19$ and $\sigma = 78.0$

$c_{Cl^-} = 0.117$ M is decreased to 0.114 M and $c_{Cl^-} = 0.157$ M is decreased to 0.148 M

pH 8: $\nu = 10.84$ and $\sigma = 65.6$

$c_{Cl^-} = 0.117$ M is decreased to 0.111 M and $c_{Cl^-} = 0.157$ M is decreased to 0.147 M

pH 9: $\nu = 12.87$

If Figures 6-13 and 6-16 are compared, it is observed that the correlation of the isotherms at a pH of 7 is not improved much when the Cl^--concentrations are decreased, but a comparison of Figures 6-14 and 6-17 shows that the correlation of the isotherms at a pH of 8 is improved when the Cl^--concentrations are decreased. Especially, the two isotherms where the Cl^--concentrations are decreased. The correlation of the retention volumes (Figure 6-17) is also improved a little compared to the correlation where the Cl^--concentrations are not decreased (Figure 6-14).
In Figure 6-18 the retention volumes calculated from the capacity data is plotted. The retention volumes are calculated by the Cl^--concentrations 0.114 M and 0.148 M at a pH of 7 and the Cl^--concentration 0.147 M at a pH of 8, but they are plotted at the original Cl^--concentrations (0.117 M and 0.157 M). The calculated retention volumes agree well with the experimental data and the model, but perfect fits of both the retention volumes and the isotherms would require a steeper slope of the retention volumes.

There is no evidence for lowering of the Cl^--concentrations as much as it has been done above, because the uncertainty of the Cl^--concentration in the two buffers is only around ±0.002 M (see Appendix A.I). The decrease of the Cl^--concentration was done to see if it was possible to obtain a better correlation of the isotherms at the highest concentration, if the initial slopes of these isotherms were increased.

Simultaneous correlation of isocratic retention volumes and capacity data. Change of Cl⁻-concentrations and determination of two shielding factors; one at each pH value

It was tried to make a fit where only one shielding factor common to a pH of both 7 and 8 was determined, when the two highest Cl⁻-concentrations were decreased.

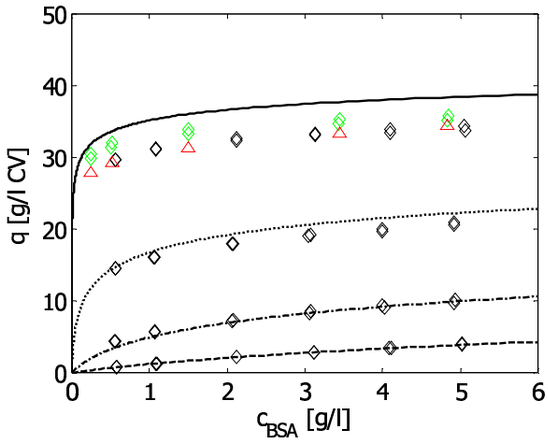

Figure 6-19: Adsorption isotherms for BSA on Source 30Q at a pH of 7. Fitted parameters: $\Delta G^0_{ads,BSA}/RT$, ν and one σ value common to a pH of 7 and 8. The Cl⁻-concentrations 0.117 M and 0.157 M are decreased to 0.116 M and 0.147 M, respectively.

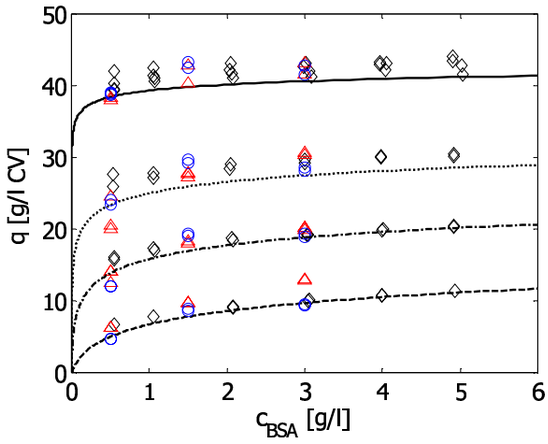

Figure 6-20: Adsorption isotherms for BSA on Source 30Q at a pH of 8. Fitted parameters: $\Delta G^0_{ads,BSA}/RT$, ν and one σ value common to a pH of 7 and 8. The Cl⁻-concentrations 0.117 M and 0.157 M are decreased to 0.106 M and 0.142 M, respectively.

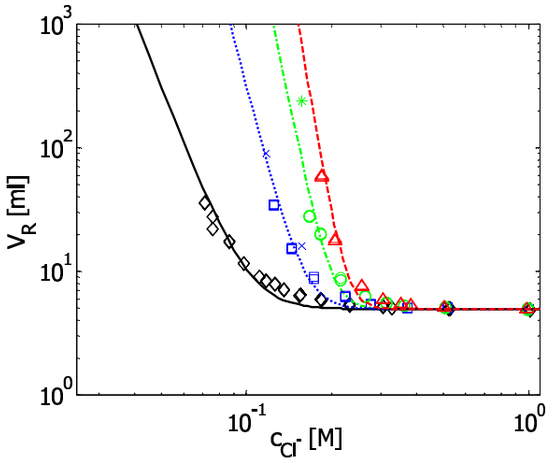

Figure 6-21: The isocratic retention volumes for BSA on Source 30Q, fitted simultaneously with the capacity data. Symbols and colors: ◊ pH 6, □ pH 7, ○ pH 8, △ pH 9. × retention volume calculated from the capacity data at a pH of 7 and the Cl⁻-concentrations 0.116 M and 0.147 M. ✳ retention volume calculated from the capacity data at a pH of 8 and the Cl⁻-concentration 0.142 M.

The fitted parameters:

$\Delta G^0_{ads,BSA} / RT = 7.202$

pH 6: $\nu = 5.80$

pH 7: $\nu = 8.59$ $c_{Cl^-} = 0.116$ M decreased to 0.114 M and $c_{Cl^-} = 0.157$ M decreased to 0.147 M

pH 8: $\nu = 11.09$ $c_{Cl^-} = 0.117$ M decreased to 0.106 M and $c_{Cl^-} = 0.157$ M decreased to 0.142 M

pH 9: $\nu = 13.28$

$\sigma = 68.2$

From Figures 6-19 and 6-20 it is obvious that it is not possible to correlate the isotherms with a shielding factor common to a pH of 7 and 8, even though the Cl^--concentrations 0.117 M and 0.157 M are decreased. To be able to correlate the isotherms with a common shielding factor the Cl^--concentrations 0.037 M and 0.077 M would have to be increased at a pH of 7 and decreased at a pH of 8, and there is no support for this. Some of the experiments are made with the same buffer solution. The only difference is the titration with 5 N NaOH. Some of the buffer is titrated to a pH of 7 and some of the buffer is titrated to a pH of 8. The volume increased due to the titration with NaOH has been neglected in the calculation of the Cl^--concentration, but at a pH of 7 and 8 the volume increase will result in a lower Cl^--concentration. An addition of 10 ml NaOH to 1 l solution with a Cl^--concentration of 0.0372 M will lower the concentration to 0.0368 M and an addition of 20 ml will lower the concentration to 0.0365 M. The volume increase is therefore negligible, when the Cl^--concentration is calculated.

Comparison with the literature

It has not been possible to find any isotherm data for BSA on Source 30Q in the literature. Gadam et al. measured SMA isotherms of β-lactoglobulin A and B at a pH of 7 at the Cl^--concentrations 100 mM and 150mM [Gadam et al., 1993]. As in the present work, they determined K and ν from linear elution data and the shielding factor from capacity measurements. Gadam et al. used one shielding factor per protein, and it is observed that the model correlates the experimental data perfectly at the lowest Cl^--concentration, but at the highest concentration there is a pronounced difference between the experimental data and the model. Gadam et al. also measured the adsorption isotherms for cytochrome c and α-chymotrypsinogen at two different salt concentrations (75 mM and 150 mM/130 mM), and here the SMA model correlates the experimental data very well at both salt concentrations.

Lewus et al. measured adsorption isotherms at a pH of 6.5 for lysozyme and cytochrome c [Lewus et al. 1999]. For lysozyme they used the salt concentrations 0 mM, 75 mM, 100 mM and 150 mM NaCl and for cytochrome c they used the NaCl concentration in the range 0 mM to 150 mM with intervals of 25 mM. For both proteins they used the same shielding factor at all salt concentrations, and they fitted K, ν and σ from the capacity measurements. For cytochrome c the SMA model

provides a very good correlation of the experimental data. For lysozyme the correlation is not so good. Here they weighted the measurements at 0 mM NaCl and the correlation at this concentration is therefore very good, but the differences between the model and the experimental data at the higher concentrations are considerable. If they had not weighted any of the data they might have obtained better correlations at the high concentrations, but the correlation at 0 mM NaCl would be worse.

In most cases the SMA model gives a satisfactory correlation of the adsorption isotherms when the shielding factor is assumed to be independent of the salt concentration. Some of the deviations from "ideal" SMA behavior observed for some proteins may be caused by the assumptions in the SMA formalism not always being valid. Neglecting: the effects of co-ions, protein-protein interactions in solution, protein-protein interactions while adsorbed, changes in the tertiary structure of the protein and hydrophobic interactions with the stationary phase are some of the assumptions in the SMA formalism that may not always be valid.

General discussion

In solution the BSA molecule is a prolate ellipse with an axial ratio of about four [Raje et al., 1997; Bosma et al., 1998]. This means that many orientations of the BSA molecule are possible when it binds to the anion exchanger. If the orientation of the BSA molecule is different at a pH of 7 and 8 due to e.g. the higher binding charge at a pH of 8 this could be an explanation for the different shielding factors. If the binding charge at a pH of 8 is located more on the minor axis than at a pH of 7, it is possible that the contact area between the BSA molecule and the adsorbent surface is smaller at a pH of 8 than at a pH of 7. A smaller contact area will result in a smaller number of sterically hindered exchange sites on the adsorbent surface and thus a smaller shielding factor.

The best correlations are obtained when the isocratic retention volumes and the capacity data is correlated simultaneously. The correlations are further improved when the highest Cl^--concentrations are decreased a little, but the uncertainty calculations cannot justify this decrease in the Cl^--concentrations. It is possible that simultaneous correlations of the retention volumes of all four proteins and capacity measurements at all four pH values would improve the correlations, because when all the data is correlated simultaneously it will be possible also to adjust the standard Gibbs energy change of the Cl^--ions. The SMA parameters are strongly correlated, and a change of the standard Gibbs energy change of the Cl^--ions will probably not result in a deterioration of the correlations of the retention volume for the other three proteins. The standard Gibbs energy change and the ν values for the other three proteins will just change a little to adjust for the change in the standard Gibbs energy change of the Cl^--ions.

7 MASS TRANSPORT

The mass transport in packed beds can be divided into an external transport and an intraparticle transport. The external transport is the transport of solute from the mobile phase to the particle surface, and the intraparticle transport is the transport of solute from the interface to the solid phase. The intraparticle transport is in this work assumed to occur by two distinct mechanisms; pore diffusion and solid diffusion (also called surface diffusion).

An excellent overview of mass transfer in ion-exchange chromatography is given by LeVan, Carta and Carmen in Section 16 in Perry's Chemical Engineers' handbook [Perry, 1997]. Another recommendable piece of writing concerning mass transfer in ion-exchange chromatography is the thesis "Application of the Linear Driving Force Approximation to the Study of Mass Transfer in Ion-Exchange Chromatography" [Hansen, 2000]. The thesis includes both experimental and theoretical studies.

7.1 The Mass Balance

The differential mass balance over a column segment is given by

$$\varepsilon\frac{\partial c}{\partial z}+(1-\varepsilon)\frac{\partial s}{\partial t}+\varepsilon v\frac{\partial c}{\partial z}-\varepsilon(E_D+D_m)\frac{\partial^2 c}{\partial z^2}=0 \qquad \textbf{(7-1)}$$

s is the average concentration in the particle, $s=K_d\varepsilon_p(c_{pore}+q)$ and $\frac{\partial s}{\partial t}=K_d\varepsilon_p\left(\frac{\partial c_{pore}}{\partial t}+\frac{\partial q}{\partial t}\right)$.

The mass balance states that the accumulation in the mobile phase, the pore phase and the adsorbed phase equals the transport into the segment by convection and axial diffusion. The axial diffusion consists of eddy diffusion E_D and ordinary diffusion D_m. The first term in the equation is the transport into the segment by convection, and the last term is the transport due to axial diffusion. The second term is the accumulation in the pore phase and in the adsorbing phase, and the third term is the accumulation in the mobile phase.

7.2 External Mass Transport

The external mass transport or the film mass transport is the transfer from the mobile phase to the particle surface. The mass transfer from the mobile phase is not momentary and the film mass transport coefficient k_f is introduced to account for this resistance to mass transport. In the mobile phase the velocity is v and on the particle surface the velocity is normally assumed to be 0. The change in velocity from v to 0 takes place in a boundary layer on the particle surface, the film layer. It takes some time before equilibrium between the concentration in the mobile phase and on the particle surface is reached, because the mass transfer from the mobile phase to the particle

surface takes time. The film mass transport coefficient is the reciprocal of the resistance to the mass transfer across the film.

The flux J, the velocity of the mass transport, through the film layer is given as

$$Ja_p = \frac{\partial s}{\partial t} = k_f a_p (c - c_0) \qquad \textbf{(7-2)}$$

where c is the concentration in the mobile phase and c_0 is the concentration in the film on the particle surface. a_p is the ratio between the surface area and the volume, $a_p = 6/d_p$, for a sphere.

The film mass transport coefficient is only constant if the concentration is low, the density of the solution is constant, the flux is low and the solution is ideal, because k_f depends on the diffusivity of the solute, the diameter of the particles, the velocity and the density of the mobile phase.

The film mass transfer coefficient can be estimated from correlations in terms of the Sherwood number $Sh = k_f d_p/D_i$, the Reynolds number $Re = \varepsilon v d_p/\nu$ and the Schmidt number $Sc = \nu/D_i$, where D_i is the diffusion coefficient and ν the kinematic viscosity. The most frequently used correlation for calculation of the film mass transport coefficient for packed beds is given in Section 16 in Perry's Chemical Engineers' Handbook [Perry, 1997].

In this work the simple correlation $k_f = \alpha v^{\beta}$ will be used for the film mass transport coefficient.

7.3 Intraparticle Mass Transport

The intrapartide mass transport takes place by two mechanisms; pore diffusion and solid diffusion. The transport in the liquid filled pores is called pore diffusion and gives access to the adsorption sites. An adsorbent may attach and detach many times, while it is transported by pore diffusion. The attachment may also be more permanent, and when the adsorbent moves along the solid phase without detaching, or by ion transport in charged ion-exchange media, the transport is taking place by solid diffusion [Perry, 1997].

When the transport is taking place by pore diffusion and solid diffusion, respectively, the flux is given as

$$Ja_p = \frac{\partial s}{\partial t} = -a_p K_d \varepsilon_p D_p \left(\frac{\partial c_{pore}(r)}{\partial r} \right)_R \qquad \textbf{(7-3)}$$

$$Ja_p = \frac{\partial s}{\partial t} = -a_p K_d \varepsilon_p D_s \left(\frac{\partial q(r)}{\partial r} \right)_R \qquad \textbf{(7-4)}$$

where D_p and D_s are the pore and the solid diffusion coefficients. The diffusivity in the pores is smaller than the diffusivity in a straight cylindrical pore because of the random orientation of the pores and the variation in the pore diameter.

The interface is given by r = R. For ion exchange the adsorption is assumed to be fast compared to the mass transfer and the local equilibrium is therefore assumed to be between the pore and solid phase $q = q(c_{pore})$.

The intraparticle mass transport is often described by mass transport coefficients and the linear driving force (LDF) approximation. In the LDF approximation the mass transport is assumed to take place over a small film layer. The flux on the particle surface is calculated on the assumption that the intraparticle resistance can be considered as the resistance offered by a thin film, and that the transport through this film can be represented as a pseudo-steady-state diffusion process. The LDF approximation is most accurate for describing the external mass transport, but in many cases it is a good approximation for the intraparticle transport as well, especially when the adsorption isotherm is linear [Carta, 1998].

By use of mass transport coefficients and the LDF approximation, the flux equations corresponding to Equation 7-3 and 7-4 are combined with Equation 7-2 given as:

Pore diffusion:
$$\frac{\partial s}{\partial t} = a_p k_f (c - c_0) = a_p k_p K_d \varepsilon_p (c_0 - c_{pore}) \qquad \textbf{(7-5)}$$

Solid diffusion:
$$\frac{\partial s}{\partial t} = a_p k_f (c - c_0) = a_p k_s K_d \varepsilon_p (q_0 - q) \qquad \textbf{(7-6)}$$

The subscript 0 refers to the concentration at the interface between the film layer and the particle surface where the two phases per definition are in equilibrium. c_{pore} and q are average concentrations. k_p is the pore mass transfer coefficient and k_s is the solid mass transfer coefficient. In the linear range of the isotherm where q is a linear function of c at equilibrium, q = Ac, the intraparticle concentration gradient to be linearized is independent of the choice of the gradient to be linearized, and q can be replaced by Ac. The solid diffusion is now expressed as

$$\frac{\partial s}{\partial t} = a_p k_s K_d \varepsilon_p A (c_0 - c_{pore}) \qquad \textbf{(7-7)}$$

When the intraparticle mass transfer is controlled neither by pore diffusion nor by solid diffusion, but by the two diffusions working in parallel, the following expression is obtained:

$$\frac{\partial s}{\partial t} = a_p k_f (c - c_0) = a_p K_d \varepsilon_p (k_p + k_s A)(c_0 - c_{pore}) \qquad \textbf{(7-8)}$$

In the following the van Deemter equation will be used for the study of mass transfer when the adsorption is linear. If the adsorbing conditions are varied from weak to strong retention the intrapartide mass transfer will range from pore to solid diffusion control.

7.4 The van Deemter Equation

In ideal chromatography there will be no band broadening when the isotherm is linear. When experiments are made under conditions where the isotherm is linear, it will be experienced that band broadening is taking place. This band broadening is caused by eddy diffusion and mass transport. In liquid chromatography the ordinary diffusion will normally have no influence.

In chromatography the term "height equivalent to a theoretical plate" H is used as a measure for the column efficiency. H is defined for the Gaussian distribution as

$$H = \frac{\sigma_z^2}{l_{col}} = \frac{\sigma_V^2}{V_R^2} l_{col} \qquad \textbf{(7-9)}$$

where σ_z^2 and σ_V^2 is the variance of the peak in the units of length and volume, respectively.

H is defined for a Gaussian distribution but is often used with good approximation for other distributions as well.

The number of plates N in a column is defined as

$$N = \frac{l_{col}}{H} \qquad \textbf{(7-10)}$$

N is also a measure of the efficiency of the column. A small H and a large N give very narrow peaks.

The reduced plate height h = H/d_p is given by the van Deemter equation [van Deemter, 1956]:

$$h = 2\lambda + 2\left(\frac{k'}{1+k'}\right)^2 \frac{v\varepsilon}{6(1-\varepsilon)K_m} = 2\lambda + 2\left(\frac{1+A}{p+1+A}\right)^2 \frac{v\varepsilon}{6(1-\varepsilon)K_m} \qquad \textbf{(7-11)}$$

λ is a constant related to the axial dispersion coefficient $D_{ax} = \lambda v d_p$, usually in the range 1-3. Here λ is assessed at 2 for all the columns. v is the interstitial velocity and $p = \varepsilon/(1-\varepsilon)K_d\varepsilon_p$. K_m is the overall mass transfer coefficient corresponding to an overall driving force in the liquid phase concentration c - c_{pore}. A is the equilibrium ratio between the solid and the pore phase in the linear

range and is determined from Equation 4-4, since the van Deemter equation is only valid in the linear range of the isotherm.

In the equation for the reduced plate height (Equation 7-11) the following assumptions are made:

- The rate of mass transfer can be described by the linear driving force approximation
- Local equilibrium exists between the pore and the solid phase
- The contribution from ordinary diffusion can be neglected
- The eddy diffusion coefficient is proportional to the velocity

The expression for the overall mass transfer coefficient K_m depends on the controlling intrapartide mass transfer mechanism. The intrapartide mass transfer can be controlled by pore, solid or parallel diffusion. The expression for K_m when intraparticle diffusion is controlled by

- Pore diffusion $$\frac{1}{K_m} = \frac{1}{k_f} + \frac{1}{K_d \varepsilon_p k_p} \quad \textbf{(7-12)}$$
- Solid diffusion $$\frac{1}{K_m} = \frac{1}{k_f} + \frac{1}{K_d \varepsilon_p A k_s} \quad \textbf{(7-13)}$$
- Parallel diffusion $$\frac{1}{K_m} = \frac{1}{k_f} + \frac{1}{K_d \varepsilon_p (k_p + A k_s)} \quad \textbf{(7-14)}$$

k_f is the velocity dependent film coefficient for the external mass transfer, determined by the simple correlation $k_f = \alpha v^{\beta}$ where α and β are constants. k_s is the solid mass transfer coefficient, and k_p is the pore mass transfer coefficient.

The development of the plate height with increasing retention reveals a characteristic behavior for each of the rate mechanisms. When pore diffusion is in control, the plate heights increase toward a constant value at strong retention, and when solid diffusion is in control, the plate heights decrease and approach a constant value at strong retention. When neither of the mechanisms control and the diffusion is parallel, the model coincides with the pore diffusion model at weak retention and the solid diffusion model at strong retention. A maximum is reached at intermediate retention resulting in a bell-shaped curve.

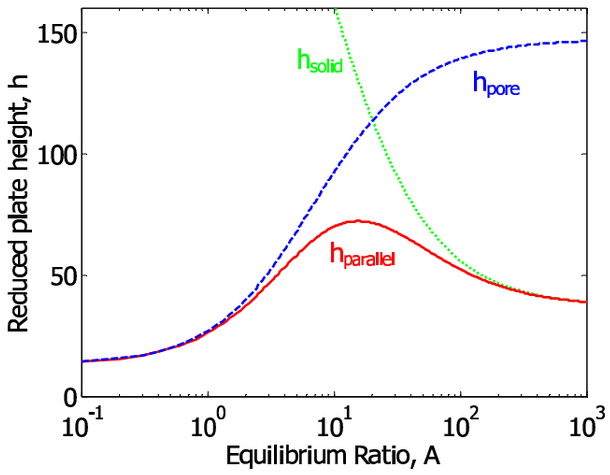

Figure 7-1: The plate height with increasing retention for pore --, solid ··· and parallel — diffusion. Parameters used in the figure: ε = 0.45, ε_p = 0.50, K_d = 0.55, λ = 2, α = 0.005, β = 2/3, v_0= 0.1 cm/s, k_p = 0.002 cm/s, k_s = 0.0001 cm/s.

7.5 Modeling Experimental Data

The van Deemter equation and the parallel diffusion model have been used to investigate the behavior of the plate heights as a function of the equilibrium ratio. The data used for the correlation is the data obtained by isocratic elution in the linear range described in Chapter 4. From the variance of the peak the reduced plate height is calculated as

$$h = \frac{\sigma^2}{V_R^2}\frac{l_{col}}{d_p} \qquad \textbf{(7-15)}$$

The equilibrium ratio A is determined from the SMA parameters obtained by the correlation of the isocratic retention volumes given in Section 4.4. Except for the SMA parameters for BSA on Source 30Q, where the parameters obtained by simultaneous correlation of both the retention volumes and the capacity measurements are used. The parameters used are the ones obtained from the fit where one shielding factor is determined at a pH of both 7 and 8.

The film mass transfer coefficient is determined as

$k_f = \alpha v^{1/3}$ where α is determined from a correlation of experimental data with the parallel diffusion model. k_p and k_s are also determined from this correlation. The correlations are made in the program MATLAB.

7.6 Results and Discussion

Not all the data in the tables in Appendix C is included in the correlations. Appendix G.I gives a list of the excluded data. It is especially the data at very strong retention which is excluded in the correlations, because the variance of the peaks tends to be ambiguous due to impurities.

The driving forces in the flux equations and reduced plate heights depend on the equilibrium ratio A, but not on how A is obtained. This means that the driving forces and reduced plate heights do not depend on the salt concentration or pH at which A is obtained, but solely on the value of A. It has been verified that the plate heights obtained in this work do not depend on the Cl^--concentration or pH applied, but only on the resulting equilibrium ratio. Thus, the pH at which the plate heights are obtained, is for simplicity not indicated in the figures.

7.6.1 Source 30Q

The experimental data is given in Appendices C.I to C.III, and in Appendix G.I a list is given of the excluded data.

The fitted parameters are given in Table 7-1 and the correlation of the reduced plate heights is presented in Figures 7-2 to 7-4. In the figures the following symbols and colors are used for the superficial velocities: v_0 = 0.021 cm/s (+), v_0 = 0.062 cm/s (×) and v_0 = 0.126 cm/s (*).

		Source 30Q		
		BSA	α-lactalbumin	β-lactoglobulin A
$\alpha \cdot 10^4$	$[(cm/s)^{2/3}$	5.96	20.1	3.64
$k_p \cdot 10^4$	[cm/s]	5.19	8.72	97.7
$k_s \cdot 10^4$	[cm/s]	1.18	2.20	ND

Table 7-1: The parameters α, k_s and k_p determined from the correlation of the reduced plate heights for Source 30Q. (ND: not determined).

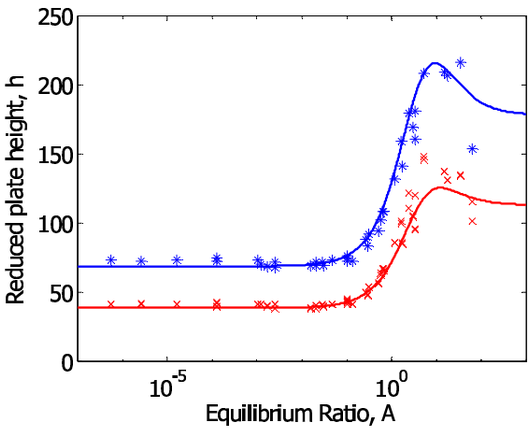

Figure 7-2: The reduced plate heights for BSA on Source 30Q correlated by the parallel diffusion model.

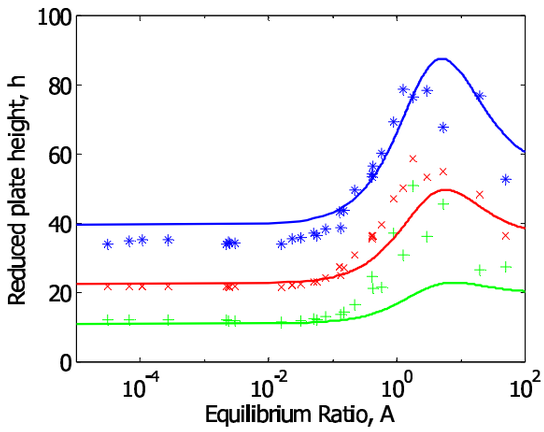

Figure 7-3: The reduced plate heights for α-lactalbumin on Source 30Q correlated by the parallel diffusion model.

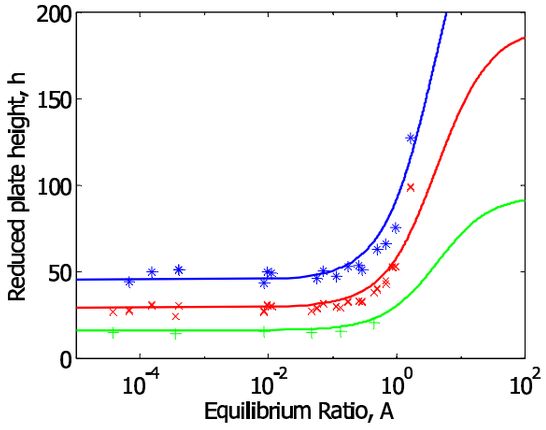

Figure 7-4: The reduced plate heights for β-lactoglobulin A on Source 30Q correlated by the pore diffusion model.

The reduced plate heights on Source 30Q for BSA and α-lactalbumin are correlated by the parallel diffusion model. The reduced plate heights for β-lactoglobulin A are correlated by the pore diffusion model due to lack of data at high equilibrium ratios. The reduced plate heights obtained by β-lactoglobulin B are not used for correlation because they are similar to the data for β-lactoglobulin A.

The correlation of the reduced plate heights for BSA is good but the determination of the solid mass transfer coefficient is quite uncertain, because of the small amount of data at high equilibrium ratios. For α-lactalbumin a few more data at high retention is available and the bell-shape behavior of the plate heights is more obvious from these data (Figure 7-3). The correlation of the plate heights for α-lactalbumin is not as good as for BSA. The model shows some deviation from the experimental data at low equilibrium ratio for v_0 = 0.126 cm/s. For v_0 = 0.021 cm/s and v_0 = 0.062 cm/s some deviation is observed between the model and the experimental data for the highest reduced plate heights (the top of the bell).

7.6.2 Q-Sepharose XL

The experimental data is given in Appendices C.V to C.VII, and in Appendix G.I a list is given of the excluded data.

The fitted parameters are given in Table 7-2 and the correlation of the reduced plate heights is presented in Figures 7-5 to 7-7. In the figures the following symbols and colors are used for the superficial velocities: v_0 = 0.0044 cm/s (*), v_0 = 0.0083 cm/s (+), v_0 = 0.016 cm/s (o) and v_0 = 0.057 cm/s (×).

		Q-Sepharose XL		
		BSA	α-lactalbumin	β-lactoglobulin B
$\alpha \cdot 10^4$	$[(cm/s)^{2/3}$	477	381	3.68
$k_p \cdot 10^4$	[cm/s]	6.84	2.38	3.43
$k_s \cdot 10^4$	[cm/s]	0.077	0.473	1.71

Table 7-2: The parameters α, k_s and k_p determined from the correlation of the reduced plate heights for Q-Sepharose XL.

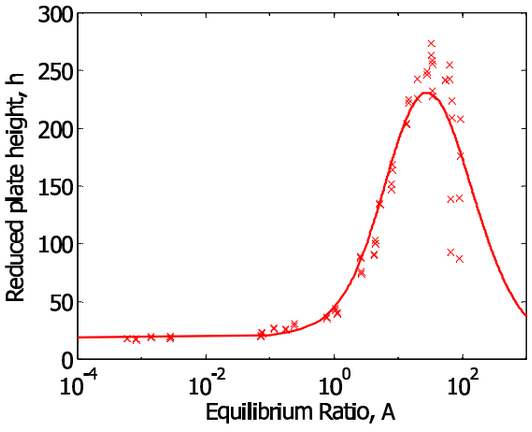

Figure 7-5: The reduced plate heights for BSA on Q-Sepharose XL correlated by the parallel diffusion model.

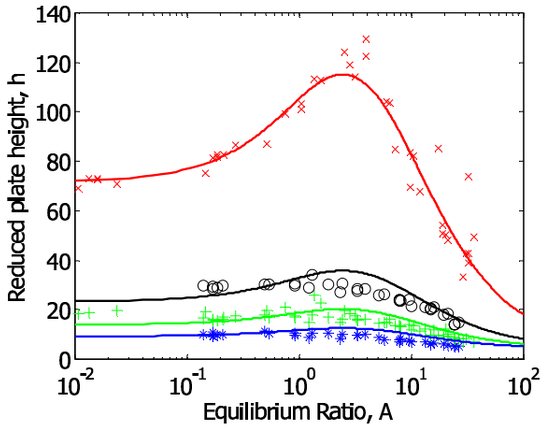

Figure 7-6: The reduced plate heights for α-lactalbumin on Q-Sepharose XL correlated by the parallel diffusion model.

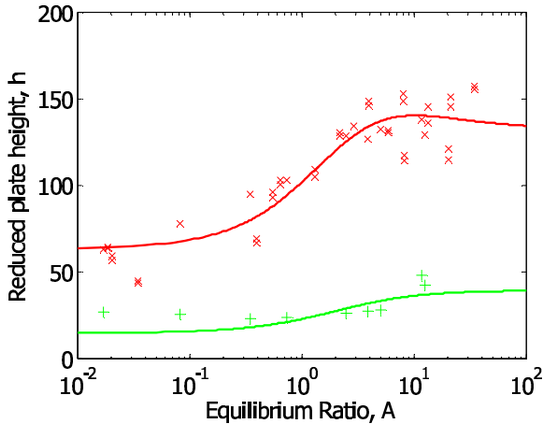

Figure 7-7: The reduced plate heights for β-lactoglobulin B on Q-Sepharose XL correlated by the parallel diffusion model.

The reduced plate heights obtained on Q-Sepharose XL are correlated very well by the parallel diffusion model. From the reduced plate heights measured by α-lactalbumin the bell-shaped behavior of the plate heights is very clear, and at all four superficial velocities the parallel diffusion model correlates the data well.

The bell-shaped behavior of the reduced plate heights is not obvious for β-lactoglobulin B, because no data is available at high equilibrium ratios. The parallel diffusion model is used for correlation of

the data but the data might have been correlated equally well by the pore diffusion model. Thus, the uncertainty of the solid mass transfer coefficient is large.

7.6.3 Ceramic Q-HyperD F

The experimental data is given in Appendices C.VIII to C.XI, and in Appendix G.I a list is given of the excluded data.

The fitted parameters are given in Table 7-3 and the correlation of the reduced plate heights is presented in Figures 7-8 to 7-12. In the figures the following symbols and colors are used for the superficial velocities: v_0 = 0.021 cm/s (+), v_0 = 0.062 cm/s (×) and v_0 = 0.126 cm/s (*).

		Ceramic Q-HyperD F				
		BSA	α-lactalbumin	β-lactoglobulin A		β-lactoglobulin B
$\alpha \cdot 10^4$	$[(cm/s)^{2/3}$	3.66	16.8	0.812	6470	16.6
$k_p \cdot 10^4$	[cm/s]	33.4	7.14	3.72	9.40	6.60
$k_s \cdot 10^4$	[cm/s]	0.405	0.473	3.76	ND	0.150

Table 7-3: The parameters α, k_s and k_p determined from the correlation of the reduced plate heights for Ceramic Q-HyperD F. (ND: not determined).

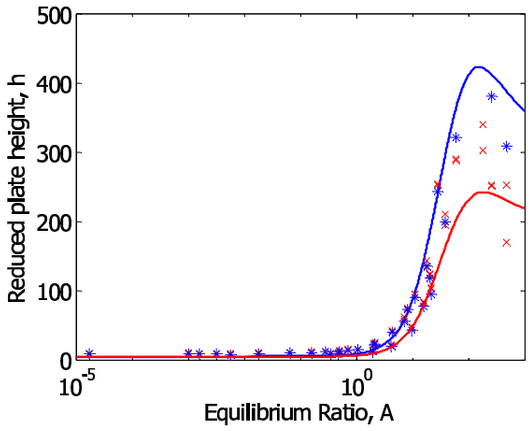

Figure 7-8: The reduced plate heights for BSA on Ceramic Q-HyperD F correlated by the parallel diffusion model.

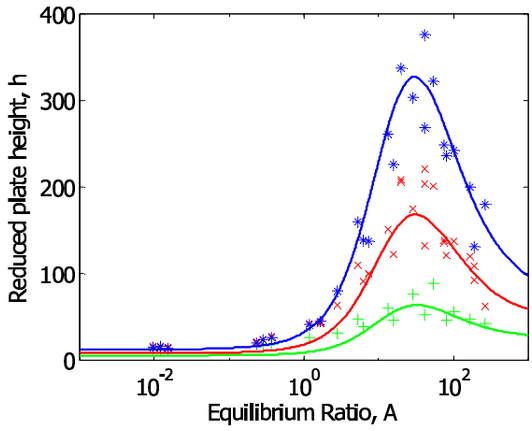

Figure 7-9: The reduced plate heights for α-lactalbumin on Ceramic Q-HyperD F correlated by the parallel diffusion model.

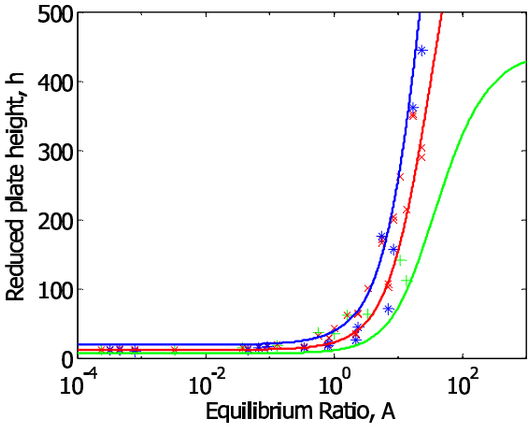

Figure 7-10: The reduced plate heights for β-lactoglobulin A on Ceramic Q-HyperD F correlated by the parallel diffusion model.

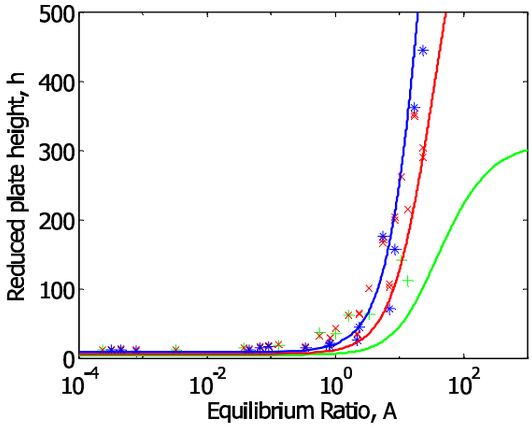

Figure 7-11: The reduced plate heights for β-lactoglobulin A on Ceramic Q-HyperD F correlated by the pore diffusion model.

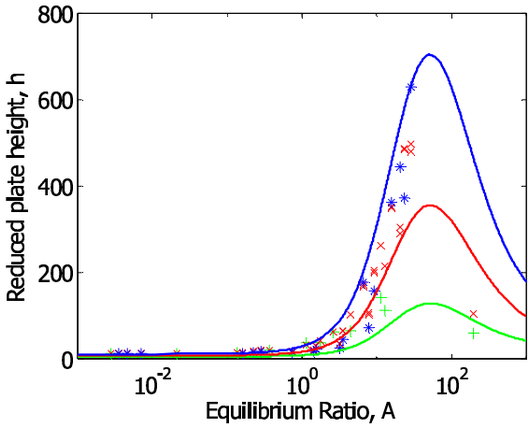

Figure 7-12: The reduced plate heights for β-lactoglobulin B on Ceramic Q-HyperD F correlated by the parallel diffusion model.

As for Source 30Q only a few experimental data is obtained by BSA at high equilibrium ratio, and the determination of k_s is very uncertain. Ernst Hansen has determined k_s for BSA on Q-HyperD 35 (similar to Q-HyperD F) and on Q-HyperD 20 (similar to Q-HyperD F, but with small particle size, d_p = 20 μm) by the flux curve procedure [Hansen et al., 1998]. He found the values $2.9 \cdot 10^{-5}$ cm/s for Q-HyperD 35 and $4.5 \cdot 10^{-5}$ cm/s for Q-HyperD 20, which is close to the value of $4.05 \cdot 10^{-5}$ cm/s determined for Q-HyperD F in this work.

For α-lactalbumin experimental data at high retention is obtained and the bell-shaped behavior of the plate heights is more easily observed. The parallel diffusion model correlates the reduced plate heights for α-lactalbumin well.

The reduced plate heights for β-lactoglobulin A are correlated both with the parallel diffusion model and the pore diffusion model. Only minor effects are observed in the correlation of the data

(Figures 7-10 and 7-11) but the choice of model has a large influence on the determination of α (Table 7-3). α is 8000 times larger when the pore diffusion model is used for the correlation.

The experimentally determined reduced plate heights for β-lactoglobulin A and B are very similar, except for the two data points at high equilibrium ratio for v_0 = 0.021 cm/s and v_0 = 0.062 cm/s for β-lactoglobulin B. These two data points make it possible to determine a value for k_s although it is associated with some uncertainty, due to the very small amount of data at high retention. More data points are needed at high equilibrium ratio in order to determine k_s with sufficient precision.

7.6.4 Fractogel EMD TMAE 650(s)

The experimental data is given in Appendices C.XII and C.XIII, and in n Appendix G.I a list is given of the excluded data.

The fitted parameters are given in Table 7-4 and the correlation of the reduced plate heights is presented in Figures 7-13 to 7-14. In the figures the following symbols and colors are used for the superficial velocities: v_0 = 0.021 cm/s (+), v_0 = 0.062 cm/s ($\times$) and v_0 = 0.126 cm/s ($*$).

		Fractogel EMD TMAE 650(s)	
		BSA	α-lactalbumin
$\alpha \cdot 10^4$	$[(cm/s)^{2/3}]$	8.86	24.3
$k_p \cdot 10^4$	[cm/s]	2.31	7.16
$k_s \cdot 10^4$	[cm/s]	1.52	6.45

Table 7-4: The parameters α, k_s and k_p determined from the correlation of the reduced plate heights for Fractogel EMD TMAE 650(s).

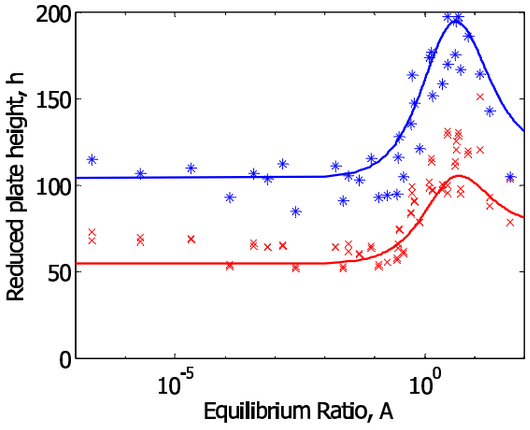

Figure 7-13: The reduced plate heights for BSA on Fractogel EMD TMAE 650(s) correlated by the parallel diffusion model.

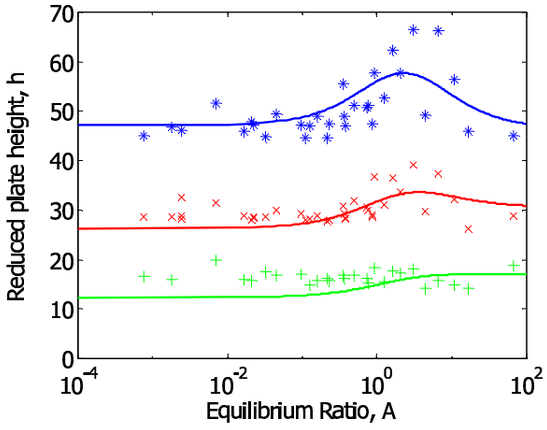

Figure 7-14: The reduced plate heights for α-lactalbumin on Fractogel EMD TMAE 650(s) correlated by the parallel diffusion model.

Reasonably good correlations of the reduced plate heights for BSA and α-lactalbumin on Fractogel EMD TMAE 650(s) are obtained by the parallel diffusion model. Some scattering of the experimental data is observed even at low equilibrium ratio, and for α-lactalbumin the bell-shaped behavior of the plate heights is not as obvious as for BSA.

7.6.5 General

The whey proteins used in this work are not the best suited for a study of the parallel diffusion model, since the peaks at high retention tend to be disturbed by impurities. The best data for the study is obtained on Q-Sepharose XL, because for this column data is also available at high equilibrium ratio. This is probably because the peaks at high retention are not disturbed by impurities, due to the poor separation skills of the Q-Sepharose XL media. The reduced plate heights obtained by all three proteins on the Q-Sepharose XL column are correlated very well by the parallel diffusion model. The reduced plate heights measured by BSA and α-lactalbumin for the three other columns are also correlated well by the parallel diffusion model. Neither the pore diffusion model nor the solid diffusion model is capable of correlating this data since none of these two models can describe the observed maximum in the plate heights.

As expected the size of the plate heights reflects the size of the proteins. The largest reduced plate heights are observed for the largest molecule, BSA, and the smallest are observed for the smallest molecule, α-lactalbumin, since the mass transfer rate decreases with increasing size of the molecule.

The simple correlation $k_f = \alpha v^{\beta} = \alpha v^{1/3}$ used in this work corresponds to $Sh = \alpha' Re^{1/3}$. The Sherwood number is given as $Sh = k_f d_p/D_i$, the Reynolds number is given as $Re = \varepsilon v d_p/\nu$ and α is then related to α' as: $\alpha = \alpha' \frac{D_i}{d_p}\left(\frac{d_p \varepsilon}{\nu}\right)^{1/3}$. For a given protein and buffer solution, D and ν are constant and α will only depend on the particle diameter d_p and the porosity ε. The influence of the porosity is negligible, and it would therefore be expected that α, for a given protein, is related to the particle diameter as $\alpha = \text{constant} \cdot d_p^{-2/3}$. From this correlation the constant is calculated for the proteins BSA and α-lactalbumin and the results are given in Table 7-5.

	BSA	α-lactalbumin
Source 30Q	$1.24 \cdot 10^{-5}$	$4.18 \cdot 10^{-5}$
Q-Sepharose XL	$2.06 \cdot 10^{-3}$	$1.65 \cdot 10^{-3}$
Q-HyperD F	$1.07 \cdot 10^{-5}$	$4.91 \cdot 10^{-5}$
Fractogel EMD TMAE 650(s)	$1.84 \cdot 10^{-5}$	$5.05 \cdot 10^{-5}$

Table 7-5: The constant in the expression α = constant $\cdot d_p^{-2/3}$ calculated from the α values determined from the correlation of the reduced plate heights.

From Table 7-5 it is observed that the values for the constant for both BSA and α-lactalbumin on Source 30Q, Q-HyperD F and Fractogel EMD TMAE 650(s) are very close and within the uncertainty. The values calculated for the constant on Q-Sepharose XL differ considerably from the values calculated for the other three columns. This may be due to the strong correlation between α and k_p. α for BSA on Q-Sepharose XL is determined from a single superficial velocity so that the uncertainty may be rather high due to the strong correlation between α and k_p. For α-lactalbumin α is determined from four superficial velocities, but from Figure 7-6 it is seen that the plateau at low equilibrium ratio is not reached. This may cause some uncertainty of the α and k_p values resulting in a too high α value.

Diffusion coefficients

In order to compare the mass transfer coefficients obtained on the different columns, the diffusion coefficients are calculated by the relation $k_i = 10 D_i/d_p$ where i is p or s. Because of the general lack of data for the β-lactoglobulins at high equilibrium ratio the diffusion coefficients are only calculated for BSA and α-lactalbumin. The calculated values are given in table 7-6.

	BSA		α-lactalbumin	
	$D_p \cdot 10^7$ [cm²/s]	$D_s \cdot 10^8$ [cm²/s]	$D_p \cdot 10^7$ [cm²/s]	$D_s \cdot 10^8$ [cm²/s]
Source 30Q	1.56	3.54	2.62	6.60
Q-Sepharose XL	6.16	0.693	2.14	4.26
Ceramic Q-HyperD F	16.7	2.03	3.57	2.37
Fractogel EMD TMAE 650(s)	0.693	4.56	2.15	19.4

Table 7-6: Pore and solid diffusion coefficients for BSA and α-lactalbumin on the four anion exchangers.

Comparison with the literature

Fernandez et al. determined solid diffusion coefficients with BSA and α-lactalbumin on Q-HyperD F and Q-HyperD M. The only difference between the Q-HyperD F and M media is the particle size of 50 μm and 75 μm, respectively. They determined the solid diffusion coefficients both by batch uptake in agitated contactors [Fernandez et al., 1996 (169-183)] and by breakthrough experiments in shallow beds [Fernandez et al., 1996 (185-198)], and they found the same values by both methods. The values are given in table 7-7.

	$D_s \cdot 10^8$ [cm²/s]	
	BSA	α-lactalbumin
Q-HyperD F	0.92	---
Q-HyperD M	0.92	1.6

Table 7-7: Solid diffusion coefficients determined by Fernandez et al. [Fernandez et al., 1996 (169-183) and (186-198)].

The solid diffusion coefficient for BSA is a little lower than the value determined in this work. If it is taken into account that the solid mass transfer coefficient determined by Hansen et al. 1998 was also lower, the value determined in this work is probably a little too high. The solid diffusion coefficient for α-lactalbumin determined by Fernandez et al. is closer to the value determined in this work, than the diffusion coefficient for BSA. Probably because the uncertainty of the diffusion coefficient determined for α-lactalbumin in this work is lower than for BSA, due to the larger amount of experimental data at high equilibrium ratio.

On FF Sepharose (this media is similar but not identical to Q-Sepharose XL) diffusion coefficients for α-chymotrypsinogen A, Mw = 24 kD, and ribonuclease A, Mw = 13 kD, have been determined [Natarajan et al., 2000].

	$D_p \cdot 10^7$ [cm^2/s]	$D_s \cdot 10^8$ [cm^2/s]
α-chymotrypsinogen A	2.9	1.45
Ribonuclease A	3.2	4.85

Table 7-8: Diffusion coefficients determined by Natarajan et al. [Natarajan et al., 2000].

If the solid diffusion coefficients determined for BSA and α-lactalbumin on Q-Sepharose XL are compared to the solid diffusion coefficients determined by Natarajan et al. for α-chymotrypsinogen A and ribonuclease A, it is observed that the solid diffusion coefficients as expected decrease with increasing molecular weight. The molecular weights for ribonuclease A and α-lactalbumin are very close and the solid diffusion coefficients are also very close. The same trend is not observed for the pore diffusion coefficients. The diffusion coefficients for BSA and α-lactalbumin are of the same order of magnitude as the diffusion coefficients determined for chymotrypsinogen A and ribonuclease A, but they increase with increasing molecular weight. The pore diffusion coefficients for α-chymotrypsinogen A and ribonuclease A decrease with increasing molecular weight as expected. The same is observed for Ceramic Q-HyperD F where the pore diffusion coefficient determined for BSA is higher than the one determined for α-lactalbumin, and the solid diffusion coefficient is lower. The solid and pore diffusion coefficients determined for BSA and α-lactalbumin on Source 30Q and Fractogel EMD TMAE 650(s) both decrease with increasing molecular weight.

8 SCALE-UP

The production of biomolecules requires the use of large scale chromatography. The method development and the parameter estimation are done in a small column to reduce the process time, buffer and sample consumption. When the method has been developed and the process requirements have been fulfilled in the small column, it has to be transferred to a larger scale. This is often done by keeping the column length constant and increase the diameter of the column [Avci et al., 2000; Williams et al. 2002]. In the following some rule of thumb guidelines for scaling where both the diameter and the column length are changed will be given. The only limitations to the scaling are a minimum requirement for the column diameter and a maximum column length determined by the pressure drop.

8.1 Theory

The van Deemter equation can be used to derive rule of thumb guidelines for scaling of chromatographic columns. In order to use the van Deemter equation for scale-up it is convenient to adopt the simple form of the van Deemter equation:

$$H = A_H + \frac{B_H}{v} + C_H v \qquad \textbf{(8-1)}$$

where $A_H = 5\lambda d_p$. $B_H = 2D_m$ and $C_H = 2\left(\frac{1+A}{p+1+A}\right)^2 \cdot \frac{\varepsilon}{6(1-\varepsilon)K_m}$. It should be mentioned that narrow tubes give increased axial dispersion, and $A = 5\lambda d_p$ is only valid when $d_{col} > 200d_p$. C_H depends on the eluting conditions and the overall mass transfer coefficient. The B_H term is normally not important in liquid chromatography, and if the B_H term is neglected the equation is reduced to

$$H = A_H + C_H v \qquad \textbf{(8-2)}$$

The time constant for the flow t_0 is given as

$$t_0 = \frac{\varepsilon V_{col}}{Q} = \frac{l_{col}}{v} \qquad \textbf{(8-3)}$$

From Equation 8-3 it is seen that the time scale for flow can be kept constant by scaling the volumetric flow rate to εV_{col}. On the assumption that the interstitial porosity is constant the time scale can be kept constant by scaling the volumetric flow rate to the column volume.

The time scale for mass transfer (except for slim tubes and shallow beds) will essentially be independent of the flow rate, because the band broadening due to mass transfer resistance (the C_H term) predominates, when compared to dispersion (the A_H term). The mass transfer is controlled by the intraparticle mass transfer, which is independent of the flow rate. Only the external mass transfer depends on the flow rate. When slim tubes ($d_{col} < 200d_p$) are used the axial dispersion is increased, and band broadening due to mass transfer resistance will not predominate, when compared to dispersion. The time scale for mass transfer therefore depends on the flow rate. When very short columns (shallow beds) are used the A_H term will also be dominating and the time scale for mass transfer will not be independent of the flow rate.

To preserve the plate numbers when scaling up or down takes place, a simple relation between the column length and the time constant for flow can be derived.
By inserting Equation 8-3 in Equation 8-2 the number of plates is given as

$$N = \frac{l_{col}}{H} = \frac{l_{col}}{A_H + C_H v} = \frac{1}{\frac{A_H}{l_{col}} + \frac{C_H}{t_0}} \qquad \textbf{(8-4)}$$

If the number of plates two columns 1 and 2 has to be identical, $N_1 = N_2$, when the column length is increased from $l_{col,1}$ to $l_{col,2}$ the time constant for the flow has to be

$$t_{0,2} = \frac{t_{0,1}}{1 + \frac{A_H}{C_H}\left(\frac{l_{col,2} - l_{col,1}}{l_{col,2}\, l_{col,1}}\right) t_{0,1}} \qquad \textbf{(8-5)}$$

From the equations it can be concluded that

- If $l_{col,2} > l_{col,1}$ and $N_2 = N_1$ then $t_{0,2} < t_{0,1}$
- If $l_{col,2} > l_{col,1}$ and $t_{0,2} = t_{0,1}$ then $N_2 > N_1$

8.2 Experimental

Isocratic elutions were performed with BSA and linear gradient elutions were performed with β-lactoglobulin A and B. The experiments were performed as described in Section 4.3.
Five columns of different dimensions all packed with Source 30Q were used for the experiments. To achieve identical time scales in the five columns, the flow rate, the gradient length and the load were scaled to the column volume V_{col}.

The isocratic elutions with BSA were performed at a pH of 8 with Cl^--concentrations of 0.20 M and 1.95 M and flow rates of 0.50 V_{col}/min and 1.0 V_{col}/min. The gradient elutions of β-lactoglobulin A and B were performed at a pH of 8 with a linear Cl^--concentration gradient from 72 mM to 326 mM and a gradient length of 32 V_{col}.

8.3 Results and Discussion

To distinguish between the columns, each column is represented by a color and in all the figures the colors are as follows:

- V_{col} = 0.98 ml
- V_{col} = 1.35 ml
- V_{col} = 8.07 ml
- V_{col} = 9.39 ml
- V_{col} = 55.61 ml

Isocratic elution of BSA

The flow rate and the load were scaled to the column volume to achieve identical time scales in all the columns. The chromatograms from the isocratic elutions of BSA are shown in Figures 8-1 to 8-3. In order to compare the peak shapes and the retention times, the retention times have been corrected by the dead times. (The dead times have been calculated from the dead volumes as $t_{dead} = V_{dead}/Q$).

Tables 8-1 to 8-3 give the column data, the retention times and the plate numbers corresponding to the chromatograms in Figures 8-1 to 8-3.

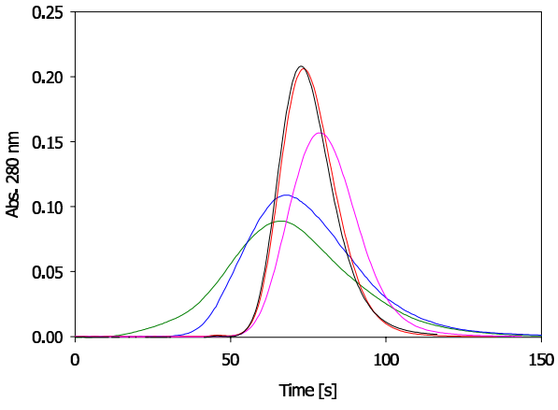

Figure 8-1: Isocratic elution of BSA on Source 30Q. Q = 0.50 V_{col}/min and c_{Cl^-} = 1.95 M.

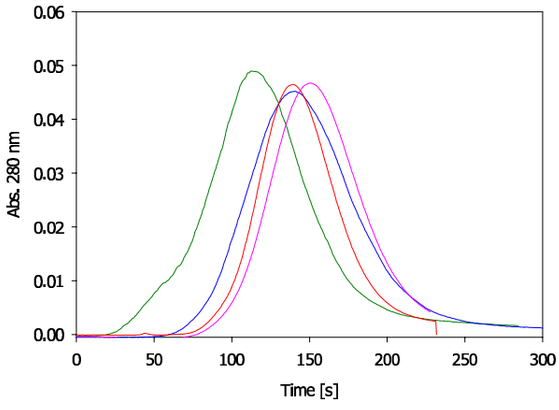

Figure 8-2: Isocratic elution of BSA on Source 30Q. Q = 0.50 V_{col}/min and c_{Cl^-} =0.20 M.

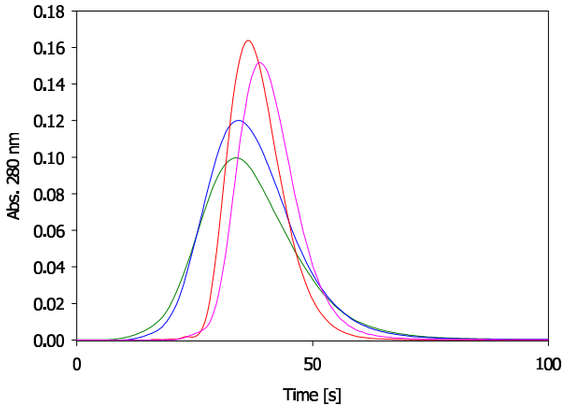

Figure 8-3: Isocratic elution of BSA.
Q = 1.00 V_{col}/min and c_{Cl^-} = 1.95 M.

Cl^--concentration 0.20 M								
Q	[V_{col}/min]	0.50	0.50	0.50	0.50	1.00	1.00	1.00
V_{col}	[ml]	0.98	1.35	8.07	9.39	0.98	8.07	9.39
l_{col}	[cm]	4.99	1.72	10.27	4.67	4.99	10.27	4.67
d_{col}	[cm]	0.5	1.0	1.0	1.6	0.5	1.0	1.6
v	[cm/min]	2.50	0.86	5.14	2.34	4.99	10.27	4.67
t_R	[min]	2.11	2.61	2.43	2.60	1.14	1.24	1.32
N		15.60	17.05	30.19	23.89	11.55	15.97	15.74

Table 8-1: Retention times and plate numbers for isocratic elution of BSA on Source 30Q at c_{Cl^-} = 0.20 M.

Cl^--concentration 1.95 M						
Q	[V_{col}/min]	0.50	0.50	0.50	0.50	0.50
V_{col}	[ml]	0.98	1.35	8.07	9.39	55.61
l_{col}	[cm]	4.99	1.72	10.27	4.67	17.70
d_{col}	[cm]	0.5	1.0	1.0	1.6	2.0
v	[cm/min]	2.50	0.86	5.14	2.34	8.85
t_R	[min]	1.25	1.30	1.25	1.33	1.27
N		16.33	24.46	66.28	53.16	57.94

Table 8-2: Retention times and plate numbers for isocratic elution of BSA on Source 30Q at c_{Cl^-} = 1.95 M.

Cl^--concentration 1.95 M						
Q	[V_{col}/min]	0.25	1.00	1.00	1.00	1.00
V_{col}	[ml]	55.61	0.98	1.35	8.07	9.39
l_{col}	[cm]	17.70	4.99	1.72	10.27	4.67
d_{col}	[cm]	2.0	0.5	1.0	1.0	1.6
v	[cm/min]	4.43	4.99	1.72	10.27	4.67
t_R	[min]	2.46	0.63	0.67	0.64	0.68
N		96.85	17.92	24.75	36.52	37.92

Table 8-3: Retention times and plate numbers for isocratic elution of BSA on Source 30Q at c_{Cl^-} = 1.95 M.

From Figures 8-1 to 8-3 and Tables 8-1 to 8-3 it is observed that the retention times are almost identical in the columns, when the flow rate and the load are scaled to the column volume. The small variances in the retention times are probably caused by uncertainties in the dead volumes and small variances in the interstitial porosities. By scaling to the column volume identical retention times are only obtained, if the interstitial porosities are the same in all the columns. To obtain identical retention times when the interstitial porosities are not identical, the flow rate and the load should be scaled to the void volume (εV_{col}). The relative uncertainties for the dead volumes and the column volumes are smallest for the three largest columns (V_{col} = 8.07 ml, 9.39 ml and 55.61 ml). If the retention times obtained in these three columns are compared, it is observed that the retention time of the column with V_{col} = 9.39 ml is a little larger than for the two other columns. This could be due to the scaling, because the interstitial porosity of this column is 0.47 and the two other columns only have an interstitial porosity of 0.40. The larger interstitial porosity will result in larger retention time, when the flow rate is scaled to the column volume and not the void volume.
From Figures 8-1 to 8-3 and Tables 8-1 to 8-3 it is also observed that the variances of the peaks decrease with increasing column length except for the small narrow column, which means that the plate number, and thus the column efficiency, increases with increasing column length.

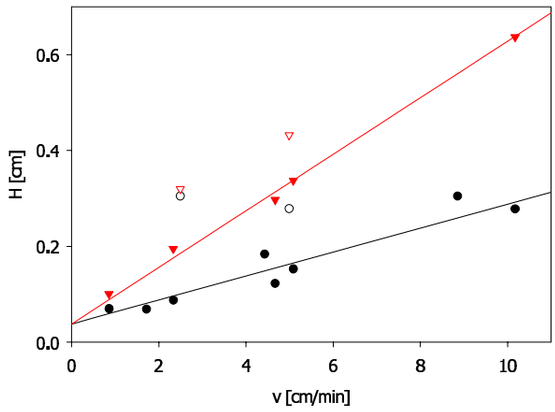

Figure 8-4: **van Deemter plots corresponding to the isocratic scale-up experiments in tables 8-1 to 8-3. The lines represents the model and the symbols represents the experimental data.**
Symbols and colors: • c_{Cl^-} = 0.20 M and ▼ c_{Cl^-} = 1.95 M. The open symbols represents the data obtained at the column with V_{col} = 0.98 ml.

From Figure 8-4 it is seen that the plate heights depend strongly on the eluting conditions. This is caused by the C term in the van Deemter equation, the slope of the lines. The A term (related to the axial dispersion) in the van Deemter equation, the intercept of the lines, is constant.
The plate heights obtained by the smallest column differ from the straight lines, because of increased axial dispersion due to the diameter of the column being too small; $d_{col} < 200d_p$.

Linear gradient elution of β-lactoglobulin A and B

The flow rate, the load and the gradient volume were scaled to the column volume to achieve identical time scales in all the columns. The chromatograms from the linear gradient elutions of β-lactoglobulin A and B are shown in Figures 8-5 and 8-6. In order to compare the peak shapes and the retention times, the retention times have been corrected by the dead times. Tables 8-4 and 8-5 give the column data and the retention times corresponding to the chromatograms in Figures 8-5 and 8-6.

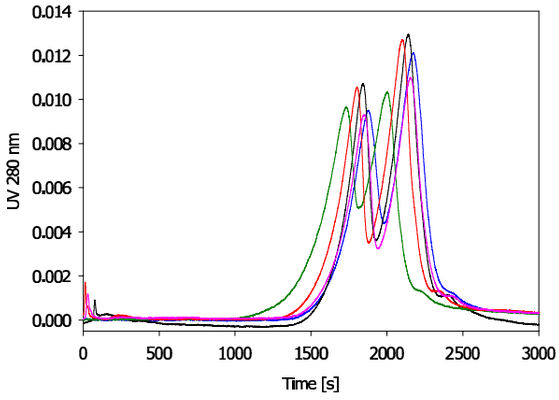

Figure 8-5: Linear gradient elution of β-lactoglobulin A and B on Source 30Q. Q = 0.50 V_{col}/min.

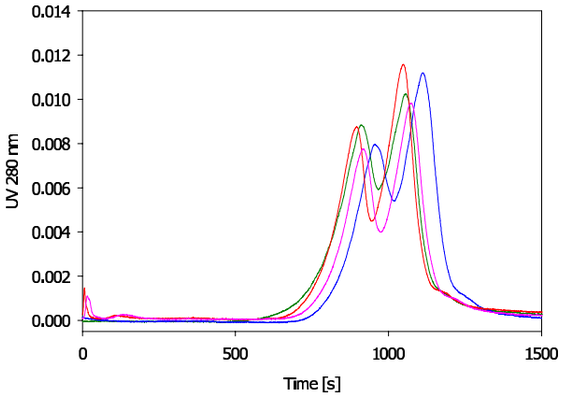

Figure 8-6: Linear gradient elution of β-lactoglobulin A and B on Source 30Q. Q = 1.00 V_{col}/min.

Gradient elution at Q = 0.50 V_{col}/min						
V_{col}	[ml]	0.98	1.35	8.07	9.39	55.61
l_{col}	[cm]	4.99	1.72	10.27	4.67	17.70
d_{col}	[cm]	0.5	1.0	1.0	1.6	2.0
$t_{R, peak1}$	[min]	29.59	31.50	30.03	30.87	30.71
$t_{R, peak2}$	[min]	34.11	36.43	35.03	35.92	35.68
$\Delta t_{R,12}$	[min]	4.52	4.93	5.00	5.05	4.97

Table 8-4: Retention times for gradient elution of β-lactoglobulin A and B on Source 30Q. V_g = 32 V_{col}, Q = 0.50 V_{col}/min.

Gradient elution at Q = 1.00 V_{col}/min					
V_{col}	[ml]	0.98	1.35	8.07	9.39
l_{col}	[cm]	4.99	1.72	10.27	4.67
d_{col}	[cm]	0.5	1.0	1.0	1.6
$t_{R, peak1}$	[min]	15.29	15.89	14.84	15.31
$t_{R, peak2}$	[min]	17.70	18.44	17.41	17.90
$\Delta t_{R,12}$	[min]	2.41	2.55	2.57	2.59

Table 8-5: Retention times for gradient elution of β-lactoglobulin A and B on Source 30Q. V_g = 32 V_{col}, Q = 1.00 V_{col}/min.

As for the isocratic elutions the retention times obtained by gradient elution are very close. By measuring the difference between the retention times of peak 1 and 2, the uncertainty of the dead volumes is eliminated. The small difference between $\Delta t_{R,12}$ for the different columns may by due to the scaling. Both the flow rate and the gradient length are scaled to the column volume and not the void volume. Also for the gradient elutions the smallest column differs considerably from the other four columns, because it is too narrow.

The concept of time scales is a very easy and reliable method for scale-up. It can be used for isocratic and gradient elution no matter if the column length, the diameter or both are changed. The only limitation is a minimum column diameter and a maximum column length. The column diameter has to be more than 200 times the particle diameter. The maximum column length is given by the pressure drop, which must not exceed the limit specified by the manufacturer.

9 CONCLUSION

Different methods for determination of the ion-exchange capacity have been studied. For the batch determination by acid-base titration it was not possible to obtain reproducible results. The in-column determination showed a relatively good repeatability with both acid-base titration and breakthrough curves with nitrate. The ion-exchange capacities determined by the breakthrough experiments with nitrate are in most cases higher than the capacities determined by acid-base titration. The determination with nitrate was chosen in preference to the acid-base determination mainly because of the reproducibility for very small columns, but also because it is very fast and easy to perform. The Q-Sepharose XL and the Q-HyperD F are classified as high-capacity media and the highest ion-exchange capacity is also determined for these two media. The two media are not suited for separation of the four whey proteins but will be very useful in a capture step. Fractogel EMD TMAE 650(s) has a much lower capacity than the other three columns. It may be possible to separate the four whey proteins on Fractogel EMD TMAE 650(s) at a pH of 6, but the best separation of the proteins will be achieved on Source 30Q at a pH of 6, which has an ion-exchange capacity around four times that of Fractogel EMD TMAE 650(s).

The isocratic retention volumes were correlated well by the SMA model. The retention volumes at linear gradient elution were predicted with reasonable precision by the SMA model with the parameters determined from correlation of the isocratic retention volumes.
The highest standard Gibbs energy change was found for Ceramic Q-HyperD F and the smallest for Fractogel EMD TMAE 650(s) which reflects the environment in the pores. Q-HyperD F has the most hydrophilic environment in the pores and Fractogel EMD TMAE 650(s) the most hydrophobic. The standard Gibbs energy change for the proteins primarily reflects the change in the conformation of the protein upon binding but may also reflect typical matrix characteristics. The binding charges of the proteins are related to the size of the proteins, or more precisely the number of sites in the protein that can be ionized. For all four media the largest binding charges are observed for BSA and the smallest for α-lactalbumin. The binding charge of β-lactoglobulin A is a little higher than the binding charge of β-lactoglobulin B. This is because amino acid number 64 is different in the two proteins. In β-lactoglobulin A amino acid number 64 is aspartic acid, which is negatively charged, and in β-lactoglobulin B amino acid number 64 is glycine, which is neutral. β-lactoglobulins A and B also have a different amino acid in position 118. In β-lactoglobulin A it is valine and in β-lactoglobulin B it is alanine, but since both the amino acids are hydrophilic the difference is negligible.

The capacity measurements with BSA on Source 30Q were correlated by the SMA formalism and the shielding factor was determined from the correlations. When one shielding factor was fitted at each pH the model could not correlate the isotherms at the highest Cl^--concentrations. Especially at a pH of 8 the correlations were very poor. A simultaneous correlation of the isocratic retention

volumes and the capacity measurements was made. From this correlation the standard Gibbs energy change, the binding charges and the shielding parameters were fitted. The correlation of the isotherms obtained by this fit shows a reasonably good agreement with the experimental data at all four Cl^--concentrations. The correlation of the isocratic retention volumes got a little worse compared to the fit where only the retention volumes were correlated, but the agreement between the experimental data and the correlations is still reasonable. If the two highest Cl^--concentrations are lowered a little it is possible to improve the correlations of both the isotherms and the isocratic retention volumes, but the uncertainty of the Cl^--concentrations in the buffer cannot justify the lowering of the Cl^--concentrations. Even with the lowering of the Cl^--concentrations it was not possible to correlate the isotherms at a pH of 7 and 8 with one common shielding factor.

From the isocratic retention volumes the reduced plate heights were determined. The largest reduced plate heights were observed for BSA and the smallest for α-lactalbumin. This is due to the size of the proteins, because the mass transfer rate decreases with increasing molecular size.
Where experimental data was available at strong retention a bell-shaped behavior of the reduced plate heights as a function of the equilibrium ratio was observed. The plate heights are constant at the lowest equilibrium ratios, then they increase and attain a maximum before they decrease again.
The plate heights were correlated with the van Deemter equation and an overall mass transfer coefficient. If the overall mass transfer coefficient is described by the film mass transfer coefficient and the pore or solid diffusion model, it is not possible to correlate the bell-shaped behavior, but it can be correlated by the parallel diffusion model. Even the plate heights for which no or few data was available at strong retention could be correlated by the parallel diffusion model, but the uncertainty of the solid mass transfer coefficients determined from these correlations is rather high.
The best data for determination of the mass transfer coefficients was obtained for Q-Sepharose XL. This is probably because the variance of the peaks is not influenced by impurities due to the poor separation skills of the Q-Sepharose XL media.

The concept of time scale was used for scale-up experiments on five columns of different dimensions all packed with Source 30Q. When the time constant for the flow is kept constant and the load is scaled to the column volume, the longer columns give a slightly better performance than the shorter columns, provided that the columns are not too narrow. Scaling by keeping the time scales identical is a very easy and reliable method, which can be used no matter if the column length, the diameter or both are changed. Rules of thumb guidelines can be derived from the simple van Deemter equation.

10 FUTURE WORK

First of all the gradient elutions with α-lactalbumin have to be repeated on the four columns to find out if the deviations between the correlations and the experimental data is caused by a change in the mixer.
Next it would be interesting to see if it is possible to separate the four proteins on Source 30Q by linear gradient elution at a pH of 6 as theoretically predicted by the SMA model.

Some work is still left to be done in the large project before the scope is fulfilled and a complete set of chromatographic data is available for all four columns and proteins. Capacity measurements with BSA on Source 30Q at a pH of 6 and 9 have to be made as well as capacity measurements with the other three proteins. To reduce the amount of experiments the number of pH values could be reduced to two. If experiments are only performed at two pH values a pH of 6 and 9 are suggested in order to represent the largest pH difference. A pH of 6 is especially interesting because, from the experiments in the linear range, it is known to be the only pH value where a separation of the four proteins can be achieved.
When capacity measurements with all four proteins have been made on Source 30Q it is possible to make a simultaneous correlation of the retention volumes and the capacity measurements for all four proteins. In the correlation all the SMA parameters for the proteins and the standard Gibbs energy change for the Cl^--ions should be determined. Due to the strong correlation of the SMA parameters it may be possible to obtain better correlations of the isotherms, when also the standard Gibbs energy for the Cl^--ions is determined from a correlation of retention volumes and capacity measurements. After the determination of the isotherms it will be possible to make some predictions about the preparative separation of the four proteins with a subsequent verification through experiments.

More work has also to be done as regards the determination of mass transport coefficients. The solid mass transfer coefficients have to be determined from non-linear mass transfer. First of all for the proteins where no plate height data is available at strong retention and the solid diffusion coefficient therefore could not be determined. The solid mass transfer coefficients should also be determined from non-linear mass transfer for the proteins for which the coefficient has already been determined from the plate height data to see how consistent the two methods are.
When the work on Source 30Q has been finished it should be repeated on the other three columns, in order to get a complete set of chromatographic data for all four columns.

PART 2

PREFACE

As a part of the fulfillment of the requirements for admission to the candidacy of the Ph.D. degree at the Technical University of Denmark I spent the time from 15 October 2001 to 15 February 2002 at Amersham Biosciences in Uppsala, Sweden.

At Amersham Biosciences I joined the section for Bioprocess System Integration, Separations R&D, with Rolf Hjorth as Section Manager. My supervisors at Amersham Biosciences were: Scientist Thorvald Andersson and Ph.D. Karol Lacki.
I want to thank all in the group for their kindness, and special thanks go to Thorvald Andersson for the joyful time I spent with him and for his patience with me in the laboratory.

The content of this report is the work I did during my stay at Amersham Biosciences. All the experimental work was done at Amersham Biosciences.

SYMBOLS

CV: Column volume

H: Height of a theoretical plate

l_{bed}: Length of the bed

$P_{packing}$: Packing pressure

V_{elu}: Measured retention volume

$V_{forward}$: The volume run through the column before the flow is reversed

$V_{inj.\ point}$: Point of injection

V_{liq} Liquid volume

V_R: Retention volume ($V_{elu} - V_{inj.\ point}$)

$V_{R,cor}$: Retention volume, corrected for the dead volumes

$V_{R,cor,\ bottom}$: Retention volume, corrected for the dead volumes, obtained by injection at the bottom of the column and forward flow

$V_{R,cor,\ top}$: Retention volume, corrected for the dead volumes, obtained by injection at the top of the column and forward flow

V_{void}: Void volume

Q: Volumetric flow rate

Greek Letters

α: Slope of the line through the data points obtained by reversed flow

α_{bottom}: Slope of the line through the data points obtained by reversed flow and injection at the bottom

α_{top}: Slope of the line through the data points obtained by reversed flow and injection at the top

β: Intercept for the line through the data points obtained by reversed flow

β_{bottom}: Intercept with the y-axis for the line through the data points obtained by reversed flow and injection at the bottom

β_{top}: Intercept with the y-axis for the line through the data points obtained by reversed flow and injection at the top

ε: Interstitial porosity

ε_t: Total porosity

σ^2: Variance

σ^2_{bottom}: Variance of the entire bed calculated from the equation obtained for injections at the bottom of the column and reversed flow

$\sigma^2_{bottom} = V_{R,cor,\ bottom} \cdot \alpha_{bottom} + \beta_{bottom}$

Dextran: $\sigma^2_{bottom} = 159.6\ ml \cdot 0.082\ ml + 8.5\ ml^2 = 21.6\ ml^2$

NaCl: $\sigma^2_{bottom} = 507.7\ ml \cdot 0.151\ ml + 10.0\ ml^2 = 86.6\ ml^2$

$\sigma^2_{cor,forw,bottom}$: Variance corrected for the variance of the empty column, obtained by injection at the bottom of the column and forward flow

$\sigma^2_{cor,forw,top}$: Variance corrected for the variance of the empty column, obtained by injection at the top of the column and forward flow

$\sigma^2_{intercept}$: Intercept with the y-axis (offset)

σ^2_{liq}: Variance corresponding to the liquid volume

σ^2_{top}: Variance of the entire bed calculated from the equation obtained for injections at the top of the column and reversed flow

$\sigma^2_{top} = V_{R,cor,top} \cdot \alpha_{top} + \beta_{top}$

Dextran: $\sigma^2_{top} = 157.0\ ml \cdot 0.115\ ml + 6.1\ ml^2 = 24.1\ ml^2$

NaCl: $\sigma^2_{top} = 503.8\ ml \cdot 0.153\ ml + 17.6\ ml^2 = 94.7\ ml^2$

σ^2_{void}: Variance corresponding to the void volume

11 INTRODUCTION

The work at Amersham Biosciences was started in the search for a bed characterization method which is easy to use, fast, cheap and does not destroy the column packing. The reversed flow technique seemed promising as such a method.

In the reversed flow technique, the flow through the column is reversed when the front has reached a specified fraction of the column length. The reversal of the flow makes it possible to distinguish between microscopic and macroscopic factors contributing to the band broadening, because the contributions from macroscopic factors are reversible, while the contributions from microscopic factors are irreversible and additive. By reversing the flow the contribution to band broadening due to macroscopic effects is eliminated and only the contributions from microscopic factors, the structure of the bed, are left. This makes it possible to examine the influence of different factors, e.g. slurry, packing pressure and flow velocity during packing, on the performance of the packed bed and thus find the optimum packing conditions for a given media and column. Further, the performance of a column can be tested after packing without the packing is destroyed.

12 THEORY

Poor efficiency of packed column can have the following reasons [Kaminski, 1992]: (1) Poor structure of the packed bed caused by (a) non plug flow of the mobile phase in the bed or (b) insufficient stable packing of the bed. (2) Incorrect design of the flow distributors which can cause (a) distortion of the zone of the injected sample solution or (b) significant band broadening. The reversed flow technique makes it possible to distinguish between the two reasons for poor efficiency of the packed bed. Two different groups of factors contribute to band broadening: microscopic and macroscopic factors. The structure of the packed bed belongs to the microscopic factors and the design of the flow distributor belongs to the macroscopic factors. The microscopic factors contributing to band broadening are: intraparticle diffusion, boundary layer mass transfer, axial dispersion and adsorption-desorption kinetics [Moscariello et al., 2001]. In a linear system the effects of these four factors are additive, and if a non-binding tracer is chosen there will be no broadening effect due to adsorption-desorption kinetic.

The flow in the packed bed and in the flow distributors normally takes place at a very low Reynolds number, Re << 1. Such a flow is governed by the creeping flow equation of motion $\nabla^2 \upsilon = 0$ and the continuity equation $(\nabla \cdot \upsilon) = 0$ [Moscariello et al., 2001]. Such creeping flows are reversible in that they change sign but not magnitude with the sign of the driving pressure. From this it follows that effects due to macroscopically non-uniform flow will be reversible [Roper et al., 1995]. Thus by reversing the flow, contributions to band broadening due to the flow variations in the distributors and in the packing will be eliminated in the resulting effluent. The microscopic factors are additive and when the flow is reversed, the band broadening due to the microscopic effects will be twice that occurring at the end of the normal flow period [Teeters et al., 2002].

The variance, the second moment, of an effluent peak resulting from a small pulse injection of a non-binding tracer will be:

Forward (normal) flow: $\sigma^2_{forward,total} = \sigma^2_{macroscopic\,effects} + \sigma^2_{microscopic\,effects} \approx \sigma^2_{distributors} + \sigma^2_{bed}$ **(12-1)**

Reversed flow: $\sigma^2_{reversed,total} = \sigma^2_{microscopic\,effects} \approx \sigma^2_{bed}$ **(12-2)**

If the packing conditions are kept constant and only the packing length is varied, a plot of the total variance vs. the bed length will result in a linear correlation if the bed is homogeneous. The correlation between the bed length and the variances for the reversed flow experiments, where the flow is reversed at half the mean residence time, will then be a straight line through (0,0). The correlation between the bed length and the variances for the forward flow experiments will also be a straight line and the y-intercept will be equal to $\sigma^2_{distributor}$. The contributions due to packing inhomogeneity are reversible and will therefore only contribute to the band broadening for the

forward flow experiments. A comparison of the slopes of the forward and the reversed flow experiments will quantify the effects of macroscopic packing inhomogeneity.

If instead the flow is reversed in different places in the column and the variances are plotted vs. the retention volume, the correlation will be linear if the bed is homogeneously packed. A comparison of the slopes of the lines for columns packed at different pressures will quantify the effect of the packing pressure on the performance of the bed.

13 EQUIPMENT

The column used was a FineLINE 70 with adjustable length and an inner diameter of 7.0 cm. The experiments were performed by a Controller LCC-501 Plus with two P-6000 pumps. The injections were made by a Superloop 50.0 ml and controlled by a motor valve IMV-7. Three IMV-8 motor valves controlled the flow path through the column. The effluent from the column was analyzed by an UV detector or a refractive index detector. Data was acquired on a computer with FPLC director software.

All the equipment and the media were from Pharmacia LKB/Pharmacia Biotech/Amersham Biosciences.

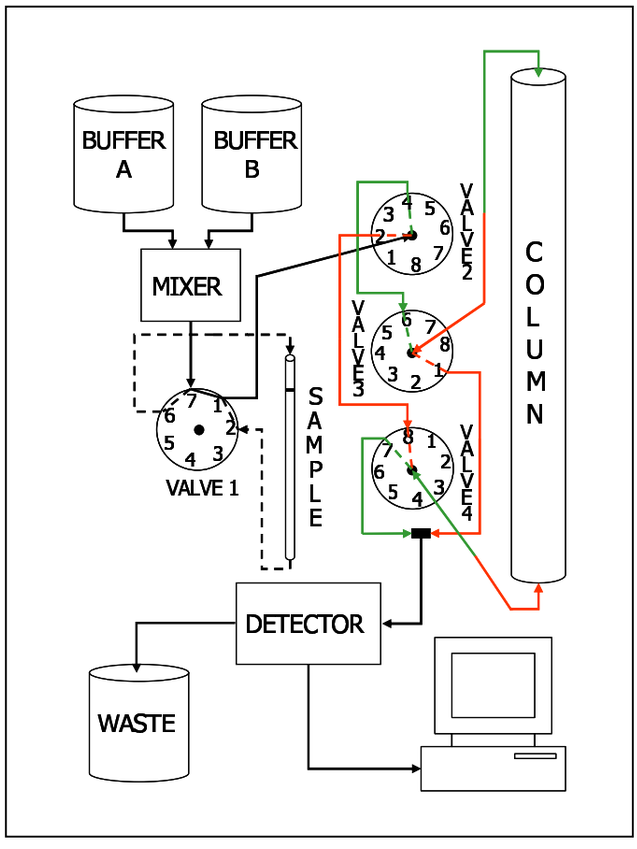

Figure 13-1: The experimental set-up.

When an injection is performed the flow through valve 1 follows the dashed line, and when no injection takes place the flow follows the solid line. From valve 1 the flow enters valve 2. When the flow path is from the bottom to the top of the column, the flow follows the red arrows. From valve 2 it enters valve 4 and continues to the bottom of the column. From the top of the column it enters valve 3 before it reaches the detector and finally the waste can.

When the flow path is from the top to the bottom of the column, the flow follows the green arrows. From valve 2 it enters valve 3 and continues to the top of the column. From the bottom of the column it enters valve 4 before it reaches the detector and finally the waste can.

14 DETERMINATION OF DEAD VOLUMES

Before any experiments on the packed columns were performed the dead volumes in the system were determined. All dead volumes were determined by injection at the bottom of the column. For the dead volume determined without a column, the same flow path as with the column present was used. The dead volume from the injection to the UV detector was determined by injection of a small pulse of 0.75 M $NaNO_3$ in a 1.0 M $NaNO_3$ buffer. The volume was determined without a column by connecting the tubes from the column inlet and outlet. The volume incl. the empty column was determined with the top and the bottom distributor plates touching. The dead volume of the column found in this way was compared to the dead volume calculated from a drawing with measurements of the column, and very good agreement was found.
The dead volume from injection to the column inlet was determined by connecting the column inlet tube direct to the UV detector and injecting a small pulse of $NaNO_3$. The dead volume in the bottom of the column to the distributor was calculated from the drawing with measurements. The dead volume of the flow distributor was found by weighing an empty distributor and a water filled distributor. The dead volume from the injection to the bottom of the bed was obtained by adding these three dead volumes.
The volume from the bottom of the bed to the UV detector was determined by adding the dead volume of the flow distributor, the dead volume of the bottom of the column and the volume of the tubes and the valves from the column inlet to the UV detector. The volume in the tubes and the valves was determined by connecting the inlet tube to the sample injection valve and inject a small pulse of $NaNO_3$.
To acquire the true retention volumes of the bed the retention volumes obtained by normal elution are corrected by the dead volume of the system incl. the empty column. The retention volumes obtained by reversed flow are corrected by the sum of the dead volume from the injection to the bed and the dead volume from the bed to the UV detector.

The measured and the calculated dead volumes are given in Appendix H.I. For the measured dead volumes the corresponding variances are also given. The determined dead volumes and variances are as follows:

Measured values:
V_{sys} = 2.10 ml
σ_{sys} = 0.28 ml^2
$V_{sys+col}$ = 12.06 ml
$\sigma_{sys+col}$ = 19.18 ml^2
$V_{distributor}$ = 2.10 ml
$V_{inj-col}$ = 1.69 ml (measured by direct connection to the UV detector)
$\sigma_{inj-col}$ = 0.24 ml^2 (measured by direct connection to the UV detector)

$V_{inj\text{-}col*}$ = 1.90 ml (measured by direct connection to the conductivity sensor)
$\sigma_{inj\text{-}col*}$ = 0.23 ml^2 (measured by direct connection to the conductivity sensor)

Calculated values:
$V_{col,empty}$ = 10.23 ml
$V_{top\ adaptor}$ = 7.54 ml
V_{bottom} = 2.69 ml
$V_{col\text{-}UV}$ = 1.32 ml
$V_{inj\text{-}bed,bottom}$ = 4.38 ml
$V_{inj\text{-}bed,top}$ = 9.23 ml
$V_{bed,bottom\text{-}UV}$ = 4.01 ml
$V_{bed,top\text{-}UV}$ = 8.86 ml

A comparison of the measured and the calculated volumes of the empty column shows a good agreement. From the measured values the volume of the empty column is:
V_{col} = 12.06 ml – 2.10 ml = 9.96 ml and the calculated value is 10.23 ml. With this good agreement it was decided to use the measured value for the system including the empty column, $V_{sys+col}$ = 12.06 ml, because it was estimated that a value from a single measurement was more precise than a value from both a measurement and a calculation.

The dead volumes and the variances used for corrections are:

- Forward flow experiments and injection at the bottom or the top of the column:
  $V_{sys+col}$ = 12.06 ml and σ^2 = 18.09 ml^2
- Reversed flow experiments and injection at the bottom of the column:
  $V_{inj\text{-}bed,bottom} + V_{bed,bottom\text{-}UV}$ = 4.38 ml + 4.01 ml = 8.39 ml
- Reversed flow experiments and injection at the top of the column:
  $V_{inj\text{-}bed,top} + V_{bed,top\text{-}UV}$ = 4.38 ml + 4.01 ml = 8.39 ml

The variances determined from the reversed flow experiments are not corrected.

15 THE PROTOTYPE MEDIA

15.1 Experimental

15.1.1 The Columns

A reversed phase prototype chromatographic media was used for the experiments. The columns were packed by use of a 60% slurry of media in 100% 2-propanol and a flow rate of 37.5 ml/min. The packing pressure was varied from 7.2 bars to 21.2 bars. The packing pressure was controlled by a pressure relief valve.

Column no.	$P_{packing}$ [bar]	l_{bed} [cm]	CV [ml]
2	7.2	19.60	754.3
3	7.2	19.73	759.3
6	9.8	18.25	702.3
5	10.0	19.25	740.8
1	14.1	18.70	719.7
8	14.1	17.90	688.9
7	16.9	17.05	656.2
4	21.2	16.05	617.7

Table 15-1: The columns packed with the prototype media.

15.1.2 Buffer and Sample Solutions

The used buffer solutions were 1.0 M $NaNO_3$ and 5% 2-propanol. The two sample solutions were 0.75 M $NaNO_3$ and 1 wt% latex beads in 5% 2-propanol. The sample solution with latex beads was filtered through 0.45 μm filters.

15.1.3 Experimental Measurements

For all experimental measurements a flow rate of 15.0 ml/min (0.39 cm/min) was used and the column was loaded with 1.0 ml sample solution. All the injections were performed at the bottom of the column, and the effluent was analyzed by an UV detector.

After packing the column was equilibrated with 5% 2-propanol until constant UV and conductivity signals were reached.

After equilibration the void volume was determined by a pulse of latex beads (forward flow experiments). Then the reversed flow experiments with latex beads were performed. A pulse of latex beads was injected at the bottom of the column, and after a specified volume the flow through the column was reversed and the latex beads were eluted through the bottom of the column (the former inlet).

After the experiments with latex beads the column was equilibrated with 1.0 M $NaNO_3$ until constant UV and conductivity signals were reached. The total liquid volume was determined by a pulse of 0.75 M $NaNO_3$ in 1.0 M $NaNO_3$, and reversed flow experiments with $NaNO_3$ were performed as with the latex beads.

15.1.4 Fitting and Data Reduction

The first and the second moments of a peak were determined by fitting the response curve to the Exponential Modified Gauss (EMG) function. Except for the peaks obtained by latex beads by the reversed flow experiments. Due to the shape of these peaks, the non-sharp front, it was not possible to use the EMG function for the fits. Therefore, the Pearson VII function was used to fit these peaks. An example of the peak shapes from the reversed flow experiments is shown in Figure 15-1.

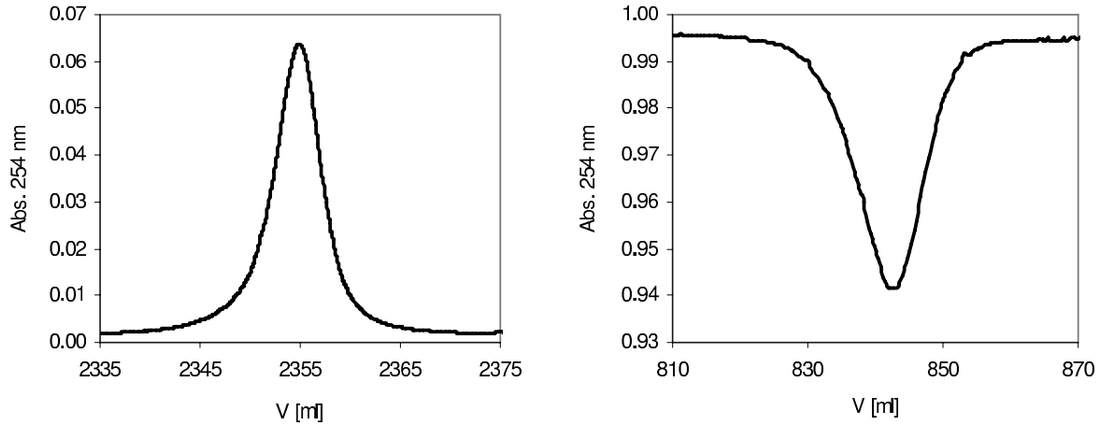

Figure 15-1: Example of peak shapes from reversed flow experiments with nitrate (left) and latex beads (right) on the prototype media.

The first and the second moments of the Pearson VII function were determined by numerical integration.

The retention volumes were calculated by subtracting the dead volumes from the first moment. The variances under normal eluting conditions were calculated by subtracting the variances measured by an empty column from the second moment. The variances measured by the empty column include both the contributions from the system and the column. The variances obtained by reversed flow experiments are not corrected in any way.

15.2 Void Volume, Liquid Volume and Porosities

The experimental data for determination of the void and the liquid volumes with corresponding variances is given in Appendices H.II and H.III. For some of the columns two tables with data for determination of the void volume are given. The data in the first table is obtained before any experiments with $NaNO_3$ are performed, and the data in the second table is obtained after determination of the liquid volume and reversed flow experiments with $NaNO_3$. The data is given in two tables because it was observed that the bed had changed after the nitrate experiments. The observations concerning these changes are described in Chapter 15.6.

Column no.	$P_{packing}$ [bar]	CV [ml]	Before nitrate experiments V_{void} [ml]	σ^2_{void} [ml^2]	ε	After nitrate experiments V_{void} [ml]	σ^2_{void} [ml^2]	ε
2	7.2	754.3	180.0	13.4	0.24	---	---	---
3	7.2	759.3	185.9	49.2	0.24	197.5	70.9	0.26
6	9.8	702.3	167.6	74.0	0.24	185.9	40.6	0.26
5	10.0	740.8	202.7	37.2	0.27	200.0	66.8	0.27
1	14.1	719.7	171.0	6.3	0.24	170.1	22.9	0.24
8	14.1	688.9	143.1	10.8	0.21	137.3	39.8	0.20
7	16.9	656.2	148.3	24.1	0.23	138.7	14.3	0.21
4	21.2	617.7	104.4	38.2	0.17	124.5	24.5	0.20

Table 15-2: Void volumes, variances and interstitial porosities for the eight columns with the prototype media.

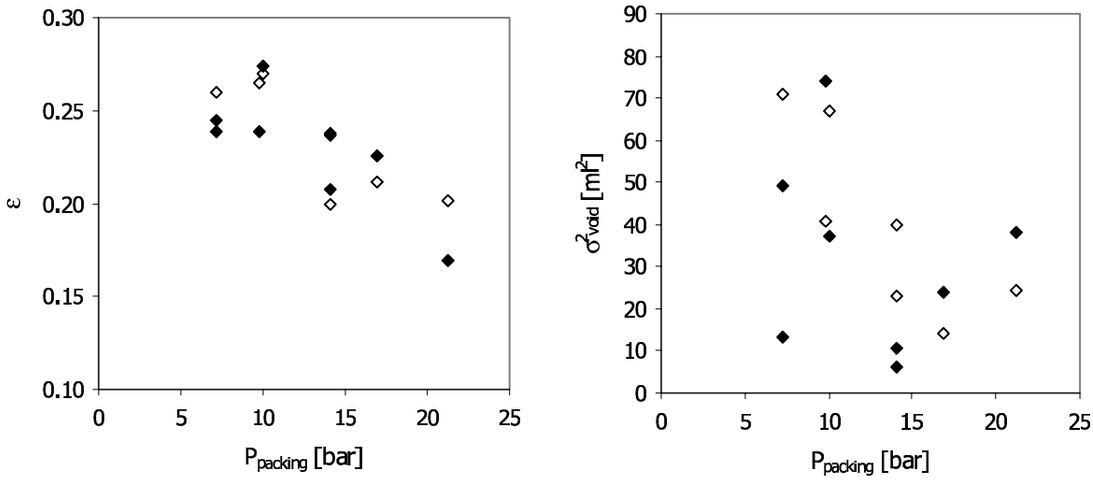

Figure 15-2: The interstitial porosity (left) and the variances for the forward flow experiments with latex beads (right) as functions of the packing pressure for the prototype media. Before nitrate experiments ♦, after nitrate experiments ◇.

From Figure 15-2 it is seen that the interstitial porosity is approximately constant up to a pressure of around 15 bars where the porosity starts to decrease when the pressure is increased. The porosities are very low, especially the porosities determined before the nitrate experiments. This means that the prototype particles are compressible, and according to the Amersham Biosciences the particles can be compressed up to 25%.

It is not possible to find any tendency in the variances as a function of the packing pressure. It was expected that the variance would decrease when the packing pressure was increased, because the interstitial porosity decreases, but it is not possible to draw any conclusion from the presented measurements.

After unpacking the media from the columns, it was examined if the particles were broken during the packing. The used media was allowed to settle and samples were taken from the supernatant and from a suspension of the particles. The size distribution in the samples was determined to see

if the particles were broken. For all the samples, except the ones from the media used at 7.2 and 14.1 bars, the size distribution was very narrow. Only one peak with a maximum at 13.7 μm was detected, so no particles were broken. For the samples from the media used for columns at 7.2 and 14.1 bars a large peak at 13.7 bars was detected, but also some small peaks were detected. The largest of the small peaks was detected around 2.5 μm. This indicates that a small part of the particles was broken. The samples were then studied in electron microscope, and here it became clear that a small part of the particles was broken. After this observation the media was only used for column packing once. It is not possible to tell if the particles were broken during unpacking of the first column packed at 7.2 bars or during packing or unpacking of the second column (packed at 14.1 bars).

The total dead volume $V_{sys+col}$ is measured by $NaNO_3$ and the much larger latex beads may be excluded in some parts of the system that are accessible for the smaller nitrate ions. This will result in a lower total dead volume for the latex beads and an underestimation of the interstitial porosity. But even if the void volumes are not corrected by the total dead volume, some of the interstitial porosities would still be lower than the theoretical limit for monosized beads of 0.26. Thus, this hypothesis can only in combination with other factors explain the low interstitial porosities measured.

Column no.	$P_{packing}$ [bar]	CV [ml]	V_{liq} [ml]	σ^2_{liq} [ml^2]	ε_t
3	7.2	759.3	589.3	250.6	0.78
6	9.8	702.3	537.3	95.3	0.77
5	10.0	740.8	571.5	163.7	0.77
1	14.1	719.7	548.6	420.4	0.76
8	14.1	688.9	496.0	226.3	0.72
7	16.9	656.2	525.1	168.6	0.80
4	21.2	617.7	454.0	117.7	0.74

Table 15-3: Liquid volumes, variances and total porosities for the eight columns with the prototype media.

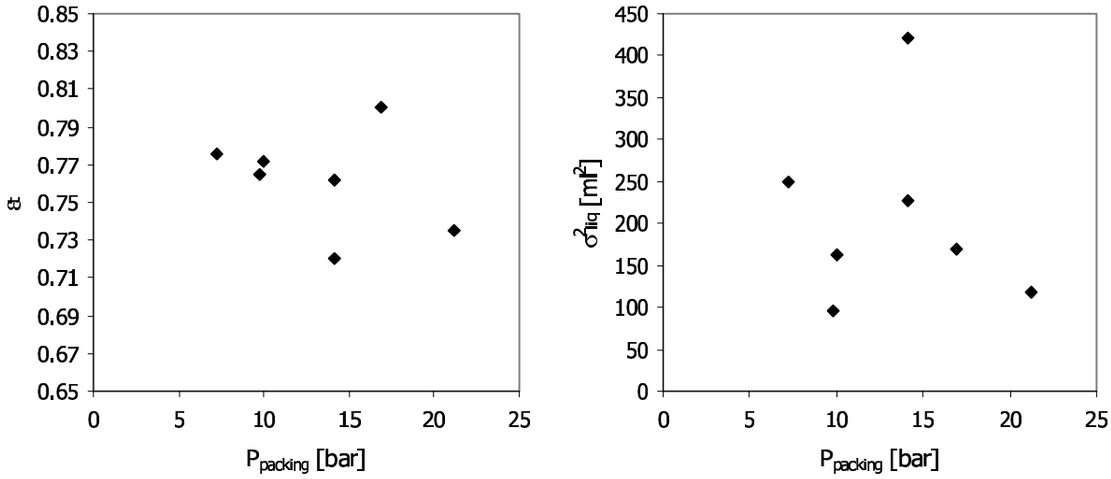

Figure 15-3: The total porosity (left) and the variances for the experiments with nitrate (right) as functions of the packing pressure for the prototype media.

There is some scattering in the total porosity data (Figure 15-3). But as for the interstitial porosity, it seems that the porosity is independent of the packing pressure up to around 15 bars and then decreases when the packing pressure is further increased. In the variance data there is also some scattering, but it seems that the variance, as the porosity, is constant up to 15 bars and then decreases when the pressure is further increased. As expected, the total porosity and the variance show the same pattern. When the porosity is constant the variance is also constant, and when the porosity decreases the variance also decreases.

15.3 Reversed Flow Experiments with Latex Beads on the Prototype Media

All the experimental data is given in Appendix H.IV.

To compare the columns the retention volumes are made dimensionless: $\frac{V_{R,cor.}}{2V_{void}}$

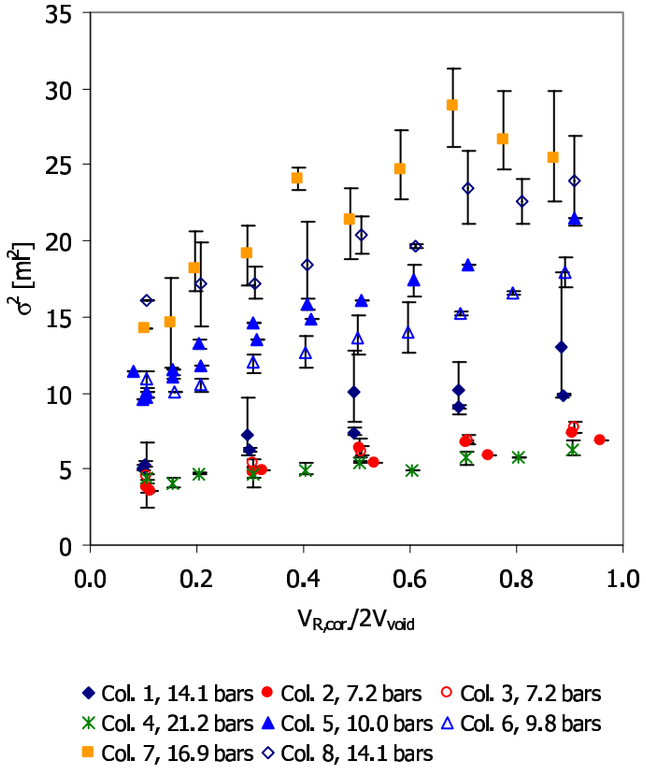

Figure 15-4: The variance as a function of the dimensionless retention volume for the reversed flow experiments with latex beads on the prototype media.

From Figure 15-4 it is not possible to find any connection between the packing pressure and the variances. The highest variances are obtained by column 7, packed at 16.9 bars, and the lowest variances are obtained by column 2, 3 and 4 packed at 7.2 and 21.2 bars. Columns 1 and 8 are packed at 14.1 bars, but the difference between the variances obtained by the two columns is very large. So from the reversed flow experiments with latex beads it is not possible to find any relation between the packing pressure and the performance of the bed.

If the variances obtained by the forward and the reversed flow experiments are compared, it is observed that the variances obtained by the forward flow experiments, for most of the columns, are much higher than the variances obtained by the reversed flow experiments. Only for columns

1, 7 and 8 the variances obtained by the forward flow experiments are of the same size as the ones obtained by the reversed flow experiments.

For most of the columns the correlation between the variance and the dimensionless retention volume seems to be linear.

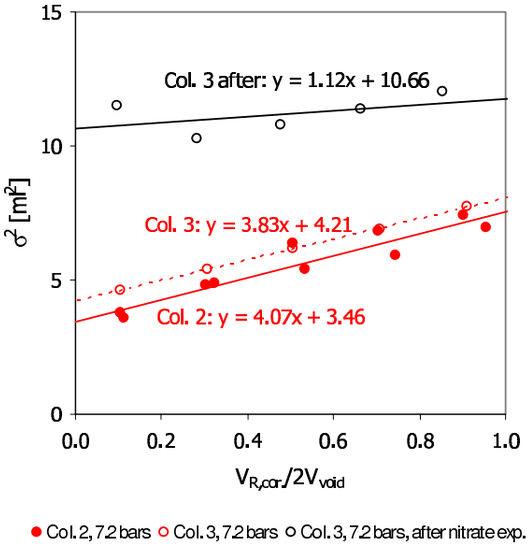

Figure 15-5: Reversed flow experiments with latex beads on columns 2 and 3. On column 3 experiments are performed both before and after the experiments with nitrate.

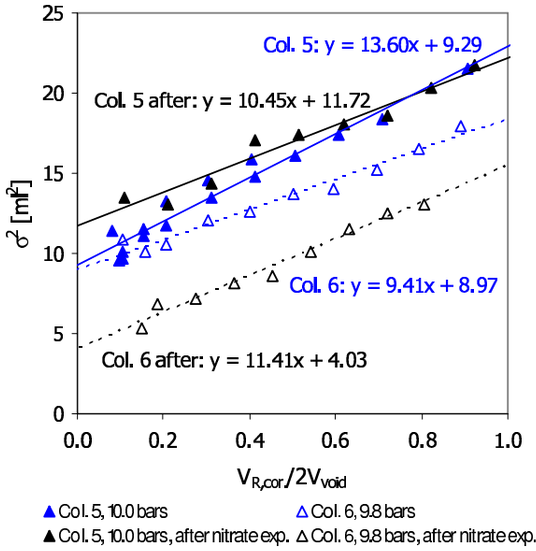

Figure 15-6: Reversed flow experiments with latex beads on columns 5 and 6. On both columns experiments are performed both before and after the nitrate experiments.

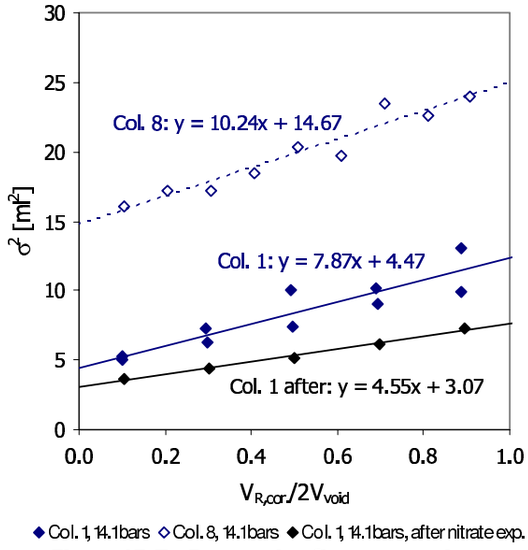

Figure 15-7: Reversed flow experiments with latex beads on columns 1 and 8. On column 1 experiments are performed both before and after the experiments with nitrate.

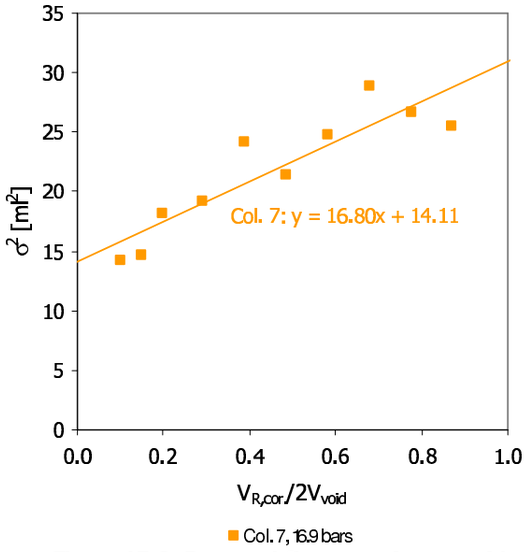

Figure 15-8: Reversed flow experiments with latex beads on column 7.

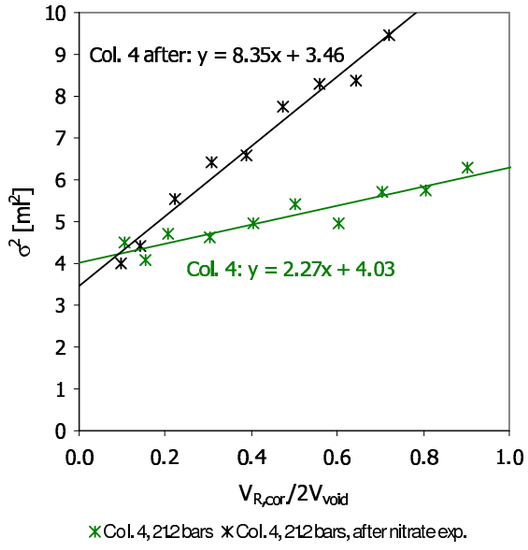

Figure 15-9: Reversed flow experiments with latex beads on column 4. Experiments are performed both before and after the experiments with nitrate.

Column no.	$P_{packing}$ [bar]	CV [ml]	$\sigma^2_{intercept, before}$ [ml²]	$\sigma^2_{intercept, after}$ [ml²]	$Slope_{before}$ [ml²]	$Slope_{after}$ [ml²]
2	7.2	754.3	3.5	---	4.1	---
3	7.2	759.3	4.2	10.7	3.8	1.1
6	9.8	702.3	9.0	4.0	9.4	11.4
5	10.0	740.8	9.3	11.7	13.6	10.5
1	14.1	719.7	4.5	3.1	7.9	4.6
8	14.1	688.9	14.7	---	10.2	---
7	16.9	656.2	14.1	---	16.8	---
4	21.2	617.7	4.0	3.5	2.3	8.4

Table 15-4: Intercept and slope of the linear relation between the variances and the dimensionless retention volumes for the reversed flow experiments with latex beads in the eight columns with the prototype media.

From Figures 15-5 to 15-9 it is observed that the variances as a function of the dimensionless retention volume are well represented by straight lines. Thus, the columns are homogeneously packed. Not even at the lowest or the highest packing pressure a density gradient can be observed in the packed beds.

None of the lines goes through (0,0), as expected, if the macroscopic effects are reversible. Therefore, some effects in the system must be irreversible. The intercept with the y-axis is not a constant value and is not related to the packing pressure. If the offset from zero was caused by a single part of the system, such as the flow distributor the irreversible effects, the offset, could be expected to be constant. This is not the case and therefore it is difficult to find a logic explanation for the offset.

From the columns where experiments are also made after the experiments with nitrate it can be seen that the columns somehow change. The variances measured before and after the nitrate experiments are different, but no clear tendency is observed. Sometimes the variances measured

after the nitrate experiments are lower than before the nitrate experiments and sometimes they are higher. The lines are not even parallel.

15.4 Reversed Flow Experiments with $NaNO_3$ on the Prototype Media

All the experimental data is given in Appendix H.V.

To compare the columns the retention volumes are made dimensionless: $\frac{V_{R,cor.}}{2V_{liq}}$

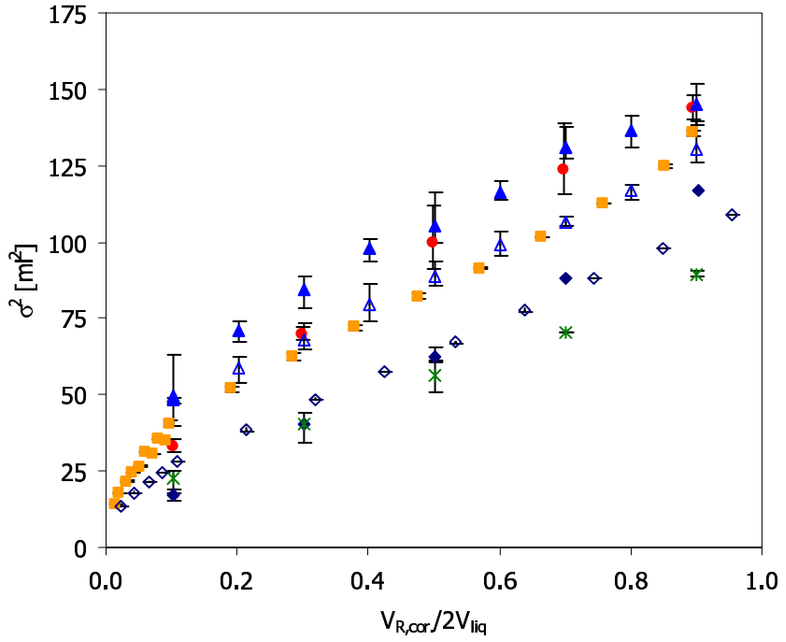

Figure 15-10: The variance as a function of the dimensionless retention volume for the reversed flow experiments with nitrate on the prototype media.

There seems to be a tendency that the variances decrease when the packing pressure is increased (Figure 15-10). The tendency is not unambiguous because the lowest variances are measured by the column packed at 10.0 bars, and the variances measured by the column packed at 16.9 bars are higher than the variance measured by the columns packed at 14.1 bars.

As for the latex beads experiments the variances measured by the forward flow experiments are higher than the variances measured by the reversed flow experiments.

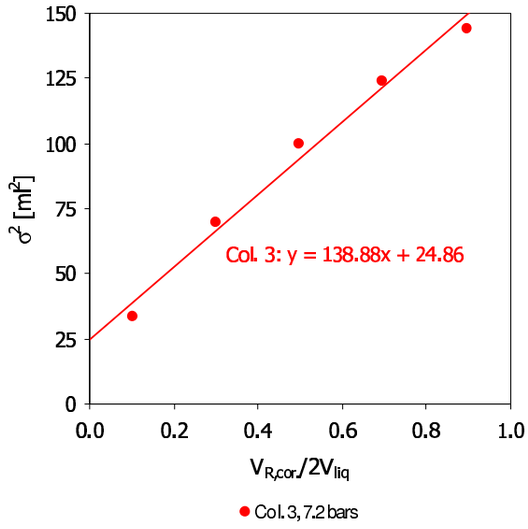

Figure 15-11: Reversed flow experiments with sodium nitrate on column 3.

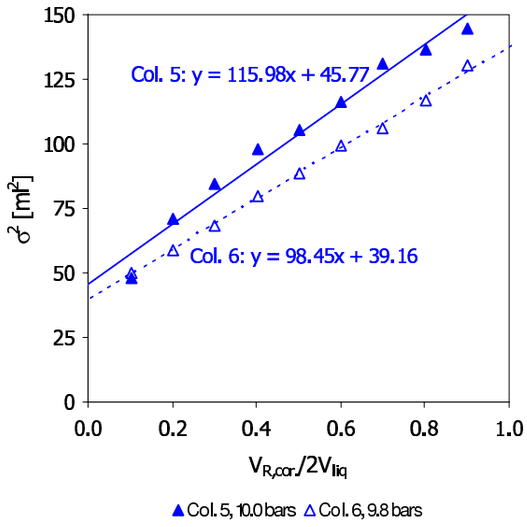

Figure 15-12: Reversed flow experiments with sodium nitrate on columns 5 and 6.

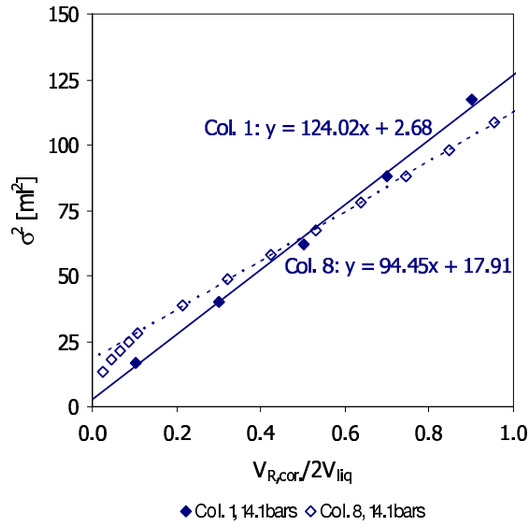

Figure 15-13: Reversed flow experiments with sodium nitrate on columns 1 and 8. For column 8 the four lowest data points are not included in the fit.

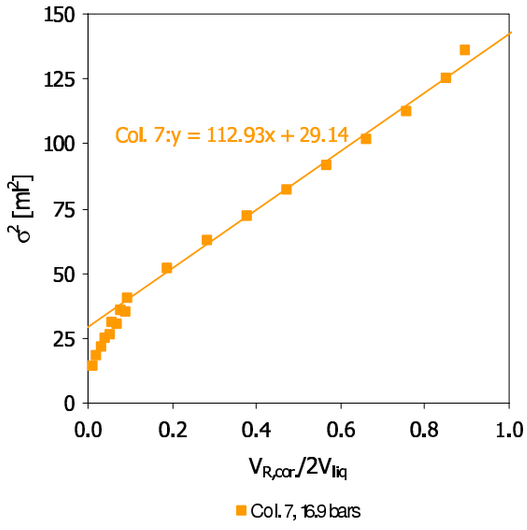

Figure 15-14: Reversed flow experiments with sodium nitrate on column 7. The nine lowest data points are not included in the fit.

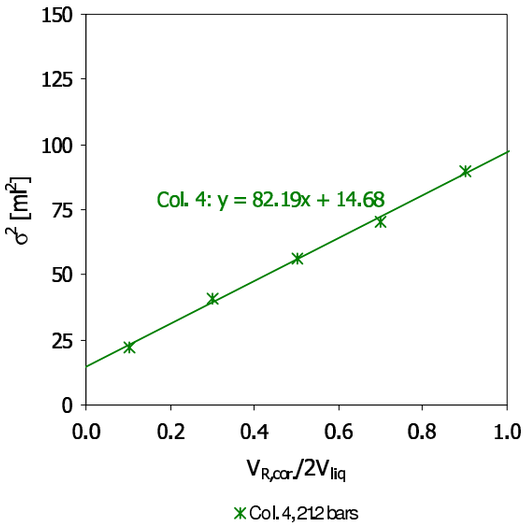

Figure 15-15: Reversed flow experiments with sodium nitrate on column 4.

From Figures 15-11 to 15-15 it is seen that the data points are well represented by straight lines, and the columns are thus homogenously packed. For columns 7 and 8 experiments where the flow is reversed after a very small volume has passed through the column ($V_{R,cor.}/2V_{liq} < 0.1$) were made. These data points do not follow the straight line. This could be due to inhomogeneous packing at these 10% of the column, or it may be contributions from a liquid gap. Another possible explanation is that not all the sample solution has left the flow distributor and entered the column before the flow is reversed.

As for the reversed flow experiments with latex beads none of the lines passes through (0,0). The intercept with the y-axis and the slope are given in the table below.

Column no.	$P_{packing}$ [bar]	CV [ml]	$\sigma^2_{intercept}$ [ml²]	Slope [ml²]
3	7.2	759.3	24.9	138.9
6	9.8	702.3	39.2	98.5
5	10.0	740.8	45.8	116.0
1	14.1	719.7	2.7	124.0
8	14.1	688.9	17.9	94.5
7	16.9	656.2	29.1	112.9
4	21.2	617.7	14.7	82.2

Table 15-5: Intercept and slope of the linear relation between the variances and the dimensionless retention volumes for the reversed flow experiments with nitrate in the eight columns with the prototype media.

As for the reversed flow experiments with latex beads the intercept with the y-axis is not a constant value and it is not related to the packing pressure.

15.5 Comparison of the Reversed Flow Experiments with Latex Beads and $NaNO_3$

It was not possible to find a connection between the packing pressure and the intercept and the slope of the lines for the reversed flow experiments. In the following it will be examined if there is a connection between the results obtained by the reversed flow experiments with latex beads and with nitrate. The intercepts with the y-axis was plotter against the packing pressure and the column number to see if there is any connection.

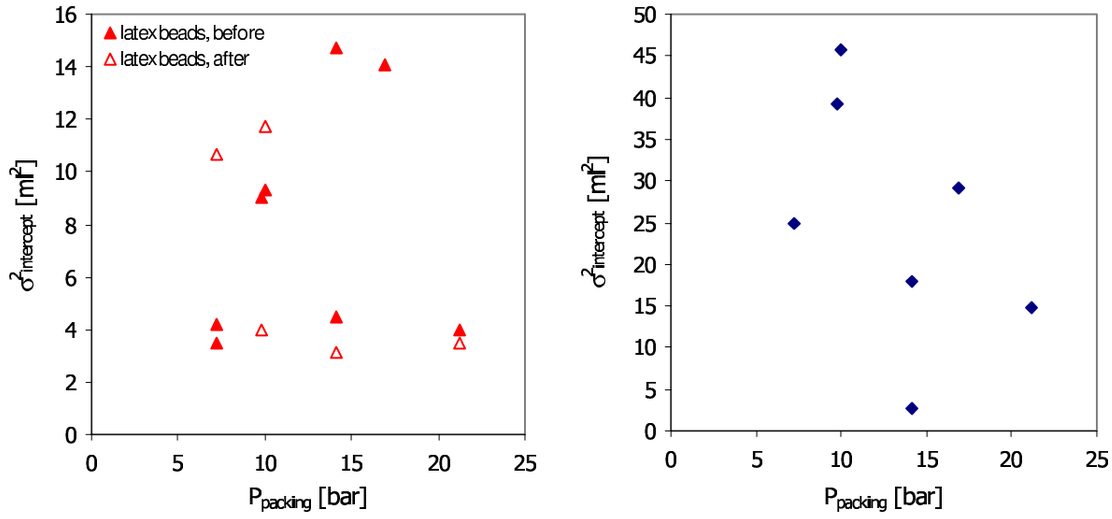

Figure 15-16: The intercept vs. the packing pressure for the reversed flow experiments with latex beads (left) and with nitrate (right).

From Figure 15-16 it is seen that the intercepts found with the latex beads are separated in two groups. The first group has an intercept of about 4 ml^2 and the other group has a higher intercept and the data is more scattered. The grouping of the data is not related to the packing pressure. The intercepts found with the nitrate are not grouped in a similar manner. They are more or less spread at random.

All packings were made in the same column and to see if the intercepts are related to order of column packing, the column number, the plots in Figure 15-17 were made.

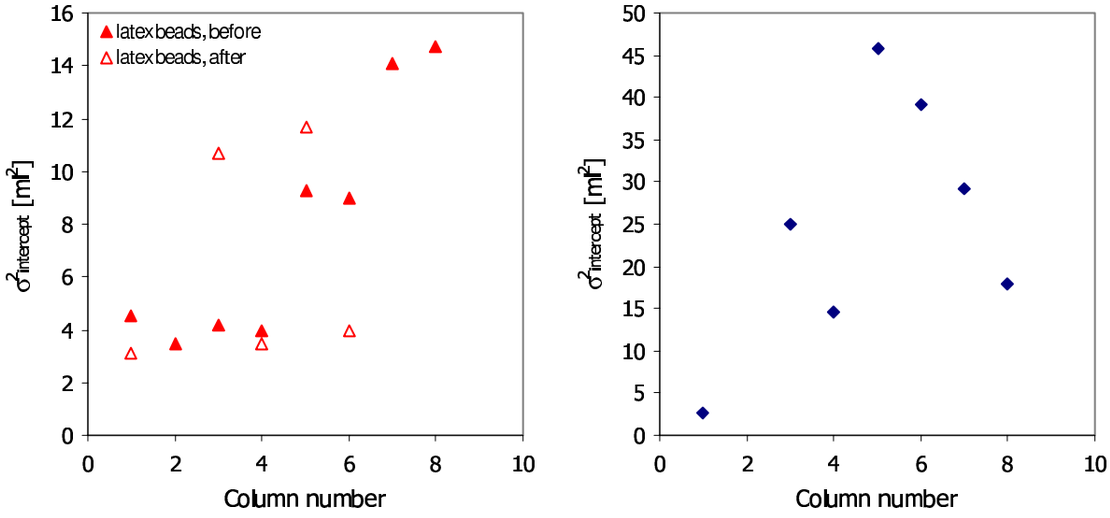

Figure 15-17: The intercept vs. the column number for the reversed flow experiments with latex beads (left) and with nitrate (right).

For the reversed flow experiments with latex beads the intercept is constant for the first 4 columns and then starts to increase with the column number. For the experiments with nitrate the intercept increases with the column number for the first 4 columns and for the last 3 columns the intercept decreases with the column number. From the comparison it is also observed that the intercept with the y-axis is no column constant because the values determined by nitrate are higher than the values determined by the latex beads. This means that the intercept depends on the experiment rather than on the packing pressure or the column number.

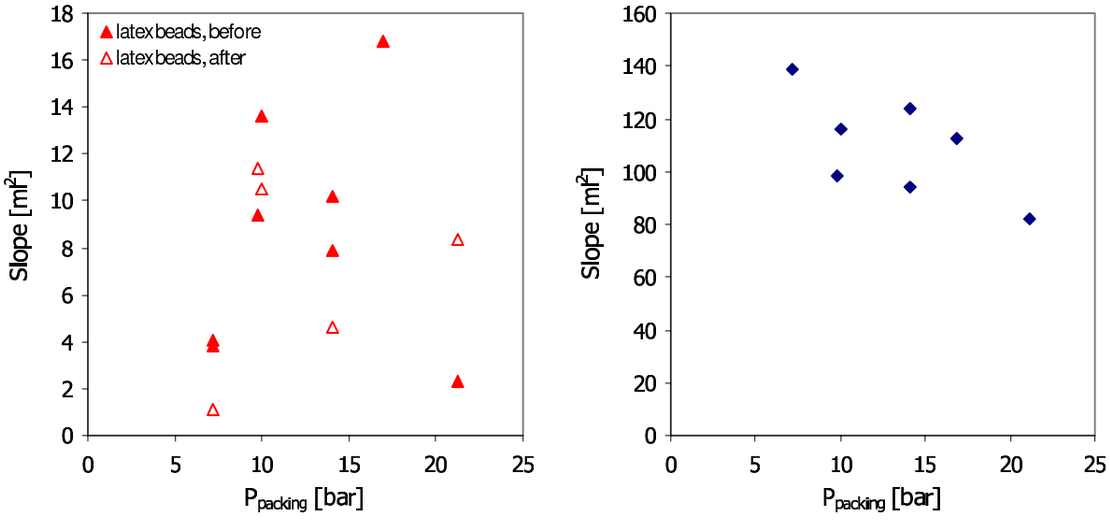

Figure 15-18: The slope vs. the packing pressure for the reversed flow experiments with latex beads (left) and with nitrate (right).

The slopes obtained by the latex beads experiments are randomly spread but for the nitrate experiments there is a tendency that the slope decreases with increased packing pressure. But again it is not possible to find a connection between the experiments with latex beads and with nitrate.

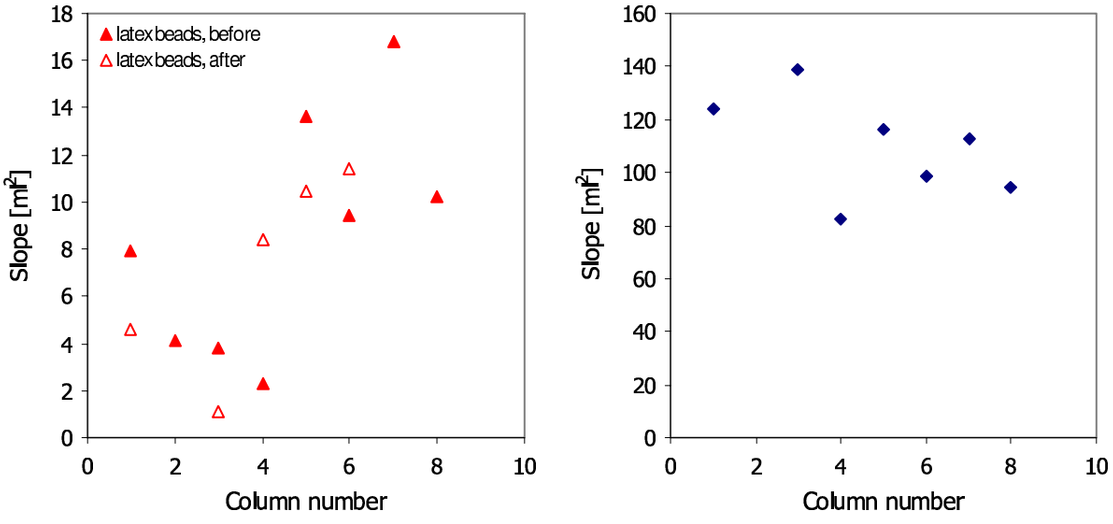

Figure 15-19: The slope vs. the column number for the reversed flow experiments with latex beads (left) and with nitrate (right).

From Figure 15-19 it is seen that there is a small tendency that the slope measured by nitrate decreases when the column number is increased. The slope measured by the latex beads decreases a little for the first four columns and then increases. As in the case of the intercepts it is observed that the slopes are grouped in two. The first four columns have a small slope and the last four columns have a higher slope. The same picture was seen for the intercepts. Maybe something has happened to the column or the flow distributors between the packing of columns 4 and 5.

The height equivalent of a theoretical plate, H, is calculated for the entire bed from the reversed flow experiments:

$$H = l_{bed} \cdot \frac{\sigma^2}{V_R^2} \qquad \textbf{(15-1)}$$

The height equivalent of a theoretical plate is only defined for a Gaussian distribution, and the use for a non-Gaussian distribution is an approximation. Even though it is defined for the Gaussian distribution it gives a good estimate of the column efficiency for non-Gaussian distributions as well.

The retention volume for the entire bed is $V_R = V_{void}$ for the latex beads experiments and $V_R = V_{liq}$ for the nitrate experiments.

The variance is calculated from the linear correlation:

$$\sigma^2 = \alpha \cdot \frac{V_R}{2V_{void}} + \beta \qquad \textbf{(15-2)}$$

where α is the slope of the line and β is the intercept. At $\frac{V_R}{2V_{void}} = 1$ the variance is twice that of the bed because this corresponds to a reversing of the flow at the end of the bed. The variance of the entire bed is given by

$$\sigma^2_{bed} = \frac{\sigma^2}{2} = \frac{\alpha \cdot 1 + \beta}{2} = \frac{\alpha + \beta}{2} \qquad \textbf{(15-3)}$$

H can now be calculated as

$$H = l_{bed} \cdot \frac{\alpha + \beta}{2V^2_{void}} \quad \text{(Latex experiments)} \qquad \textbf{(15-4)}$$

$$H = l_{bed} \cdot \frac{\alpha + \beta}{2V^2_{liq}} \quad \text{(Nitrate experiments)} \qquad \textbf{(15-5)}$$

If the data is corrected for the irreversible effects, by subtraction of the intercept, the H-value is calculated as

$$H = l_{bed} \cdot \frac{\alpha}{2V^2_{void}} \quad \text{(Latex experiments)} \qquad \textbf{(15-6)}$$

$$H = l_{bed} \cdot \frac{\alpha}{2V^2_{liq}} \quad \text{(Nitrate experiments)} \qquad \textbf{(15-7)}$$

For the experiments with latex only the data obtained before the nitrate experiments is included.

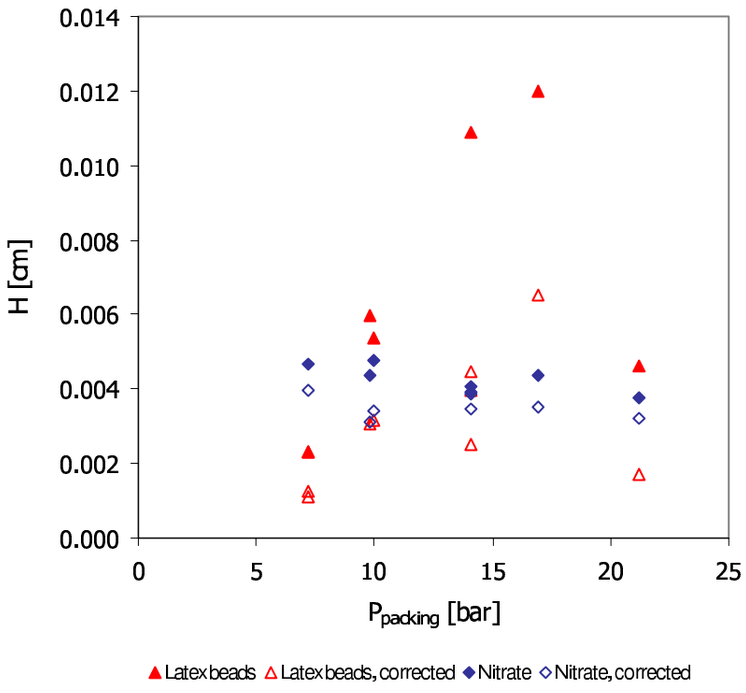

Figure 15-20: The height equivalent of a theoretical plate vs. the packing pressure for the reversed flow experiments with latex beads and nitrate. Both data corrected for the intercept (open marks) and data not corrected for the intercept (solid marks) is shown.

Except for the column packed at 21.1 bars the H-values for the latex beads experiments increase with increasing packing pressure, both for the non-corrected and the corrected data. This corresponds to a decrease in the performance of the bed when the packing pressure is increased. The H-values for the nitrate experiments are almost constant but there is a slight tendency that the H-values decrease with increasing packing pressure, both for the non-corrected and the corrected data. Thus, the results obtained by latex beads and nitrate are opposite. For the latex beads the best performance of the bed is achieved at the lowest packing pressure and for nitrate the best performance is achieved at the highest packing pressure.

The tendency for the H-values has to be considered with caution because the column number seems to influence the variances.

15.6 Observations Concerning the Development of Gas in the Prototype Media

As a consequence of the columns changing after the experiments with nitrate and some observations concerning gas development in the columns, it was decided to investigate the cause of the gas development. It was hoped that an explanation for the gas development would lead to an explanation for the change of the columns after the nitrate experiments and for the y-intercept.

To investigate the cause of the gas development a number of experiments were performed. First on a FineLINE 70 column, then on an INdEX HR16/30 column and finally on a FineLINE 35 column. The FineLINE 70 is a steel column but the INdEX HR16/30 and the FineLINE 35 columns are glass columns, which makes it possible to observe the bed during the experiments.

15.6.1 The FineLINE 70 Column

The column was packed at 10.0 bars and 37.5 ml/min in 100% 2-propanol.
CV = 702.3 ml.

The experimental sequence:

- After packing the column is equilibrated with 5% 2-propanol and the void volume is determined by latex beads. Then reversed flow experiments with latex beads are performed.
- The column is equilibrated with 1.0 M $NaNO_3$ and the total porosity is determined by pulse injection of 0.75 M $NaNO_3$. After this reversed flow experiments are also performed by injections of 0.75 M $NaNO_3$.
- The column is equilibrated with 5% 2-propanol and after 1 to 1½ column volume, it is observed that air or some kind of gas is eluted from the column. No air/gas has been entering the column, so it must develop in the column. After about 3 column volumes the gas has been removed from the column and the experiments with the latex beads are repeated.
  Now the void volume has increased by 9.5% and σ^2 has decreased by 17.6%. For the reversed flow experiments σ^2 has also decreased.
- The column is equilibrated with 1.0 M $NaNO_3$ and no gas is observed. The experiments with injection of 0.75 M $NaNO_3$ in 1.0 M $NaNO_3$ are repeated. No changes are observed in the retention volume or the variance.
- The column is equilibrated with 5% 2-propanol and gas is again observed after 1 to 1½ column volume. After about 3 column volumes the gas has been removed from the column and injections of a mixture of $NaNO_3$ and latex beads are made. In the first run two injections are made. For both injections peaks are only observed at a volume corresponding to the total liquid volume.

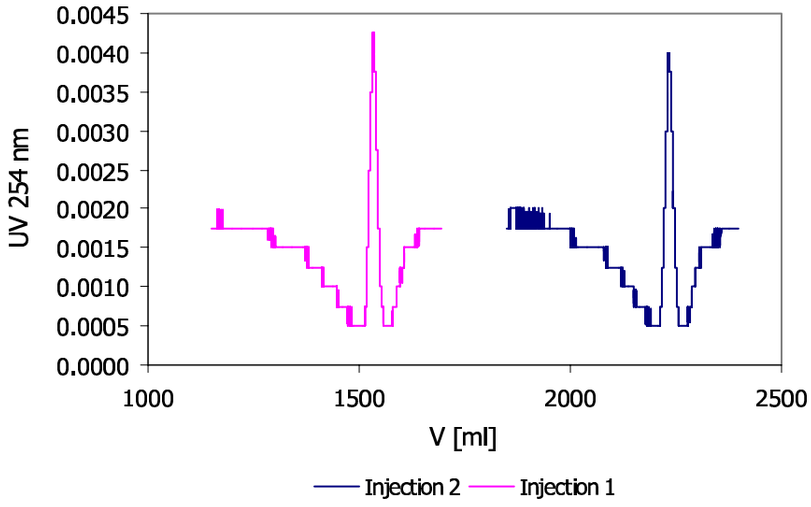

Figure 15-21: First run with mixed injections of nitrate and latex beads in 2-propanol.

In the second run also two injections are made and now peaks are observed at a volume corresponding to the void volume and a volume corresponding to the total liquid volume.

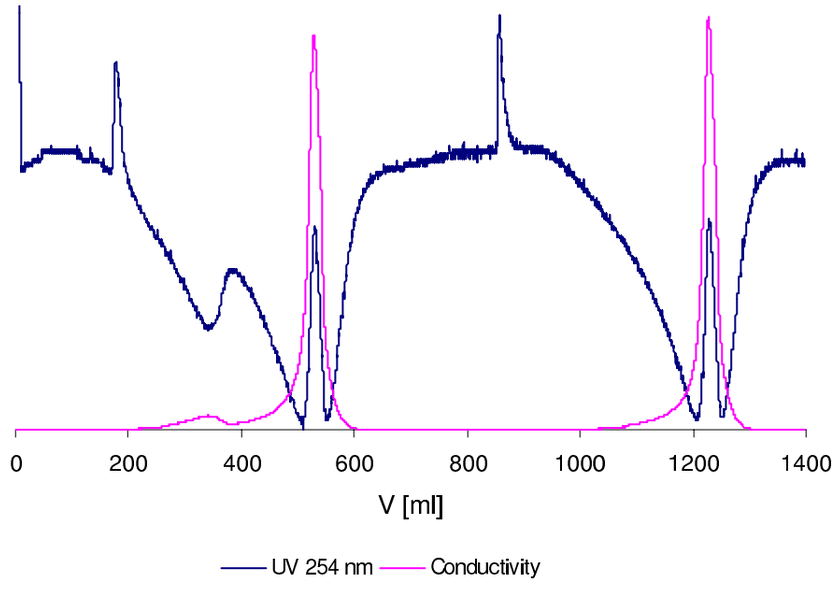

Figure 15-22: Second run with mixed injections of nitrate and latex beads in 2-propanol.

The retention volume of the peaks corresponding to the liquid volume is 3% less than the retention volume measured by a single injection of 0.75 M $NaNO_3$. The retention volume of the void peak from the first injection has not changed, compared to the retention volume measured for the single latex beads injections. The retention volume of the void peak from the

second injection is 10% less than the retention volume measured for the single latex beads injections.

Common to both runs is the lack of a stable baseline. The baseline drops before the peak with a retention volume corresponding to the total liquid volume is eluted. Immediately after the peak the baseline increases again.

- The column is now equilibrated with 1.0 M NaCl, and a large peak with a retention volume corresponding to the total liquid volume is eluted.

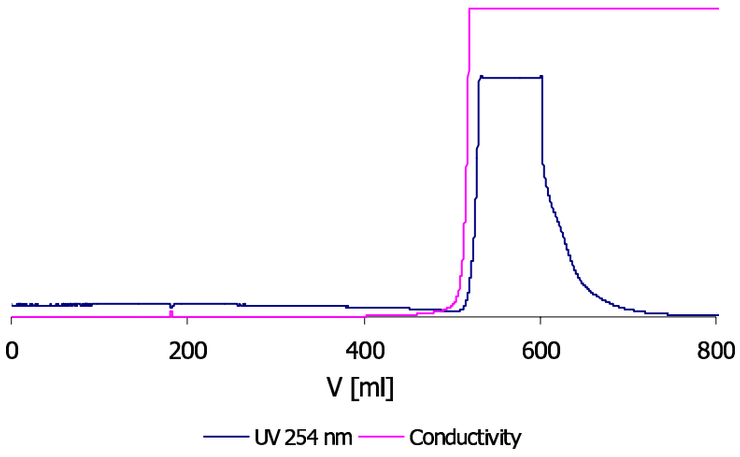

Figure 15-23: Shift of buffer from 5% 2-propanol to 1.0 M NaCl.

- The column is equilibrated with 5% 2-propanol and no gas development is observed.
- The column is equilibrated with 1.0 M $NaNO_3$. The conductivity curve does not look as smooth as expected but otherwise nothing unusual is observed.

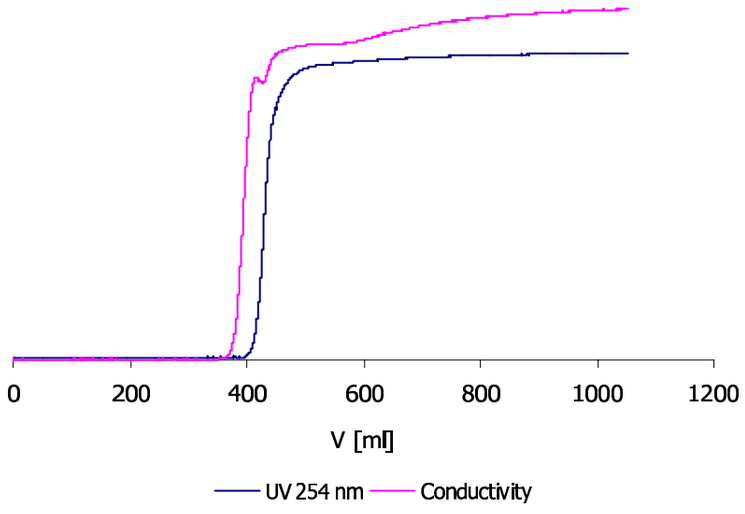

Figure 15-24: Shift of buffer from 5% 2-propanol to 1.0 M $NaNO_3$.

- The column is equilibrated with 5% 2-propanol but after about 2 column volumes no gas has been observed. A run with three injections of a mixture of latex beads and $NaNO_3$ is made. Only peaks being eluted at the total liquid volume are observed, and after the first peak gas is eluted from the column.

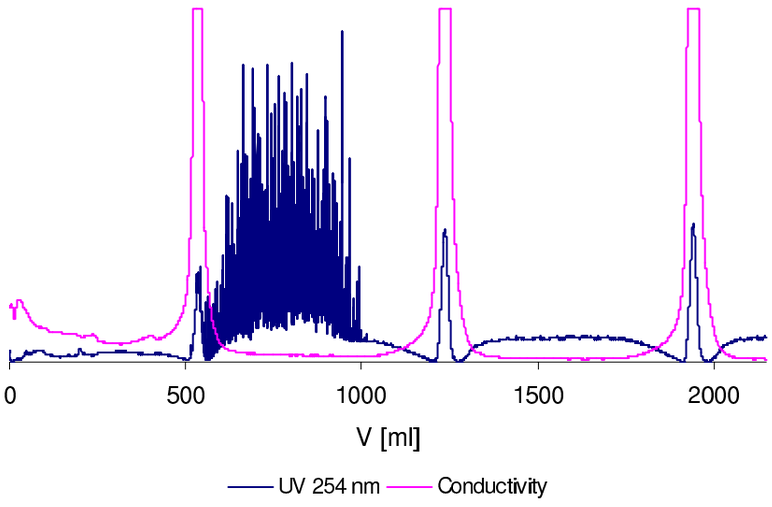

Figure 15-25: Third run with mixed injections of nitrate and latex beads in 2-propanol.

The concentration of latex beads in the sample is increased and three more runs with injections of the mixture are made. In none of these runs a peak with a retention volume corresponding to the void volume is observed. In all the runs the pattern of the baseline is the same. The baseline drops before the peak is eluted and increases again immediately after the peak.
Also this time the retention volumes are 3% less than the retention volumes measured by the single $NaNO_3$ injections.

The development of gas when the mobile phase is shifted from 1.0 M $NaNO_3$ to 5% 2-propanol has also been observed for others of the FineLINE 70 columns packed with the prototype. At the beginning we thought that the phenomenon was caused by air in the 5% 2-propanol buffer. But then the air should also appear when the column is equilibrated after packing, and no air is observed at this stage.

15.6.2 The INdEX HR16/30 Column

The column was packed at 10.0 bars and 10.0 ml/min in 100% 2-propanol.
CV = 61.5 ml (before compression of the bed).

- After packing the column is equilibrated with 5% 2-propanol, and the void volume is determined by latex beads. During these experiments the media is compressed 0.3 mm, even though the flow rate is only 5.0 ml/min and the pressure about 6 bars. The adaptor is adjusted so the filter again touches the bed. The void volume is determined again and the reversed flow experiments are made.
- The column is equilibrated with 1.0 M $NaNO_3$ and the liquid volume is determined by 0.75 M $NaNO_3$. But the column is compressed again, and after adjustment of the adaptor it is decided only to focus on the formation of gas in the column. So no more injections are made.
- The column is equilibrated with 5% 2-propanol and after about 1½ column volume gas is observed.

The packing of the INdEX HR16/30 column was repeated with fresh media and a packing pressure of 14.0 bars. After running the column a couple of hours with 5% 2-propanol at 10 ml/min a liquid gap appeared. The experiment was stopped after additional 3 hours, and at that time the liquid gap was about 1 cm in height.

The compression of the bed is also observed with a FineLINE 35 column run at 15 ml/min with 5% 2-propanol. After about 20 hours of use the liquid gap in the column is about 1 cm.

The observations described above indicate that compression of the bed and formation of a liquid gap take place in the FineLINE 70 steel column as well.

15.7 Conclusion

The 80 % in the middle of the columns were homogeneously packed, despite the packing pressure. It is not possible to say anything about the packing of the first and the last 10% of the column. If the flow is reversed before the sample solution has reached around 10% of the bed, some of the sample solution may not have left the flow distributor and entered the column, and if the flow is reversed after the sample solution has reached 90% of the bed some of the solution may have left the column and entered the flow distributor before the flow is reversed. This, as an inhomogeneously packed bed, results in data points which differ from the straight line.
Some effects related to the columns are irreversible, because for the reversed flow experiments with latex beads and those with nitrate an offset from zero is observed in the lines where the variances are plotted against the dimensionless retention volumes. It is not possible to find an explanation for the y-intercept. If a liquid gap is formed in the FineLINE 70 columns as well as in

the glass columns, the y-intercept could be due to this liquid gap. The size of the y-intercept would then reflect the size of the liquid gap. On the other hand a liquid gap is expected to increase with decreasing packing pressure, but the offset does not seem to be related to the packing pressure. Thus, this explanation can only be true, if the liquid gap increases more with increasing time of use than with decreasing packing pressure.

When the buffer solution is changed from 1.0 M $NaNO_3$ to 5% 2-propanol some kind of gas develops in the prototype media. If the $NaNO_3$ solution is replaced by a NaCl solution no gas development occurs. If mixed injections with latex beads and nitrate are performed the void peak may sometimes be missing, and it is not possible to obtain a stable baseline. This indicates that some kind of reaction takes place between the latex beads and the nitrate and maybe also between the media. It is not possible to find the exact cause of the gas formation, but the columns change after the nitrate experiments and the gas development. The experiments with latex beads could therefore not be reproduced after the nitrate experiments.

16 THE SUPERDEX 30 PREP GRADE MEDIA

It was decided to make some experiments on the media Superdex 30 prep grade (Superdex 30pg) to see if the irreversible effects found with the prototype media were due to the media or the column.

16.1 Experimental

16.1.1 The Column

The chromatographic media Superdex 30pg was used for the experiments. The column was packed by use of a 60% slurry of media in 2-3% ethanol, and a flow rate of 37.5 ml/min. A pressure relief valve controlled the packing pressure to 2.7 bars.

l_{bed} = 16.3 cm

CV = 627.3 ml

16.1.2 Buffer and Sample Solutions

The used buffer solution 0.40 M NaCl. The two sample solutions were 0.80 M NaCl and 2 wt% Dextran in 0.40 M NaCl.

16.1.3 Experimental Measurements

For all experimental measurements a flow rate of 15.0 ml/min (0.39 cm/min) was used and the column was loaded with 1.0 ml sample solution. In the experiments with dextran the effluent wss analyzed by the UV detector, and in the experiments with NaCl the effluent was analyzed by the conductivity detector.

After packing the column was equilibrated with 0.40 M NaCl until a constant detector signal was reached.

After equilibration the void volume was determined by dextran and then the reversed flow experiments with dextran were performed.

After the experiments with dextran the total liquid volume was determined by a pulse of 0.80 M NaCl, and reversed flow experiments were performed as with dextran.

16.1.4 Fitting and Data Reduction

The Exponential Modified Gauss (EMG) function was used to fit the peaks, except for the peaks obtained by reversed flow experiments with NaCl. Due to the shape of these peaks the Pearson VII function was used for fitting.

The retention volumes and the variances were determined as for the prototype media, except that dextran were used instead of latex beads and NaCl was used instead of $NaNO_3$.

16.2 Void Volume, Liquid Volume and Porosities

The experimental data for determination of the void and the liquid volumes with corresponding variances is given in Appendix H.VI and H.VII. Injections were made both at the top and at the bottom of the column and the corresponding data is given in two separate tables in the appendices.

Injection	CV [ml]	V_{void} [ml]	σ^2_{void} [ml^2]	ε	V_{liq} [ml]	σ^2_{liq} [ml^2]	ε_t
Top	627.3	157.0	53.1	0.25	503.8	98.0	0.80
Bottom		159.6	123.8	0.25	507.7	153.0	0.81

Table 16-1: Void volumes, liquid volumes and corresponding variances, interstitial and total porosities measured by injections at the top and the bottom of the column with Superdex 30pg.

From the table it is seen that the variances depend on whether the injections are performed at the top or the bottom of the column. The variances measured when the injections are performed at the bottom of the column are much higher than the variances measured when the injections are performed at the top of the column. This is very surprising because, according to Amersham Biosciences, the top and the bottom flow distributors should be identical. The variances for the empty column are unfortunately only measured with injections at the bottom of the column. The difference between the variances measured with injection at the top and at the bottom is 70.7 ml^2 for dextran and 55.0 ml^2 for NaCl. Because the difference is not constant it cannot be explained only by a difference in the variances for the empty column between injections made at the top and the bottom of the column.

16.3 Reversed Flow with Dextran

The experimental data for the reversed flow experiments with dextran is given in Appendix H.VIII. Again injections were made both at the top and at the bottom of the column and the data is given in two separate tables.

In Figure 16-1 the variances are plotted against the retention volumes. The data is fitted both with a straight line and a second order polynomial.

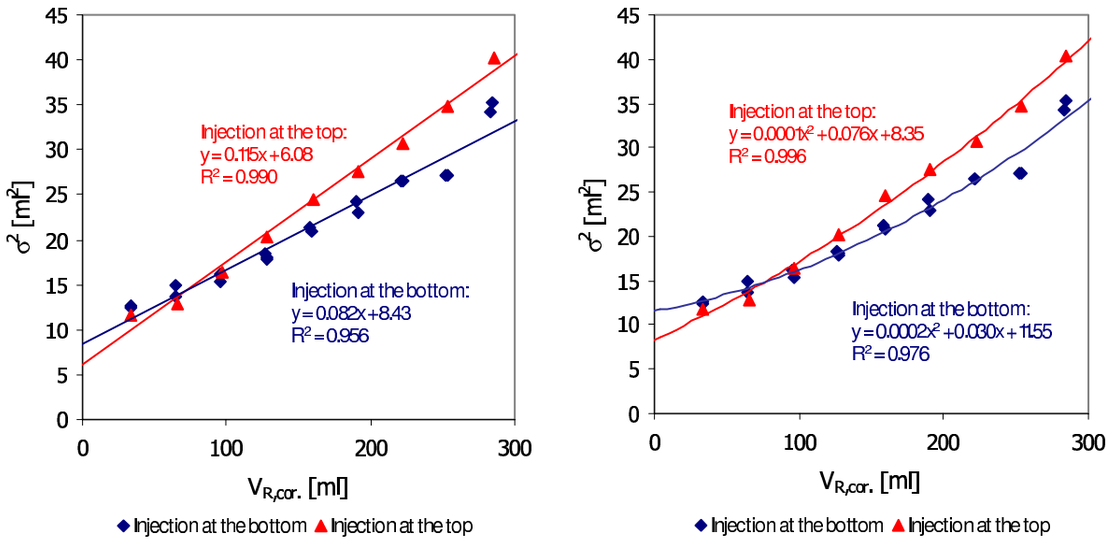

Figure 16-1: The variance as a function of the retention volume for reversed flow with dextran on Superdex 30pg. Fitted with a straight line (left) and with a second order polynomial (right).

When the data is fitted with a second order polynomial the fit is improved a little compared to the fit with a straight line. Whether the fit is improved due to experimental uncertainties or due to the bed being inhomogeneously packed is not possible to decide against a background of these data alone.

Independent of how the data is fitted the lines do not pass through (0,0). This means that the offset is not due to the media but must be due to some irreversible effects in the system as e.g. the flow distributors. Furthermore, it seems that the irreversible effects depend on whether the injections are made at the top or the bottom of the column, but the differences between the offsets are very small (linear: 2.35 ml^2 and polynomial: 3.20 ml^2) and may be caused by experimental uncertainties.

16.4 Reversed Flow with NaCl

The experimental data for the reversed flow experiments with NaCl is given in Appendix H.IX. Injections are made both at the top and the bottom of the column and the data is given in two separate tables.

In Figure 16-2 the variances are plotted against the retention volumes. As for the experiments with dextran the data is fitted both with a straight line and a second order polynomial.

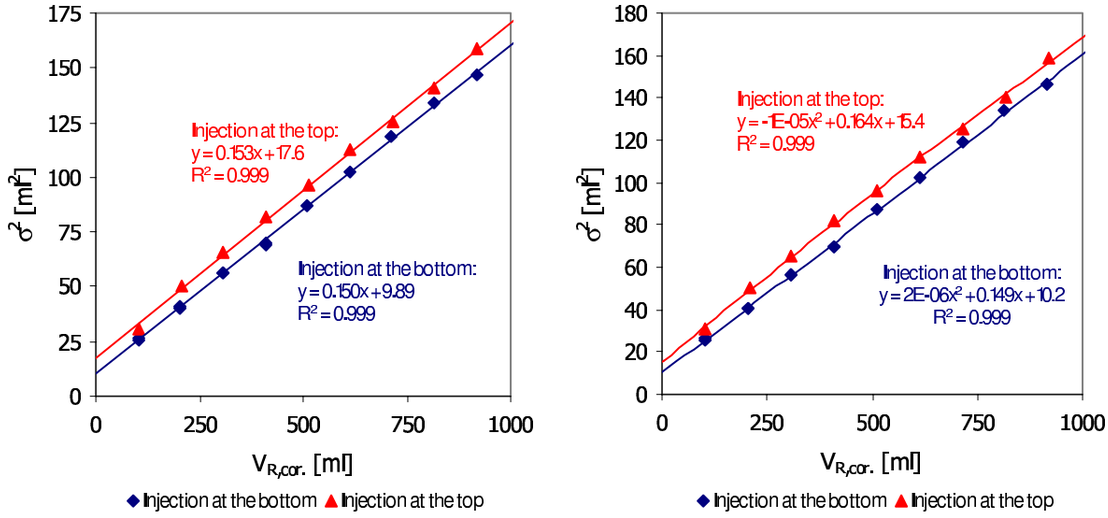

Figure 16-2: The variance as a function of the retention volume for reversed flow with NaCl on Superdex 30pg fitted with a straight line (left) and with a second order polynomial (right).

The differences between the linear and the polynomial fits are negligible. Therefore, it can be concluded that the column is homogeneously or almost homogeneously packed. As for the reversed flow experiments with dextran the lines do not pass through (0,0), and the size of the offset depends on whether the injections are made at the top or the bottom of the column. The differences between the offsets are very small, and because the lines are parallel they can be brought to coincide by changing the dead volume. It was examined how much the dead volume should be changed to make the lines coincide. The dead volume when injection takes place at the bottom of the column has to be around 55 ml higher than the dead volume when injection takes place at the top of the column. This is not possible at all because the dead volume of the entire empty system is only 12.06 ml and, furthermore, the dead volume at the top of the column is larger than that at the bottom of the column. The irreversible effects are therefore different for the top and the bottom of the column.

16.5 Conclusion

In the table below all the results obtained by the Superdex 30pg column are given. It was concluded earlier that the column is homogeneously or almost homogeneously packed and therefore only the results for the linear fits are listed in the table.

		Dextran	NaCl
$V_{R,cor,\ bottom}$	[ml]	159.6	507.7
$V_{R,cor,\ top}$	[ml]	157.0	503.8
$\sigma^2_{cor,forw,bottom}$	[ml^2]	126.1	155.3
$\sigma^2_{cor,forw,top}$	[ml^2]	55.4	100.3
σ^2_{bottom}	[ml^2]	21.6	86.6
σ^2_{top}	[ml^2]	24.1	94.7
α_{bottom}	[ml]	0.082	0.151
α_{top}	[ml]	0.115	0.153
β_{bottom}	[ml^2]	8.5	10.0
β_{top}	[ml^2]	6.1	17.6

Table 16-2: The retention volumes and variances for the forward flow experiments. Intercept, slope and variances calculated from the linear relation between the variances and the retention volumes for the reversed flow experiments.

σ^2_{bottom} and σ^2_{top} are the variances calculated from the equation obtained for the reversed flow experiments with injections at the top and the bottom of the column respectively. The variances are calculated by the retention volumes obtained for the forward flow experiments to acquire the variance of one bed height (the entire bed) and not the double bed height.

$$\sigma^2_{bottom} = V_{R,cor,\ bottom} \cdot \alpha_{bottom} + \beta_{bottom} \qquad \textbf{(16-1)}$$

$$\sigma^2_{top} = V_{R,cor,\ top} \cdot \alpha_{top} + \beta_{top} \qquad \textbf{(16-2)}$$

Dextran: $\sigma^2_{bottom} = 159.6\ ml \cdot 0.082\ ml + 8.5\ ml^2 = 21.6\ ml^2$

$\sigma^2_{top} = 157.0\ ml \cdot 0.115\ ml + 6.1\ ml^2 = 24.1\ ml^2$

NaCl: $\sigma^2_{bottom} = 507.7\ ml \cdot 0.151\ ml + 10.0\ ml^2 = 86.6\ ml^2$

$\sigma^2_{top} = 503.8\ ml \cdot 0.153\ ml + 17.6\ ml^2 = 94.7\ ml^2$

The variances obtained by injections at the bottom of the column and forward flow are much higher than the variances obtained by injection at the top of the column and forward flow. If the variances for the entire bed calculated from the reversed flow experiments are compared only a

very small difference is observed. The variances obtained by injections at the top of the column are a little higher than the variances obtained by injections at the bottom of the column.
A very big difference is observed between the variances for the entire bed calculated from the reversed flow experiments and the variances obtained by the forward flow experiments. The cause of this big difference is unknown, but it is probably due to some irreversible effects in the system or/and the flow distributors.

If the variances from injections at the top and the bottom of the column for reversed flow are compared a very good agreement is found. Especially for the NaCl-experiments where the lines are completely parallel. That the lines are parallel and not identical shows that the bed is homogeneous, but the irreversible effects are larger for injections at the top of the column than for injections at the bottom of the column. This result is opposite to the result found for the forward flow experiments, where the largest variances were found for injections at the bottom of the column. This indicates that the largest contribution to the variance is the variance from the flow distributor at the top of the column when it is entered from the bed side.

17 DISCUSSION

For all the packed columns the bed was homogeneous but some irreversible effects were observed for all the columns. The irreversible effects were not constant and could not be related to the packing pressure or the column number. After discovering the formation of a liquid gap in the smaller columns packed with the prototype media, it was thought that the irreversible effects might be caused by a liquid gap. If the irreversible effects are caused by a liquid gap, a liquid gap is formed in the column with Superdex 30pg media as well, because the irreversible effects are also observed for this column. The Superdex 30pg media is an old and well known media and problems with formation of liquid gabs have never been reported. Thus, it is unlikely that the irreversible effects are caused only by a liquid gap.

The reversible effects could be caused by the flow distributors and to clarify whether this is the case some additional experiments have to be made. The experiments should be performed with an empty column and some additional tubes before and after the column, so that it will be possible to reverse the flow when the sample has passed both the flow distributors. Because of the differences between the irreversible effects for injections at the top and the bottom of the column, the experiments could be made with injections at both ends of the column.

The determination of the variance with an empty column was only done for injections at the bottom of the column. However, this measurement has to be done for injections at the top of the column as well, because large differences were also encountered in the variances for the forward flow experiments and the injections at the top and the bottom of the column. Amersham Biosciences stated that the flow distributors were identical. The results obtained by the Superdex 30pg media indicate that this is not the case, because the variances depend on whether the injection is performed at the top or the bottom of the column.

Owing to the unexpected results obtained and the resulting lack of convincing conclusions, it would be a good idea to see if it is possible to reproduce the results of Moscariello et al. 2001 by the system and the column used in this project. The media and the trace should be the same as the ones used by Moscariello, and the experiments should be performed in exactly the same manner. For each column the variance should be measured by forward flow experiments and experiments where the flow is reversed when the tracer has reached the middle of the column. (Injections should be made both at the top and at the bottom of the column). Then it will be possible to make the same plot as Moscariello et al. made in the paper (Figure 6) [Moscariello et al., 2001]. If it is possible to reproduce the results of Moscariello, there are no irreversible effects in the system or the flow distributors, and the offset could be due to the media, the tracer or the differences in the way we make the experiments. Moscariello only reverses the flow when the tracer has reached 50% of the column length, and we have reversed the flow from 10% to 90% of the column length. If it is not possible to reproduce the results, we have some irreversible effects in our system that Moscariello does not have in his system, and then we have to find a way to determine these irreversible effects. The first attempt could be to change the flow distributors.

18 CONCLUSION

The axial packing technique gives homogenously packed beds with the prototype media in the range 7 to 21 bars. With Superdex 30pg at 2.7 bars it also gives a homogeneously packed bed.
The interstitial porosity and the total porosity for the prototype media are constant up to around 15 bars and then decreased with increasing pressure because of the compressibility of the media. The interstitial porosities determined for the prototype media are very low, but porosities in the same range have been determined by others at Amersham Biosciences.

The intercept with the y-axis established for the reversed flow experiments with both the prototype media and Superdex 30pg is caused by some unexpected irreversible effects in the system. The irreversible effects are not constant and are not related to the packing pressure or the column number, but they depend on whether the injection is performed at the top or the bottom of the column. The reversed flow experiments performed by the Superdex 30pg column indicate that the largest contribution to the irreversible effects is due to the flow distributor at the top of the column, when this is entered from the bed side.

The performance of the prototype media does not seem to be related to the packing pressure. For the experiments with latex beads there is a tendency that the performance of the bed decreases with increasing packing pressure and for the nitrate experiments the tendency is opposite. Because of the problems with the gas development, the liquid gap and the bed changing after the nitrate experiments, it is very difficult to draw any definitive conclusions from the experiments on the prototype media.

REFERENCES

Avci, A.K.; Çamurdan, M.; Ülgen, K.Ö.; *Quantitative description of protein adsorption by frontal analysis*, Process Biochem., 2000, 36, 141-148.

Bentorp, D.; Engelhardt, H.; *Chromatographic characterization of ion exchangers for high-performance liquid chromatography of proteins, I. Chromatographic determination of loading capacity for low- and high-molecular mass anions*, Jour. Chrom., 1991, 556, 363-372.

BioSepra; Product news. Q, S, DEAD, CM Ceramic HyperD*, Ion Exchange Sorbents and Ion Exchange Chromatography, Ceramic HyperD® 20 and F*, www.biosepra.com, 2002.

Bosma, J.C.; Wesselingh, J.A.; pH *dependence of Ion-Exchange Equilibrium of Proteins*, AIChE Journal, 1998, 44, 2399-2409.

Brooks, C. A.; Cramer, S.M.; *Steric Mass-Action Ion-Exchange: Displacement Profiles and Induced Salt Gradients*, AIChE Journal, 1992, 38, 1969-1978.

Carta, G.; Cincotti, A.; *Film model approximation for non-linear adsorption and diffusion in spherical particles*, Chem. Eng. Sci., 1998, 53, 3483-3488.

Fernandez, M.A.; Carta, G.; *Characterization of protein adsorption by composite silica-polyacrylamide gel anion exchangers I. Equilibrium and mass transfer in agitated contactors*, Jour. Chrom. A, 1996, 746, 169-183.

Fernandez, M.A.; Carta, G.; *Characterization of protein adsorption by composite silica-polyacrylamide gel anion exchangers II. Mass transfer in packed columns and predictability of breakthrough behavior*, Jour. Chrom. A, 1996, 746, 185-198.

Freitag, R.; Vogt, S.; *Comparison of particulate and continuous-bed columns for protein displacement chromatography*, Jour. Biotech., 2000, 78, 69-82.

Gebauer, K.H.; Thömmes, J.; Kula, M.R.; *Breakthrough performance of high capacity membrane adsorbers in protein chromatography*, Chem. Eng. Sci., 1997, 52, 405-419.

Gedam, S.D.; Jayaraman, G.; Cramer, S.M.; *Charaterization of non-linear adsorption properties of dextrane-based polyelectrolyte displacers in ion-exchange systems*, Jour. Chrom. 1993, 630, 37-52.

Gerstner J. A.; Bell, J. A.; Cramer, S.M.; *Gibbs free energy of adsorption for biomolecules in ion exchange systems*, Biophysical Chemistry, 1994, 52, 97-106.

Guiochon, G.; Shirazi, S.G.; Katti, A.M.; *Fundamentals of Preparative and Non-linear Chromatography*, Academic Press, 1994.

Hansen, E.; *Application of the Linear Driving Force Approximation to the study of Mass Transfer in Ion-exchange Chromatography*, Ph.D. Thesis, IVC-SEP, The Techical University of Denmark, 2002.

Hansen, E.; Mollerup, J.; *Application of the two-film theory to the determination of mass transfer coefficients for bovine serum albumin on anion-exchanger columns*, Jour. Chrom. A, 1998, 827, 259-267.

Helfferich, F.; *Ion Exchange*, Dover Publication, Inc., New York, 1995, ch. 4.

Kaminski, M.; *Simple test for determination of the degree of distortion of the liquid-phase flow profile in columns for preparative liquid chromatography*, Jour. Chrom., 1992, 589, 61-70.

Kundu A.; Barnthouse, K.A.; Cramer, S.M.; *Selective displacement Chromatography of Proteins*, Biotech. and Bioeng., 1997, 56, 119-129.

Lewus, R.K.; Carta, G.; *Binary Protein Adsorption on Gel-Composite Ion-Exchange Media*, AIChE Jour., 1999, 45, 512-522.

Li, Y.-L.; Pinto, N.G.; *Influence of lateral interactions on preparative protein chromatography, I. Isotherm behavior*, Jour. Chrom A, 1994, 658, 445-457.

Merck KGaA; *Fractogel® EMD process media*, www.merck.de, 2002.

Moscariell, J.; Purdom, G.; Coffman, J.; Root, T.W.; Lightfoot, E.N.; *Characterizing the performance of industrial-scale columns*, Jour. Chrom A, 2001, 908, 131-141.

Nash, D.C.; Chase, H.A.; *Comparison of diffusion and diffusion-convection matrices for use in ion-exchange separations of proteins*, Jour. Chrom. A, 1998, 807, 185-207.

Natarajan, V.; Cramer, S.; *A methodology for the Characterization of Ion-Exchange Resins*, Sep. Sci. and Tech., 2000, 35, 1719-1742.

National Dairy Council; *National Dairy Council, Health-Enhancing Properties of Dairy Ingredients, Composition of Whey*, www.nationaldairycouncil.org/lvl04/nutrilib/digest/dairydigest_722b.htm, 2001.

Perry, R.H.; Green, D.W.; Maloney, J.O.; *Perry's Chemical Engineers' Handbook*, 7. ed., McGraw-Hill, New York, 1997, Section 16.

Pharmacia Biotech*; Q Sepharose® XL, SP Sepharose® XL*, www.amershambiosciences.com, 2002, data file 18-1123-82, Ed. AB.

Pharmacia Biotech; *Source 30Q, Source 30S*, www.amershambiosciences.com, 2002, data file 18-1107-12, Ed. AB.

Raje, P.; Pinto, N.G.; *Combination of the steric mass action and non-ideal surface solution models for overload protein ion-exchange chromatography*, Jour. Chrom. A, 1997, 760, 89-103.

Roper, D.K.; Lightfoot, E.N.; *Estimating plate heights in stacked-membrane chromatography by flow reversal*, Jour. Chrom A, 1995, 702, 69-80.

Soldatov, V.S.; *Potentiometric titration of ion exchangers*, Reactive & Functional Polymers, 1998, 38, 73-112.

Soldatov, V.S.; *Quantitative Presentation of Potentiometric Titration Curves of Ion Exchangers*, Ind. Eng. Chem. Res.,1995, 34, 2605-2611.

Son, W.-K.; Kim, S.H.; Kim, T.I.; *Calculation on Ion Exchange Capacity for an Ion Exchanger Using the Potentiometric Titration*, J. Poly. Sci. B, 2000, 38, 3181-3188.

Suzuki, H.; Wang, B.; Yoshida, R.; Kokufuta, E.; *Potentiometric Titration Behaviors of a Polymer and Gel Consisting of N-Isopropylacrylamide and Acrylic Acid*, Langmuir, 1999, 15, 4283-4288.

Teeters, M.A.; Root, T.W.; Lightfoot, E.N.; *Performance and scale-up of adsorptive membrane chromatography*, Jour. Chrom A, 2002, 944, 129-139.

van Deemter, J.J.; Zuiderweg, F.J.; Klinkenberg, A.*; Longitudinal diffusion and resistance to mass transfer as causes of nonideality in chromatography*, Chem. Eng. Sci., 1956, 5, 271-289.

Vejledning til øvelser i proteinkemi, Molekylærbiologisk Institut, Københavns Universitet, 2001.

Williams, A.; Taylor, K.; Dambuleff, K.; Persson, O.; Kennedy, R.M.; *Maintenance of column performance at scale*, Jour. Chrom. A, 2002, 944, 69-75.

Zuyi, T.; Jinzhou, D.; Taiwei, C.; *Potentiometric titration in studies of ion exchangers*, Reac. & Func. Poly., 1996, 31, 17-24.

Modeling Retention Volumes, Isotherms and Plate Heights for Whey Proteins in Anion-exchange Chromatography

APPENDICES

by

Linda Pedersen

Ph.D. Thesis

IVC-SEP, Department of Chemical Engineering, Technical University of Denmark

INTRODUCTION

The content of these appendices are experimental data, calibrations and uncertainty calculations.

Appendix A contains calibrations and uncertainty calculations.

Appendix B contains experimental data and calculations for determination of dead volumes of the BioCAD system and the empty columns. Appendix B also includes the experimental data for determination of retention volumes under non-adsorbed conditions, total porosity of the columns and ion-exchange capacity.

Appendix C contains the experimental data obtained by isocratic elution of BSA, α-lactalbumin, β-lactoglobulin A and B on Source 30Q, Q-Sepharose XL, Ceramic Q-HyperD F and Fractogel EMD TMAE 650(s).

Appendix D contains the experimental data from gradient elution of BSA, α-lactalbumin, β-lactoglobulin A and B on Source 30Q, Q-Sepharose XL, Ceramic Q-HyperD F and Fractogel EMD TMAE 650(s).

Appendix E contains the Cl^--concentrations used for investigation of the possibility for separation of the four proteins by gradient elution.

In appendix F contains the experimental data from capacity measurements with BSA on Source 30Q.

Appendix G is related to the correlation of the reduced plate heights.

Appendix H contains the experimental data from the work at Amersham Biosciences.

CONTENTS

APPENDIX F: CAPACITY MEASUREMENTS

APPENDIX G: REDUCED PLATE HEIGHTS

APPENDIX H: WORK DONE AT AMERSHAM BIOSCIENCES

APPENDIX A.I: UNCERTAINTY BUDGET FOR DETERMINATION OF V_R

This uncertainty budget was made as a part of the requirements for the fulfillment of the Ph.D. course "Quality Assurance in Chemical Measurements".

Step 1: Specification

The measurand:

The measurand is the retention volume of a protein measured at a specified pH and counterion concentration.

Procedure:

The column is equilibrated with mobile phase and the UV-detector is reset. The sample solution is loaded onto the column and the absorbance of the column effluent is measured by an UV-detector at 280 nm and a computer logs the signal. The mobile phase has no absorbance at 280 nm, so no absorbance is observed until the protein starts to elute.
The logged signal (the peak) is fitted with the EMG-function in the program TableCurve 2D.

A more detailed description of the procedure is given in the SOP. (The SOP is given later in this appendix).

Calculation:

$$V_R = (b + d)k - V_{R,empty}$$

Where $V_{R,empty} = (b_{empty} + d_{empty})k_{empty}$ and $k = \frac{Q_{act}}{Q_{nom}}$

V_R: Retention volume of the protein [ml]
b: Parameter from the EMG-fit [ml]
d: Parameter from the EMG-fit [ml]
$V_{R,empty}$: Dead volume measured for an empty column [ml]
k: Correction factor
Q_{act}: Actual flow rate [ml/min]
Q_{nom}: Flow rate specified on the BioCAD [ml/min]

The subscript empty refers to the empty column.

Step 2: Identifying and analyzing uncertainty sources

The standard deviation of the parameter b and d are given by the program TableCurve 2D, but they depend a little on the shape of the peak (see the Figures 1 to 3).

The standard deviation of the parameter b and d are higher for the peak in Figure 2 than for the peak in Figure 1. This is due to the fact that some impurities elute before the protein in Figure 2 and this gives a relative large deviation between the fitted function and the data points.

In Figure 3 some deviation between the peak and the fitted function is observed and this results in very high and unrealistic standard deviations. The standard deviations for the peaks where the function does not pass through all data points have to be used with care.

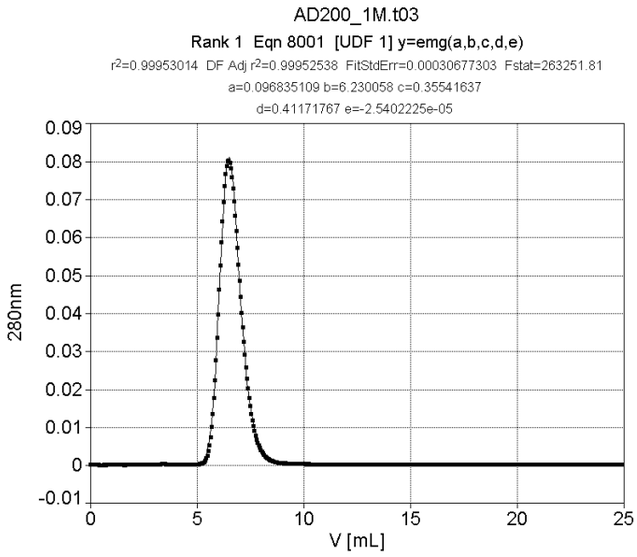

Figure 1: Fit with the EMG-function.

$s_b^2 = 0.0014148$ and $s_d^2 = 0.0024684$.

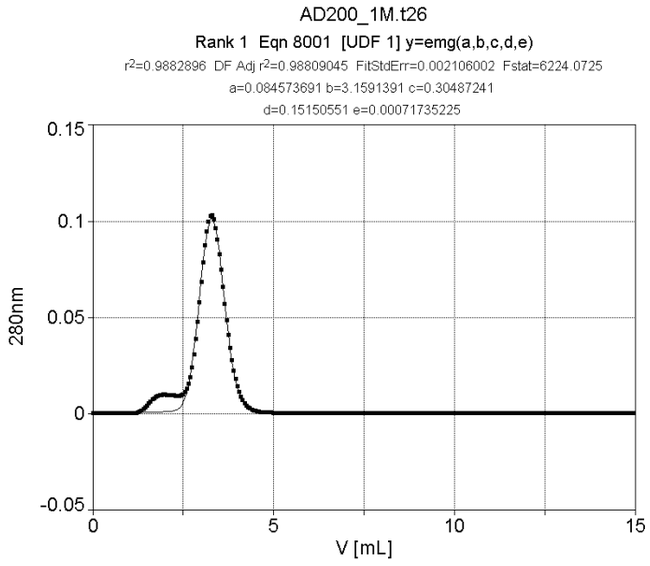

Figure 2: Fit with the EMG-function.

$$s_b^2 = 0.019269 \text{ and } s_d^2 = 0.025757 .$$

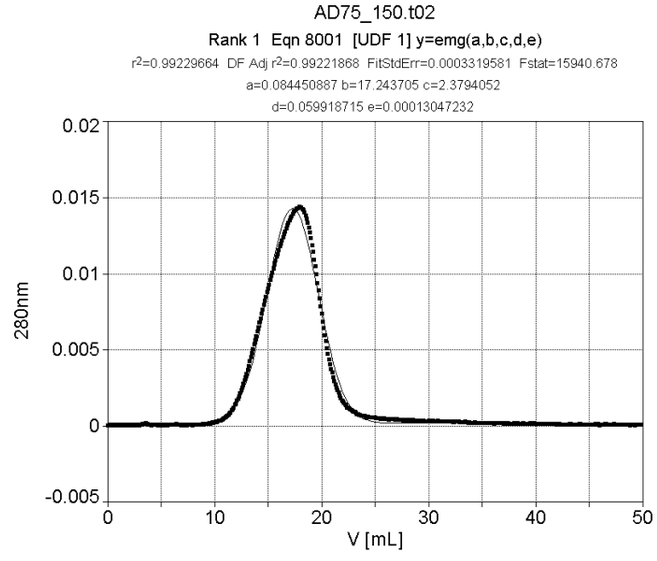

Figure 3: Fit with the EMG-function.

$$s_b^2 = 29.485 \text{ and } s_d^2 = 29.500 .$$

Step 3: Quantifying Uncertainty

Q_{act}: A calibration curve will be made and the uncertainties will be estimated from the calibration curve.

k: The uncertainty of the correction factor is the same as the uncertainty of the flow rate.

$V_{R,empty}$: The uncertainty of $V_{R,empty}$ will be estimated by combining the uncertainties of k_{empty}, and of the parameters b and d.

V_R: The uncertainty of $V_{R,empty}$ will be estimated by combining the uncertainties of $V_{R,empty}$, k and the parameters b and d.

Load: To estimate the uncertainty caused by different amounts of load experiments where only the load was change has been performed.

Repeatability: The repeatability standard deviation will be determined from V_R obtained by experiment performed at identical conditions (same buffer, sample solution, flow rate, amount of load and performed on the same day).

Reproducibility: The precision will be determined from V_R obtained by experiments performed under non-identical conditions (different buffer, sample solution, flow rate, amounts of load and performed on different days).

Step 4: Calculating Uncertainty

The calculations described in this part are given as Excel sheet later in this appendix.

Calibration of the flow rate

The flow rate was calibrated in the interval 0.50 ml/min to 35 ml/min. The flow rate 0.50 ml/min is the lowest possible flow rate and the highest flow rate I have used is 27.50 ml/min.
The experiments for the calibration curve were performed as described in the SOP.

The flow rate is calculated as:

$$Q_{i,act} = \frac{m}{\rho \cdot t} = \frac{m}{((T - 22\,°C) \cdot 0.000255 + 0.9978) \cdot t} \cdot f_{drop}$$

The factor f_{drop} is 1 and was included because the T-test showed that I had forgotten an uncertainty source. The water from the waste tube is falling as drops. This causes an uncertainty because are the last 1 or 2 drops falling into the glass flask or are they staying in the tube?

The uncertainty of the balance is given by the manufacture as ± 0.001 g, and by use of a rectangular distribution and taking into account that the balance is used twice this gives:

$$u(m) = \sqrt{\frac{2}{3}} \cdot 0.001 = 0.000816 \text{ g}$$

The uncertainty of the thermometer is given by the manufacture as ± 0.1 °C, and by use of a rectangular distribution this gives:

$$u(T) = \frac{0.1}{\sqrt{3}} = 0.057735 \text{ °C}$$

The uncertainty of the time is estimated as ± 1 second = ± 1/60 min, and by use of a triangular distribution this gives:

$$u(t) = \frac{1/60}{\sqrt{6}} = 0.013608 \text{ min}$$

The uncertainty arising from the drops falling are estimated to ± 2 drops, which is approximately ± 0.090 g. Use of a rectangular distribution gives:

$$u(\text{drop}) = \frac{0.090}{\sqrt{3}} = 0.051962 \text{ g}$$

With f_{drop} = 1 the partial derivatives can be expressed as:

$$\frac{\partial Q_{act}}{\partial m} = \frac{1}{((T - 22\,°C) \cdot 0.000255 + 0.9978) \cdot t}$$

$$\frac{\partial Q_{act}}{\partial T} = \frac{-0.00255 \cdot m \cdot t}{(((T - 22\,°C) \cdot 0.000255 + 0.9978) \cdot t)^2}$$

$$\frac{\partial Q_{act}}{\partial t} = \frac{-m}{((T - 22\,°C) \cdot 0.000255 + 0.9978) \cdot t^2}$$

$$\frac{\partial Q_{act}}{\partial f_{drop}} = \frac{m}{((T - 22\,°C) \cdot 0.000255 + 0.9978) \cdot t}$$

The combined uncertainty is calculated as:

$$u(Q_{i,act,cal}) = \sqrt{\left(\frac{\partial Q_{act}}{\partial m}\right)^2 \cdot u^2(m) + \left(\frac{\partial Q_{act}}{\partial T}\right)^2 \cdot u^2(T) + \left(\frac{\partial Q_{act}}{\partial t}\right)^2 \cdot u^2(t) + \left(\frac{\partial Q_{act}}{\partial f_{drop}}\right)^2 \cdot u^2(drop)}$$

The weights assigned to each $Q_{i,act}$ can now be determined as:

$$w_i = \frac{1}{u^2(Q_{i,act,cal})}$$

The weighted mean values for each flow rate is calculated as:

$$Q_{j,mean} = \frac{\sum_{i=1}^{n} w_i \cdot Q_{i,act,cal}}{\sum_{i=1}^{n} w_i}$$

To see if the mean values are in statistical control the T-test is performed on each mean value:

$$T = \sum_{i=1}^{n} \frac{(Q_{i,act,cal} - Q_{j,mean})^2}{u^2(Q_{i,act,cal})}$$

After introducing the parameter f_{drop} the weighted mean values are in statistical control, and can be used instead of the individual measurements.

The uncertainty of the mean values is calculated as:

$$u(Q_{j,mean,cal}) = \sqrt{\frac{1}{\sum_{i=1}^{n} w_i}}$$

The repeatability standard deviation and the repeatability uncertainty for each flow rate are calculated as:

$$s_{j,repeat} = \sqrt{\frac{1}{1-n} \cdot \sum_{i=1}^{n} (Q_{i,act,cal} - Q_{j,mean})^2}$$

$$u(j,repeat) = \frac{s_{j,repeat}}{\sqrt{2 \cdot (n-1)}}$$

The uncertainty of the mean values is determined by combining the repeatability uncertainty and the calculated uncertainty for the mean values:

$$u(Q_{j,mean}) = \sqrt{u^2(Q_{j,mean,cal}) + u^2(j,repeat)}$$

The weights assigned to each mean value is calculated as:

$$w_j = \frac{1}{u^2(Q_{j,mean})}$$

The calibration is assumed to be linear and the constants a and b in the equation:

$Q_{act} = a \cdot Q_{nom} + b$ is determined by weighted regression.

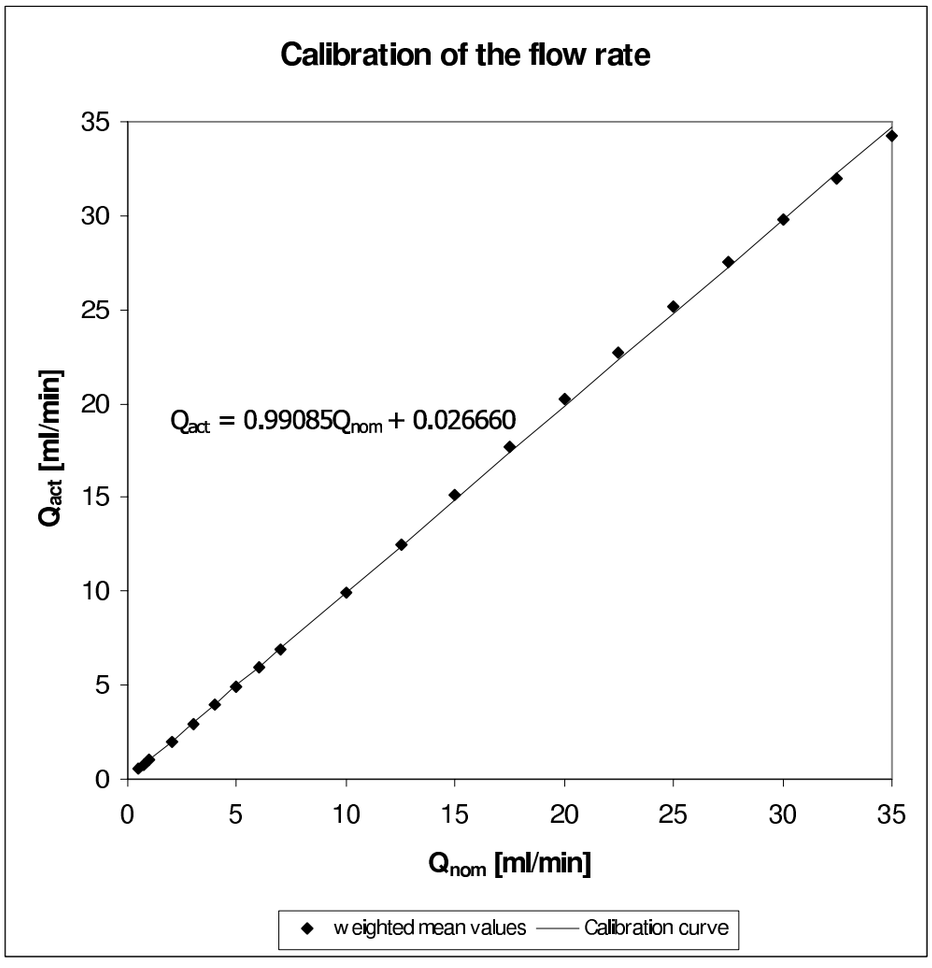

Figure 4: Calibration curve for the flow rate.

The T-test is performed to see if the regression line is in statistical control:

$$T = \sum_{i=1}^{n} \frac{(Q_{j,mean} - Q_{act,pred})^2}{u^2(Q_{j,mean})}$$

From the T-value = 2.656 it is clear that the calibration is in statistical control.
It is now investigated if there is a connection between the flow rate and the standard deviation. The standard deviation is calculated from the uncertainty as:

$$SD = u(Q_{act,pred}) \cdot \sqrt{2 \cdot (n-1)}$$

The SD at Q_{nom} = 35.0 ml/min is an outlier and is not included in the regression.
Two equations $SD = a \cdot Q_{act,pred} + b$ and $SD^2 = m \cdot (Q_{act,pred})^2 + c$ are investigated in order to find a relationship between SD and $Q_{act,pred}$. From the T values it is observed that the equation $SD = a \cdot Q_{act,pred} + b$ gives the best description of the relation between SD and $Q_{act,pred}$. The equation: $u(Q_{act,pred}) = 0.053066 \cdot Q_{act,pred} + 0.002987$ is therefore used to calculate the standard uncertainty of $Q_{act,pred}$.

The correction factor for the flow rate k is calculated as:

$$k = \frac{Q_{act,pred}}{Q_{nom}}$$

And while Q_{nom} has no uncertainty the uncertainty of k is determined as:

$$u(k) = \sqrt{SD^2 \cdot \frac{1}{Q_{nom}^2}} = \frac{SD}{Q_{nom}}$$

The retention volume of the empty column, $V_{R,empty}$:
$V_{R,empty}$ is determined for the column with V_{col} = 9.39 ml by two different loads, 50 µl and 100 µl. The nominal flow rates used are 1 and 3 ml/min.

First the retention volume and the uncertainty of the retention volume are calculated without taking the flow rate into account:

$$V_{obs,empty} = (b + d)$$
$$u(V_{obs,empty}) = \sqrt{u^2(b) + u^2(d)}$$

The actual flow rate k and u(k) are calculated as described above. The retention volume corrected for the flow rate is now calculated as:

$$V_{R,empty,cal} = V_{obs,empty} \cdot k$$

And the uncertainty $u(V_{R,empty,cal})$ is calculated as:

$$u(V_{R,empty,cal}) = \sqrt{k^2 \cdot u(V_{obs,empty}) + V_{obs,empty}^2 \cdot u^2(k)}$$

$V_{R,empty}$ is now determined as the weighted mean value, and the T-test is performed to see if the mean value is in statistical control. The mean value is in statistical control while T = 1.265 for the load 100 µl and T = 0.110 for the load 50 µl.

The repeatability standard deviation and the repeatability uncertainty are now calculated and the uncertainty of $V_{R,empty}$ is determined as:

$$u(V_{R,empty}) = \sqrt{u^2(V_{R,empty,mean}) + u^2(repeat)}$$

Where $u(V_{R,empty,mean}) = \sqrt{\frac{1}{\sum_{i=1}^{n} w_i}}$

This gives:

- Load 100 µl: $V_{R,empty}$ = 0.937 ml $u(V_{R,empty})$ = 0.012
- Load 50 µl: $V_{R,empty}$ = 0.902 ml $u(V_{R,empty})$ = 0.021

The retention volume of the protein BSA, V_R:

These calculations are similar to the calculations for the retention volume of the empty column.

The calculation of the retention volume of BSA without correction for the retention volume of the empty column is made for 4 different columns. The retention volumes determined are:

- V_{col} = 0.98 ml: $V_{R,uncor}$ = 1.634 ml with $u(V_{R,uncor})$ = 0.045 ml at c_s = 0.20 M
- V_{col} = 7.99 ml: $V_{R,uncor}$ = 10.34 ml with $u(V_{R,uncor})$ = 0.25 ml at c_s = 0.20 M
- V_{col} = 9.39 ml: $V_{R,uncor}$ = 13.32 ml with $u(V_{R,uncor})$ = 0.32 ml at c_s = 0.20 M
- V_{col} = 55.61 ml: $V_{R,uncor}$ = 35.6 ml with $u(V_{R,uncor})$ = 1.1 ml at c_s = 1.95 M

I have only made calculations of the retention volume of the empty column for the column with V_{col} = 9.39 ml. Thus, only the retention volume measured for this column is corrected for the retention volume of the empty column. The load was 100 µl, so the retention volume of the empty column used, is the one at the load = 100 µl.

$V_{R,9.39} = V_{R,uncor} - V_{R,empty} = 13.320\ ml - 0.916\ ml = 12.40\ ml$

$$u(V_{R,9.39}) = \sqrt{u^2(V_{R,uncor}) + u^2(V_{R,empty})}$$
$$= \sqrt{0.319^2 + 0.0125^2}$$
$$= 0.32\ ml$$

Contribution to the uncertainty:

For the column with V_{col} = 9.39 ml a histogram of the different contributions to the uncertainty of the retention volume was made.

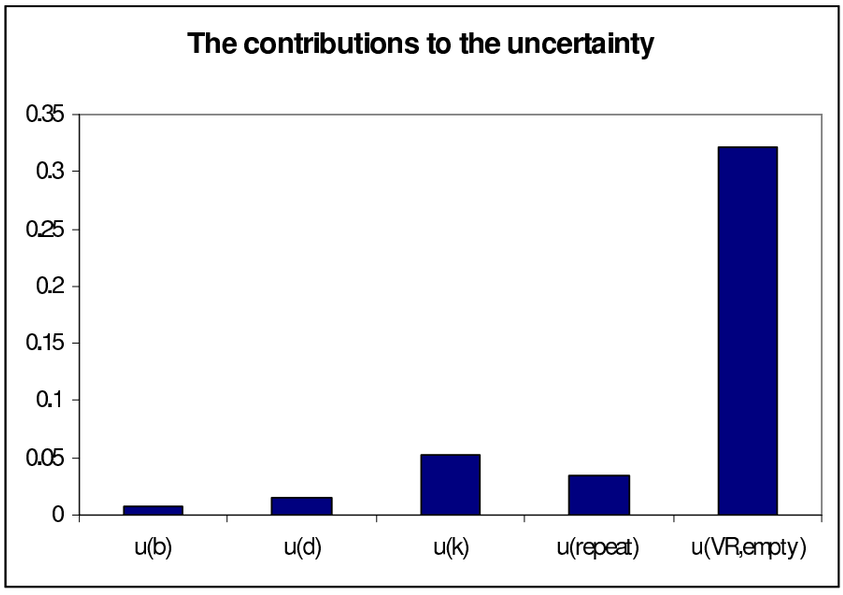

Figure 5: A histogram of the contributions to the uncertainty.

From the histogram it is seen that all the contributions are small. The largest contribution is the uncertainty of the correction factor, but it is still small.

Conclusion:

It seems like the uncertainty budget is capable of describing the uncertainty of the retention volume of the protein. All the uncertainty contributions are so small, that it will not be worth the effort to try to make them even smaller.

THE FOLLOWING WAS GIVEN AS APPENDICES TO THE UNCERTAINTY BUDGET.

STANDARD OPERATING PROCEDURE FOR DETERMINATION OF RETENTION VOLUMES OF WHEY PROTEINS ON THE BIOCAD WORKSTATION

In this SOP it is assumed that the mobile phase and the sample solution are prepared, and that the user is familiar with the software to the BioCAD and the program TableCurve 2D.

1) Fill 10 ml of the sample solution in a 10 ml test tube and place it on one of the sample inlets.
2) Prime the sample inlet 3 times with 100 µl sample solution.
3) Place the mobile phase on one of the mobile phase inlets A, B, C, D or E (F is used for water).
4) Purge the mobile phase inlet by 20 ml at a flow rate of 10 ml/min.
5) If a new flow rate is used it must be calibrated. (See the description later).
6) Make a method in the BioCAD method editor.
   Method:
   A) Specify the column position and the flow rate.
   B) Equil Block: Equilibrate the column with 40 ml mobile phase and reset the UV-detector after 39 ml.
   C) Load Block: Load the appropriate amount of sample solution to the column and start the data collection.
   D) Elute Block: Specify the elution mode and the amount of mobile phase for the elution.
   E) Regen Block: Regenerate the column with 40 ml of 2 M salt solution.
7) If no measurements of the retention volume of the empty column is made, repeat 6) with an empty column where the top and bottom assemblies are as close together as possible (no volume between).
8) Fit the peaks with the EMG-function in TableCurve 2D, and calculated the retention volumes: $V_{R,cal} = (b + d)\cdot k$, where b and d are parameters in the EMG-function, and k is the correction factor for the flow rate.
9) Calculate the retention volume of the protein: $V_R = V_{R,cal} - V_{empty}$

Calibration of flow rate:

1) Weigh a glass bottle, m_1 [g]
2) On the BioCAD method editor: Select the flow rate in question, Q_{nom} [ml/min], and specify the time, t [min], for the experiment and set the column position in bypass.
3) During the experiment the water from the waste tube is collected in the glass bottle.
4) Collect at least 2 minutes and at least 10 ml of water.
5) Weight the glass bottle with the water, m_2 [g] and measure the temperature, T [°C].
6) Calculated the amount of water: $m = m_2 - m_1$ [g].
7) Calculate the actual flow rate: $Q_{act} = m/\rho\cdot t$ [ml/min].
   $\rho = (T - 22°C)\cdot 0.000255 + 0.9978$ [g/cm^3].

CAUSE AND EFFECT DIAGRAM FOR DETERMINATION OF RETENTION VOLUMES OF WHEY PROTEINS ON THE BIOCAD WORKSTATION

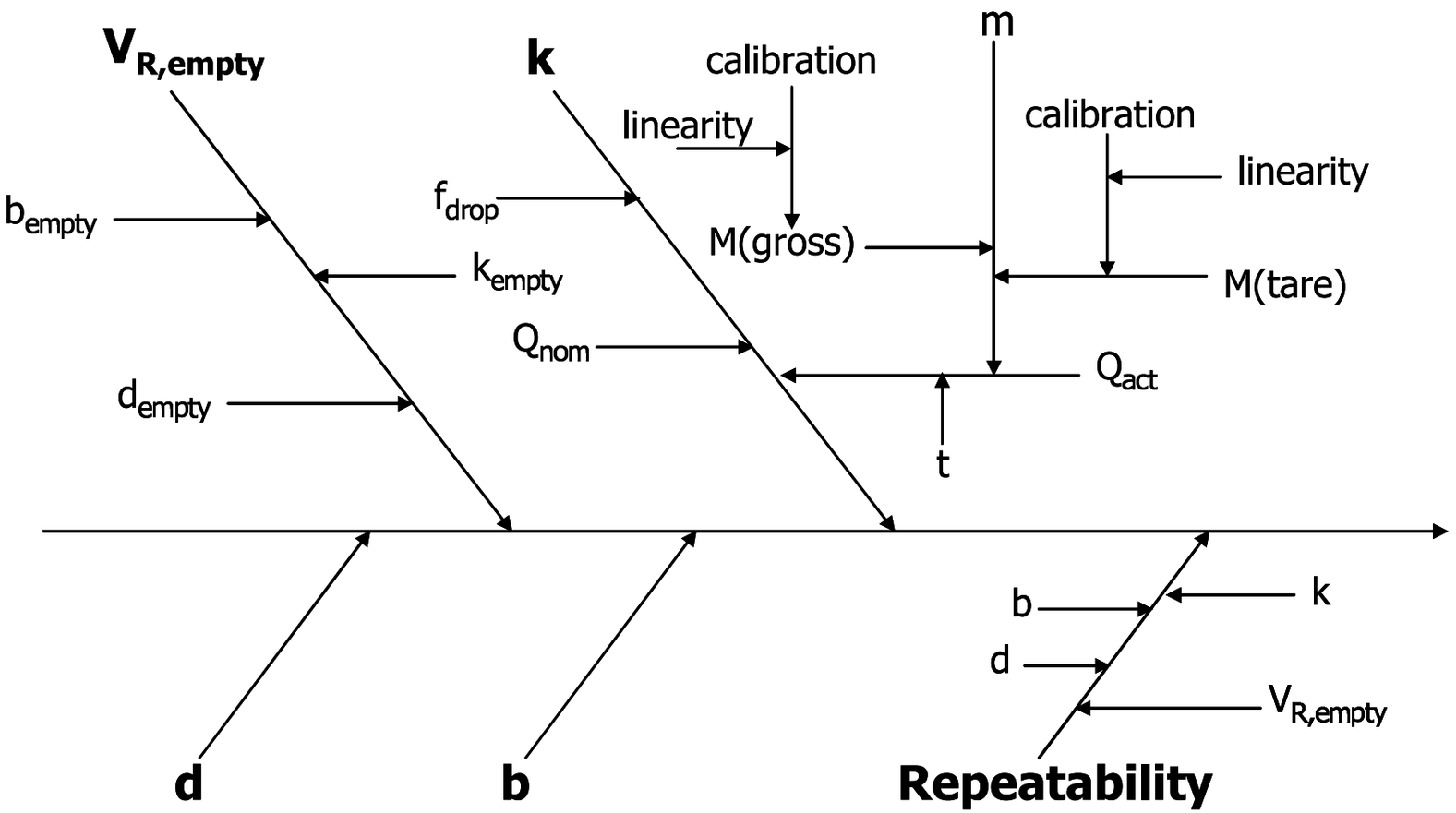

CALIBRATION OF THE FLOW RATE

Calculation of $Q_{i,act}$ and $u(Q_{i,act,cal})$:

Q_{nom} [ml/min]	T [°C]	t [min]	m_1 [g]	m_2 [g]	M [g]	Q [g/min]	$Q_{i,act}$ [ml/min]	$Q_{act}'(t)$	$Q_{act}'(T)$	$Q_{act}'(m)$	$Q_{act}'(drop)$	$u(Q_{i,act,cal})$
0.50	21.9	24	89.5653	102.2101	12.6448	0.52687	0.52804	-0.02200	-0.00013	0.04176	0.52804	0.02744
	21.9	20	90.9048	101.4620	10.5572	0.52786	0.52904	-0.02645	-0.00014	0.05011	0.52904	0.02749
	22.0	50	101.4620	127.8965	26.4345	0.52869	0.52986	-0.01060	-0.00014	0.02004	0.52986	0.02753
0.75	22.0	100	91.1650	168.0696	76.9046	0.76905	0.77074	-0.00771	-0.00020	0.01002	0.77074	0.04005
	22.0	40	90.5285	121.1884	30.6599	0.76650	0.76819	-0.01920	-0.00020	0.02506	0.76819	0.03992
	22.2	30	91.1076	114.0707	22.9631	0.76544	0.76709	-0.02557	-0.00020	0.03341	0.76709	0.03986
1.00	22.0	10	91.1750	101.2138	10.0388	1.00388	1.00609	-0.10061	-0.00026	0.10022	1.00609	0.05230
	22.0	20	101.2138	121.2992	20.0854	1.00427	1.00648	-0.05032	-0.00026	0.05011	1.00648	0.05230
2.00	22.0	10	91.3048	111.0288	19.7240	1.97240	1.97675	-0.19767	-0.00051	0.10022	1.97675	0.10275
	22.0	16	111.0288	142.4214	31.3926	1.96204	1.96636	-0.12290	-0.00050	0.06264	1.96636	0.10219
	21.8	20	90.5619	129.9083	39.3464	1.96732	1.97176	-0.09859	-0.00050	0.05011	1.97176	0.10246
3.00	22.0	10	91.3558	120.6110	29.2552	2.92552	2.93197	-0.29320	-0.00075	0.10022	2.93197	0.15240
	22.0	15	120.6110	164.6072	43.9962	2.93308	2.93955	-0.19597	-0.00075	0.06681	2.93955	0.15277
4.00	21.9	15	129.9083	188.9809	59.0726	3.93817	3.94696	-0.26313	-0.00101	0.06682	3.94696	0.20512
	21.9	10	91.7087	131.1176	39.4089	3.94089	3.94968	-0.39497	-0.00101	0.10022	3.94968	0.20530
5.00	21.9	10	91.2860	140.5653	49.2793	4.92793	4.93892	-0.49389	-0.00126	0.10022	4.93892	0.25672
	21.9	6	140.5653	170.1333	29.5680	4.92800	4.93899	-0.82317	-0.00126	0.16704	4.93899	0.25688
6.00	21.9	5	91.9963	121.5872	29.5909	5.91818	5.93138	-1.18628	-0.00152	0.20045	5.93138	0.30863
	21.9	10	121.5872	180.7761	59.1889	5.91889	5.93209	-0.59321	-0.00152	0.10022	5.93209	0.30835
7.00	21.9	4	91.7330	119.3716	27.6386	6.90965	6.92506	-1.73127	-0.00177	0.25056	6.92506	0.36061
	21.9	10	91.6614	160.8374	69.1760	6.91760	6.93303	-0.69330	-0.00177	0.10022	6.93303	0.36037
10.00	21.9	3	119.3716	149.2099	29.8383	9.94610	9.96828	-3.32276	-0.00255	0.33408	9.96828	0.51994
	21.9	7	91.0234	160.6217	69.5983	9.94261	9.96479	-1.42354	-0.00255	0.14318	9.96479	0.51815
12.50	21.9	6	90.4178	165.3285	74.9107	12.48512	12.51296	-2.08549	-0.00320	0.16704	12.51296	0.65081
	21.9	3	91.1378	128.4542	37.3164	12.43880	12.46654	-4.15551	-0.00319	0.33408	12.46654	0.65024

Calculation of $Q_{i,act}$ and $u(Q_{i,act,cal})$ continued:

Q_{nom} [ml/min]	T [°C]	t [min]	m_1 [g]	m_2 [g]	M [g]	Q [g/min]	$Q_{i,act}$ [ml/min]	$Q_{act}'(t)$	$Q_{act}'(T)$	$Q_{act}'(m)$	$Q_{act}'(drop)$	$u(Q_{i,act,cal})$
15.00	21.9	6	91.2675	181.6920	90.4245	15.07075	15.10436	-2.51739	-0.00386	0.16704	15.10436	0.78559
	21.9	3	91.1856	136.4398	45.2542	15.08473	15.11838	-5.03946	-0.00386	0.33408	15.11838	0.78856
17.50	22.1	6	91.4695	197.2649	105.7954	17.63257	17.67099	-2.94517	-0.00452	0.16703	17.67099	0.91909
	22.1	4	91.2739	161.6395	70.3656	17.59140	17.62974	-4.40743	-0.00451	0.25054	17.62974	0.91803
20.00	22.1	5	91.5197	192.3900	100.8703	20.17406	20.21802	-4.04360	-0.00517	0.20044	20.21802	1.05200
	22.0	4	90.0740	170.2512	80.1772	20.04430	20.08849	-5.02212	-0.00513	0.25055	20.08849	1.04606
	22.1	3	91.4586	152.3480	60.8894	20.29647	20.34070	-6.78023	-0.00520	0.33406	20.34070	1.06095
22.50	22.2	5	91.4694	205.0165	113.5471	22.70942	22.75833	-4.55167	-0.00582	0.20043	22.75833	1.18418
	22.2	3	91.5712	159.6345	68.0633	22.68777	22.73663	-7.57888	-0.00581	0.33405	22.73663	1.18592
25.00	22.2	4.5	91.4079	204.1353	112.7274	25.05053	25.10448	-5.57877	-0.00642	0.22270	25.10448	1.30667
	22.2	2	91.0792	141.3864	50.3072	25.15360	25.20777	-12.60389	-0.00644	0.50108	25.20777	1.32102
27.50	22.2	4	91.3472	200.8963	109.5491	27.38728	27.44626	-6.86156	-0.00701	0.25054	27.44626	1.42920
	22.2	2	91.0398	145.9505	54.9107	27.45535	27.51448	-13.75724	-0.00703	0.50108	27.51448	1.44190
30.00	22.2	3.5	91.2001	195.1714	103.9713	29.70609	29.77006	-8.50573	-0.00761	0.28633	29.77006	1.55122
	22.2	2	90.9393	150.4224	59.4831	29.74155	29.80560	-14.90280	-0.00762	0.50108	29.80560	1.56197
32.50	22.2	3.5	91.0466	202.8970	111.8504	31.95726	32.02608	-9.15031	-0.00818	0.28633	32.02608	1.66878
	22.2	2	91.2906	155.1470	63.8564	31.92820	31.99696	-15.99848	-0.00818	0.50108	31.99696	1.67680
35.00	22.2	2	91.1301	159.5988	68.4687	34.23435	34.30808	-17.15404	-0.00877	0.50108	34.30808	1.79792
	22.2	3	90.7800	193.2496	102.4696	34.15653	34.23009	-11.41003	-0.00875	0.33405	34.23009	1.78541
	22.2	2	91.7512	160.2641	68.5129	34.25645	34.33023	-17.16511	-0.00877	0.50108	34.33023	1.79908
	22.2	3	90.7693	193.4077	102.6384	34.21280	34.28648	-11.42883	-0.00876	0.33405	34.28648	1.78835

Calculation of $Q_{j,mean}$, T-test and $u(Q_{j,mean})$:

Q_{nom} [ml/min]	$Q_{i,act}$ [ml/min]	$u(Q_{i,act,cal})$	w_i	$Q_{j,mean}$	T	$u(Q_{j,mean,cal})$	s(j,repeat)	u(j,repeat))	$u(Q_{j,mean})$
0.50	0.52804	0.02744	1328.15	0.5290	0.002185	0.01587	0.00091	0.00045	0.01588
	0.52904	0.02749	1323.09						
	0.52986	0.02753	1319.19						
0.75	0.77074	0.04005	623.47	0.7687	0.004403	0.02306	0.00188	0.00094	0.02308
	0.76819	0.03992	627.60						
	0.76709	0.03986	629.38						
1.00	1.00609	0.05230	365.65	1.0063	2.79E-05	0.03698	0.00028	0.00020	0.03698
	1.00648	0.05230	365.55						
2.00	1.97675	0.10275	94.72	1.9716	0.005139	0.05916	0.00519	0.00260	0.05922
	1.96636	0.10219	95.76						
	1.97176	0.10246	95.25						
3.00	2.93197	0.15240	43.05	2.9357	0.001233	0.10789	0.00536	0.00379	0.10796
	2.93955	0.15277	42.85						
4.00	3.94696	0.20512	23.77	3.9483	8.8E-05	0.14511	0.00193	0.00136	0.14511
	3.94968	0.20530	23.73						
5.00	4.93892	0.25672	15.17	4.9390	3.73E-08	0.18159	0.00005	0.00004	0.18159
	4.93899	0.25688	15.15						
6.00	5.93138	0.30863	10.50	5.9317	2.66E-06	0.21813	0.00050	0.00036	0.21813
	5.93209	0.30835	10.52						
7.00	6.92506	0.36061	7.69	6.9290	0.000244	0.25491	0.00563	0.00398	0.25494
	6.93303	0.36037	7.70						
10.00	9.96828	0.51994	3.70	9.9665	2.27E-05	0.36702	0.00247	0.00175	0.36702
	9.96479	0.51815	3.72						
12.50	12.51296	0.65081	2.36	12.4897	0.002546	0.45999	0.03282	0.02321	0.46058
	12.46654	0.65024	2.37						

Calculation of $Q_{j,mean}$, T-test and $u(Q_{j,mean})$ continued:

Q_{nom} [ml/min]	$Q_{i,act}$ [ml/min]	$u(Q_{i,act,cal})$	w_i	$Q_{j,mean}$	T	$u(Q_{j,mean,cal})$	s(j,repeat)	u(j,repeat))	$u(Q_{j,mean})$
15.00	15.10436	0.78559	1.62	15.1113	0.000159	0.55654	0.00991	0.00701	0.55659
	15.11838	0.78856	1.61						
17.50	17.67099	0.91909	1.18	17.6503	0.001009	0.64952	0.02917	0.02063	0.64985
	17.62974	0.91803	1.19						
20.00	20.21802	1.05200	0.90	20.2146	0.028669	0.60792	0.08918	0.04459	0.60956
	20.08849	1.04606	0.91						
	20.34070	1.06095	0.89						
22.50	22.75833	1.18418	0.71	22.7475	0.000168	0.83796	0.01534	0.01085	0.83803
	22.73663	1.18592	0.71						
25.00	25.10448	1.30667	0.59	25.1556	0.00309	0.92899	0.07304	0.05164	0.93042
	25.20777	1.32102	0.57						
27.50	27.44626	1.42920	0.49	27.4801	0.001129	1.01506	0.04824	0.03411	1.01563
	27.51448	1.44190	0.48						
30.00	29.77006	1.55122	0.42	29.7877	0.000261	1.10066	0.02513	0.01777	1.10080
	29.80560	1.56197	0.41						
32.50	32.02608	1.66878	0.36	32.0116	0.000152	1.18283	0.02059	0.01456	1.18292
	31.99696	1.67680	0.36						
35.00	34.30808	1.79792	0.31	34.2885	0.001728	0.89633	0.04297	0.01754	0.89650
	34.23009	1.78541	0.31						
	34.33023	1.79908	0.31						
	34.28648	1.78835	0.31						

Calculation of w_j, $Q_{nom,pred}$ and T-test:

Q_{nom} [ml/min]	$Q_{j,mean}$	$u(Q_{j,mean})$	w_j	$Q_{act,pred}$	$res^2/u^2(Q_{j,mean})$
0.50	0.5290	0.01588	3967.182	0.522087	0.188265035
0.75	0.7687	0.02308	1877.349	0.769801	0.002421146
1.00	1.0063	0.03698	731.1761	1.017515	0.092141257
2.00	1.9716	0.05922	285.1784	2.008369	0.385449542
3.00	2.9357	0.10796	85.79801	2.999223	0.345670714
4.00	3.9483	0.14511	47.48853	3.990077	0.082815058
5.00	4.9390	0.18159	30.32729	4.980932	0.053433904
6.00	5.9317	0.21813	21.01637	5.971786	0.033709643
7.00	6.9290	0.25494	15.38635	6.96264	0.017362437
10.00	9.9665	0.36702	7.423658	9.935203	0.007286136
12.50	12.4897	0.46058	4.714047	12.41234	0.0282372
15.00	15.1113	0.55659	3.22798	14.88947	0.158902964
17.50	17.6503	0.64985	2.367989	17.36661	0.190629602
20.00	20.2146	0.60956	2.69137	19.84375	0.370059162
22.50	22.7475	0.83803	1.423915	22.32088	0.259149238
25.00	25.1556	0.93042	1.155155	24.79802	0.147674009
27.50	27.4801	1.01563	0.969456	27.27515	0.04070679
30.00	29.7877	1.10080	0.825242	29.75229	0.001035353
32.50	32.0116	1.18292	0.714642	32.22942	0.033910752
35.00	34.2885	0.89650	1.244219	34.70656	0.217462172
				T =	2.656

$Q_{act} = 0.99085\, Q_{nom} + 0.02666$

Correlation of the flow rate and the standard uncertainty:

$Q_{act,pred}$ [ml/min]	$u(Q_{j,mean})$	n	SD	$Q^2_{act,pred}$ [ml/min]	SD^2	SD^2_{pred}	$(SD^2 - SD^2_{pred})^2/u(Q_{j,mean})^2$	SD_{pred}	$(SD - SD_{pred})^2/u(Q_{j,mean})^2$
0.522	0.01588	3	0.0318	0.2726	0.0010	0.0198	1.4020	0.0307	0.00447
0.770	0.02308	3	0.0462	0.5926	0.0021	0.0207	0.6468	0.0438	0.01012
1.018	0.03698	2	0.0523	1.0353	0.0027	0.0219	0.2690	0.0570	0.01603
2.008	0.05922	3	0.1184	4.0335	0.0140	0.0302	0.0747	0.1096	0.02243
2.999	0.10796	2	0.1527	8.9953	0.0233	0.0439	0.0365	0.1621	0.00769
3.990	0.14511	2	0.2052	15.921	0.0421	0.0631	0.0209	0.2147	0.00429
4.981	0.18159	2	0.2568	24.810	0.0659	0.0877	0.0143	0.2673	0.00335
5.972	0.21813	2	0.3085	35.662	0.0952	0.1177	0.0107	0.3199	0.00273
6.963	0.25494	2	0.3605	48.478	0.1300	0.1531	0.0082	0.3725	0.00219
9.935	0.36702	2	0.5190	98.708	0.2694	0.2921	0.0038	0.5302	0.00092
12.412	0.46058	2	0.6514	154.07	0.4243	0.4452	0.0021	0.6617	0.00050
14.889	0.55659	2	0.7871	221.70	0.6196	0.6322	0.0005	0.7931	0.00012
17.367	0.64985	2	0.9190	301.60	0.8446	0.8532	0.0002	0.9246	0.00007
19.844	0.60956	3	1.2191	393.77	1.4862	1.1082	0.3847	1.0560	0.07159
22.321	0.83803	2	1.1851	498.22	1.4046	1.3970	0.0001	1.1875	0.00001
24.798	0.93042	2	1.3158	614.94	1.7314	1.7199	0.0002	1.3189	0.00001
27.275	1.01563	2	1.4363	743.93	2.0630	2.0766	0.0002	1.4504	0.00019
29.752	1.10080	2	1.5568	885.20	2.4235	2.4673	0.0016	1.5818	0.00052
32.229	1.18292	2	1.6729	1038.7	2.7986	2.8920	0.0062	1.7133	0.00116
34.707	0.89650	4	2.1960	1204.5	4.8223	3.3506	---	1.8447	---
							T = 2.883		T = 0.148

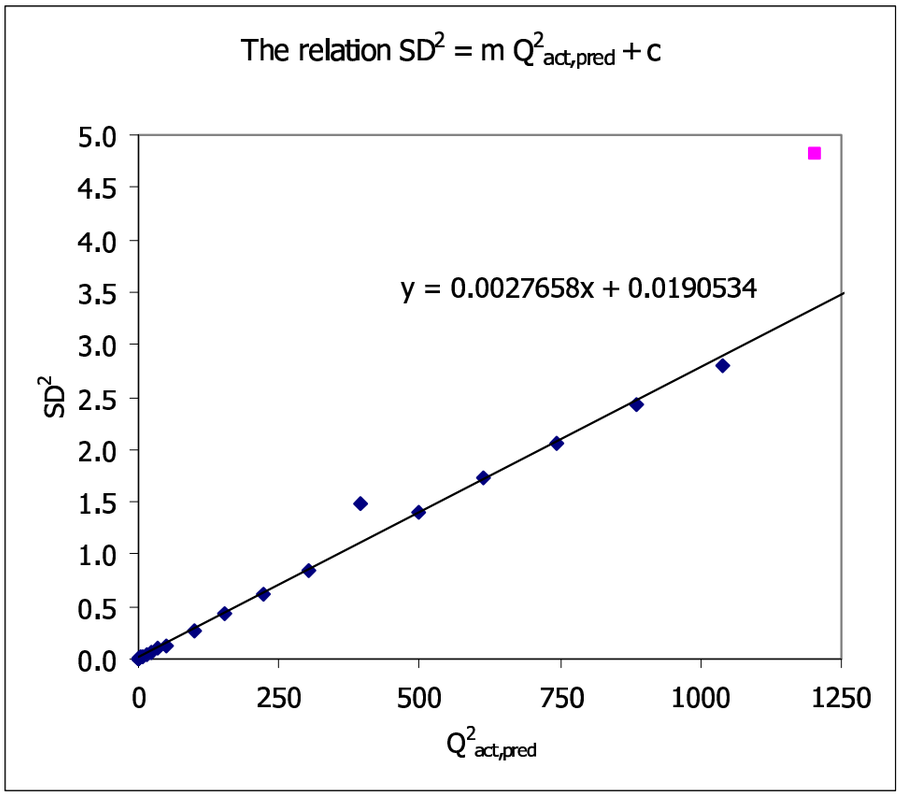
The relation $SD^2 = m\ Q^2_{act,pred} + c$
y = 0.0027658x + 0.0190534
SD^2
$Q^2_{act,pred}$
0.0
0.5
1.0
1.5
2.0
2.5
3.0
3.5
4.0
4.5
5.0
0
250
500
750
1000
1250

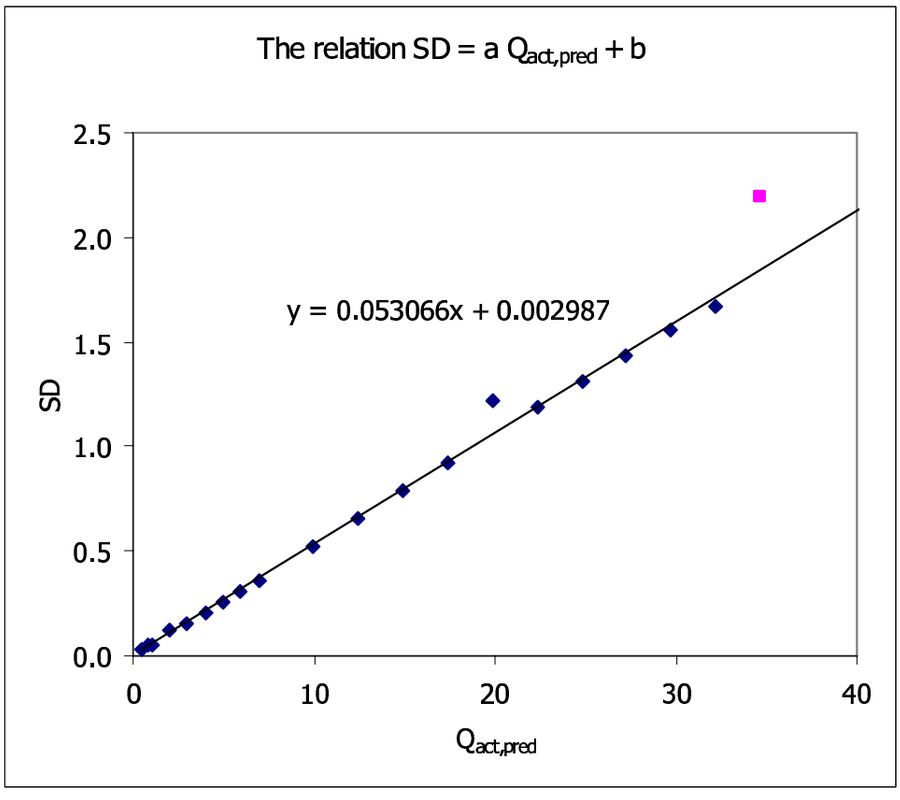
The relation $SD = a\ Q_{act,pred} + b$
y = 0.053066x + 0.002987
SD
$Q_{act,pred}$
0.0
0.5
1.0
1.5
2.0
2.5
0
10
20
30
40

CALCULATION OF $v_{R,EMPTY}$ FOR THE COLUMN HR16

Q_{nom} [ml/min]	Load [µl]	d	b	SD(b) = u(b)	SD(d) = u(d)	$V_{obs,empty}$ [ml]	u($V_{obs,empty}$)	$V_{R,empty,cal}$ [ml]
1.0	100	0.17440	0.73814	0.00074	0.0016	0.9125	0.001763	0.92853
1.0	100	0.25623	0.67650	0.00032	0.0011	0.9327	0.001146	0.94907
1.0	100	0.25465	0.68039	0.00029	0.0010	0.9350	0.001041	0.95141
1.0	100	0.25575	0.68211	0.00029	0.0010	0.9379	0.001041	0.95428
1.0	100	0.26059	0.66702	0.00033	0.0012	0.9276	0.001245	0.94386
1.0	100	0.26093	0.66679	0.00033	0.0012	0.9277	0.001245	0.94396
1.0	100	0.12079	0.78577	0.00058	0.0011	0.9066	0.001244	0.92243
1.0	100	0.12005	0.78156	0.0006	0.0011	0.9016	0.001253	0.91741
1.0	100	0.12076	0.78198	0.0006	0.0011	0.9027	0.001253	0.91855
1.0	100	0.11979	0.78226	0.0006	0.0011	0.9020	0.001253	0.91785
1.0	100	0.11923	0.78610	0.0006	0.0011	0.9053	0.001253	0.92118
1.0	100	0.11864	0.78835	0.00059	0.0011	0.9070	0.001248	0.92288
3.0	100	0.23266	0.72521	0.00068	0.0021	0.9579	0.002207	0.95762
3.0	100	0.23745	0.71807	0.00065	0.0021	0.9555	0.002198	0.95527
3.0	100	0.23621	0.70777	0.00067	0.0021	0.9440	0.002204	0.94374
3.0	100	0.23346	0.70820	0.00066	0.0021	0.9417	0.002201	0.94142
3.0	100	0.23097	0.70880	0.0006	0.0019	0.9398	0.001992	0.93953
3.0	100	0.23050	0.70342	0.00062	0.0020	0.9339	0.002094	0.93367
1.0	50	0.24659	0.64788	0.0002	0.0008	0.8945	0.000786	0.91014
1.0	50	0.24585	0.64711	0.00022	0.0008	0.8930	0.000868	0.90860
1.0	50	0.24603	0.64306	0.0002	0.0008	0.8891	0.000776	0.90467
1.0	50	0.24521	0.64389	0.0002	0.0008	0.8891	0.000776	0.90467
1.0	50	0.24530	0.63135	0.0002	0.0008	0.8766	0.000786	0.89200
1.0	50	0.24586	0.63320	0.00021	0.0008	0.8791	0.000837	0.89446

Q_{nom} [ml/min]	$u(V_{R,empty,cal})$	w_i	$V_{R,empty}$ [ml]	T	s(repeat)	u(repeat)	$u(V_{R,empty,mean})$	$u(V_{R,empty})$
1.0	0.0520	369.393						
1.0	0.0532	353.825						
1.0	0.0533	352.120						
1.0	0.0535	350.007						
1.0	0.0529	357.712						
1.0	0.0529	357.633						
1.0	0.0517	374.514						
1.0	0.0514	378.623						
1.0	0.0515	377.683	0.916	1.2647	0.0142	0.00243	0.01222	0.01246
1.0	0.0514	378.260						
1.0	0.0516	375.528						
1.0	0.0517	374.150						
3.0	0.0518	372.425						
3.0	0.0517	374.265						
3.0	0.0511	383.445						
3.0	0.0509	385.340						
3.0	0.0508	387.019						
3.0	0.0505	391.814						
1.0	0.0510	384.836						
1.0	0.0509	386.116						
1.0	0.0507	389.506	0.902	0.11037	0.00748	0.00237	0.02063	0.02077
1.0	0.0507	389.501						
1.0	0.0500	400.642						
1.0	0.0501	398.430						

Q_{nom} [ml/min]	$Q_{act,pred}$ [ml/min]	$u(Q_{act,pred})$	k	u(k)
1.0	1.0175	0.05698	1.01751	0.05698
3.0	2.9992	0.16214	0.99974	0.05405

CALCULATION OF THE RETENTION VOLUME OF THE PROTEIN BSA

V_{col} [ml]	C_s [M]	Q [ml/min]	b	d	u(b)	u(d)	$V_{R,obs}$ [ml]	$u(V_{obs,empty})$	$V_{R,cal}$ [ml]
55.61	1.95	27.8	32.8382	3.6498	0.0123	0.0228	36.488	0.0259	36.189
55.61	1.95	13.9	32.8625	2.6224	0.0047	0.0082	35.485	0.0095	35.228
55.61	1.95	13.9	32.9752	2.6113	0.0045	0.0078	35.587	0.0089	35.329
9.39	0.20	9.39	10.9572	2.5657	0.0073	0.0152	13.523	0.0169	13.438
9.39	0.20	9.39	10.8804	2.6046	0.0060	0.0127	13.485	0.0141	13.400
9.39	0.20	4.695	11.4461	1.8670	0.0029	0.0051	13.313	0.0059	13.267
9.39	0.20	4.695	11.5040	1.8491	0.0028	0.0050	13.353	0.0057	13.307
9.39	0.20	4.695	11.3323	1.9068	0.0028	0.0049	13.239	0.0057	13.193
8.07	0.20	8.07	8.3916	2.0137	0.0059	0.0117	10.405	0.0131	10.345
8.07	0.20	8.07	8.4337	2.0626	0.0060	0.0121	10.496	0.0134	10.435
8.07	0.20	3.995	8.8412	1.4112	0.0048	0.0085	10.252	0.0098	10.227
8.07	0.20	3.995	9.1816	1.0752	0.0066	0.0102	10.257	0.0121	10.231
8.07	0.20	3.995	9.1042	1.3815	0.0038	0.0067	10.486	0.0077	10.460
0.98	0.20	0.980	1.3969	0.2489	0.0022	0.0037	1.646	0.0043	1.676
0.98	0.20	0.980	1.4097	0.2523	0.0021	0.0036	1.662	0.0042	1.692
0.98	0.20	0.510	1.3549	0.1818	0.0025	0.0039	1.537	0.0047	1.603
0.98	0.20	0.510	1.3516	0.1763	0.0029	0.0043	1.528	0.0052	1.594
0.98	0.20	0.510	1.3666	0.1715	0.0032	0.0048	1.538	0.0058	1.605

V_{col} [ml]	$u(V_{R,cal})$	w_i	$V_{R,uncork}$ [ml]	T	s(repeat)	u(repeat)	$u(V_{R,uncor,mean})$	$u(V_{R,uncor})$
55.61	1.9245	0.2700						
55.61	1.8771	0.2838	35.573	0.15298	0.5281	0.2641	1.0937	1.1251
55.61	1.8824	0.2822						
9.39	0.7176	1.9421						
9.39	0.7155	1.9533						
9.39	0.7125	1.9697	13.320	0.01017	0.0991	0.0350	0.3192	0.3211
9.39	0.7147	1.9580						
9.39	0.7086	1.9918						
8.07	0.5530	3.2700						
8.07	0.5578	3.2135						
8.07	0.5505	3.3002	10.338	0.00459	0.1096	0.0387	0.2482	0.2512
8.07	0.5507	3.2969						
8.07	0.5630	3.1554						
0.98	0.0940	113.082						
0.98	0.0950	110.918						
0.98	0.0942	112.693	1.634	6.78E-07	0.0462	0.0163	0.0421	0.0452
0.98	0.0937	113.925						
0.98	0.0944	112.323						

Q_{nom} [ml/min]	$Q_{act,pred}$ [ml/min]	$u(Q_{act,pred})$	k	u(k)
27.80	27.58	1.4663	0.9918	0.0527
13.90	13.80	0.7354	0.9928	0.0529
9.390	9.331	0.4981	0.9937	0.0530
7.990	7.944	0.4245	0.9942	0.0531
4.695	4.679	0.2513	0.9965	0.0535
3.995	3.985	0.2145	0.9975	0.0537
0.980	0.998	0.0559	1.0181	0.0571
0.510	0.532	0.0312	1.0432	0.0612

Retention volume and uncertainty for the elution of BSA on the column with V_{col} = 9.39 ml

$V_{R,9.39}$ = 13.320 – 0.916 ml = 12.40 ml

$u(V_{R,9.39})$ = 0.32 ml

APPENDIX A.II: CALIBRATION OF THE MIXER

The mixer was calibrated by mixing a solution of pure milliQ water and a solution of $NaNO_3$. Before the calibration was started the water solution was run through the system until the UV-signal was constant, and the UV-detector was reset. Then the absorbance of the pure nitrate solution at 280 nm was measured. The calibration is started at 2.0% nitrate solution and 98.0% MilliQ water, and kept constant for 5 milliliters before the gradient is started. The gradient starts at 2% nitrate solution and is increased to 100% nitrate solution during a specified volume.
The actual % of mixing is calculated as:

$$\%\,\text{mixing} = \frac{\text{Abs.}}{\text{Abs.}_{\text{pure nitrate}}}$$

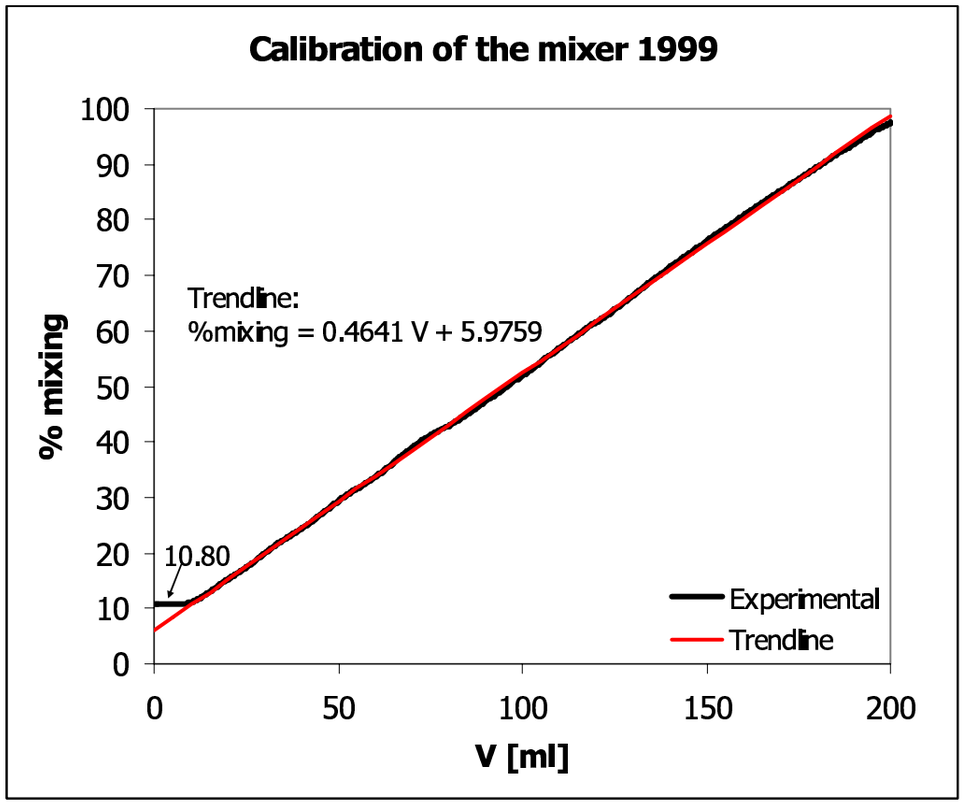

From the figure it appears that programmed 2% mixing is actual 10.80%, and that the mixing is linear from that point. The curve does not reach 100% because the method was stopped at 100% mixing and the dead volume from the mixer to the detector is around 5 ml. The last 5 ml therefore never reached the detector.

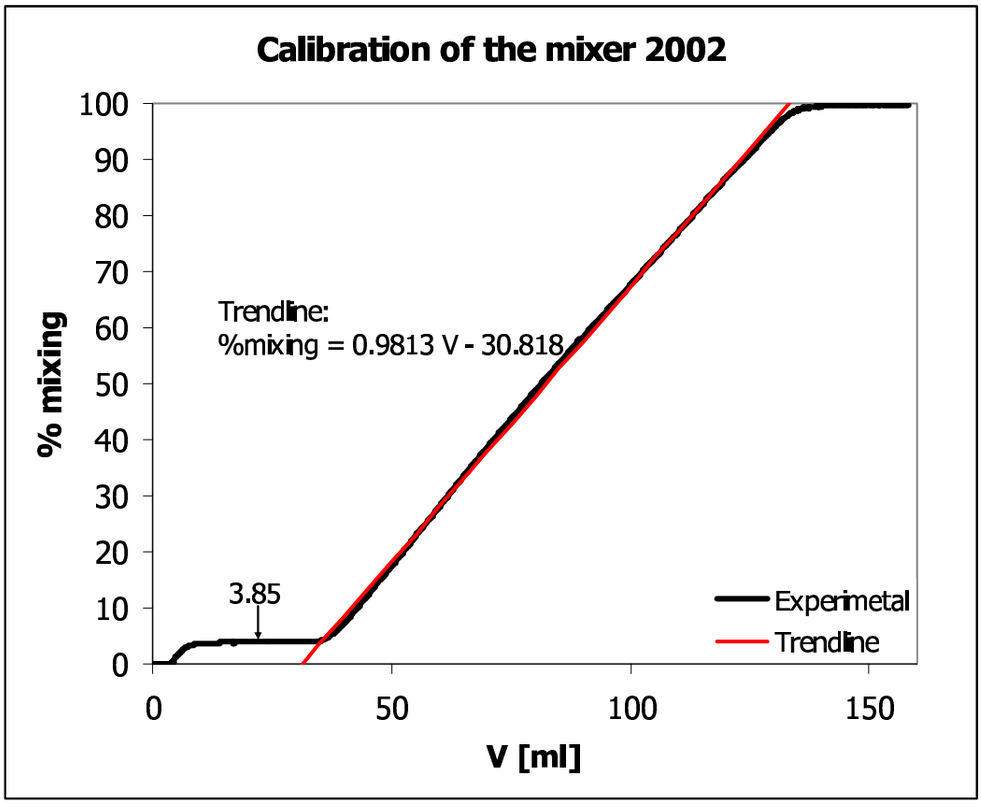

From the figure it appears that the mixer has changed since 1999. The programmed 2% mixing is now actual 3.85% and not 10.80% as in 1999. The mixer is still linear from the nominal 2% to 100% mixing.

APPENDIX A.III: CALIBRATION CURVE FOR $NaNO_3$

Date: 13/12-99	
C_{NaNO3}	Abs. 280 nm
0.0	0
0.1	0.1891
0.1	0.1923
0.2	0.3753
0.2	0.3784
0.4	0.7396
0.4	0.7431
0.6	1.0853
0.6	1.0589
0.8	1.429
0.8	1.4379
1.0	1.7682
1.0	1.776
1.0	1.773
1.0	1.7821
1.2	2.091
1.2	2.1028
1.5	2.55
1.5	2.54
2.0	above 3

Date: 9/4-02	
C_{NaNO3}	Abs. 280 nm
0.0	0
0.095	0.1905
0.19	0.3766
0.38	0.7243
0.57	1.0653
0.76	1.3765
0.95	1.6885

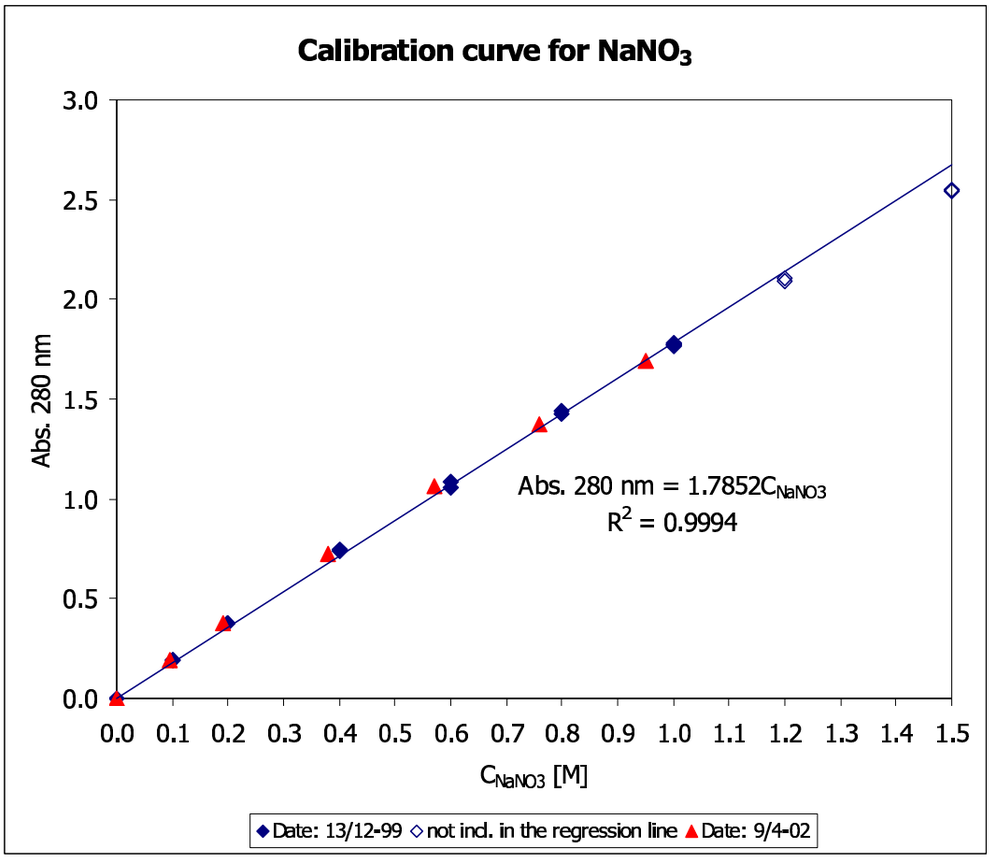

APPENDIX A.IV: CALIBRATION CURVE FOR BSA

Date: 14/12-99	
C_{BSA} [g/l]	Abs. 280 nm
0.015	0.006
0.030	0.011
0.061	0.023
0.122	0.045
0.304	0.114
0.608	0.226
1.215	0.449
2.025	0.739
2.430	0.889
3.038	1.108
4.050	1.476
4.860	1.754
6.075	2.174
8.100	2.736

Date: 30/8-01	
C_{BSA} [g/l]	Abs. 280 nm
0.502	0.186
1.005	0.368
2.512	0.916
3.015	1.092

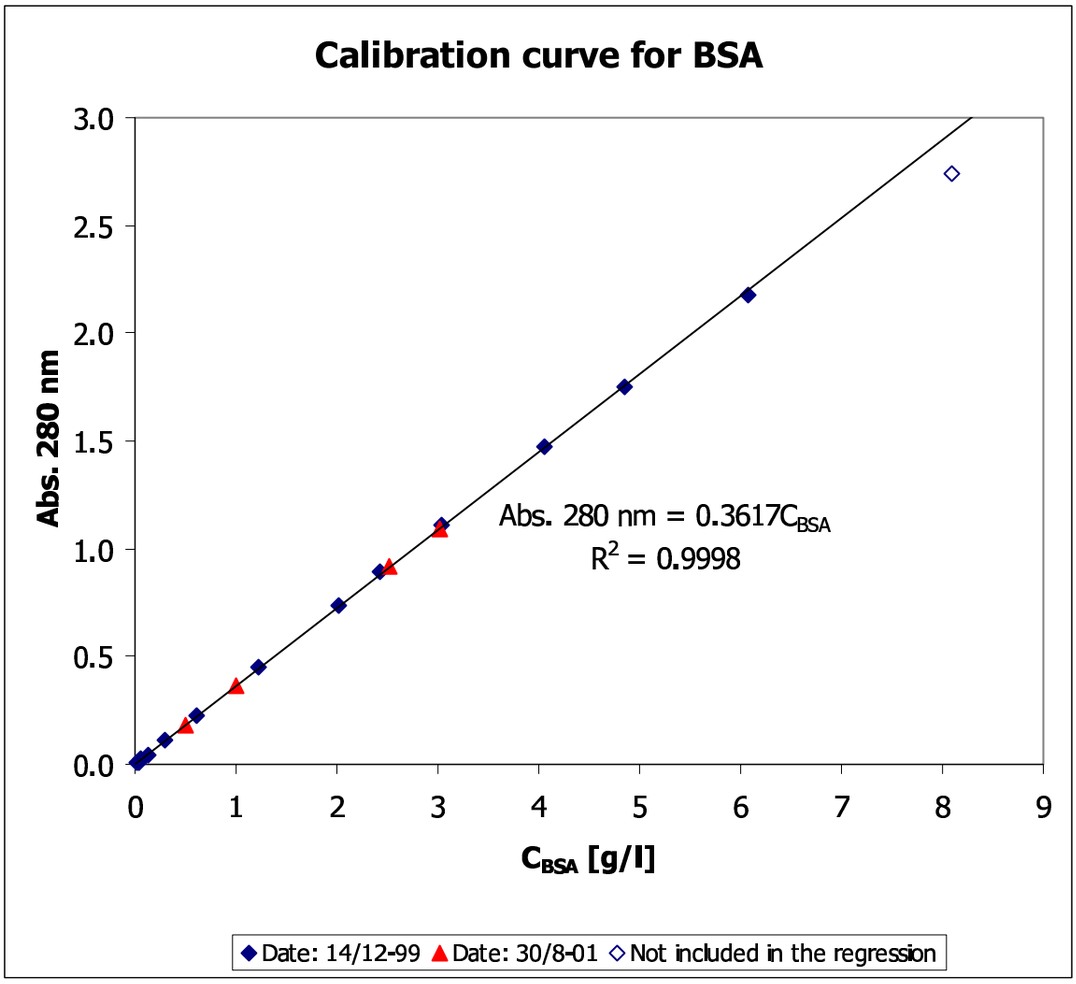

APPENDIX A.V: CALCULATION OF THE UNCERTAINTY OF THE Cl^--CONCENTRATION IN THE BUFFER SOLUTIONS

The stock solution without NaCl, buffer A:

The amount of Cl^--ions in this solution is added by titration with 5N HCl and the concentration is calculated as:

$$c_{Cl^-,A} = \frac{c_{HCl} \cdot V_{HCl}}{V_{water} + V_{HCl}} = 0.0372\,M$$

Where c_{HCl} = 5N, $V_{HCl} \approx$ 37.5 ml (this is the approximate amount added to obtain a pH of 6 in a 5 liter solution) and V_{water} = 5.0 l (most often 5 liters is prepared).

The 5 liter water for the solution is added in three portions by use of a 1 liter calibrated flask and a 2 liter calibrated flask.
The uncertainty of the calibrated flasks is by the manufacture stated as: 1000 ml ± 0.4 ml and 2000 ml ± 0.6 ml. There is an additional uncertainty from the readings of the volume. This additional uncertainty is estimated to ± 0.2 ml for both calibrated flasks, wherefore the uncertainties become: 1000 ml ± 0.6 ml and 2000 ml ± 0.8 ml.

The volume of the solution V_{water} is calculated as:

$$V_{water} = V_1 + 2V_2$$

By use of a rectangular distribution the uncertainties are given as:

$$u(V_1) = \sqrt{\frac{1}{3}} \cdot 0.0006\,l = 0.000346\,l$$
$$u(V_2) = \sqrt{\frac{1}{3}} \cdot 0.0008\,l = 0.000462\,l$$

With the partial derivatives:

$$\frac{\partial V_{water}}{\partial V_1} = 1$$
$$\frac{\partial V_{water}}{\partial V_2} = 2$$

The combined uncertainty of V_{water} becomes:

$$u(V_{water}) = \sqrt{\left(\frac{\partial V_{water}}{V_1}\right)^2 u^2(V_1) + \left(\frac{\partial V_{water}}{V_2}\right)^2 u^2(V_2)}$$
$$= 0.000987\,l$$

The first 36 ml of HCl is added by pipette and the rest as drops. The uncertainty of V_{HCl} is estimated to ± 0.2 ml. The uncertainty of the concentration of the 5N HCl solution is by the manufacture stated as ± 0.5% which gives ± 0.025 N.
By use of a rectangular distribution the uncertainties are given as:

$$u(V_{HCl}) = \sqrt{\frac{1}{3}} \cdot 0.0002\,l = 0.000115\,l$$
$$u(c_{HCl}) = \sqrt{\frac{1}{3}} \cdot 0.025\,N = 0.014434\,N$$

The partial derivatives:

$$\frac{\partial c_{Cl^-}}{\partial V_{water}} = \frac{-c_{HCl} V_{HCl}}{(V_{water} + V_{HCl})^2} = -0.007389\ mol/l^2$$
$$\frac{\partial c_{Cl^-}}{\partial c_{HCl}} = \frac{V_{HCl}}{V_{water} + V_{HCl}} = 0.007444$$
$$\frac{\partial c_{Cl^-}}{\partial V_{HCl}} = \frac{c_{HCl} V_{water}}{(V_{water} + V_{HCl})^2} = 0.98517\ mol/l^2$$

The uncertainty of the Cl^--concentration in the solution without NaCl added is now calculated as:

$$u(c_{Cl^-,A}) = \sqrt{u^2(V_{water})\left(\frac{\partial c_{Cl^-}}{\partial V_{water}}\right)^2 + u^2(c_{HCl})\left(\frac{\partial c_{Cl^-}}{\partial c_{HCl}}\right)^2 + u^2(V_{HCl})\left(\frac{\partial c_{Cl^-}}{\partial V_{HCl}}\right)^2}$$
$$= 0.00016\,M$$

The stock solution with 58.44 g NaCl per liter water, buffer B:

The calculation of the uncertainty of the solution with 58.44 g NaCl per liter water will also be based on a 5 liter solution, because most often 5 liter is prepared.

The volume correction factor φ is calculated as:

$$\varphi = \frac{1}{\left(1 - \alpha \cdot c^m_{NaCl}\right) \cdot \left(1 + c^m_{NaCl} \cdot Mw_{NaCl}\right)} = 0.9792$$

Where $c^m_{NaCl} = \frac{m_{NaCl}}{Mw_{NaCl}\, V_{water}\, \rho_{water}} = 1.00\,mol/kg$ and m_{NaCl} = 292.2 g, Mw_{NaCl} = 58.44 g/mol,

$V_{water} = 5.00\,l$ and $\rho_{water} = 1.00\,kg/l$.

First the combined uncertainty of the molale NaCl-concentration is calculated. The uncertainty of the balance is by the manufacture stated as ± 1.0 g and the uncertainty of the density of water is estimated to 0.003 kg/l, because the density of water at 25 °C is 1.003 kg/l. The uncertainty of the volume of water is equal to the combined uncertainty of V_{water} calculated above.

The uncertainties are calculated by use of the rectangular distribution:

$$u(m_{NaCl}) = \sqrt{\frac{1}{3}} \cdot 0.1\,g = 0.5774\,g$$

$$u(\rho_{water}) = \sqrt{\frac{1}{3}} \cdot 0.003\,kg/l = 0.001732\,kg/l$$

The partial derivatives:

$$\frac{\partial c^m_{NaCl}}{\partial m_{NaCl}} = \frac{1}{Mw_{NaCl}\, V_{water}\, \rho_{water}} = 0.003422\,mol/g \cdot kg$$

$$\frac{\partial c^m_{NaCl}}{\partial V_{water}} = \frac{-m_{NaCl}}{Mw_{NaCl}\, V^2_{water}\, \rho_{water}} = -0.2000\,mol/l \cdot kg$$

$$\frac{\partial c^m_{NaCl}}{\partial \rho_{water}} = \frac{-m_{NaCl}}{Mw_{NaCl}\, V_{water}\, \rho^2_{water}} = -1.000\,mol \cdot l/kg^2$$

The combined uncertainty of the molale NaCl-concentration:

$$u(c^m_{NaCl}) = \sqrt{u^2(m_{NaCl})\left(\frac{\partial c^m_{NaCl}}{\partial m_{NaCl}}\right)^2 + u^2(V_{water})\left(\frac{\partial c^m_{NaCl}}{\partial V_{water}}\right)^2 + u^2(\rho_{water})\left(\frac{\partial c^m_{NaCl}}{\partial \rho_{water}}\right)^2}$$
$$= 0.002635\ mol/kg$$

It is now possible to calculate the combined uncertainty of the volume correction factor. The uncertainty of the parameter α is estimated to ±0.0005 kg/mol.

$$u(\alpha) = \sqrt{\frac{1}{3}} \cdot 0.0005\,\text{kg/mol} = 0.0002887\,\text{kg/mol}$$

The partial derivatives:

$$\frac{\partial\varphi}{\partial\alpha} = \frac{-c^m_{NaCl}}{\left(1-\alpha c^m_{NaCl}\right)^2\left(1+c^m_{NaCl}Mw_{NaCl}\right)} = -1.01477\,\text{mol/kg}$$

$$\frac{\partial\varphi}{\partial c^m_{NaCl}} = \frac{\alpha+2\alpha c^m_{NaCl}Mw_{NaCl}-Mw_{NaCl}}{\left(1-\alpha c^m_{NaCl}\right)^2\left(1+c^m_{NaCl}Mw_{NaCl}\right)^2} = -0.01844\ \text{kg/mol}$$

(Mw_{NaCl} = 0.05844 kg/mol)

The combined uncertainty of φ:

$$u(\varphi) = \sqrt{u^2(\alpha)\left(\frac{\partial\varphi}{\partial\alpha}\right)^2 + u^2\left(c^m_{NaCl}\right)\left(\frac{\partial\varphi}{\partial c^m_{NaCl}}\right)^2}$$
$$= 0.000297$$

The corrected volume is calculated as:

$$V_{cor.} = \frac{V_{water}}{\varphi} = 5.106\,\text{l}$$

The partial derivatives:

$$\frac{\partial V_{cor.}}{\partial V_{water}} = \frac{1}{\varphi} = 1.0213$$

$$\frac{\partial V_{cor.}}{\partial\varphi} = \frac{-V_{water}}{\varphi^2} = -5.2152\,\text{l}$$

The combined uncertainty of the corrected volume:

$$u(V_{cor.}) = \sqrt{u^2(V_{water})\left(\frac{\partial V_{cor.}}{\partial V_{water}}\right)^2 + u^2(\varphi)\left(\frac{\partial V_{cor.}}{\partial\varphi}\right)^2}$$
$$= 0.00185\,\text{l}$$

The molar concentration of NaCl before titration is calculated as:

$$c_{NaCl,before} = \frac{m_{NaCl}}{Mw_{NaCl} V_{cor.}} = 0.9792\,M$$

The partial derivatives:

$$\frac{\partial c_{NaCl,before}}{\partial m_{NaCl}} = \frac{1}{Mw_{NaCl} V_{cor.}} = 0.003351\ mol/g \cdot l$$
$$\frac{\partial c_{NaCl,before}}{\partial V_{cor.}} = \frac{-m_{NaCl}}{Mw_{NaCl} V_{cor.}^2} = -0.19178\ mol/l^2$$

$$u(c_{NaCl,before}) = \sqrt{u^2(m_{NaCl})\left(\frac{\partial c_{NaCl,before}}{\partial m_{NaCl}}\right)^2 + u^2(V_{cor.})\left(\frac{\partial c_{NaCl,before}}{\partial V_{cor.}}\right)^2}$$
$$= 0.0020\ M$$

The actual concentration of Cl^--ions after adjustment of pH is calculated as:

$$c_{Cl^-,B} = \frac{c_{NaCl,before} \cdot V_{cor.} + c_{HCl} \cdot V_{HCl}}{V_{cor.} + V_{HCl}} = 1.0085 M$$

As for buffer A the amount of HCl added to obtain a pH of 6 is around 37.5 ml with an uncertainty of ± 0.2 ml. The uncertainty of the variables in the expression for c_{Cl^-} has been calculated above and the partial derivatives are given as:

$$\frac{\partial c_{Cl^-}}{\partial c_{NaCl,before}} = \frac{V_{cor.}}{V_{cor.} + V_{HCl}} = 0.9927$$
$$\frac{\partial c_{Cl^-}}{\partial V_{cor.}} = \frac{V_{HCl}(c_{NaCl,before} - c_{HCl})}{(V_{cor.} + V_{HCl})^2} = -0.005699\ mol/l^2$$
$$\frac{\partial c_{Cl^-}}{\partial c_{HCl}} = \frac{V_{HCl}}{V_{cor.} + V_{HCl}} = 0.007291$$
$$\frac{\partial c_{Cl^-}}{\partial V_{HCl}} = \frac{V_{cor.}(c_{HCl} - c_{NaCl,before})}{(V_{cor.} + V_{HCl})^2} = 0.7760\ mol/l^2$$

The combined uncertainty of the actual concentration of Cl^--ions after adjustment of pH is now calculated as:

$$u(c_{Cl^-,B}) = \sqrt{u^2(c_{NaCl,before})\left(\frac{\partial c_{Cl^-}}{\partial c_{NaCl,before}}\right)^2 + u^2(V_{cor.})\left(\frac{\partial c_{Cl^-}}{\partial V_{cor.}}\right)^2 + u^2(c_{HCl})\left(\frac{\partial c_{Cl^-}}{\partial c_{HCl}}\right)^2 + u^2(V_{HCl})\left(\frac{\partial c_{Cl^-}}{\partial V_{HCl}}\right)^2}$$
$$= 0.0020 \text{ M}$$

The concentration of Cl^--ions in the solutions prepared by mixing of the two stock solutions is calculated as:

$$c_{Cl^-,AB} = \frac{V_A c_{Cl^-,A} + V_B c_{Cl^-,B} + V_{HCl}\, c_{HCl}}{V_A + V_B + V_{HCl}}$$

After mixing pH is increased a little, wherefore pH again is adjusted to a pH of 6. The raise in pH depends on the concentration in buffer AB after mixing. Wherefore the amount of HCl added varies a little, but for simplicity a value of 1.0 ml ±0.1 ml will be used.
For the buffers with a pH of 7, 8 and 9 5N NaOH is added to reach the pH in question. The addition of NaOH does of cause not increase the amount of Cl^--ions, but the volume is increased. The volume increase is not included in the calculation of the Cl^--concentration, and will therefore be included in the uncertainty calculations. The uncertainty calculations are made for a solution with pH > 6 in order to include the contribution to the uncertainty caused by the volume not being corrected for the addition of NaOH. The total volume is calculated as $V_{total} = V_A + V_B + V_{HCl} = 1.001$ l. The Cl^--concentration is now given as:

$$c_{Cl^-,AB} = \frac{V_A\, c_{Cl^-,A} + V_B\, c_{Cl^-,B} + V_{HCl}\, c_{HCl}}{V_{total}}$$

Because of the volume increase by addition of NaOH is neglected the uncertainty of V_{total} is assessed a value of ± 25 ml incl. the uncertainty of the volume of buffer A and B and HCl.
The uncertainty of the volume of buffer A and B depends on the calibrated flasks. The uncertainty of the calibrated flasks is by the manufacture stated as: 500 ml ±0.3 ml, 250 ml ±0.23 ml, 200 ml ±0.15 ml, 100 ml ±0.15 ml and 50 ml ±0.06 ml. Using the rectangular distribution for the uncertainty of the calibrated flasks, the volume of HCl and the total volume these becomes:

$$u(V_{500}) = \sqrt{\frac{1}{3}} \cdot 0.0003\text{l} = 0.0001732\text{l}$$
$$u(V_{250}) = \sqrt{\frac{1}{3}} \cdot 0.00023\text{l} = 0.0001328\text{l}$$
$$u(V_{200}) = u(V_{100}) = \sqrt{\frac{1}{3}} \cdot 0.00015\text{l} = 0.00008660\text{l}$$
$$u(V_{50}) = \sqrt{\frac{1}{3}} \cdot 0.00006\text{l} = 0.00003464\text{l}$$

$$u(V_{25}) = \sqrt{\frac{1}{3}} \cdot 0.00004\,l = 0.00002309\,l$$
$$u(V_{HCl}) = \sqrt{\frac{1}{3}} \cdot 0.0001\,l = 0.00005774\,l$$
$$u(V_{total}) = \sqrt{\frac{1}{3}} \cdot 0.020\,l = 0.01443\,l$$

The uncertainty of the Cl^--concentration in buffer A and B are calculated above.

The partial derivatives are given as:

$$\frac{\partial c_{Cl^-,AB}}{\partial V_A} = \frac{c_A}{V_{total}} = 0.03716\,mol/l^2$$
$$\frac{\partial c_{Cl^-,AB}}{\partial c_A} = \frac{V_A}{V_{total}}$$
$$\frac{\partial c_{Cl^-,AB}}{\partial V_B} = \frac{c_B}{V_{total}} = 1.0075\,mol/l^2$$
$$\frac{\partial c_{Cl^-,AB}}{\partial c_B} = \frac{V_B}{V_{total}}$$
$$\frac{\partial c_{Cl^-,AB}}{\partial V_{HCl}} = \frac{c_{HCl}}{V_{total}} = 4.995\,mol/l^2$$
$$\frac{\partial c_{Cl^-,AB}}{\partial c_{HCl}} = \frac{V_{HCl}}{V_{total}} = 0.0004995\,mol/l^2$$
$$\frac{\partial c_{Cl^-,AB}}{\partial V_{total}} = \frac{-(V_A c_A + V_B c_B + V_{HCl} c_{HCl})}{V_{total}^2}$$

The partial derivatives that do not depend on the volume of buffer A or B are calculated and the other derivatives are given in the table below. The uncertainties of the volume of buffer A and B are calculated from the uncertainties of the calibrated flasks. With the volumes V_A = 0.80 l and V_B = 0.20 l the uncertainties are:

$$u(V_A) = u(V_{500}) + u(V_{200}) + u(V_{100}) = 0.0003464\,l$$
$$u(V_B) = u(V_{200}) = 0.00008660\,l$$

The combined uncertainty of the Cl^--concentration in the buffers prepared by mixing of buffer A and B are given as:

$$u\left(c_{Cl^-,AB}\right)=\sqrt{\begin{array}{l}u^2(V_A)\left(\frac{\partial c_{Cl^-,AB}}{\partial V_A}\right)^2+u^2(c_A)\left(\frac{\partial c_{Cl^-,AB}}{\partial c_A}\right)^2+u^2(V_B)\left(\frac{\partial c_{Cl^-,AB}}{\partial V_B}\right)^2+u^2(c_B)\left(\frac{\partial c_{Cl^-,AB}}{\partial c_B}\right)^2\\+u^2(V_{HCl})\left(\frac{\partial c_{Cl^-,AB}}{\partial V_{HCl}}\right)^2+u^2(c_{HCl})\left(\frac{\partial c_{Cl^-,AB}}{\partial c_{HCl}}\right)^2+u^2(V_{total})\left(\frac{\partial c_{Cl^-,AB}}{\partial V_{total}}\right)^2\end{array}}$$

In the table below are given the volume of buffer A and B and the corresponding Cl^--concentration, the partial derivatives that depends on V_A or V_B, the uncertainty of V_A and V_B and the uncertainty of the Cl^--concentration.

V_A [ml]	V_B [ml]	$c_{Cl^-,AB}$ [M]	$\frac{\partial c_{Cl^-,AB}}{\partial c_A}$	$\frac{\partial c_{Cl^-,AB}}{\partial c_B}$	$\frac{\partial c_{Cl^-,AB}}{\partial V_{total}}$	$U(V_A)$ [l]	$U(V_B)$ [l]	$u\left(c_{Cl^-,AB}\right)$ [M]
0.950	0.050	0.088	0.9491	0.0500	-0.0881	0.000393	0.000035	0.0013
0.925	0.075	0.113	0.9241	0.0749	-0.1123	0.000370	0.000058	0.0017
0.900	0.100	0.137	0.8991	0.0999	-0.1366	0.000346	0.000087	0.0020
0.850	0.150	0.185	0.8492	0.1499	-0.1850	0.000393	0.000121	0.0027
0.800	0.200	0.234	0.7992	0.1998	-0.2335	0.000346	0.000087	0.0034
0.750	0.250	0.283	0.7493	0.2498	-0.2820	0.000306	0.000133	0.0041
0.600	0.400	0.428	0.5994	0.3996	-0.4274	0.000260	0.000173	0.0062
0.500	0.500	0.525	0.4995	0.4995	-0.5243	0.000173	0.000173	0.0076

APPENDIX A.VI: SPECIFICATIONS OF THE pH ELECTRODE

pHC2401-7: "Red Rod" Combined pH Electrode

pH range: 0 to 12

Temperature range: -10 to 100 °C

Zero point: pH 6.65 ± 0.5

Sensitivity: > 97%

Reference system: symmetrical light protected Ag/AgCl cartridges ("Red Rod")

Min. immersion depth: 14 mm

Junction type: annular ring

Salt-bridge solution: saturated KCl

Connection: cable with type 7 plug.

APPENDIX B.I: DEAD VOLUMES OF THE BIOCAD SYSTEM

Position 1

Volume between mixer and detector, V_{MD}

Measurements with $NaNO_3$:
Q = 2.94 ml/min

C_{NaNO3} [M]	Baseline	Area	A [UV·s]	A [UV·ml]	V [ml]
0.967	0	Total	2040.764	43.141	24.992
		Below		34.013	19.704
		Above		9.128	**5.288**
0.965	0.0021	Total	2053.641	43.058	24.992
		Below		34.227	19.866
		Above		8.831	**5.126**
0.974	0.0042	Total	563.369	52.130	29.975
		Below		9.389	**5.399**
		Above		42.740	24.576
0.985	0.00375	Total	2585.329	52.761	29.992
		Below		43.089	24.493
		Above		9.673	**5.498**
0.985	0.0044	Total	589.929	52.713	29.992
		Below		9.832	**5.594**
		Above		42.881	24.398
0.968	0.0036	Total	561.936	51.800	29.975
		Below		9.366	**5.420**
		Above		42.434	24.555
0.966	0.0036	Total	2530.194	51.692	29.975
		Below		42.170	24.453
		Above		9.522	**5.522**
0.966	0.0037	Total	574.024	51.683	29.975
		Below		9.567	**5.549**
		Above		42.116	24.426

Measurements with BSA:
Q = 2.94 ml/min

C_{BSA} [mg/ml]	Baseline	Area	A [UV·s]	A [UV·ml]	V [ml]
2.983	-0.00092	Below	113.315	32.128	29.500
		Above		5.666	**5.202**
		Total		26.463	24.298
2.929	-0.00144	Below	112.187	37.422	35.000
		Above		5.609	**5.246**
		Total		31.813	29.754

For each measurement the value in bold is the value of interest (the volume from the mixer to the detector). V_{MD} is determined as the mean value of the 10 measurements.

- V_{MD} = 5.38 ml

Volume between mixer and column inlet, V_{MC}

Q = 1.01 ml/min

C_{NaNO3} [M]	Baseline	A [UV·s]	A [UV·ml]	V [ml]	Comment
0.983	0	503.992	8.400	4.786	
0.983	-0.000024	493.425	8.224	4.685	
0.990	0.00011	486.865	8.114	4.591	
0.990	-0.000067	488.544	8.142	4.607	
0.990	0.000109	512.592	8.543	4.833	Incl. Connection link

The volume is determined as the mean value of the four measurements without the connection link.

- V_{MC} = 4.67 ml
- $V_{connection\ link}$ = 4.83 ml – 4. 67 ml = 0.16 ml

Volume between column outlet and detector, V_{CD}

Q = 1.01 ml/min

C_{NaNO3} [M]	Baseline	Area	A [UV·s]	A [UV·ml]	V [ml]	Comment
		Total		5.223	2.992	
0.978	0	Below	263.428	4.390	2.515	
		Above		0.832	**0.477**	
		Total		4.326	2.494	
0.971	0	Below	47.899	0.798	**0.460**	
		Above		3.528	2.034	
		Total		5.230	2.993	
0.979	0	Below	273.434	4.557	2.608	
		Above		0.673	**0.385**	
		Total		8.727	4.994	
0.979	0	Below	476.357	7.939	4.544	Incl. Connection link
		Above		0.788	**0.451**	
		Total		8.696	4.994	
0.975	0.0001	Below	478.400	7.973	4.579	
		Above		0.723	**0.415**	
		Total		8.665	4.994	
0.972	0	Below	44.589	0.743	**0.428**	
		Above		7.921	4.566	
		Total		8.641	4.994	
0.969	0.00023	Below	469.737	7.829	4.525	Incl. Connection link
		Above		0.812	**0.469**	

The volume is determined as the mean value of the five measurements where the connection link is not included:

- V_{CD} = 0.43 ml
- $V_{connection\ link} = \frac{0.451\ ml + 0.469\ ml}{2} - 0.43\ ml = 0.03\ ml$

Volume between the inlet and outlet of the bypass valve incl. the connection link, $V_2+V_3+V_{connection\ link}$

Q = 1.01 ml/min

C_{NaNO3} [M]	Baseline	A [UV·s]	A [UV·ml]	V [ml]
0.983	0.00046	11.362	0.189	0.108
0.983	1.7361	11.005	0.183	0.104
0.983	0.0038	12.058	0.201	0.114
0.983	0.0039	11.926	0.199	0.113
0.983	1.7222	11.151	0.186	0.106
0.983	0.00431	11.795	0.197	0.112
0.983	1.7204	11.051	0.184	0.105

The volume is determined as the mean of the seven measurements

- $V_2 + V_3 + V_{connection\ link}$ = 0.11 ml

Volume between injection and detector, V_{ID}

Q = 1.01 ml/min

Mobile phase	σ [ml]	τ [ml]	$V_{R,Gauss}$ [ml]	V_R [ml]	Comment
H_2O	0.0365	0.0540	0.2957	0.3497	2 ml before injection
H_2O	0.0369	0.0550	0.2992	0.3541	2 ml before injection
H_2O	0.0390	0.0538	0.3190	0.3728	Starting with injection
H_2O	0.0373	0.0527	0.3002	0.3528	2 ml before injection
$NaNO_3$	0.0370	0.0534	0.2995	0.3528	2 ml before injection
$NaNO_3$	0.0386	0.0580	0.3178	0.3758	Starting with injection
$NaNO_3$	0.0374	0.0578	0.3000	0.3578	2 ml before injection
$NaNO_3$	0.0399	0.0521	0.3235	0.3756	Starting with injection

The volumes determined with the method that starts with injection are higher than the volumes where 2 ml of mobile phase is run through the system before injection. No reason for this trend is found, but because no method normally starts with injection, V_{ID} is determined as the mean value of the five measurements where 2 ml of mobile phase is run through the system before the injection.

- $V_{ID} + V_{connection\ link}$ = 0.35 ml

Position 2

Volume between mixer and detector, V_{MD}

Measurements with $NaNO_3$:

Q = 2.94 ml/min

C_{NaNO3} [M]	Baseline	Area	A [UV·s]	A [UV·ml]	V [ml]
0.992	-0.00693	Total	2095.219	44.240	24.992
		Below		34.920	19.727
		Above		9.320	**5.265**
0.986	0.003215	Total	569.074	43.990	24.992
		Below		9.485	**5.388**
		Above		34.506	19.603
0.987	0.001543	Total	2086.270	44.033	24.992
		Below		34.771	19.735
		Above		9.262	**5.257**
0.986	0.003478	Total	568.496	43.954	24.975
		Below		9.475	**5.384**
		Above		34.479	19.591
0.974	-0.000017	Total	2041.679	43.438	24.992
		Below		34.028	19.578
		Above		9.410	**5.414**
0.971	0.0060	Total	565.597	43.313	24.992
		Below		9.427	**5.439**
		Above		33.886	19.552

Measurements with BSA:

Q = 2.94 ml/min

C_{BSA} [mg/ml]	Baseline	Area	A [UV·s]	A [UV·ml]	V [ml]
2.881	-0.00018	Below	627.064	36.820	35.000
		Above		31.353	29.803
		Total		5.467	**5.197**
2.851	0	Below	110.742	36.428	35.000
		Above		5.537	**5.320**
		Total		30.891	29.380

For each measurement the value in bold is the value of interest (the volume from the mixer to the detector). V_{MD} is determined as the mean value of the 8 measurements.

- V_{MD} = 5.33 ml

Volume between mixer and column inlet, V_{MC}

Q = 1.01 ml/min

C_{NaNO3} [M]	Baseline	A [UV·s]	A [UV·ml]	V [ml]	Comment
0.983	-0.00021	504.654	8.411	4.792	
0.983	-0.000163	507.835	8.464	4.822	
0.983	0.00012	515.643	8.594	4.896	
0.983	0.00206	506.152	8.436	4.806	
0.990	-0.000065	498.729	8.312	4.703	
0.990	-0.000161	515.871	8.598	4.864	Incl. Connection link

The volume is determined as the mean value of the four measurements without the connection link.

- V_{MC} = 4.80 ml
- $V_{connection\ link}$ = 4.864 ml – 4.80 ml = 0.06 ml

Volume between column outlet and detector, V_{CD}

Q = 1.01 ml/min

C_{NaNO3} [M]	Baseline	Area	A [UV·s]	A [UV·ml]	V [ml]	Comment
		Total		8.608	4.992	
0.966	0	Below	51.701	0.862	**0.500**	
		Above		7.746	4.492	
		Total		8.587	4.992	
0.964	0	Below	460.785	7.680	4.464	
		Above		0.907	**0.527**	
		Total		8.580	4.992	
0.963	0.00184	Below	52.868	0.881	**0.513**	
		Above		7.699	4.479	
		Total		4.286	2.492	
0.964	0	Below	200.155	3.336	1.939	Incl. Connection link
		Above		0.950	**0.552**	
		Total		4.285	2.492	
0.963	0.00139	Below	55.692	0.928	**0.540**	Incl. Connection link
		Above		3.357	1.952	

The values of interest are in bold.

Volume is determined as the mean value of the three measurements where the connection link is not included:

- V_{CD} = 0.51 ml
- $V_{connection\ link} = \frac{0.552\ ml + 0.540\ ml}{2} - 0.51\ ml = 0.04\ ml$

Volume between the inlet and outlet of the bypass valve incl. the connection link, $V_2+V_3+V_{forb.-led}$

Q = 1.01 ml/min

C_{NaNO3} [M]	Baseline	A [UV·s]	A [UV·ml]	V [ml]
0.983	1.7652	16.745	0.279	0.159
0.983	0.0057	18.352	0.306	0.174
0.983	1.7614	16.389	0.273	0.156
0.983	1.0056	18.400	0.307	0.175
0.990	1.7247	16.041	0.267	0.151
0.990	0.0070	17.841	0.297	0.168

The volume is determined as the mean of the six measurements

- $V_2 + V_3 + V_{connection\ link}$ = 0.16 ml

Volume between injection and detector, V_{ID}

Q = 1.01 ml/min

Mobile phase	σ [ml]	τ [ml]	$V_{R,Gauss}$ [ml]	V_R [ml]	Comment
H_2O	0.04362	0.06083	0.37666	0.438	2 ml before injection
H_2O	0.04350	0.06227	0.39462	0.457	Starting with injection
H_2O	0.04312	0.06096	0.37855	0.440	2 ml before injection
H_2O	0.04737	0.06240	0.37865	0.441	Starting with injection
H_2O	0.04475	0.06199	0.50505	0.567	Starting with injection
$NaNO_3$	0.04436	0.06170	0.38217	0.444	2 ml before injection
$NaNO_3$	0.04491	0.06618	0.40101	0.467	Starting with injection
$NaNO_3$	0.04365	0.06311	0.38211	0.445	2 ml before injection
$NaNO_3$	0.04707	0.06012	0.40695	0.467	Starting with injection

As for position 1 it is observed that the volumes determined with the method that starts with injection are higher than the volumes where 2 ml of mobile phase is run through the system before the injection. Thus V_{ID} is also for position 2 is determined as the mean value of the measurements where 2 ml of mobile phase is run through the system before the injection.

- $V_{ID} + V_{connection\ link}$ = 0.44 ml

Volume of connection link, $V_{connection\ link}$

The volume of the connection link has been determined together with the volumes V_{MC} and V_{MD} in both position 1 and 2. The volumes determined are: 0.16 ml, 0.03 ml, 0.06 ml and 0.04 ml. it is obvious that the volume of 0.16 ml is too high, because it is even higher than the volume between the inlet and outlet of the bypass valves incl. the connection link. This measurement is therefore omitted in the calculation of the volume of the connection link and the volume becomes:

$$V_{connection\ link} = \frac{0.03\,ml + 0.06\,ml + 0.04\,ml}{3} = 0.04ml$$

APPENDIX B.II: DEAD VOLUMES OF THE EMPTY COLUMNS

The HR16 column

The measurements are made with an empty column without filters.
Column position: 1
Mobile phase: 2.0 M NaCl

Puls	Q [ml/min]	σ_{gauss} [m]	τ [ml]	$V_{R,gauss}$ [ml]	V_R [ml]	σ^2 [ml^2]	
25 µl BSA	1.01	0.0501	0.1957	0.6174	0.8183	0.0413	
25 µl BSA	1.01	0.0514	0.2416	0.6128	0.8597	0.0618	
25 µl BSA	1.01	0.0486	0.2586	0.6166	0.8807	0.0701	0.051
25 µl BSA	1.01	0.0467	0.2614	0.6163	0.8832	0.0714	
25 µl BSA	1.01	0.0934	0.1550	0.6868	0.8470	0.0332	
25 µl BSA	1.01	0.0935	0.1331	0.7180	0.8564	0.0268	
100 µl BSA	1.01	0.0986	0.1744	0.7381	0.9183	0.0406	
100 µl BSA	1.01	0.0619	0.2562	0.6765	0.9386	0.0704	
100 µl BSA	1.01	0.0606	0.2546	0.6804	0.9409	0.0694	0.066
100 µl BSA	1.01	0.0600	0.2557	0.6821	0.9438	0.0699	
100 µl BSA	1.01	0.0578	0.2606	0.6670	0.9334	0.0722	
100 µl BSA	1.01	0.0574	0.2609	0.6668	0.9336	0.0723	
100 µl BSA	2.94	0.0683	0.2327	0.7252	0.9374	0.0563	
100 µl BSA	2.94	0.0642	0.2374	0.7181	0.9351	0.0579	
100 µl BSA	2.94	0.0642	0.2362	0.7078	0.9238	0.0574	0.056
100 µl BSA	2.94	0.0640	0.2335	0.7082	0.9215	0.0561	
100 µl BSA	2.94	0.0632	0.2310	0.7088	0.9196	0.0549	
100 µl BSA	2.94	0.0598	0.2305	0.7034	0.9139	0.0543	
50 µl BSA	1.01	0.0465	0.2466	0.6479	0.9001	0.0638	
50 µl BSA	1.01	0.0478	0.2459	0.6471	0.8986	0.0635	
50 µl BSA	1.01	0.0474	0.2460	0.6431	0.8947	0.0636	0.063
50 µl BSA	1.01	0.0482	0.2452	0.6439	0.8947	0.0632	
50 µl BSA	1.01	0.0457	0.2453	0.6313	0.8822	0.0630	
50 µl BSA	1.01	0.0457	0.2459	0.6332	0.8846	0.0633	
100 µl	1.01	0.0966	0.1208	0.7858	0.9123	0.0242	
100 µl	1.01	0.0959	0.1201	0.7816	0.9073	0.0239	
100 µl	1.01	0.0948	0.1208	0.7820	0.9084	0.0239	0.024
100 µl	1.01	0.0949	0.1198	0.7823	0.9077	0.0237	
100 µl	1.01	0.0942	0.1192	0.7861	0.9110	0.0234	
100 µl	1.01	0.0944	0.1186	0.7883	0.9127	0.0233	

The dead volume of the HR16 column is determined as the mean value of all the measured retention volumes.

$$V_{empty16} = V_{R,mean} - V_{ID,pos.1} = 0.916\,ml - 0.31\,ml = 0.606\,ml$$

This volume is measured by two variable assemblies. The variable assembly has a longer tube than the non variable assembly (normal bottom assembly). A column with one variable and one non variable assembly will therefore have a smaller dead volume than the column with two variable assemblies. The tube of the non variable assembly is 36.1 cm shorter than the tube of the variable

assembly. The inner diameter of the tube is 0.8 mm, so the volume of the extra 36.1 cm of tube is 0.181 ml. The dead volume of a HR16 column with one variable and one non variable assembly is:

$V_{empty16} = 0.606\,ml - 0.181\,ml = 0.425\,ml$

To determined the volume of the filters measurements are made with an empty column with two variable assemblies and two filters. Measurements have been made with the column in both position 1 and 2.

Injection: 50 µl $NaNO_3$

Q = 1.01 ml/min

Position	σ_{gauss} [m]	τ [ml]	$V_{R,gauss}$ [ml]	V_R [ml]	V_R - V_{ID} [ml]	σ^2 [ml^2]	
1	0.1153	0.2337	0.8580	1.0917	0.7817	0.0679	
1	0.0951	0.2436	0.8160	1.0596	0.7496	0.0684	
1	0.0965	0.2123	0.8198	1.0322	0.7222	0.0544	0.055
1	0.0938	0.1691	0.8223	0.9914	0.6814	0.0374	
1	0.1066	0.1876	0.8412	1.0288	0.7188	0.0466	
2	0.1207	0.1785	0.9472	1.1257	0.7257	0.0464	
2	0.1179	0.1746	0.9258	1.1004	0.7004	0.0444	
2	0.1520	0.1825	0.9146	1.0971	0.6971	0.0564	0.055
2	0.1201	0.2494	0.9262	1.1756	0.7756	0.0766	
2	0.1548	0.1716	0.9430	1.1146	0.7146	0.0534	

The dead volume of the HR16 column including the filters are determined from a mean of the ten measured retention volumes.

$$V_{empty16,incl.filters} = (V_R - V_{ID})_{mean} = 0.727\,ml$$

The dead volume of the filters is:

$$V_{dead,filters} = (V_{empty16,incl.filters} - V_{empty16})_{mean} = 0.727\,ml - 0.606\,ml = 0.121\,ml$$

The volume of the filters is:

$$V_{filters} = (0.8\,cm)^2 \cdot \pi \cdot 0.2\,cm = 0.402\,ml$$

The porosity of the filters:

$$\varepsilon_{filter} = \frac{V_{dead,filters}}{V_{filters}} = \frac{0.121\,ml}{0.402\,ml} = 0.302$$

The HR10 column

The measurements are made with an empty column without filters.
Column position: 2
Mobile phase: 2.0 M NaCl

Puls	Q [ml/min]	σ_{gauss} [m]	τ [ml]	$V_{R,gauss}$ [ml]	V_R [ml]	σ^2 [ml^2]	
25 µl BSA	1.01	0.0491	0.1412	0.4576	0.6025	0.0226	
25 µl BSA	1.01	0.0502	0.1473	0.4606	0.6118	0.0245	0.025
25 µl BSA	1.01	0.0451	0.1579	0.4591	0.6208	0.0273	
100 µl BSA	1.01	0.0544	0.1670	0.5039	0.6752	0.0313	
100 µl BSA	1.01	0.0542	0.1671	0.5066	0.6779	0.0313	
100 µl BSA	1.01	0.0537	0.1672	0.4887	0.6600	0.0312	0.031
100 µl BSA	1.01	0.0545	0.1677	0.4900	0.6618	0.0315	
100 µl BSA	1.01	0.0540	0.1672	0.4946	0.6659	0.0313	
100 µl BSA	1.01	0.0539	0.1679	0.4969	0.6690	0.0315	
100 µl BSA	2.94	0.0490	0.1402	0.5226	0.6486	0.0211	
100 µl BSA	2.94	0.0483	0.1418	0.5220	0.6496	0.0215	
100 µl BSA	2.94	0.0481	0.1398	0.5190	0.6447	0.0209	0.021
100 µl BSA	2.94	0.0475	0.1394	0.5185	0.6438	0.0208	
100 µl BSA	2.94	0.0469	0.1389	0.5171	0.6420	0.0206	
100 µl BSA	2.94	0.0471	0.1392	0.5166	0.6418	0.0207	
50 µl BSA	1.01	0.0441	0.1694	0.4624	0.6358	0.0310	
50 µl BSA	1.01	0.0430	0.1707	0.4616	0.6363	0.0314	
50 µl BSA	1.01	0.0434	0.1702	0.4615	0.6357	0.0313	0.031
50 µl BSA	1.01	0.0432	0.1691	0.4462	0.6192	0.0309	
50 µl BSA	1.01	0.0431	0.1695	0.4544	0.6278	0.0310	
50 µl BSA	1.01	0.0432	0.1692	0.4558	0.6289	0.0309	
50 µl NO_3^-	1.01	0.0483	0.1529	0.4737	0.6305	0.0260	0.026
100 µl NO_3^-	1.01	0.0637	0.0761	0.5638	0.6439	0.0100	
100 µl NO_3^-	1.01	0.0635	0.0763	0.5638	0.6442	0.0100	
100 µl NO_3^-	1.01	0.0640	0.0749	0.5648	0.6437	0.0098	0.099
100 µl NO_3^-	1.01	0.0642	0.0749	0.5658	0.6446	0.0098	
100 µl NO_3^-	1.01	0.0637	0.0750	0.5707	0.6498	0.0098	
100 µl NO_{3-}	1.01	0.0637	0.0747	0.5721	0.6509	0.0098	

The dead volume of the HR10 column is determined from a mean of all the measured retention volumes except the volumes measured by an injection of 25 µl BSA. These three measurements are not included, because they are smaller than all the other measurements and none of the experiments in the linear range are made with such a small injection volume.

$$\begin{aligned} V_{empty10} &= V_{R,mean} - V_{ID,pos.2} \\ &= 0.647\,ml - 0.40\,ml \\ &= 0.247\,ml \end{aligned}$$

As for the HR16 column this volume is measured by two variable assemblies. The tube of the non variable assembly is 27.1 cm shorter than the tube of the variable assembly. The inner diameter of the tube is 0.5 mm, so the volume of the extra 27.1 cm of tube is 0.053 ml. The dead volume of a

HR10 column with one variable and one non variable assembly is:

$$V_{empty10} = 0.247\,ml - 0.053\,ml$$
$$= 0.194\,ml$$

The dead volume of the 2 filters is calculated from the porosity of the filters for the HR16 column.

$$V_{filters} = (0.5\,cm)^2 \cdot \pi \cdot 0.18\,cm = 0.141\,ml$$

$$V_{dead,filters} = V_{filters} \cdot \varepsilon_{filters} = 0.141\,ml \cdot 0.302 = 0.043\,ml$$

APPENDIX B.III: RETENTION VOLUMES UNDER NON-ADSORBED CONDITIONS

The Source 30Q column (CV = 8.07 ml) used for experiments in the linear range

Column position: 1
Q = 1.01 ml/min, 2.94 ml/min and 5.93 ml/min
$V_{NA} = V_R - V_{dead}$
Where $V_{dead} = V_{10empty} + V_{ID,pos.1} + V_{filters}$ = 0.194 ml + 0.31 ml + 0.043 ml = 0.547 ml

Protein	Load [ml]	c_{NaCl} [mM]	V_R [ml]	V_{NA} [ml]	
BSA	20	2000	5.504	4.957	4.93
	100	2000	5.544	4.997	
	100	2000	5.541	4.994	
	100	1009	5.469	4.922	
	100	1009	5.487	4.940	
	100	1009	5.435	4.888	
	100	1011	5.425	4.878	
	100	1011	5.414	4.867	
	100	1011	5.416	4.869	
	100	1006	5.495	4.948	
	100	1006	5.533	4.986	
	100	1006	5.469	4.922	
	100	996	5.433	4.886	
	100	996	5.572	5.025	
	100	996	5.451	4.904	
	100	989	5.446	4.899	
	100	989	5.535	4.988	
	100	989	5.439	4.892	
α-lactalbumin	20	2000	5.762	5.215	5.28
	100	2000	5.803	5.256	
	100	997	5.813	5.266	
	100	997	5.789	5.242	
	100	997	5.859	5.312	
	100	1005	5.814	5.267	
	100	1005	5.878	5.331	
	100	1005	5.807	5.260	
	100	1011	5.845	5.298	
	100	1011	5.866	5.319	
β-lactoglobulin A & B	20	2000	5.684	5.137	5.17
	20	2000	5.742	5.195	
	100	2000	5.772	5.225	
	100	2000	5.715	5.168	
	100	2000	5.719	5.172	
	100	989	5.758	5.211	
	100	989	5.785	5.238	
	100	996	5.736	5.189	
	100	996	5.758	5.211	
	100	996	5.701	5.154	
	100	1001	5.654	5.107	
	100	1001	5.694	5.147	
	100	1001	5.665	5.118	
	100	1010	5.632	5.085	
	100	1010	5.710	5.163	
	100	1010	5.708	5.161	

The Q-Sepharose XL column used for experiments in the linear range

Measurements are made both with the column in position 1 and 2.
Q = 1.01 ml/min, 6.93 ml/min and 15.1 ml/min
Load: 100 µl
$V_{NA} = V_R - V_{dead}$
Position 1: $V_{dead} = V_{16empty} + V_{ID,pos.1} + V_{filters}$ = 0.425 ml + 0.40 ml + 0.121 ml = 0.946 ml
Position 2: $V_{dead} = V_{16empty} + V_{ID,pos.2} + V_{filters}$ = 0.425 ml + 0.31 ml + 0.121 ml = 0.856 ml

Protein	c_{NaCl} [mM]	V_R [ml]	V_{NA} [ml]	
BSA	989	3.710	2.764	2.80
	989	3.697	2.751	
	989	3.722	2.776	
	996	3.740	2.794	
	996	3.816	2.870	
	1006	3.824	2.878	
	1006	3.866	2.920	
	1006	3.770	2.824	
	1009	3.762	2.816	
	1009	3.831	2.885	
	1009	3.660	2.714	
	1011	3.665	2.719	
	1011	3.717	2.771	
	1011	3.692	2.746	
α-lactalbumin	990	5.488	4.542	4.46
	990	5.295	4.349	
	997	5.450	4.504	
	997	5.497	4.551	
	997	5.238	4.292	
	1005	5.477	4.531	
	1005	5.459	4.513	
	1011	5.396	4.450	
	1011	5.469	4.523	
	1011	5.276	4.330	
β-lactoglobulin A & B	1001	4.531	3.585	3.52
	1001	4.559	3.613	
	1010	4.428	3.482	
	1010	4.359	3.413	
	1010	4.431	3.485	

The Ceramic Q-HyperD F column used for experiments in the linear range

Column position: 1
Q = 1.01 ml/min, 2.94 ml/min and 5.93 ml/min
$V_{NA} = V_R - V_{dead}$
Where $V_{dead} = V_{10empty} + V_{ID,pos.1} + V_{filters}$ = 0.194 ml + 0.31 ml + 0.043 ml = 0.547 ml

Protein	Load [ml]	c_{NaCl} [mM]	V_R [ml]	V_{NA} [ml]	
BSA	100	2000	4.038	3.491	3.53
	100	2000	4.114	3.567	
	100	990	4.048	3.501	
	100	990	4.081	3.534	
	100	990	4.042	3.495	
	100	996	4.066	3.519	
	100	996	4.067	3.520	
	100	1007	4.061	3.514	
	100	1007	4.053	3.506	
	100	1007	4.071	3.524	
	100	1010	4.079	3.532	
	100	1010	4.152	3.605	
	100	1010	4.085	3.538	
α-lactalbumin	20	2000	4.187	3.640	3.64
	100	2000	4.156	3.609	
	100	2000	4.251	3.704	
	100	2000	4.192	3.645	
	100	990	4.204	3.657	
	100	990	4.165	3.618	
	100	990	4.206	3.659	
	100	997	4.196	3.649	
	100	997	4.182	3.635	
	100	997	4.223	3.676	
	100	1005	4.129	3.582	
	100	1005	4.194	3.647	
	100	1005	4.149	3.602	
β-lactoglobulin A & B	100	989	4.149	3.602	3.58
	100	989	4.141	3.594	
	100	996	4.072	3.525	
	100	996	4.148	3.601	
	100	996	4.084	3.537	
	100	1001	4.132	3.585	
	100	1001	4.167	3.620	
	100	1001	4.101	3.554	
	100	1010	4.145	3.598	
	100	1010	4.119	3.572	

The Fractogel EMD TMAE 650(s) column used for experiments in the linear range

Column position: 2
Q = 1.01 ml/min, 2.94 ml/min and 5.93 ml/min
$V_{NA} = V_R - V_{dead}$
Where $V_{dead} = V_{10empty} + V_{ID,pos.1} + V_{filters}$ = 0.247 ml + 0.40 ml + 0.043 ml = 0.690 ml

Protein	Load [ml]	c_{NaCl} [mM]	V_R [ml]	V_{NA} [ml]	
BSA	20	2000	2.831	2.141	2.19
	100	2000	2.908	2.218	
	100	2000	2.831	2.141	
	100	2000	2.908	2.218	
	100	2000	2.831	2.141	
	100	990	2.844	2.154	
	100	990	2.882	2.192	
	100	990	2.902	2.212	
	100	996	2.927	2.237	
	100	996	2.865	2.175	
	100	1007	2.861	2.171	
	100	1007	2.932	2.242	
	100	1007	2.857	2.167	
	100	1010	2.861	2.171	
	100	1010	2.939	2.249	
	100	1010	2.875	2.185	
α-lactalbumin	100	2000	3.151	2.461	2.73
	100	990	3.233	2.543	
	100	990	3.233	2.543	
	100	990	3.318	2.628	
	100	997	3.215	2.525	
	100	997	3.156	2.466	
	100	997	3.178	2.488	
	100	1005	3.225	2.535	
	100	1005	3.262	2.572	
	100	1005	3.207	2.517	
	100	1005	3.161	2.471	
	100	1011	3.275	2.585	
	100	1011	3.243	2.553	
	100	1011	3.291	2.601	
β-lactoglobulin A & B	100	2000	2.995	2.305	2.34
	100	989	3.036	2.346	
	100	989	3.094	2.404	
	100	996	3.031	2.341	
	100	996	3.051	2.361	
	100	996	3.007	2.317	
	100	1001	2.970	2.280	
	100	1001	3.094	2.404	
	100	1001	2.986	2.296	
	100	1010	3.029	2.339	
	100	1010	2.969	2.279	

Source 30Q columns used for scale-up

$V_{NA} = V_R - V_{dead}$

V_{col} = 0.46 ml: Column position 2, V_{dead} = 1.127 ml, load: 20 µl, Q = 1.01 ml/min
V_{col} = 0.98 ml: Column position 2, V_{dead} = 0.550 ml, load: 25 µl, Q = 1.01 ml/min
V_{col} = 1.35 ml: Column position 1, V_{dead} = 0.600 ml, load: 25 µl, Q = 1.01 ml/min
V_{col} = 9.29 ml: Column position 2, V_{dead} = 1.127 ml, load: 100 µl, Q = 1.01 ml/min
V_{col} = 55.61 ml: Column position 2, V_{dead} = 1.40 ml, load: 100 µl, Q = 5.93 ml/min

Media	V_{col} [ml]	V_R [ml]	$V_{NA,BSA}$ [ml]	
Source 30Q	0.46	1.465 1.462 1.468	0.338 0.335 0.341	0.34
Source 30Q	0.98	1.142 1.131 1.142 1.134 1.137	0.592 0.581 0.592 0.584 0.587	0.59
Source 30Q	1.35	1.420 1.421 1.424 1.425	0.820 0.821 0.824 0.825	0.82
Source 30Q	9.39	7.179 7.171 7.155 7.159	6.052 6.044 6.028 6.032	6.04
Source 30Q	55.61	35.238 35.435 35.455 35.504 35.464	33.838 34.035 34.055 34.104 34.064	34.02

Different Source 30Q columns used for examination of the different methods for determination of ion-exchange capacity

Column position: 1
Q = 1.01 ml/min
$V_{NA} = V_R - V_{dead}$
V_{dead} = 0.856 ml (for both columns)

Media	V_{col} [ml]	Load [µl]	V_R [ml]	$V_{NA,BSA}$ [ml]	
Source 30Q	13.57	100	9.350	8.494	8.47
		20	9.318	8.462	
		100	9.335	8.479	
		100	9.322	8.466	
		20	9.282	8.426	
Source 30Q	13.07	100	8.860	8.004	8.01
		20	8.854	7.998	
		20	8.859	8.003	
		100	8.890	8.034	
		100	8.875	8.019	
		20	8.855	7.999	

APPENDIX B.IV: DETERMINATION OF TOTAL POROSITY

The columns used for experiments in the linear range

$V_{NA} = V_R - V_{dead}$
Where $V_{dead} = V_{empty} + V_{ID,pos.} + V_{filters}$

Source 30Q: Column position 1, V_{dead} = 0.547 ml, Q = 1.01 ml/min
Q-Sepharose XL: Column position 2, V_{dead} = 0.946 ml, Q = 1.01 ml/min
Q-HyperD F: Column position 1, V_{dead} = 0.547 ml, Q = 1.01 ml/min
Fractogel EMD TMAE 650(s): Column position 2, V_{dead} = 0.690 ml, Q = 1.01 ml/min

Media	V_{col} [ml]	Load [µl]	V_R [ml]	V_t [ml]		ε_t
Source 30Q	8.07	20	6.584	6.037	6.00	0.75
		20	6.467	5.920		
		20	6.549	6.002		
		100	6.598	6.051		
		100	6.555	6.008		
		20	6.516	5.969		
Q-Sepharose XL	7.56	100	8.077	7.131	7.07	0.93
		20	7.994	7.048		
		20	7.963	7.017		
		100	8.117	7.171		
		100	8.023	7.077		
		20	7.902	6.956		
Q-HyperD F	7.56	20	6.620	6.073	6.09	0.81
		100	6.664	6.117		
		20	6.636	6.089		
		100	6.652	6.105		
		100	6.663	6.116		
		20	6.597	6.050		
Fractogel	3.93	20	3.602	2.912	2.94	0.75
		100	3.642	2.952		
		20	3.641	2.951		
		20	3.611	2.921		
		100	3.651	2.961		
		100	3.648	2.958		
		20	3.616	2.926		

Source 30Q columns used for scale-up

$V_{NA} = V_R - V_{dead}$

V_{col} = 0.46 ml: Column position 2, V_{dead} = 1.127 ml, load: 20 µl, Q = 1.01 ml/min
V_{col} = 0.98 ml: Column position 2, V_{dead} = 0.550 ml, load: 25 µl, Q = 1.01 ml/min
V_{col} = 1.35 ml: Column position 1, V_{dead} = 0.600 ml, load: 25 µl, Q = 1.01 ml/min
V_{col} = 9.29 ml: Column position 2, V_{dead} = 1.127 ml, load: 50 µl, Q = 1.01 ml/min
V_{col} = 55.61 ml: Column position 2, V_{dead} = 1.40 ml, load: 100 µl, Q = 5.93 ml/min

Media	V_{col} [ml]	Load [µl]	V_R [ml]	V_t [ml]		ε_t
Source 30Q	0.46	20	1.482	0.355	0.37	0.79
		20	1.495	0.368		
		20	1.478	0.351		
		20	1.506	0.379		
		20	1.498	0.371		
		20	1.497	0.370		
Source 30Q	0.98	25	1.284	0.734	0.74	0.76
		25	1.297	0.747		
		25	1.291	0.741		
		25	1.302	0.752		
		25	1.293	0.743		
Source 30Q	1.35	25	1.620	1.020	1.00	0.74
		25	1.605	1.005		
		25	1.595	0.995		
		25	1.604	1.004		
		25	1.599	0.999		
Source 30Q	9.39	50	8.431	7.304	7.23	0.77
		50	8.331	7.204		
		50	8.318	7.191		
		50	8.369	7.242		
		50	8.391	7.264		
		50	8.328	7.201		
Source 30Q	55.61	100	41.813	40.413	41.33	0.74
		100	42.349	40.949		
		100	44.300	42.900		
		100	42.818	41.418		
		100	42.850	41.450		
		100	42.721	41.321		
		100	42.395	40.995		
		100	42.627	41.227		

Different Source 30Q columns used for examination of the different methods for determination of ion-exchange capacity

Column position: 1
Q = 1.01 ml/min
$V_{NA} = V_R - V_{dead}$
V_{dead} = 0.856 ml (for all three columns)

Media	V_{col} [ml]	Load [µl]	V_R [ml]	V_t [ml]		ε_t
Source 30Q	13.57	100	11.250	10.394	10.39	0.77
		100	11.277	10.421		
		20	11.301	10.445		
		20	11.252	10.396		
		100	11.203	10.347		
		100	11.193	10.337		
		20	11.235	10.379		
Source 30Q	13.07	100	10.716	9.860	9.90	0.76
		20	10.876	10.020		
		20	10.819	9.963		
		100	10.725	9.869		
		100	10.714	9.858		
		20	10.680	9.824		
Source 30Q	11.76	100	9.881	9.025	9.05	0.77
		100	9.919	9.063		
		100	9.928	9.072		
		100	9.908	9.052		

APPENDIX B.V: DETERMINATION OF ION-EXCHANGE CAPACITY BY IN-COLUMN ACID-BASE TITRATION

The columns used for experiments in the linear range

Media	V_{col} [ml]	Q [ml/min]	V_{NaOH} [ml]	V_{H_2O} [ml]	V_{NaCl} [ml]	V_{HCl} [ml]	λ [mmol]	Λ [mmol/ml pore volume]
Source 30Q	8.07	10	100	65	75	6.92	0.692	0.688	0.251
		10	75	65	75	6.86	0.686		
		10	100	75	100	6.89	0.689		
		10	75	65	75	6.83	0.683		
		10	75	65	125	6.95	0.695		
		10	75	65	150	6.79	0.679		
		10	100	65	125	6.87	0.687		
		10	150	75	125	6.94	0.694		
		10	75	65	150	6.83	0.683		
		10	100	75	125	6.94	0.694		
Q-Sepharose XL	7.56	10	100	75	125	16.99	1.699	1.693	0.352
		10	100	75	125	16.86	1.686		
		10	125	75	125	16.86	1.686		
		10	100	75	125	17.02	1.702		
		10	100	75	125	16.90	1.690		
		10	125	75	125	16.97	1.697		
Q-HyperD F	7.56	10	125	75	125	18.12	1.812	1.811	0.590
		10	125	75	125	18.17	1.817		
		10	125	75	125	18.05	1.805		
		10	125	75	125	18.08	1.808		
Fractogel EMD TMAE	3.93	6	100	75	125	0.72	0.072	0.0685	0.0503
		6	75	75	100	0.65	0.065		
		6	100	75	125	0.68	0.068		
		6	100	75	100	0.69	0.069		

Source 30Q columns used for scale-up

Media	V_{col} [ml]	Q [ml/min]	V_{NaOH} [ml]	V_{H_2O} [ml]	V_{NaCl} [ml]	V_{HCl} [ml]	λ [mmol]	Λ [mmol/ml pore volume]
Source 30Q	0.46	10	40	55	45	0.37	0.037	0.291
		10	40	55	45	0.37	0.037	
		10	50	65	75	0.36	0.036	
		10	40	55	45	0.36	0.036	
Source 30Q	1.35	10	50	55	60	1.05	0.105	0.226
		10	60	55	75	1.06	0.106	
		10	60	55	75	1.06	0.106	
		10	60	60	75	1.03	0.103	
Source 30Q	9.39	10	125	75	125	8.67	0.867	0.303
		10	125	75	125	8.72	0.872	
		10	125	75	125	8.74	0.874	
		10	140	80	150	8.57	0.857	
		10	125	75	125	8.62	0.862	
		10	125	80	125	8.60	0.860	
Source 30Q	55.61	15	300	125	300	52.79	5.279	0.277
		15	300	125	300	52.94	5.294	
		15	250	125	250	52.85	5.285	
		15	300	125	300	52.88	5.288	

Different Source 30Q columns used for investigation of the different methods for determination of ion-exchange capacity

Media	V_{col} [ml]	Q [ml/min]	V_{NaOH} [ml]	V_{H_2O} [ml]	V_{NaCl} [ml]	V_{HCl} [ml]	λ [mmol]	Λ [mmol/ml pore volume]
Source 30Q	13.57	5	125	80	125	9.96	0.996	1.008	0.239
		5	150	80	100	10.24	1.024	
		5	175	100	150	10.33	1.033	
		5	175	100	150	9.84	0.984	
		10	175	100	150	10.18	1.018	
		10	250	150	200	9.99	0.999	
		10	175	75	125	10.03	1.003	
		5-10	?	?	?	10.05	1.005	
		5-10	?	?	?	9.95	0.995	
		8-10	192	75	160	10.20	1.020	
		8-10	175	75	143	10.10	1.010	
		8-10	175	78	125	10.09	1.009	
Source 30Q	13.07	10	175	75	125	9.52	0.952	0.951	0.226
		5	150	75	125	9.54	0.954	
		10	150	75	125	9.47	0.947	
		5	150	75	125	9.52	0.952	
Source 30Q	11.76	10	150	125	75	11.30	1.130	1.131	0.315
		10	150	125	75	11.31	1.131	
		10	150	125	75	11.29	1.129	
		10	150	125	75	11.36	1.136	

In the last five runs for the column with a volume of 13.57 ml another pump than the one on the BioCAD was used. This pump was not calibrated so the exact flow rate is not known, and furthermore the flow rate is not constant. The volumes in the different steps for the last three runs are determined by weighing.

APPENDIX B.VI: DETERMINATION OF ION-EXCHANGE CAPACITY BY IN-COLUMN EXPERIMENTS WITH NITRATE

The columns used for experiments in the linear range

Media	V_{col} [ml]	A_{peak} [abs. 280 nm·ml]	λ [mmol]		Λ [mmol/ml pore vol.]
Source 30Q	8.07	1.502 1.509 1.504	0.8414 0.8454 0.8427	0.843	0.308
Q-Sepharose XL	7.56	3.842 3.848 3.845 3.845	2.1524 2.1554 2.1539 2.1539	2.154	0.448
Q-HyperD F	7.56	4.254 4.258	2.3827 2.3849	2.384	0.777
Fractogel	3.93	0.200 0.201 0.201	0.1119 0.1129 0.1126	0.112	0.0825

Column used for frontal analysis with BSA

Media	V_{col} [ml]	A_{peak} [abs. 280 nm·ml]	λ [mmol]		Λ [mmol/ml pore vol.]
Source 30Q	0.46	0.1146 0.1149 0.1136	0.0493 0.0495 0.0489	0.049	0.392
Source 30Q	0.98	0.2103 0.2092 0.2132	0.0905 0.0900 0.0918	0.091	0.290
Source 30Q	1.35	0.2038 0.2005 0.2062	0.114 0.112 0.116	0.114	0.246

Different Source 30Q columns used for examination of the different methods for determination of ion-exchange capacity

V_{col} = 13.57 ml: Q_{load} = 1.01 ml/min, $Q_{eluting}$ = 9.97 ml/min
V_{col} = 13.07 ml: Q_{load} = 1.01 ml/min and 4.94 ml/min, $Q_{eluting}$ = 4.94 ml/min
V_{col} = 11.76 ml: Q_{load} = 4.94 ml/min and 9.97 ml/min, $Q_{eluting}$ = 4.94 ml/min

Media	V_{col} [ml]	V_{load} [ml]	V_{wash} [ml]	A_{peak} [abs. 280 nm·ml]	λ [mmol]	Λ [mmol/ml pore vol.]
		40	25	1.978	1.1080	
		40	25	2.011	1.1267	
		30	25	2.011	1.1262	
		30	25	2.019	1.1308	
		50	25	2.043	1.1443	
		50	25	2.057	1.1522	
		100	25	2.095	1.1735	
Source 30Q	13.57	100	100	2.092	1.1720	1.140 0.270
		75	25	1.970	1.1036	
		100	25	2.007	1.1245	
		150	25	2.045	1.1454	
		50	25	2.019	1.1309	
		75	25	2.039	1.1421	
		100	25	2.068	1.1582	
		150	25	2.075	1.1625	
		75	25	1.912	1.0708	
		75	25	1.885	1.0561	
		50	25	1.917	1.0739	
Source 30Q	13.07	75	25	1.936	1.0846	1.067 0.254
		75	25	1.905	1.0670	
		75	40	1.884	1.0552	
		75	40	1.891	1.0590	
		75	75	1.947	1.0906	
		75	75	1.958	1.0970	
		75	75	1.958	1.0966	
		75	50	1.987	1.1132	
		75	100	1.946	1.0899	
		100	75	1.968	1.1026	
Source 30Q	11.76	75	100	1.922	1.0766	1.100 0.306
		75	100	1.972	1.1048	
		100	100	1.947	1.0907	
		100	75	1.960	1.0978	
		75	100	1.913	1.0717	
		100	75	2.024	1.1337	
		75	100	1.983	1.1105	
		100	100	2.015	1.1288	

APPENDIX B.VII: DETERMINATION OF ION-EXCHANGE CAPACITY BY BACK TITRATION

Sample no.		1	2	3
$m_{glass\ container}$	[g]	6.6242	6.6296	6.5637
$m_{glass\ container\ +\ drained\ media}$	[g]	6.7449	6.8686	6.8122
$m_{drained\ media}$	[g]	0.1207	0.2390	0.2485
$m_{after\ oven}$	[g]	6.6711	6.7190	6.6610
$m_{dry\ media}$	[g]	0.0469	0.0894	0.0973
Water content after draining	[%]	61.1	62.6	60.8

Water content in the drained media:

$$water\% = \frac{61.1\% + 62.6\% + 60.8\%}{3} = 61.5\%$$

$m_{drained\ media}$	$m_{dry\ media}$ [g]	c_{HCl} [M]	V_{HCl} [ml]	V_{NaOH} [ml]	λ [mmol]	Λ [mmol/g dry	
0.7504	0.289	0.010	10.0	0.50	0.050	0.866	0.57
				0.84	0.016	0.277	
1.2810	0.493	0.050	10.0	4.51	0.049	0.497	0.50
				4.51	0.049	0.497	
1.4219	0.547	0.100	10.0	9.31	0.069	0.631	0.62
				9.33	0.067	0.612	
0.8208	0.316	0.100	10.0	9.58	0.042	0.665	0.70
				9.54	0.046	0.728	
0.8249	0.317	0.100	10.0	9.58	0.042	0.662	0.68
				9.56	0.044	0.693	

The mass of dry media is calculated from the water content in the drained media:

$$m_{dry\ media} = m_{drained\ media} \cdot \left(1 - \frac{water\%}{100\%}\right)$$

The capacities determined in the samples added 0.050 and 0.010 M NaCl are lower than the capacities determined in the samples added 0.100 M NaCl. This could be due to not all OH^--ions has been exchanged with Cl^--ions. Therefore the capacity is determined as the mean of the capacities determined in 0.100 M NaCl.

$$\Lambda = 0.67\,mmol/g\ dry\ media$$

APPENDIX B.VIII: DETERMINATION OF ION-EXCHANGE CAPACITY BY BATCH ACID-BASE TITRATION

New media

Sample no.		1	2	3
$m_{glass\ container}$	[g]	6.6242	6.6296	6.5637
$m_{glass\ container\ +\ drained\ media}$	[g]	6.7449	6.8686	6.8122
$m_{drained\ media}$	[g]	0.1207	0.2390	0.2485
$m_{after\ oven}$	[g]	6.6711	6.7190	6.6610
$m_{dry\ media}$	[g]	0.0469	0.0894	0.0973
Water content after draining	[%]	61.1	62.6	60.8

The water content is calculated as the mean of the three samples: water% = 61.5%

The mass of dry media is calculated from the water content in the drained media:

$$m_{dry\ media} = m_{drained\ media} \cdot \left(1 - \frac{water\%}{100\%}\right)$$

Blank titration of 100.0 ml NaCl

	pH 2.50			pH 2.00		
$C_{NaCl,\ added}$ [M]	V_{HCl} [ml]	n_{HCl} [ml]		V_{HCl} [ml]	n_{HCl} [ml]	
1.0	7.04	0.704		14.27	1.427	
1.0	7.07	0.707	0.706	14.23	1.423	1.427
1.0	7.07	0.707		14.31	1.431	
0.10	5.35	0.535		14.91	1.491	
0.10	5.34	0.534	0.535	14.92	1.492	1.487
0.10	5.35	0.535		14.78	1.478	

Titration of the media samples

			pH 2.50					pH 2.00				
$m_{drained\ media}$	$m_{dry\ media}$ [g]	$C_{NaCl,added}$ [M]	V_{HCl} [ml]	n_{HCl} [mmol]	λ [mmol]	Λ [mmol/g dry		V_{HCl} [ml]	n_{HCl} [mmol]	λ [mmol]	Λ [mmol/g dry	
1.4703	0.566	1.0	8.06	0.806	0.100	0.177		15.37	1.537	0.110	0.194	
0.9924	0.382	1.0	7.80	0.780	0.074	0.194	0.176	14.93	1.493	0.066	0.173	0.185
1.3620	0.524	1.0	7.89	0.789	0.083	0.158		15.25	1.525	0.098	0.187	
1.0319	0.397	0.10	6.26	0.626	0.091	0.230	0.220	15.55	1.555	0.068	0.171	0.176
1.4488	0.557	0.10	6.51	0.651	0.116	0.209		15.88	1.588	0.101	0.181	

Media that has been used in a column

The media used in the titrations described below has been used in the Source 30Q column with the column volume 11.76 ml. The column was packed with a new media and the total porosity and the capacity was determined. The porosity was determined both by acid-base titration and by breakthrough experiments with nitrate. The column was regenerated before it was unpacked. All the media from the column was drained in a glass filter funnel and weighted, and three samples for determination of the water content were taken. The rest of the media was equilibrated with NaOH and washed to a neutral pH before it was drained again. From this filter cake 6 samples for titration and three samples for determination of the water content were taken.

Determination of media amount in the column

Sample no.		1	2	3
$m_{glass\ container}$	[g]	6.6075	6.6292	6.6336
$m_{glass\ container\ +\ drained\ media}$	[g]	6.6876	6.7854	6.845
$m_{drained\ media}$	[g]	0.0801	0.1562	0.2114
$m_{after\ oven}$	[g]	6.6404	6.6934	6.7196
$m_{dry\ media}$	[g]	0.0329	0.0642	0.086
Water content after draining	[%]	58.9	58.9	59.3

Water% = 59.0 %

The total amount of drained media from the column:

$m_{drained\ media}$ = 8.3777 g

This corresponds to:

$$m_{dry\ media} = 8.3777\,g \cdot \left(1 - \frac{59.0\%}{100\%}\right) = 3.43\,g$$

The media samples for titration were all prepared the same day. Three of them were titrated the day of preparation and the last three was titrated three days later. At both days blank titrations of the 1.0 M NaCl-solution were performed before the media samples were titrated.

Determinations of water content in the drained samples

Sample no.		1	2	3
$m_{glass\ container}$	[g]	6.6794	6.5529	6.6065
$m_{glass\ container\ +\ drained\ media}$	[g]	6.8028	6.7174	6.7803
$m_{drained\ media}$	[g]	0.1234	0.1645	0.1738
$m_{after\ oven}$	[g]	6.7288	6.6173	6.6750
$m_{dry\ media}$	[g]	0.0494	0.0644	0.0685
Water content after draining	[%]	60.0	60.9	60.6

The water content is calculated as the mean of the three samples: water% = 60.5%

Titrations performed the day the media samples were prepared

Blank titration of 100.0 ml NaCl

	pH 2.50			pH 2.00		
$C_{NaCl,added}$ [M]	V_{HCl} [ml]	n_{HCl} [ml]		V_{HCl} [ml]	n_{HCl} [ml]	
1.0	6.58	0.658		12.97	1.297	
1.0	6.60	0.660	0.656	12.86	1.286	1.290
1.0	6.50	0.650		12.86	1.286	

Titration of the media samples

			pH 2.50					pH 2.00				
$m_{drained\ media}$	$m_{dry\ media}$ [g]	$C_{NaCl,added}$ [M]	V_{HCl} [ml]	n_{HCl} [mmol]	λ [mmol]	Λ [mmol/g dry		V_{HCl} [ml]	n_{HCl} [mmol]	λ [mmol]	Λ [mmol/g dry	
0.9524	0.376	1.0	7.60	0.760	0.104	0.276		14.15	1.415	0.125	0.333	
1.2344	0.488	1.0	7.77	0.777	0.121	0.248	0.261	14.31	1.431	0.141	0.290	0.310
1.1752	0.465	1.0	7.76	0.776	0.120	0.258		14.32	1.432	0.142	0.306	

Titrations performed three days after the media samples were prepared:

Blank titration of 100.0 ml NaCl

	pH 2.50			pH 2.00		
$C_{NaCl,added}$ [M]	V_{HCl} [ml]	n_{HCl} [ml]		V_{HCl} [ml]	n_{HCl} [ml]	
1.0	7.14	0.714		14.09	1.409	
1.0	7.18	0.718		13.93	1.393	
1.0	7.20	0.720	0.719	14.15	1.415	1.414
1.0	7.17	0.717		14.20	1.420	
1.0	7.17	0.717		14.24	1.424	
1.0	7.30	0.730		14.24	1.424	

Titration of the media samples

			pH 2.50					pH 2.00				
$m_{drained\ media}$	$m_{dry\ media}$ [g]	$C_{NaCl,added}$ [M]	V_{HCl} [ml]	n_{HCl} [mmol]	λ [mmol]	Λ [mmol/g dry		V_{HCl} [ml]	n_{HCl} [mmol]	λ [mmol]	Λ [mmol/g dry	
1.3411	0.530	1.0	8.46	0.846	0.127	0.239		15.64	1.564	0.150	0.283	
1.3550	0.536	1.0	8.51	0.851	0.132	0.246	0.242	15.60	1.56	0.146	0.272	0.278
1.2636	0.500	1.0	8.39	0.839	0.120	0.240		15.53	1.553	0.139	0.278	

APPENDIX C.I: EXPERIMENTAL DATA FOR ISOCRATIC ELUTION OF BSA ON SOURCE 30Q

The peaks are fitted with the EMG function. The retention volumes and the variances are calculated as:

$V_R = V_{R,Gauss} + \tau - V_{dead}$

$\sigma^2 = \sigma^2_{Gauss} + \tau^2$

Where $V_{dead} = V_{empty10,\ incl.\ filters} + V_{ID,\ pos.1}$ = 0.237 ml + 0.31 ml = 0.547 ml

Column position: 1
Load: 100 µl

Q [ml/min]	c_s [mM]	$V_{R,Gauss}$ [ml]	pH 6 σ_{gauss} [ml]	τ [ml]	V_R [ml]	σ^2 [ml^2]
2.94	71	27.81	3.66	8.16	35.4	79.9
5.93	71	25.86	5.14	11.07	36.4	149.1
2.94	71	27.47	3.77	8.46	35.4	85.7
2.94	76	20.98	3.02	7.43	27.9	64.3
5.93	76	20.09	3.90	7.97	27.5	78.8
2.94	76	20.96	3.02	7.34	27.8	62.9
2.94	76	17.06	2.47	5.50	22.0	36.4
5.93	76	16.32	3.09	6.10	21.9	46.8
2.94	76	17.13	2.51	5.58	22.2	37.4
2.94	87	13.98	1.87	3.93	17.4	18.9
5.93	87	13.60	2.38	4.35	17.4	24.6
2.94	87	13.86	1.83	3.98	17.3	19.2
2.94	98	10.10	1.27	2.06	11.6	5.83
5.93	98	9.75	1.56	2.41	11.6	8.21
2.94	98	10.15	1.26	2.06	11.7	5.84
2.94	111	8.18	0.852	1.32	8.94	2.46
5.93	111	7.90	1.03	1.75	9.10	4.11
2.94	111	8.17	0.850	1.31	8.93	2.44
2.94	117	7.46	0.785	1.35	8.26	2.43
5.93	117	7.31	0.923	1.70	8.46	3.75
2.94	117	7.62	0.755	1.31	8.38	2.28
2.94	126	7.18	0.630	1.19	7.82	1.81
5.93	126	6.98	0.792	1.52	7.96	2.95
2.94	126	7.20	0.632	1.18	7.84	1.80
2.94	136	6.61	0.565	0.959	7.02	1.24
5.93	136	6.52	0.702	1.23	7.21	2.01
2.94	136	6.63	0.559	0.967	7.05	1.25
2.94	154	6.13	0.509	0.723	6.30	0.782
5.93	154	5.98	0.642	0.932	6.36	1.28
2.94	154	6.16	0.508	0.717	6.33	0.772
2.94	155	6.23	0.502	0.746	6.43	0.808
5.93	155	6.03	0.633	0.960	6.45	1.32
2.94	155	6.22	0.501	0.745	6.42	0.806
2.94	183	5.87	0.475	0.570	5.90	0.550
5.93	183	5.69	0.599	0.763	5.91	0.941
2.94	183	5.89	0.476	0.566	5.91	0.547
2.94	185	5.83	0.465	0.506	5.79	0.472
5.93	185	5.67	0.589	0.692	5.81	0.825
2.94	185	5.84	0.464	0.504	5.79	0.470

pH 6

Q [ml/min]	c_s [mM]	$V_{R,Gauss}$ [ml]	σ_{Gauss} [ml]	τ [ml]	V_R [ml]	σ^2 [ml^2]
2.94	232	5.52	0.478	0.388	5.36	0.378
5.93	232	5.42	0.581	0.569	5.45	0.662
2.94	232	5.54	0.478	0.381	5.38	0.374
2.94	232	5.47	0.447	0.394	5.31	0.355
2.94	233	5.48	0.444	0.378	5.31	0.340
5.93	233	5.38	0.554	0.554	5.39	0.614
2.94	233	5.48	0.444	0.378	5.31	0.340
2.94	305	5.33	0.429	0.354	5.14	0.309
5.93	305	5.26	0.533	0.523	5.24	0.558
2.94	305	5.34	0.430	0.354	5.15	0.310
2.94	329	5.28	0.415	0.338	5.07	0.286
5.93	329	5.11	0.515	0.503	5.06	0.518
2.94	329	5.28	0.415	0.338	5.07	0.286
2.94	523	5.14	0.413	0.359	4.95	0.299
5.93	523	5.05	0.508	0.522	5.03	0.531
2.94	523	5.16	0.412	0.356	4.97	0.296
2.94	526	5.15	0.406	0.329	4.93	0.273
5.93	526	5.07	0.503	0.496	5.02	0.499
2.94	526	5.14	0.406	0.329	4.93	0.273
2.94	1009	5.10	0.410	0.365	4.92	0.301
5.93	1009	4.96	0.502	0.532	4.94	0.535
2.94	1009	5.08	0.410	0.360	4.89	0.298
2.94	1011	5.09	0.402	0.336	4.88	0.275
5.93	1011	4.91	0.498	0.505	4.87	0.503
2.94	1011	5.08	0.403	0.335	4.87	0.274

pH 7

Q [ml/min]	c_s [mM]	$V_{R,Gauss}$ [ml]	σ_{gauss} [ml]	τ [ml]	V_R [ml]	σ^2 [ml^2]
2.94	125	24.95	3.20	10.21	34.6	114.5
5.93	125	24.22	4.23	10.91	34.6	136.9
2.94	125	25.04	3.27	9.43	33.9	99.7
5.93	145	11.74	1.94	4.36	15.5	22.7
2.94	145	11.94	1.47	3.90	15.3	17.4
2.94	145	11.92	1.47	3.91	15.3	17.4
5.93	174	7.74	1.00	1.82	9.02	4.31
2.94	174	7.84	0.864	1.38	8.67	2.65
2.94	224	6.05	0.500	0.682	6.18	0.714
5.93	224	5.96	0.623	0.893	6.30	1.19
2.94	224	6.08	0.499	0.674	6.21	0.703
2.94	275	5.55	0.445	0.391	5.40	0.351
5.93	275	5.44	0.559	0.564	5.46	0.630
2.94	275	5.56	0.444	0.391	5.40	0.350
2.94	374	5.30	0.416	0.344	5.10	0.291
5.93	374	5.11	0.519	0.501	5.07	0.520
2.94	374	5.26	0.416	0.342	5.05	0.290
2.94	516	5.21	0.416	0.353	5.02	0.298
5.93	516	5.16	0.510	0.520	5.13	0.531
2.94	516	5.24	0.414	0.350	5.04	0.294
2.94	1006	5.14	0.412	0.359	4.95	0.298
5.93	1006	5.00	0.503	0.530	4.99	0.534
2.94	1006	5.11	0.412	0.354	4.92	0.295

pH 8

Q [ml/min]	c_s [mM]	$V_{R,Gauss}$ [ml]	σ_{gauss} [ml]	τ [ml]	V_R [ml]	σ^2 [ml^2]
2.94	167	24.42	3.91	3.90	27.8	30.5
5.93	167	23.66	4.89	5.16	28.3	50.6
2.94	167	24.38	3.92	3.85	27.7	30.2
2.94	183	17.51	2.75	2.89	19.9	15.9
5.93	183	17.05	3.41	3.62	20.1	24.7
2.94	183	17.42	2.73	2.86	19.7	15.6
2.94	215	7.97	0.875	1.13	8.55	2.04
5.93	215	7.82	1.08	1.59	8.87	3.69
2.94	215	7.97	0.877	1.13	8.55	2.05
2.94	263	6.13	0.504	0.611	6.19	0.627
5.93	263	6.10	0.657	0.833	6.39	1.13
2.94	263	6.13	0.510	0.616	6.20	0.639
2.94	314	5.65	0.471	0.410	5.51	0.390
5.93	314	5.56	0.581	0.592	5.61	0.688
2.94	314	5.66	0.469	0.407	5.52	0.385
2.94	362	5.41	0.440	0.369	5.23	0.330
5.93	362	5.31	0.544	0.540	5.30	0.588
2.94	362	5.41	0.439	0.366	5.22	0.326
2.94	508	5.20	0.417	0.362	5.02	0.305
5.93	508	5.18	0.518	0.533	5.17	0.552
2.94	508	5.21	0.418	0.360	5.03	0.305
2.94	996	5.08	0.408	0.356	4.89	0.293
5.93	996	5.03	0.503	0.533	5.02	0.537
2.94	996	5.10	0.408	0.356	4.90	0.293

pH 9

Q [ml/min]	c_s [mM]	$V_{R,Gauss}$ [ml]	σ_{gauss} [ml]	τ [ml]	V_R [ml]	σ^2 [ml^2]
2.94	185	51.85	8.14	6.93	58.2	114.3
5.93	185	54.37	11.29	5.51	59.3	157.8
2.94	185	52.59	8.27	5.47	57.5	98.2
2.94	207	15.69	2.57	2.21	17.3	11.5
5.93	207	15.61	3.28	3.01	18.1	19.8
2.94	207	15.77	2.58	2.23	17.4	11.6
2.94	256	7.02	0.676	0.965	7.44	1.39
5.93	256	6.93	0.836	1.32	7.70	2.45
2.94	256	7.03	0.677	0.960	7.44	1.38
2.94	304	5.86	0.510	0.482	5.80	0.492
5.93	304	5.73	0.633	0.699	5.89	0.891
2.94	304	5.87	0.510	0.481	5.80	0.491
2.94	354	5.54	0.458	0.376	5.37	0.351
5.93	354	5.40	0.565	0.559	5.42	0.631
2.94	354	5.54	0.456	0.373	5.36	0.347
2.94	383	5.46	0.445	0.365	5.27	0.331
5.93	383	5.34	0.548	0.542	5.33	0.594
2.94	383	5.46	0.444	0.361	5.27	0.327
2.94	501	5.23	0.423	0.359	5.04	0.308
5.93	501	5.13	0.520	0.538	5.12	0.560
2.94	501	5.23	0.424	0.361	5.05	0.311
2.94	989	5.09	0.412	0.352	4.90	0.293
5.93	989	5.00	0.501	0.530	4.98	0.532
2.94	989	5.09	0.410	0.348	4.89	0.290

APPENDIX C.II: EXPERIMENTAL DATA FOR ISOCRATIC ELUTION OF α-LACTALBUMIN ON SOURCE 30Q

For the experiments where no σ_{Gauss} and τ values are given the peaks could not be fitted due to the shape of the peaks. The retention volumes are therefore determined as the volume at the peak maximum.

The peaks are fitted with the EMG function. The retention volumes and the variances are calculated as:

$V_R = V_{R,Gauss} + \tau - V_{dead}$

$\sigma^2 = \sigma^2_{Gauss} + \tau^2$

Where $V_{dead} = V_{empty10,\ incl.\ filters} + V_{ID,\ pos.1}$ = 0.237 ml + 0.31 ml = 0.547 ml

Column position: 1
Load: 100 µl

Q [ml/min]	c_s [mM]	$V_{R,Gauss}$ [ml]	pH 6 σ_{Gauss} [ml]	τ [ml]	V_R [ml]	σ^2 [ml^2]
5.93	38	99.15	----	----	98.6	----
1.01	48	37.99	----	----	37.4	----
2.94	48	34.42	----	----	33.9	----
5.93	48	31.85	----	----	31.3	----
1.01	57	26.95	----	----	26.4	----
2.94	57	24.49	----	----	23.9	----
5.93	57	22.74	----	----	22.2	----
1.01	77	10.53	----	----	9.99	----
2.94	77	10.43	----	----	9.88	----
5.93	77	10.55	----	----	10.0	----
1.01	87	8.73	----	----	8.18	----
2.94	87	8.78	----	----	8.23	----
5.93	87	8.91	----	----	8.36	----
1.01	111	7.42	----	----	6.88	----
2.94	111	7.42	----	----	6.87	----
5.93	111	7.57	----	----	7.03	----
1.01	136	6.54	0.287	0.466	6.46	0.300
2.94	136	6.47	0.412	0.526	6.45	0.446
5.93	136	6.50	0.521	0.636	6.59	0.676
1.01	185	6.04	0.235	0.279	5.77	0.133
2.94	185	5.98	0.335	0.365	5.80	0.246
5.93	185	6.04	0.432	0.462	5.95	0.401
1.01	233	5.90	0.218	0.257	5.61	0.113
2.94	233	5.82	0.313	0.341	5.62	0.214
5.93	233	5.85	0.405	0.431	5.73	0.350
1.01	330	5.75	0.213	0.236	5.44	0.101
2.94	330	5.70	0.305	0.310	5.46	0.189
5.93	330	5.74	0.395	0.395	5.59	0.312
1.01	524	5.67	0.212	0.230	5.35	0.098
2.94	524	5.59	0.302	0.301	5.35	0.182
5.93	524	5.61	0.390	0.383	5.45	0.299
1.01	1011	5.61	0.213	0.230	5.30	0.099
2.94	1011	5.57	0.304	0.300	5.32	0.182
5.93	1011	5.60	0.392	0.387	5.44	0.304

pH 7

Q [ml/min]	c_s [mM]	$V_{R,Gauss}$ [ml]	σ_{Gauss} [ml]	τ [ml]	V_R [ml]	σ^2 [ml^2]
2.94	68	79.44	11.27	0.253	79.1	127.2
5.93	68	76.64	11.38	0.080	76.2	129.5
2.94	68	80.41	10.75	0.198	80.1	115.7
2.94	79	47.42	7.51	0.081	47.0	56.4
5.93	79	45.10	7.72	0.186	44.7	59.7
2.94	79	47.49	7.43	0.054	47.0	55.2
2.94	102	17.37	2.03	0.014	16.8	4.14
5.93	102	17.04	2.35	0.064	16.6	5.54
2.94	102	17.52	2.17	0.032	17.0	4.70
2.94	127	10.95	1.68	0.114	10.5	2.84
5.93	127	10.20	1.65	0.728	10.4	3.25
2.94	127	10.84	1.67	0.206	10.5	2.84
2.94	147	7.87	0.709	1.02	8.34	1.53
5.93	147	7.91	0.867	1.01	8.38	1.78
2.94	147	7.88	0.725	0.976	8.31	1.48
2.94	176	6.81	0.472	0.513	6.78	0.486
5.93	176	6.79	0.585	0.643	6.89	0.756
2.94	176	6.83	0.471	0.512	6.80	0.483
2.94	225	6.08	0.346	0.404	5.94	0.282
5.93	225	6.05	0.441	0.515	6.02	0.460
2.94	225	6.10	0.348	0.403	5.95	0.283
2.94	322	5.76	0.310	0.318	5.53	0.197
5.93	322	5.74	0.400	0.404	5.59	0.324
2.94	322	5.75	0.310	0.317	5.52	0.197
2.94	517	5.59	0.301	0.297	5.34	0.179
5.93	517	5.58	0.386	0.381	5.42	0.294
2.94	517	5.57	0.300	0.299	5.32	0.179
2.94	1005	5.52	0.300	0.296	5.27	0.177
5.93	1005	5.50	0.384	0.382	5.33	0.293
2.94	1005	5.51	0.300	0.294	5.26	0.177

Q [ml/min]	c_s [mM]	$V_{R,Gauss}$ [ml]	pH 8 σ_{Gauss} [ml]	τ [ml]	V_R [ml]	σ^2 [ml^2]
1.01	79	115.16	-7.55	-6.16	108.5	95.0
2.94	79	105.54	-10.85	-0.076	104.9	117.8
5.93	79	103.11	-12.75	-0.088	102.5	162.4
1.01	94	44.82	3.62	1.81	46.1	16.4
2.94	94	41.13	3.87	3.57	44.2	27.7
5.93	94	39.41	4.14	5.13	44.0	43.5
1.01	120	20.85	2.35	0.033	20.3	5.51
2.94	120	19.59	2.42	0.056	19.1	5.85
5.93	120	19.28	2.65	0.019	18.8	7.01
1.01	147	11.68	1.35	0.019	11.1	1.83
2.94	147	11.10	1.39	0.170	10.7	1.96
5.93	147	10.58	1.45	0.678	10.7	2.56
1.01	168	8.47	0.599	0.665	8.59	0.800
2.94	168	8.31	0.733	0.665	8.42	0.979
5.93	168	8.20	0.872	0.839	8.49	1.46
1.01	193	7.22	0.341	0.444	7.12	0.314
2.94	193	7.05	0.477	0.549	7.05	0.529
5.93	193	7.04	0.601	0.705	7.20	0.858
1.01	218	6.57	0.279	0.345	6.37	0.197
2.94	218	6.48	0.399	0.457	6.39	0.368
5.93	218	6.38	0.499	0.594	6.43	0.601
1.01	266	6.18	0.228	0.286	5.92	0.134
2.94	266	6.08	0.329	0.377	5.91	0.250
5.93	266	6.06	0.426	0.470	5.98	0.403
1.01	315	5.94	0.211	0.260	5.66	0.112
2.94	315	5.82	0.309	0.334	5.61	0.207
5.93	315	5.80	0.402	0.420	5.68	0.338
1.01	510	5.68	0.208	0.237	5.37	0.099
2.94	510	5.56	0.299	0.300	5.31	0.179
5.93	510	5.53	0.385	0.379	5.36	0.291
1.01	997	5.57	0.206	0.238	5.27	0.099
2.94	997	5.49	0.295	0.298	5.24	0.176
5.93	997	5.48	0.380	0.381	5.31	0.289

pH 9

Q [ml/min]	c_s [mM]	$V_{R,Gauss}$ [ml]	σ_{Gauss} [ml]	τ [ml]	V_R [ml]	σ^2 [ml^2]
1.01	110	64.10	4.97	8.75	72.3	101.3
2.94	110	59.75	6.79	9.87	69.1	143.5
5.93	110	56.67	7.18	11.92	68.0	193.5
1.01	135	21.10	1.98	1.45	22.0	6.02
2.94	135	19.66	2.04	2.28	21.4	9.36
5.93	135	19.20	2.42	2.60	21.3	12.6
1.01	160	12.30	1.12	0.589	12.3	1.60
2.94	160	11.77	1.23	0.878	12.1	2.28
5.93	160	11.63	1.47	1.11	12.2	3.41
1.01	184	8.84	0.550	0.646	8.94	0.720
2.94	184	8.58	0.721	0.791	8.82	1.14
5.93	184	8.49	0.894	1.03	8.97	1.85
1.01	208	7.57	0.367	0.468	7.50	0.354
2.94	208	7.48	0.523	0.622	7.55	0.660
5.93	208	7.47	0.659	0.787	7.71	1.05
1.01	257	6.44	0.250	0.315	6.21	0.162
2.94	257	6.31	0.364	0.414	6.17	0.304
5.93	257	6.28	0.475	0.526	6.26	0.502
1.01	305	6.14	0.223	0.276	5.87	0.126
2.94	305	6.07	0.327	0.356	5.88	0.233
5.93	305	6.02	0.426	0.446	5.92	0.380
1.01	501	5.73	0.213	0.243	5.42	0.105
2.94	501	5.65	0.304	0.311	5.42	0.189
5.93	501	5.67	0.392	0.385	5.51	0.302
1.01	990	5.60	0.209	0.238	5.30	0.100
2.94	990	5.56	0.299	0.301	5.31	0.180
5.93	990	5.59	0.385	0.379	5.42	0.292

APPENDIX C.III: EXPERIMENTAL DATA FOR ISOCRATIC ELUTION OF β-LACTOGLOBULIN A ON SOURCE 30Q

For the experiments where no σ_{Gauss} and τ values are given the peaks could not be fitted due to the shape of the peaks. The retention volumes are therefore determined as the volume at the peak maximum.

The peaks are fitted with the EMG function. The retention volumes and the variances are calculated as:

$V_R = V_{R,Gauss} + \tau - V_{dead}$

$\sigma^2 = \sigma^2_{Gauss} + \tau^2$

Where $V_{dead} = V_{empty10,\ incl.\ filters} + V_{ID,\ pos.1}$ = 0.237 ml + 0.31 ml = 0.547 ml

Column position: 1
Load: 100 µl

pH 6

Q [ml/min]	c_s [mM]	$V_{R,Gauss}$ [ml]	σ_{Gauss} [ml]	τ [ml]	V_R [ml]	σ^2 [ml^2]
2.94	116	48.36	----	----	47.8	----
5.93	116	46.69	----	----	46.1	----
2.94	116	48.95	----	----	48.4	----
2.94	136	23.51	----	----	23.0	----
5.93	136	22.61	----	----	22.1	----
2.94	136	23.35	----	----	22.8	----
1.01	154	17.41	----	----	16.9	----
1.01	184	10.01	----	----	9.46	----
2.94	232	6.04	0.475	0.494	5.98	0.470
5.93	232	6.00	0.565	0.630	6.08	0.716
2.94	232	6.07	0.469	0.485	6.01	0.454
2.94	280	5.70	0.381	0.389	5.54	0.297
5.93	280	5.66	0.481	0.517	5.63	0.499
2.94	280	5.71	0.382	0.387	5.55	0.296
2.94	330	5.58	0.352	0.362	5.39	0.255
5.93	330	5.60	0.446	0.475	5.53	0.424
2.94	330	5.59	0.350	0.363	5.40	0.254
2.94	379	5.49	0.339	0.354	5.30	0.240
5.93	379	5.52	0.434	0.459	5.43	0.399
2.94	379	5.50	0.339	0.351	5.31	0.238
2.94	524	5.36	0.337	0.350	5.16	0.236
5.93	524	5.34	0.428	0.464	5.25	0.399
2.94	524	5.36	0.337	0.348	5.17	0.235
2.94	1010	5.28	0.336	0.348	5.09	0.234
5.93	1010	5.24	0.425	0.468	5.16	0.400
5.93	1010	5.24	0.425	0.466	5.16	0.398

pH 7

Q [ml/min]	c_s [mM]	$V_{R,Gauss}$ [ml]	σ_{Gauss} [ml]	τ [ml]	V_R [ml]	σ^2 [ml^2]
2.94	147	49.11	----	----	48.6	----
2.94	147	48.64	----	----	48.1	----
2.94	159	33.58	----	----	33.0	----
5.93	159	32.11	----	----	31.6	----
2.94	159	33.80	----	----	33.3	----
2.94	185	16.19	----	----	15.6	----
5.93	185	15.58	----	----	15.0	----
2.94	185	16.37	----	----	15.8	----
2.94	225	7.37	0.974	0.870	7.70	1.71
5.93	225	7.21	1.02	1.10	7.77	2.25
2.94	225	7.42	0.979	0.890	7.76	1.75
2.94	249	6.96	0.661	0.557	6.97	0.747
2.94	249	6.89	0.657	0.549	6.89	0.733
2.94	273	6.30	0.491	0.457	6.21	0.450
5.93	273	6.14	0.582	0.605	6.20	0.706
2.94	273	6.20	0.486	0.457	6.11	0.446
2.94	322	5.79	0.396	0.390	5.64	0.309
5.93	322	5.71	0.493	0.505	5.67	0.498
2.94	322	5.80	0.393	0.386	5.64	0.303
2.94	371	5.58	0.359	0.382	5.41	0.275
5.93	371	5.53	0.454	0.489	5.48	0.446
2.94	371	5.57	0.358	0.377	5.40	0.271
2.94	516	5.39	0.342	0.364	5.21	0.249
5.93	516	5.32	0.431	0.462	5.23	0.399
2.94	516	5.41	0.338	0.361	5.22	0.245
2.94	1001	5.30	0.338	0.354	5.11	0.239
5.93	1001	5.24	0.424	0.457	5.15	0.388
2.94	1001	5.32	0.335	0.350	5.12	0.234

pH 8

Q [ml/min]	c_s [mM]	$V_{R,Gauss}$ [ml]	σ_{Gauss} [ml]	τ [ml]	V_R [ml]	σ^2 [ml^2]
1.01	166	59.20	----	----	58.7	----
2.94	166	57.57	----	----	57.0	----
1.01	191	24.80	----	----	24.2	----
2.94	191	23.61	----	----	23.1	----
1.01	240	10.43	----	----	9.88	----
2.94	240	9.17	----	----	8.62	----
2.94	264	7.40	0.799	0.424	7.28	0.818
5.93	264	7.24	0.861	0.680	7.37	1.20
2.94	264	7.40	0.803	0.417	7.27	0.819
2.94	313	6.26	0.433	0.408	6.12	0.354
5.93	313	6.22	0.533	0.541	6.21	0.577
2.94	313	6.24	0.432	0.413	6.10	0.358
2.94	508	5.54	0.325	0.352	5.34	0.229
5.93	508	5.50	0.417	0.443	5.39	0.370
2.94	508	5.52	0.325	0.350	5.33	0.228
2.94	996	5.40	0.318	0.341	5.19	0.217
5.93	996	5.32	0.407	0.434	5.21	0.354
2.94	996	5.36	0.318	0.339	5.15	0.216

pH 9

Q [ml/min]	c_s [mM]	$V_{R,Gauss}$ [ml]	σ_{Gauss} [ml]	τ [ml]	V_R [ml]	σ^2 [ml^2]
1.01	183	55.19	----	----	54.6	----
2.94	183	52.81	----	----	52.3	----
1.01	208	24.34	----	----	23.8	----
2.94	208	23.61	----	----	23.1	----
1.01	232	15.49	----	----	14.9	----
1.01	232	15.32	----	----	14.8	----
1.01	256	10.25	----	----	9.70	----
1.01	305	6.86	0.421	0.298	6.61	0.266
2.94	305	6.67	0.504	0.484	6.61	0.489
1.01	354	6.18	0.276	0.293	5.92	0.162
2.94	354	6.10	0.383	0.393	5.95	0.301
1.01	403	5.88	0.242	0.288	5.62	0.141
2.94	403	5.80	0.344	0.370	5.63	0.256
1.01	501	5.67	0.229	0.282	5.41	0.132
2.94	501	5.60	0.333	0.344	5.40	0.229
1.01	745	5.52	0.220	0.261	5.23	0.116
2.94	745	5.64	0.318	0.327	5.42	0.208
1.01	989	5.49	0.225	0.266	5.21	0.121
2.94	989	5.45	0.325	0.333	5.24	0.217

APPENDIX C.IV: EXPERIMENTAL DATA FOR ISOCRATIC ELUTION OF β-LACTOGLOBULIN B ON SOURCE 30Q

For the experiments where no σ_{Gauss} and τ values are given the peaks could not be fitted due to the shape of the peaks. The retention volumes are therefore determined as the volume at the peak maximum.

The peaks are fitted with the EMG function. The retention volumes and the variances are calculated as:

$V_R = V_{R,Gauss} + \tau - V_{dead}$

$\sigma^2 = \sigma^2_{Gauss} + \tau^2$

Where $V_{dead} = V_{empty10,\ incl.\ filters} + V_{ID,\ pos.1}$ = 0.237 ml + 0.31 ml = 0.547 ml

Column position: 1
Load: 100 µl

Q [ml/min]	c_s [mM]	$V_{R,Gauss}$ [ml]	pH 6 σ_{Gauss} [ml]	τ [ml]	V_R [ml]	σ^2 [ml^2]
2.94	85	52.58	----	----	52.0	----
5.93	85	49.55	----	----	49.0	----
2.94	85	52.58	----	----	52.0	----
2.94	96	32.05	----	----	31.5	----
5.93	96	30.83	----	----	30.3	----
2.94	96	32.83	----	----	32.3	----
2.94	116	17.64	----	----	17.1	----
5.93	116	17.29	----	----	16.7	----
2.94	116	18.18	----	----	17.6	----
2.94	136	11.11	----	----	10.6	----
5.93	136	11.10	----	----	10.6	----
2.94	136	11.11	----	----	10.6	----
2.94	155	9.05	----	----	8.51	----
5.93	155	9.41	----	----	8.86	----
2.94	155	8.83	----	----	8.29	----
1.01	154	9.26	----	----	8.71	----
2.94	184	7.57	----	----	7.03	----
5.93	184	7.70	----	----	7.15	----
2.94	184	7.54	----	----	6.99	----
1.01	184	7.34	----	----	6.79	----
2.94	232	6.04	0.475	0.494	5.98	0.470
5.93	232	6.00	0.565	0.630	6.08	0.716
2.94	232	6.07	0.469	0.485	6.01	0.454
2.94	280	5.70	0.381	0.389	5.54	0.297
5.93	280	5.66	0.481	0.517	5.63	0.499
2.94	280	5.71	0.382	0.387	5.55	0.296
2.94	330	5.58	0.352	0.362	5.39	0.255
5.93	330	5.60	0.446	0.475	5.53	0.424
2.94	330	5.59	0.350	0.363	5.40	0.254
2.94	379	5.49	0.339	0.354	5.30	0.240
5.93	379	5.52	0.434	0.459	5.43	0.399
2.94	379	5.50	0.339	0.351	5.31	0.238

pH 6

Q [ml/min]	c_s [mM]	$V_{R,Gauss}$ [ml]	σ_{Gauss} [ml]	τ [ml]	V_R [ml]	σ^2 [ml^2]
2.94	524	5.36	0.337	0.350	5.16	0.236
5.93	524	5.34	0.428	0.464	5.25	0.399
2.94	524	5.36	0.337	0.348	5.17	0.235
2.94	1010	5.28	0.336	0.348	5.09	0.234
5.93	1010	5.24	0.425	0.468	5.16	0.400
5.93	1010	5.24	0.425	0.466	5.16	0.398

pH 7

Q [ml/min]	c_s [mM]	$V_{R,Gauss}$ [ml]	σ_{Gauss} [ml]	τ [ml]	V_R [ml]	σ^2 [ml^2]
2.94	117	59.78	----	----	59.2	----
2.94	117	59.25	----	----	58.7	----
2.94	128	41.13	----	----	40.6	----
2.94	128	40.36	----	----	39.8	----
2.94	147	21.27	----	----	20.7	----
2.94	147	21.27	----	----	20.7	----
2.94	159	16.36	----	----	15.8	----
5.93	159	15.81	----	----	15.3	----
2.94	159	16.19	----	----	15.6	----
2.94	185	10.47	----	----	9.92	----
5.93	185	11.29	----	----	10.7	----
2.94	185	10.47	----	----	9.92	----
2.94	225	7.37	0.974	0.870	7.70	1.71
5.93	225	7.21	1.02	1.10	7.77	2.25
2.94	225	7.42	0.979	0.890	7.76	1.75
2.94	249	6.96	0.661	0.557	6.97	0.747
2.94	249	6.89	0.657	0.549	6.89	0.733
2.94	273	6.30	0.491	0.457	6.21	0.450
5.93	273	6.14	0.582	0.605	6.20	0.706
2.94	273	6.20	0.486	0.457	6.11	0.446
2.94	322	5.79	0.396	0.390	5.64	0.309
5.93	322	5.71	0.493	0.505	5.67	0.498
2.94	322	5.80	0.393	0.386	5.64	0.303
2.94	371	5.58	0.359	0.382	5.41	0.275
5.93	371	5.53	0.454	0.489	5.48	0.446
2.94	371	5.57	0.358	0.377	5.40	0.271
2.94	516	5.39	0.342	0.364	5.21	0.249
5.93	516	5.32	0.431	0.462	5.23	0.399
2.94	516	5.41	0.338	0.361	5.22	0.245
2.94	1001	5.30	0.338	0.354	5.11	0.239
5.93	1001	5.24	0.424	0.457	5.15	0.388
2.94	1001	5.32	0.335	0.350	5.12	0.234

pH 8

Q [ml/min]	c_s [mM]	$V_{R,Gauss}$ [ml]	σ_{Gauss} [ml]	τ [ml]	V_R [ml]	σ^2 [ml^2]
1.01	142	66.97	----	----	66.4	----
2.94	142	65.13	----	----	64.6	----
1.01	166	28.24	----	----	27.7	----
2.94	166	26.60	----	----	26.1	----
1.01	191	15.44	----	----	14.9	----
2.94	191	14.50	----	----	14.0	----
1.01	240	8.87	----	----	8.32	----
2.94	240	9.17	----	----	8.62	----
2.94	264	7.40	0.799	0.424	7.28	0.818
5.93	264	7.24	0.861	0.680	7.37	1.20
2.94	264	7.40	0.803	0.417	7.27	0.819
2.94	313	6.26	0.433	0.408	6.12	0.354
5.93	313	6.22	0.533	0.541	6.21	0.577
2.94	313	6.24	0.432	0.413	6.10	0.358
2.94	508	5.54	0.325	0.352	5.34	0.229
5.93	508	5.50	0.417	0.443	5.39	0.370
2.94	508	5.52	0.325	0.350	5.33	0.228
2.94	996	5.40	0.318	0.341	5.19	0.217
5.93	996	5.32	0.407	0.434	5.21	0.354
2.94	996	5.36	0.318	0.339	5.15	0.216

pH 9

Q [ml/min]	c_s [mM]	$V_{R,Gauss}$ [ml]	σ_{Gauss} [ml]	τ [ml]	V_R [ml]	σ^2 [ml^2]
1.01	158	68.66	----	----	68.1	----
2.94	158	66.78	----	----	66.2	----
1.01	158	69.41	----	----	68.9	----
1.01	183	26.70	----	----	26.2	----
2.94	183	25.54	----	----	25.0	----
1.01	208	14.85	----	----	14.3	----
2.94	208	14.39	----	----	13.8	----
1.01	232	11.06	----	----	10.5	----
1.01	232	11.08	----	----	10.5	----
1.01	256	8.48	----	----	7.93	----
1.01	305	6.86	0.421	0.298	6.61	0.266
2.94	305	6.67	0.504	0.484	6.61	0.489
1.01	354	6.18	0.276	0.293	5.92	0.162
2.94	354	6.10	0.383	0.393	5.95	0.301
1.01	403	5.88	0.242	0.288	5.62	0.141
2.94	403	5.80	0.344	0.370	5.63	0.256
1.01	501	5.67	0.229	0.282	5.41	0.132
2.94	501	5.60	0.333	0.344	5.40	0.229
1.01	745	5.52	0.220	0.261	5.23	0.116
2.94	745	5.64	0.318	0.327	5.42	0.208
1.01	989	5.49	0.225	0.266	5.21	0.121
2.94	989	5.45	0.325	0.333	5.24	0.217

APPENDIX C.V: EXPERIMENTAL DATA FOR ISOCRATIC ELUTION OF BSA ON Q-SEPHAROSE XL

The peaks are fitted with the EMG function. The retention volumes and the variances are calculated as:

$V_R = V_{R,Gauss} + \tau - V_{dead}$

$\sigma^2 = \sigma^2_{Gauss} + \tau^2$

Where $V_{dead} = V_{empty16,\ incl.\ filters} + V_{ID,\ pos.2}$ = 0.546 ml + 0.40 ml = 0.946 ml

Column position: 2
Load: 100 µl

Q [ml/min]	c_s [mM]	$V_{R,Gauss}$ [ml]	pH 6 σ_{Gauss} [ml]	τ [ml]	V_R [ml]	σ^2 [ml^2]
6.93	126	19.58	10.54	40.12	58.8	1721
15.1	126	6.69	9.93	75.90	81.6	5860
6.93	126	20.31	11.24	30.11	49.5	1033
6.93	135	20.45	7.69	23.67	43.2	620
15.1	135	16.81	7.90	22.05	37.9	549
6.93	135	22.02	7.77	15.22	36.3	292
6.93	136	10.03	6.14	29.44	38.5	904
15.1	136	4.92	3.00	36.48	40.5	1340
6.93	136	10.64	7.24	26.85	36.5	773
6.93	154	5.19	1.76	15.00	19.2	228
15.1	154	3.80	0.553	11.14	14.0	124
6.93	154	5.21	1.82	14.94	19.2	226
6.93	155	5.51	2.96	17.98	22.5	332
15.1	155	4.01	0.793	13.21	16.3	175
6.93	155	5.59	3.04	16.62	21.3	286
6.93	183	4.07	0.708	8.29	11.4	69.2
15.1	183	3.61	0.319	5.21	7.88	27.3
6.93	183	4.10	0.710	8.48	11.6	72.4
6.93	185	3.83	0.625	6.62	9.50	44.2
15.1	185	3.50	0.308	3.78	6.34	14.4
6.93	185	3.75	0.626	6.40	9.21	41.3
6.93	232	3.24	0.220	2.24	4.54	5.08
15.1	232	3.32	0.203	1.25	3.63	1.62
6.93	232	3.26	0.223	2.21	4.53	4.95
6.93	232	3.23	0.224	2.17	4.46	4.77
6.93	233	3.22	0.227	1.97	4.24	3.92
15.1	233	3.27	0.215	1.17	3.50	1.42
6.93	233	3.21	0.226	1.94	4.21	3.82
6.93	305	3.25	0.184	1.01	3.31	1.05
15.1	305	3.41	0.203	0.663	3.13	0.480
6.93	305	3.19	0.185	0.977	3.22	0.988
6.93	329	3.13	0.194	0.866	3.05	0.787
15.1	329	3.24	0.217	0.636	2.93	0.451
6.93	329	3.07	0.195	0.863	2.98	0.782
6.93	523	3.15	0.184	0.646	2.85	0.452
15.1	523	3.31	0.201	0.501	2.87	0.291
6.93	523	3.19	0.187	0.635	2.88	0.438
6.93	526	3.18	0.189	0.596	2.83	0.391
15.1	526	3.34	0.216	0.488	2.88	0.285
6.93	526	3.20	0.188	0.596	2.85	0.391

pH 6

Q [ml/min]	c_s [mM]	$V_{R,Gauss}$ [ml]	σ_{Gauss} [ml]	τ [ml]	V_R [ml]	σ^2 [ml^2]
6.93	1009	3.17	0.186	0.587	2.82	0.379
15.1	1009	3.37	0.203	0.462	2.88	0.255
6.93	1009	3.10	0.188	0.558	2.71	0.346
6.93	1011	3.14	0.188	0.527	2.72	0.313
15.1	1011	3.27	0.217	0.445	2.77	0.245
6.93	1011	3.16	0.189	0.529	2.75	0.315

pH 7

Q [ml/min]	c_s [mM]	$V_{R,Gauss}$ [ml]	σ_{Gauss} [ml]	τ [ml]	V_R [ml]	σ^2 [ml^2]
6.93	203	9.39	4.85	24.89	33.3	643
15.1	203	5.26	2.21	26.34	30.7	699
6.93	203	9.26	5.41	23.90	32.2	600
6.93	224	5.23	1.57	14.19	18.5	204
15.1	224	4.15	0.559	9.94	13.1	99.2
6.93	224	5.22	1.73	13.63	17.9	189
6.93	272	3.51	0.336	3.85	6.42	15.0
15.1	272	3.56	0.235	2.04	4.65	4.21
6.93	272	3.53	0.337	3.74	6.32	14.1
6.93	370	3.18	0.192	1.05	3.29	1.145
15.1	370	3.22	0.200	0.698	2.97	0.527
6.93	370	3.22	0.192	1.04	3.31	1.110
6.93	516	3.22	0.181	0.756	3.03	0.604
15.1	516	3.32	0.200	0.518	2.89	0.308
6.93	516	3.25	0.180	0.734	3.04	0.571
6.93	1006	3.23	0.179	0.591	2.88	0.381
15.1	1006	3.42	0.201	0.447	2.92	0.241
6.93	1006	3.19	0.181	0.580	2.82	0.369

pH 8

Q [ml/min]	c_s [mM]	$V_{R,Gauss}$ [ml]	σ_{Gauss} [ml]	τ [ml]	V_R [ml]	σ^2 [ml^2]
6.93	241	13.22	8.01	29.72	42.0	948
6.93	241	13.72	8.66	25.86	38.6	744
6.93	263	6.66	2.86	15.76	21.5	257
15.1	263	4.46	0.913	14.09	17.6	199
6.93	263	6.59	2.72	15.06	20.7	234
6.93	314	3.63	0.391	4.62	7.30	21.5
15.1	314	3.57	0.252	2.59	5.21	6.77
6.93	314	3.62	0.394	4.47	7.15	20.1
6.93	362	3.24	0.213	1.68	3.97	2.87
15.1	362	3.43	0.208	1.03	3.51	1.11
6.93	362	3.25	0.216	1.65	3.96	2.78
6.93	508	3.22	0.192	0.729	3.00	0.568
15.1	508	3.53	0.207	0.580	3.17	0.379
6.93	508	3.28	0.194	0.731	3.06	0.572
6.93	996	3.19	0.192	0.548	2.79	0.337
15.1	996	3.53	0.210	0.473	3.06	0.268
6.93	996	3.26	0.191	0.552	2.87	0.341

pH 9

Q [ml/min]	c_s [mM]	$V_{R,Gauss}$ [ml]	σ_{Gauss} [ml]	τ [ml]	V_R [ml]	σ^2 [ml^2]
6.93	256	31.52	16.38	32.91	63.5	1351
15.1	256	18.24	10.88	33.91	51.2	1268
6.93	256	36.30	16.76	17.32	52.7	581
6.93	304	4.80	1.48	12.12	16.0	149
15.1	304	3.73	0.457	8.97	11.8	80.7
6.93	304	4.97	1.39	10.72	14.7	117
6.93	354	3.40	0.296	3.19	5.64	10.3
15.1	354	3.30	0.228	1.77	4.12	3.19
6.93	354	3.36	0.296	3.12	5.54	9.83
6.93	383	3.24	0.227	1.93	4.22	3.78
15.1	383	3.25	0.213	1.15	3.46	1.37
6.93	383	3.23	0.227	1.91	4.19	3.71
6.93	501	3.19	0.186	0.803	3.05	0.680
15.1	501	3.19	0.208	0.589	2.83	0.390
6.93	501	3.19	0.189	0.767	3.01	0.624
6.93	989	3.17	0.184	0.540	2.76	0.325
15.1	989	3.23	0.210	0.463	2.75	0.258
6.93	989	3.18	0.186	0.541	2.78	0.327

APPENDIX C.VI: EXPERIMENTAL DATA FOR ISOCRATIC ELUTION OF α-LACTALBUMIN ON Q-SEPHAROSE XL

The peaks are fitted with the EMG function. The retention volumes and the variances are calculated as:

$V_R = V_{R,Gauss} + \tau - V_{dead}$

$\sigma^2 = \sigma^2_{Gauss} + \tau^2$

Where $V_{dead} = V_{empty16,\ incl.\ filters} + V_{ID,\ pos.2}$ = 0.546 ml + 0.40 ml = 0.946 ml

Column position: 2
Load: 100 µl

pH 6

Q [ml/min]	c_s [mM]	$V_{R,Gauss}$ [ml]	σ_{Gauss} [ml]	τ [ml]	V_R [ml]	σ^2 [ml^2]
1.01	77	72.07	9.21	0.063	71.2	85
6.93	77	55.10	13.98	12.68	66.8	356
15.1	77	41.57	11.90	31.32	71.9	1123
1.01	87	48.47	8.15	0.057	47.6	66.4
6.93	87	34.21	11.30	9.79	43.1	224
15.1	87	25.27	12.17	23.08	47.4	681
1.01	111	22.82	3.43	2.82	24.7	19.7
6.93	111	15.91	4.91	9.89	24.9	122
15.1	111	11.45	5.12	16.01	26.5	283
1.01	136	17.45	3.11	1.13	17.6	10.9
6.93	136	10.88	4.15	7.86	17.8	79.0
15.1	136	6.92	2.75	14.68	20.7	223
1.01	185	8.92	1.47	1.40	9.38	4.13
6.93	185	5.82	1.39	5.44	10.3	31.5
15.1	185	4.80	0.780	6.22	10.1	39.3
1.01	233	6.82	1.08	1.48	7.35	3.36
6.93	233	4.80	0.843	4.00	7.85	16.7
15.1	233	4.18	0.538	4.21	7.44	18.0
1.01	330	5.59	0.695	1.02	5.67	1.52
6.93	330	4.20	0.607	2.60	5.86	7.14
15.1	330	3.95	0.365	2.28	5.28	5.35
1.01	524	4.93	0.620	0.814	4.79	1.05
6.93	524	3.85	0.441	2.06	4.97	4.44
15.1	524	3.61	0.285	1.89	4.55	3.64
1.01	1011	4.62	0.574	0.780	4.45	0.938
6.93	1011	3.64	0.358	1.83	4.52	3.47
15.1	1011	3.71	0.265	1.57	4.33	2.52

pH 6 (Data by Søren S. Frederiksen)

Q [ml/min]	c_s [mM]	$V_{R,Gauss}$ [ml]	σ_{Gauss} [ml]	τ [ml]	V_R [ml]	σ^2 [ml^2]
1.97	79	53.12	8.76	7.00	59.2	126
1.01	79	56.30	7.15	4.29	59.7	69.5
0.529	79	60.63	6.68	0.000	59.7	44.6
1.97	89	39.30	6.72	6.34	44.7	85.4
1.01	89	45.25	6.62	0.000	44.3	43.8
0.529	89	45.70	5.34	0.000	44.8	28.5
1.97	113	22.22	4.23	3.73	25.0	31.8
1.01	113	23.79	3.50	2.35	25.2	17.8
0.529	113	26.30	3.26	0.000	25.4	10.7
1.97	138	14.38	2.74	3.13	16.6	17.3
1.01	138	15.42	2.27	2.18	16.7	9.91
0.529	138	17.44	2.27	0.000	16.5	5.13
1.97	188	8.71	1.68	2.08	9.84	7.13
1.01	188	9.47	1.44	1.29	9.82	3.76
0.529	188	9.89	1.22	0.902	9.85	2.30
1.97	236	6.69	1.20	1.77	7.52	4.59
1.01	236	7.25	1.06	1.12	7.43	2.39
0.529	236	7.59	0.900	0.769	7.41	1.40
1.97	335	5.60	0.834	1.40	6.05	2.66
1.01	335	5.91	0.713	1.00	5.96	1.51
0.529	335	6.11	0.597	0.768	5.94	0.947
1.97	529	4.99	0.727	1.20	5.24	1.96
1.01	529	5.28	0.639	0.809	5.14	1.06
0.529	529	5.49	0.548	0.573	5.11	0.628

pH 7

Q [ml/min]	c_s [mM]	$V_{R,Gauss}$ [ml]	σ_{Gauss} [ml]	τ [ml]	V_R [ml]	σ^2 [ml^2]
6.93	127	55.53	14.61	15.68	70.3	459
15.1	127	43.39	10.20	40.33	82.8	1731
6.93	127	51.91	8.88	35.14	86.1	1314
6.93	127	54.83	14.21	18.20	72.1	533
6.93	147	31.69	8.93	12.93	43.7	247
15.1	147	23.63	9.92	25.11	47.8	729
6.93	147	32.15	8.68	12.48	43.7	231
6.93	176	15.73	4.86	9.87	24.6	121
15.1	176	11.06	5.02	14.68	24.8	241
6.93	176	16.17	4.70	8.45	23.7	93.5
6.93	225	7.44	2.70	7.02	13.5	56.5
15.1	225	5.18	1.31	9.79	14.0	97.5
6.93	225	7.60	2.56	6.90	13.6	54.2
6.93	322	4.71	0.867	3.42	7.19	12.5
15.1	322	3.98	0.552	3.85	6.89	15.1
6.93	322	4.66	0.869	3.46	7.17	12.7
6.93	517	3.93	0.515	2.26	5.24	5.38
15.1	517	3.45	0.332	2.18	4.69	4.86
6.93	517	3.89	0.516	2.26	5.21	5.38
6.93	1005	3.62	0.379	1.86	4.53	3.59
15.1	1005	3.32	0.279	1.59	3.96	2.59
6.93	1005	3.61	0.380	1.84	4.51	3.54

pH 7 (Data by Søren S. Frederiksen)

Q [ml/min]	c_s [mM]	$V_{R,Gauss}$ [ml]	σ_{Gauss} [ml]	τ [ml]	V_R [ml]	σ^2 [ml^2]
1.97	138	37.82	6.76	0.00	36.9	45.7
1.01	138	38.54	5.40	0.00	37.6	29.1
0.529	138	39.29	4.36	0.00	38.3	19.0
1.97	138	38.38	6.83	0.00	37.4	46.7
1.01	138	38.85	5.38	0.00	37.9	28.9
0.529	138	39.14	4.35	0.00	38.2	18.9
0.529	157	26.64	3.10	0.00	25.7	9.59
1.01	157	26.26	3.82	0.00	25.3	14.6
1.97	157	22.55	3.81	4.11	25.7	31.5
0.529	157	26.71	3.10	0.00	25.8	9.58
1.01	157	26.05	3.83	0.00	25.1	14.6
1.97	157	22.36	3.81	4.19	25.6	32.1
0.529	187	15.92	1.72	1.52	16.5	5.27
1.01	187	15.42	2.11	2.09	16.6	8.81
1.97	187	14.56	2.62	2.95	16.6	15.5
0.529	187	17.17	2.10	0.00	16.2	4.40
1.01	187	15.35	2.11	2.12	16.5	8.97
1.97	187	14.52	2.61	3.02	16.6	16.0
0.529	236	9.95	1.11	1.07	10.1	2.36
1.01	236	9.64	1.35	1.44	10.1	3.91
1.97	236	9.06	1.63	2.09	10.2	7.03
0.529	236	10.00	1.09	1.09	10.1	2.39
1.01	236	9.66	1.35	1.44	10.2	3.90
1.97	236	9.09	1.64	2.05	10.2	6.89
0.529	335	6.89	0.731	0.71	6.65	1.03
1.01	335	6.64	0.876	1.03	6.73	1.84
1.97	335	6.21	1.00	1.50	6.77	3.27
0.529	335	6.82	0.702	0.791	6.66	1.12
1.01	335	6.54	0.820	1.09	6.69	1.86
1.97	335	6.15	0.961	1.56	6.76	3.36
0.529	529	5.71	0.565	0.549	5.31	0.62
1.01	529	5.50	0.666	0.803	5.36	1.09
1.97	529	5.16	0.767	1.18	5.40	1.99
0.529	529	5.71	0.564	0.553	5.31	0.625
1.01	529	5.46	0.666	0.819	5.33	1.11
1.97	529	5.12	0.763	1.20	5.37	2.02
0.529	529	5.67	0.569	0.645	5.37	0.740
3.95	529	4.66	0.846	1.79	5.50	3.92
6.93	529	4.13	0.797	2.28	5.46	5.82
15.1	529	3.50	0.631	2.55	5.10	6.90

Q [ml/min]	c_s [mM]	$V_{R,Gauss}$ [ml]	pH 8 σ_{Gauss} [ml]	τ [ml]	V_R [ml]	σ^2 [ml^2]
1.01	147	79.31	10.08	3.07	81.4	111
6.93	147	62.85	14.20	27.17	89.1	940
15.1	147	56.13	14.99	29.55	84.7	1098
1.01	168	45.55	6.26	3.13	47.7	49.0
6.93	168	36.40	9.99	13.16	48.6	273
15.1	168	29.48	9.77	22.74	51.3	613
1.01	193	26.91	3.93	2.56	28.5	22.0
6.93	193	20.10	6.13	10.02	29.2	138
15.1	193	14.83	6.85	16.99	30.9	336
1.01	218	18.97	3.08	1.79	19.8	12.7
6.93	218	13.53	4.65	8.08	20.7	86.9
15.1	218	8.93	4.58	14.79	22.8	240
1.01	266	10.80	1.76	1.48	11.3	5.29
6.93	266	7.14	2.16	6.06	12.3	41.4
15.1	266	5.25	1.24	8.37	12.7	71.5
1.01	315	7.80	1.30	1.45	8.30	3.77
6.93	315	5.39	1.07	4.55	8.99	21.8
15.1	315	4.35	0.731	5.15	8.55	27.1
1.01	510	5.39	0.682	0.822	5.26	1.14
6.93	510	4.03	0.565	2.35	5.44	5.85
15.1	510	3.55	0.360	2.40	5.01	5.90
1.01	997	4.70	0.586	0.751	4.50	0.907
6.93	997	3.63	0.382	1.86	4.55	3.62
15.1	997	3.60	0.283	1.64	4.29	2.76

Q [ml/min]	c_s [mM]	$V_{R,Gauss}$ [ml]	pH 8 σ_{Gauss} [ml]	(Data by Søren S. Frederiksen) τ [ml]	V_R [ml]	σ^2 [ml^2]
1.97	168	29.72	4.90	5.15	33.9	50.5
1.01	168	31.15	3.99	3.34	33.5	27.1
0.529	168	34.13	3.83	0.00	33.2	14.6
1.97	188	20.82	3.59	3.97	23.8	28.7
1.01	188	21.30	2.91	2.73	23.1	15.9
0.529	188	22.53	2.39	1.95	23.5	9.50
1.97	212	14.97	2.68	3.03	17.1	16.4
1.01	212	15.82	2.18	2.10	17.0	9.14
0.529	212	16.22	1.77	1.55	16.8	5.54
1.97	236	11.70	2.16	2.48	13.2	10.8
1.01	236	12.43	1.76	1.69	13.2	5.98
0.529	236	12.88	1.45	1.21	13.1	3.57
1.97	286	8.43	1.51	1.84	9.32	5.68
1.01	286	9.11	1.25	1.24	9.41	3.11
0.529	286	9.53	1.01	0.896	9.48	1.83
1.97	335	6.91	1.20	1.59	7.56	3.96
1.01	335	7.58	1.04	1.02	7.65	2.11
0.529	335	7.92	0.848	0.716	7.69	1.23
1.97	529	5.25	0.777	1.22	5.52	2.10
1.01	529	5.55	0.671	0.820	5.42	1.12
0.529	529	5.77	0.570	0.579	5.40	0.660

pH 9

Q [ml/min]	c_s [mM]	$V_{R,Gauss}$ [ml]	σ_{Gauss} [ml]	τ [ml]	V_R [ml]	σ^2 [ml^2]
1.01	184	67.83	9.38	0.138	67.0	88.1
6.93	184	52.88	15.26	15.12	67.1	461
15.1	184	40.96	17.01	33.34	73.4	1401
1.01	208	42.40	6.24	0.043	41.5	38.9
6.93	208	29.31	7.57	21.00	49.4	498
15.1	208	22.81	6.34	35.56	57.4	1305
1.01	257	15.92	2.62	2.05	17.0	11.1
6.93	257	10.79	3.84	8.05	17.9	79.6
15.1	257	7.21	2.87	13.76	20.0	198
1.01	305	10.57	1.76	1.54	11.2	5.47
6.93	305	6.93	2.00	6.20	12.2	42.4
15.1	305	5.41	1.23	7.97	12.4	65.0
1.01	404	6.32	0.840	1.22	6.59	2.19
6.93	404	4.58	0.808	3.28	6.92	11.4
15.1	404	3.94	0.478	3.60	6.60	13.2
1.01	501	5.61	0.717	0.885	5.54	1.30
6.93	501	4.17	0.627	2.55	5.77	6.91
15.1	501	3.82	0.379	2.69	5.56	7.36
1.01	990	4.73	0.578	0.762	4.54	0.914
6.93	990	3.77	0.383	1.87	4.70	3.66
15.1	990	3.59	0.272	1.70	4.35	2.97

pH 9 (Data by Søren S. Frederiksen)

Q [ml/min]	c_s [mM]	$V_{R,Gauss}$ [ml]	σ_{Gauss} [ml]	τ [ml]	V_R [ml]	σ^2 [ml^2]
1.97	212	26.92	5.00	4.73	30.7	47.3
1.01	212	28.43	4.01	3.31	30.8	27.1
0.529	212	31.14	3.74	0.00	30.2	14.0
1.97	236	17.81	3.42	3.52	20.4	24.1
1.01	236	18.79	2.78	2.47	20.3	13.8
0.529	236	20.83	2.66	0.00	19.9	7.05
1.97	286	10.43	1.99	2.39	11.9	9.64
1.01	286	11.14	1.64	1.65	11.8	5.43
0.529	286	11.53	1.35	1.22	11.8	3.31
1.97	335	7.86	1.43	1.89	8.81	5.63
1.01	335	8.40	1.19	1.32	8.77	3.16
0.529	335	8.68	0.988	0.979	8.72	1.93
1.97	432	6.01	0.953	1.47	6.53	3.06
1.01	432	6.36	0.821	1.01	6.43	1.70
0.529	432	6.58	0.693	0.746	6.38	1.04
1.97	529	5.38	0.809	1.30	5.73	2.34
1.01	529	5.70	0.701	0.868	5.62	1.24
0.529	529	5.90	0.591	0.621	5.58	0.735

APPENDIX C.VII: EXPERIMENTAL DATA FOR ISOCRATIC ELUTION OF β-LACTOGLOBULIN B ON Q-SEPHAROSE XL

For the experiments where no σ_{Gauss} and τ values are given the peaks could not be fitted due to the shape of the peaks. The retention volumes are therefore determined as the volume at the peak maximum.

The peaks are fitted with the EMG function. The retention volumes and the variances are calculated as:

$V_R = V_{R,Gauss} + \tau - V_{dead}$

$\sigma^2 = \sigma^2_{Gauss} + \tau^2$

Where $V_{dead} = V_{empty16,\ incl.\ filters} + V_{ID,\ pos.2}$ = 0.546 ml + 0.40 ml = 0.946 ml

Column position: 2
Load: 100 µl

pH 6

Q [ml/min]	c_s [mM]	$V_{R,Gauss}$ [ml]	σ_{Gauss} [ml]	τ [ml]	V_R [ml]	σ^2 [ml^2]
1.01	154	50.19	----	----	49.2	----
1.01	184	26.20	----	----	25.3	----
6.93	232	6.98	2.44	8.05	14.1	70.7
15.1	232	5.04	1.24	10.27	14.4	107
6.93	232	7.00	2.50	8.42	14.5	77.2
6.93	280	4.59	0.984	5.02	8.66	26.2
15.1	280	3.89	0.412	4.79	7.73	23.1
6.93	280	4.59	0.958	5.18	8.82	27.7
6.93	330	3.82	0.528	3.56	6.43	12.9
15.1	330	3.44	0.287	2.55	5.03	6.56
6.93	330	3.83	0.530	3.51	6.39	12.6
6.93	379	3.49	0.356	2.62	5.16	6.99
15.1	379	3.53	0.237	1.72	4.31	3.02
6.93	379	3.53	0.360	2.54	5.12	6.59
6.93	524	3.35	0.221	1.63	4.04	2.71
15.1	524	3.45	0.200	1.05	3.56	1.15
6.93	524	3.39	0.222	1.61	4.05	2.63
6.93	1010	3.30	0.192	1.13	3.48	1.31
15.1	1010	3.61	0.198	0.753	3.41	0.607
6.93	1010	3.32	0.194	1.11	3.49	1.28

pH 7

Q [ml/min]	c_s [mM]	$V_{R,Gauss}$ [ml]	σ_{Gauss} [ml]	τ [ml]	V_R [ml]	σ^2 [ml^2]
6.93	225	21.18	13.05	22.84	43.1	692
15.1	225	11.17	10.37	51.75	62.0	2785
6.93	225	20.49	12.73	22.27	41.8	658
6.93	249	13.52	7.10	13.88	26.4	243
15.1	249	8.57	5.06	24.40	32.0	621
6.93	249	13.20	7.09	14.42	26.7	258
6.93	273	9.36	4.00	10.28	18.7	122
15.1	273	6.38	2.85	13.86	19.3	200
6.93	273	9.45	4.01	9.55	18.1	107
6.93	322	5.72	1.65	5.54	10.3	33.5
15.1	322	4.39	0.826	6.52	10.0	43.2
6.93	322	5.65	1.62	5.47	10.2	32.6
6.93	371	4.35	0.835	4.27	7.67	18.9
15.1	371	3.72	0.371	3.86	6.63	15.0
6.93	516	3.37	0.289	2.20	4.62	4.93
15.1	516	3.24	0.215	1.48	3.77	2.22
6.93	516	3.39	0.288	2.16	4.61	4.75
6.93	1001	3.19	0.206	1.34	3.58	1.83
15.1	1001	3.22	0.201	0.875	3.15	0.806
6.93	1001	3.24	0.207	1.31	3.61	1.77

pH 8

Q [ml/min]	c_s [mM]	$V_{R,Gauss}$ [ml]	σ_{Gauss} [ml]	τ [ml]	V_R [ml]	σ^2 [ml^2]
1.01	240	35.00	----	----	34.1	----
6.93	264	17.63	7.90	15.24	31.9	295
15.1	264	13.04	7.31	25.01	37.1	679
6.93	264	18.77	8.12	15.32	33.1	301
1.01	289	16.00	4.33	4.43	19.5	38.4
6.93	289	10.88	4.36	10.47	20.4	129
6.93	313	8.82	2.92	7.73	15.6	68.3
15.1	313	6.67	2.04	10.74	16.5	119
6.93	313	8.73	2.92	7.35	15.1	62.5
1.01	362	8.14	1.46	1.78	8.97	5.31
6.93	362	5.39	1.32	5.15	9.60	28
1.01	411	4.45	0.802	3.97	7.47	16.4
6.93	508	3.71	0.471	2.65	5.42	7.25
15.1	508	3.76	0.278	2.33	5.15	5.52
6.93	508	3.74	0.466	2.63	5.43	7.12
6.93	996	3.43	0.233	1.56	4.04	2.49
15.1	996	3.62	0.208	1.18	3.85	1.43
6.93	996	3.37	0.235	1.54	3.97	2.43

Q [ml/min]	c_s [mM]	$V_{R,Gauss}$ [ml]	pH 9 σ_{Gauss} [ml]	τ [ml]	V_R [ml]	σ^2 [ml^2]
1.01	232	76.28	----	----	75.3	----
6.93	232	69.65	----	----	68.7	----
1.01	256	38.09	----	----	37.1	----
6.93	256	37.18	----	----	36.2	----
1.01	305	15.96	4.30	5.49	20.5	48.6
6.93	305	10.96	4.26	11.78	21.8	157
1.01	354	10.05	1.92	2.25	11.4	8.78
6.93	354	6.60	1.91	6.71	12.4	48.7
1.01	403	7.36	1.19	1.61	8.02	4.02
6.93	403	4.87	1.11	4.59	8.51	22.3
1.01	501	5.41	0.803	1.04	5.51	1.73
6.93	501	3.88	0.512	2.80	5.73	8.10
1.01	574	4.94	0.684	0.931	4.92	1.34
6.93	574	3.59	0.425	2.33	4.97	5.60
1.01	745	4.39	0.582	0.908	4.35	1.16
6.93	745	3.32	0.281	1.77	4.14	3.21
1.01	989	4.19	0.541	0.905	4.15	1.11
6.93	989	3.43	0.241	1.55	4.04	2.46

APPENDIX C.VIII: EXPERIMENTAL DATA FOR ISOCRATIC ELUTION OF BSA ON CERAMIC Q-HYPERD F

The peaks are fitted with the EMG function. The retention volumes and the variances are calculated as:

$V_R = V_{R,Gauss} + \tau - V_{dead}$

$\sigma^2 = \sigma^2_{Gauss} + \tau^2$

Where $V_{dead} = V_{empty10,\ incl.\ filters} + V_{ID,\ pos.1}$ = 0.237 ml + 0.31 ml = 0.547 ml

Column position: 1
Load: 100 µl

Q [ml/min]	c_s [mM]	$V_{R,Gauss}$ [ml]	pH 6 σ_{gauss} [ml]	τ [ml]	V_R [ml]	σ^2 [ml^2]
2.94	71	23.60	3.63	19.63	42.7	398
5.93	71	22.68	4.63	13.60	35.7	206
2.94	71	24.68	3.65	15.52	39.6	254
2.94	76	18.70	2.75	10.26	28.4	113
5.93	76	17.23	3.72	11.55	28.2	147
2.94	76	18.29	2.40	11.29	29.0	133
2.94	87	13.34	4.04	4.31	17.1	34.9
5.93	87	9.10	2.66	9.14	17.7	90.7
2.94	87	9.05	1.75	9.64	18.1	96.0
2.94	98	5.25	0.454	2.27	6.97	5.34
5.93	98	5.07	0.446	2.08	6.61	4.53
2.94	98	5.18	0.458	2.10	6.73	4.61
2.94	108	4.68	0.300	1.37	5.50	1.96
5.93	108	4.65	0.293	1.32	5.42	1.82
2.94	108	4.66	0.300	1.35	5.46	1.91
2.94	111	4.80	0.346	1.54	5.79	2.50
5.93	111	4.76	0.335	1.47	5.68	2.27
2.94	111	4.74	0.343	1.45	5.64	2.21
2.94	120	4.47	0.253	1.09	5.01	1.25
5.93	120	4.52	0.248	1.07	5.04	1.20
2.94	120	4.45	0.252	1.08	4.98	1.23
2.94	126	4.40	0.223	0.910	4.76	0.877
5.93	126	4.36	0.225	0.888	4.70	0.840
2.94	126	4.38	0.230	0.894	4.73	0.853
2.94	139	4.16	0.152	0.608	4.22	0.392
5.93	139	4.21	0.156	0.594	4.25	0.377
2.94	139	4.16	0.156	0.601	4.22	0.386
2.94	157	4.04	0.136	0.408	3.90	0.185
5.93	157	4.13	0.139	0.400	3.98	0.179
2.94	157	4.00	0.136	0.405	3.86	0.182
2.94	185	3.92	0.138	0.295	3.67	0.106
5.93	185	4.00	0.140	0.287	3.74	0.102
2.94	185	3.95	0.137	0.295	3.70	0.106
2.94	196	3.94	0.121	0.278	3.67	0.092
5.93	196	4.02	0.126	0.274	3.75	0.091
2.94	196	3.91	0.121	0.278	3.64	0.092
2.94	215	3.90	0.121	0.264	3.62	0.085
5.93	215	3.99	0.126	0.260	3.71	0.084
2.94	215	3.90	0.121	0.265	3.62	0.085

pH 6

Q [ml/min]	c_s [mM]	$V_{R,Gauss}$ [ml]	σ_{gauss} [ml]	τ [ml]	V_R [ml]	σ^2 [ml^2]
2.94	236	3.91	0.126	0.250	3.61	0.078
5.93	236	3.97	0.132	0.246	3.67	0.078
2.94	236	3.88	0.127	0.252	3.59	0.080
2.94	333	3.88	0.125	0.232	3.57	0.070
5.93	333	3.99	0.130	0.230	3.68	0.070
2.94	333	3.87	0.125	0.235	3.56	0.071
2.94	527	3.87	0.125	0.230	3.56	0.069
5.93	527	3.95	0.130	0.226	3.63	0.068
2.94	527	3.89	0.125	0.232	3.57	0.069
2.94	1010	3.86	0.121	0.223	3.53	0.064
5.93	1010	3.93	0.124	0.219	3.60	0.063
2.94	1010	3.86	0.120	0.223	3.54	0.064

pH 7

Q [ml/min]	c_s [mM]	$V_{R,Gauss}$ [ml]	σ_{gauss} [ml]	τ [ml]	V_R [ml]	σ^2 [ml^2]
2.94	112	22.28	4.00	21.74	43.5	489
2.94	112	21.88	4.10	18.68	40.0	366
2.94	131	8.27	1.65	7.46	15.2	58.3
5.93	131	7.40	1.63	8.68	15.5	78.0
2.94	131	8.15	1.96	7.47	15.1	59.6
2.94	151	5.06	0.411	2.53	7.05	6.59
5.93	151	4.97	0.392	2.39	6.82	5.89
2.94	151	5.05	0.412	2.51	7.01	6.47
2.94	180	4.18	0.184	0.771	4.40	0.628
5.93	180	4.22	0.179	0.724	4.39	0.557
2.94	180	4.17	0.184	0.750	4.38	0.596
2.94	209	4.03	0.151	0.410	3.89	0.191
5.93	209	4.06	0.150	0.402	3.91	0.185
2.94	209	4.02	0.150	0.412	3.88	0.193
2.94	229	3.94	0.139	0.310	3.70	0.115
5.93	229	3.93	0.138	0.302	3.68	0.110
2.94	229	3.94	0.139	0.312	3.71	0.117
2.94	325	3.85	0.127	0.233	3.54	0.071
5.93	325	3.84	0.127	0.224	3.52	0.066
2.94	325	3.84	0.127	0.234	3.53	0.071
2.94	521	3.84	0.125	0.224	3.52	0.065
5.93	521	3.89	0.125	0.212	3.55	0.061
2.94	521	3.84	0.125	0.223	3.52	0.065
2.94	1007	3.84	0.124	0.221	3.51	0.064
5.93	1007	3.84	0.125	0.211	3.51	0.060
2.94	1007	3.85	0.124	0.222	3.52	0.065

pH 8

Q [ml/min]	c_s [mM]	$V_{R,Gauss}$ [ml]	σ_{gauss} [ml]	τ [ml]	V_R [ml]	σ^2 [ml^2]
2.94	162	45.53	14.11	18.00	63.0	523
5.93	162	43.35	14.68	20.86	63.7	651
2.94	162	49.26	12.46	13.94	62.7	349
2.94	172	26.49	7.33	11.31	37.2	182
5.93	172	23.56	8.64	14.07	37.1	273
2.94	172	26.50	7.36	11.24	37.2	181
2.94	198	6.22	0.960	3.39	9.06	12.4
5.93	198	5.73	0.862	3.39	8.57	12.3
2.94	198	6.14	0.985	3.31	8.90	11.9
2.94	218	4.60	0.297	1.18	5.23	1.48
5.93	218	4.63	0.290	1.12	5.20	1.34
2.94	218	4.66	0.309	1.18	5.29	1.50
2.94	236	4.21	0.187	0.664	4.32	0.476
5.93	236	4.30	0.183	0.635	4.39	0.437
2.94	236	4.20	0.187	0.647	4.30	0.454
2.94	256	4.05	0.151	0.380	3.88	0.167
5.93	256	4.09	0.152	0.382	3.93	0.169
2.94	256	4.05	0.153	0.390	3.89	0.176
2.94	316	3.88	0.130	0.240	3.57	0.075
5.93	316	4.03	0.131	0.236	3.72	0.073
2.94	316	3.92	0.131	0.239	3.61	0.074
2.94	511	3.85	0.125	0.220	3.53	0.064
5.93	511	3.92	0.126	0.214	3.59	0.062
2.94	511	3.87	0.124	0.221	3.55	0.064
2.94	996	3.85	0.123	0.218	3.52	0.063
5.93	996	3.99	0.127	0.211	3.66	0.061
2.94	996	3.85	0.124	0.219	3.52	0.063

pH 9

Q [ml/min]	c_s [mM]	$V_{R,Gauss}$ [ml]	σ_{gauss} [ml]	τ [ml]	V_R [ml]	σ^2 [ml^2]
2.94	211	17.71	5.70	9.77	26.9	128
2.94	211	18.70	5.44	9.54	27.7	121
2.94	259	4.41	0.267	0.973	4.83	1.02
5.93	259	4.37	0.250	0.931	4.76	0.929
2.94	259	4.43	0.271	0.980	4.87	1.03
2.94	308	3.91	0.138	0.273	3.63	0.094
5.93	308	4.00	0.143	0.271	3.73	0.094
2.94	308	3.94	0.138	0.272	3.67	0.093
2.94	356	3.89	0.128	0.217	3.56	0.064
5.93	356	3.96	0.132	0.217	3.63	0.065
2.94	356	3.88	0.128	0.217	3.55	0.064
2.94	503	3.85	0.124	0.202	3.50	0.056
5.93	503	3.92	0.129	0.200	3.57	0.056
2.94	503	3.84	0.125	0.205	3.50	0.058
2.94	990	3.85	0.124	0.198	3.50	0.055
5.93	990	3.88	0.128	0.196	3.53	0.055
2.94	990	3.84	0.123	0.199	3.49	0.055

APPENDIX C.IX: EXPERIMENTAL DATA FOR ISOCRATIC ELUTION OF α-LACTALBUMIN ON CERAMIC Q-HYPERD F

For the experiments where no σ_{Gauss} and τ values are given the peaks could not be fitted due to the shape of the peaks. The retention volumes are therefore determined as the volume at the peak maximum.

The peaks are fitted with the EMG function. The retention volumes and the variances are calculated as:

$V_R = V_{R,Gauss} + \tau - V_{dead}$

$\sigma^2 = \sigma^2_{Gauss} + \tau^2$

Where $V_{dead} = V_{empty10,\ incl.\ filters} + V_{ID,\ pos.1}$ = 0.237 ml + 0.31 ml = 0.547 ml

Column position: 1
Load: 100 µl

Q [ml/min]	c_s [mM]	$V_{R,Gauss}$ [ml]	pH 6 σ_{Gauss} [ml]	τ [ml]	V_R [ml]	σ^2 [ml^2]
1.01	57	37.94	----	----	37.4	----
2.94	57	30.77	5.43	9.11	39.3	112
5.93	57	28.25	7.31	8.33	36.0	123
1.01	77	14.95	2.27	5.37	19.8	34.0
2.94	77	13.47	2.96	4.39	17.3	28.0
5.93	77	11.40	3.23	5.43	16.3	39.9
1.01	87	10.56	1.16	6.33	16.3	41.4
2.94	87	8.71	1.52	6.19	14.4	40.7
5.93	87	7.24	1.35	6.55	13.2	44.7
1.01	111	6.89	0.730	3.03	9.37	9.7
2.94	111	5.81	0.680	3.50	8.76	12.7
5.93	111	5.17	0.497	3.66	8.28	13.7
1.01	136	5.56	0.462	2.15	7.17	4.83
2.94	136	4.91	0.383	2.26	6.62	5.23
5.93	136	4.61	0.290	2.09	6.16	4.46
1.01	185	4.63	0.226	1.17	5.26	1.43
2.94	185	4.30	0.208	1.10	4.85	1.25
5.93	185	4.25	0.182	0.974	4.68	0.982
1.01	233	4.44	0.212	0.928	4.82	0.907
2.94	233	4.20	0.190	0.865	4.52	0.785
5.93	233	4.16	0.165	0.776	4.39	0.629
1.01	330	4.17	0.168	0.711	4.33	0.533
2.94	330	3.99	0.151	0.611	4.06	0.396
5.93	330	3.97	0.142	0.533	3.96	0.305
1.01	524	4.01	0.138	0.531	4.00	0.301
2.94	524	3.93	0.135	0.449	3.83	0.220
5.93	524	3.95	0.132	0.405	3.81	0.181
1.01	1011	3.96	0.132	0.399	3.81	0.177
2.94	1011	3.92	0.131	0.360	3.73	0.147
5.93	1011	3.98	0.130	0.336	3.77	0.130

Q [ml/min]	c_s [mM]	$V_{R,Gauss}$ [ml]	pH 7 σ_{Gauss} [ml]	τ [ml]	V_R [ml]	σ^2 [ml^2]
2.94	102	40.67	6.38	10.08	50.2	142
5.93	102	39.24	8.23	9.55	48.2	159
2.94	102	41.67	6.81	8.53	49.7	119
2.94	127	18.97	4.55	3.95	22.4	36.3
5.93	127	16.73	5.19	6.06	22.2	63.7
2.94	127	19.38	4.84	3.42	22.3	35.1
2.94	147	10.39	2.69	3.69	13.5	20.9
5.93	147	8.83	2.55	5.59	13.9	37.8
2.94	147	10.50	2.72	3.42	13.4	19.0
2.94	176	6.20	0.918	2.50	8.15	7.10
5.93	176	5.50	0.733	3.45	8.40	12.4
2.94	176	6.17	0.918	2.52	8.14	7.17
2.94	225	4.69	0.360	1.15	5.29	1.45
5.93	225	4.42	0.290	1.37	5.23	1.95
2.94	225	4.68	0.354	1.15	5.28	1.45
2.94	322	4.08	0.198	0.580	4.12	0.376
5.93	322	4.00	0.167	0.596	4.05	0.383
2.94	322	4.05	0.198	0.583	4.09	0.379
2.94	517	3.92	0.147	0.355	3.73	0.148
5.93	517	3.92	0.140	0.352	3.72	0.143
2.94	517	3.90	0.147	0.355	3.71	0.148
2.94	1005	3.84	0.136	0.286	3.58	0.100
5.93	1005	3.91	0.136	0.284	3.65	0.099
2.94	1005	3.86	0.136	0.287	3.60	0.101

Q [ml/min]	c_s [mM]	$V_{R,Gauss}$ [ml]	pH 8 σ_{Gauss} [ml]	τ [ml]	V_R [ml]	σ^2 [ml^2]
1.01	120	58.27	6.81	6.69	64.4	91.1
2.94	120	68.51	12.27	0.092	68.1	150
5.93	120	55.89	9.92	21.15	76.5	546
1.01	147	25.03	3.87	2.59	27.1	21.7
2.94	147	23.57	5.32	5.41	28.4	57.6
5.93	147	20.81	5.71	8.36	28.6	103
1.01	168	13.11	2.01	2.55	15.1	10.5
2.94	168	11.73	2.39	4.44	15.6	25.4
5.93	168	10.77	2.74	6.13	16.4	45.1
1.01	193	8.38	0.850	1.70	9.53	3.61
2.94	193	7.54	1.04	2.75	9.74	8.64
5.93	193	6.75	1.09	3.86	10.1	16.1
1.01	218	6.60	0.593	0.898	6.95	1.16
2.94	218	6.06	0.715	1.67	7.18	3.29
5.93	218	5.45	0.668	2.42	7.33	6.32
1.01	266	5.17	0.397	0.632	5.26	0.557
2.94	266	4.72	0.416	1.06	5.23	1.30
5.93	266	4.44	0.325	1.37	5.26	1.99
1.01	315	4.57	0.291	0.503	4.53	0.338
2.94	315	4.27	0.267	0.779	4.51	0.678
5.93	315	4.12	0.212	0.883	4.46	0.825
1.01	510	4.03	0.165	0.321	3.80	0.130
2.94	510	3.93	0.153	0.390	3.78	0.176
5.93	510	3.94	0.144	0.398	3.79	0.179
1.01	997	3.93	0.138	0.266	3.65	0.090
2.94	997	3.88	0.132	0.299	3.63	0.107
5.93	997	3.92	0.131	0.305	3.68	0.110

Q [ml/min]	c_s [mM]	$V_{R,Gauss}$ [ml]	pH 9 σ_{Gauss} [ml]	τ [ml]	V_R [ml]	σ^2 [ml^2]
1.01	160	37.62	4.41	4.93	42.0	43.7
2.94	160	36.58	6.90	8.71	44.7	124
5.93	160	34.40	8.31	12.38	46.2	222
1.01	184	19.88	2.28	2.50	21.8	11.5
2.94	184	19.46	3.64	4.67	23.6	35.1
5.93	184	17.81	4.18	7.67	24.9	76.3
1.01	208	12.72	1.56	1.66	13.8	5.19
2.94	208	11.89	2.27	3.02	14.4	14.3
5.93	208	10.62	2.54	5.05	15.1	31.9
1.01	257	6.59	0.698	1.05	7.09	1.58
2.94	257	5.84	0.800	1.83	7.12	4.00
5.93	257	5.33	0.704	2.65	7.43	7.50
1.01	305	5.14	0.417	0.727	5.32	0.703
2.94	305	4.67	0.414	1.21	5.33	1.63
5.93	305	4.42	0.317	1.52	5.39	2.41
1.01	404	4.25	0.219	0.430	4.13	0.233
2.94	404	4.04	0.182	0.582	4.08	0.372
5.93	404	4.05	0.157	0.582	4.09	0.364
1.01	501	4.08	0.174	0.343	3.87	0.148
2.94	501	3.95	0.157	0.425	3.82	0.205
5.93	501	3.96	0.146	0.423	3.84	0.200
1.01	990	3.93	0.137	0.272	3.66	0.093
2.94	990	3.86	0.133	0.301	3.62	0.109
5.93	990	3.91	0.133	0.298	3.66	0.107

APPENDIX C.X: EXPERIMENTAL DATA FOR ISOCRATIC ELUTION OF β-LACTOGLOBULIN A ON CERAMIC Q-HYPERD F

For the experiments where no σ_{Gauss} and τ values are given the peaks could not be fitted due to the shape of the peaks. The retention volumes are therefore determined as the volume at the peak maximum.

The peaks are fitted with the EMG function. The retention volumes and the variances are calculated as:

$V_R = V_{R,Gauss} + \tau - V_{dead}$

$\sigma^2 = \sigma^2_{Gauss} + \tau^2$

Where $V_{dead} = V_{empty10,\ incl.\ filters} + V_{ID,\ pos.1}$ = 0.237 ml + 0.31 ml = 0.547 ml

Column position: 1
Load: 100 µl

pH 6

Q [ml/min]	c_s [mM]	$V_{R,Gauss}$ [ml]	σ_{Gauss} [ml]	τ [ml]	V_R [ml]	σ^2 [ml^2]
1.01	120	83.59	----	----	83.0	----
2.94	155	5.90	0.865	10.78	16.1	117
5.93	155	5.39	0.896	9.03	13.9	82.4
2.94	155	5.80	0.909	13.45	18.7	182
2.94	184	4.72	0.363	4.17	8.34	17.6
5.93	184	4.58	0.318	3.15	7.18	10.0
2.94	184	4.68	0.379	4.15	8.28	17.3
2.94	232	4.16	0.164	1.10	4.71	1.24
5.93	232	4.20	0.163	0.861	4.52	0.767
2.94	232	4.17	0.166	1.08	4.70	1.19
2.94	280	3.97	0.131	0.518	3.94	0.285
5.93	280	4.10	0.137	0.445	4.00	0.216
2.94	280	4.00	0.132	0.511	3.96	0.279
2.94	330	3.88	0.126	0.354	3.68	0.141
5.93	330	3.88	0.132	0.329	3.67	0.126
2.94	330	3.91	0.126	0.356	3.72	0.142
2.94	379	3.86	0.124	0.312	3.62	0.112
5.93	379	3.88	0.130	0.294	3.62	0.104
2.94	379	3.89	0.123	0.312	3.65	0.112
2.94	524	3.89	0.124	0.288	3.63	0.099
5.93	524	3.99	0.130	0.270	3.72	0.090
2.94	524	3.88	0.125	0.289	3.63	0.099
2.94	1010	3.88	0.126	0.260	3.60	0.084
5.93	1010	3.96	0.131	0.249	3.66	0.079
2.94	1010	3.86	0.127	0.261	3.57	0.084

Q [ml/min]	c_s [mM]	$V_{R,Gauss}$ [ml]	pH 7 σ_{Gauss} [ml]	τ [ml]	V_R [ml]	σ^2 [ml^2]
2.94	185	34.46	----	----	33.9	----
5.93	185	29.77	----	----	29.2	----
2.94	185	34.46	----	----	33.9	----
2.94	225	6.45	1.45	5.77	11.7	35.4
5.93	225	5.67	0.973	6.62	11.7	44.8
2.94	225	6.70	1.64	5.60	11.7	34.1
2.94	249	5.12	0.660	3.31	7.88	11.4
5.93	249	4.67	0.420	3.11	7.24	9.87
2.94	249	5.03	0.625	3.22	7.70	10.8
2.94	273	4.44	0.294	1.85	5.74	3.50
5.93	273	4.35	0.221	1.50	5.30	2.30
2.94	273	4.43	0.282	1.82	5.71	3.39
2.94	322	4.05	0.150	0.776	4.28	0.625
5.93	322	4.07	0.148	0.614	4.14	0.398
2.94	322	4.04	0.150	0.762	4.25	0.602
2.94	371	3.92	0.131	0.455	3.83	0.224
5.93	371	3.98	0.132	0.390	3.82	0.169
2.94	371	3.95	0.131	0.455	3.86	0.224
2.94	516	3.87	0.127	0.320	3.64	0.118
5.93	516	3.90	0.133	0.292	3.65	0.103
2.94	516	3.89	0.126	0.323	3.67	0.120
2.94	1001	3.86	0.128	0.268	3.59	0.088
5.93	1001	3.92	0.134	0.250	3.62	0.080
2.94	1001	3.83	0.128	0.267	3.55	0.088

pH 8

Q [ml/min]	c_s [mM]	$V_{R,Gauss}$ [ml]	σ_{Gauss} [ml]	τ [ml]	V_R [ml]	σ^2 [ml^2]
1.01	191	69.01	----	----	68.5	----
2.94	191	67.62	----	----	67.1	----
1.01	240	15.09	----	----	14.5	----
1.01	289	5.68	0.788	1.67	6.81	3.42
2.94	289	4.94	0.603	2.46	6.85	6.41
1.01	362	4.20	0.220	0.761	4.41	0.628
2.94	362	4.04	0.160	0.747	4.24	0.583
1.01	411	4.01	0.156	0.537	4.00	0.313
2.94	411	3.92	0.136	0.492	3.87	0.261
2.94	264	6.59	1.42	3.54	9.58	14.5
5.93	264	5.75	1.12	4.57	9.77	22.1
2.94	264	6.63	1.40	3.40	9.49	13.6
2.94	313	4.46	0.362	1.58	5.49	2.63
5.93	313	4.23	0.252	1.57	5.25	2.53
2.94	313	4.42	0.357	1.59	5.46	2.66
2.94	508	3.85	0.134	0.335	3.64	0.130
5.93	508	3.86	0.134	0.310	3.62	0.114
2.94	508	3.87	0.133	0.337	3.66	0.131
2.94	996	3.81	0.128	0.258	3.53	0.083
5.93	996	3.90	0.130	0.253	3.60	0.081
2.94	996	3.83	0.127	0.259	3.54	0.083

pH 9

Q [ml/min]	c_s [mM]	$V_{R,Gauss}$ [ml]	σ_{Gauss} [ml]	τ [ml]	V_R [ml]	σ^2 [ml^2]
1.01	208	87.90	----	----	87.4	----
1.01	232	38.73	----	----	38.2	----
2.94	232	37.73	----	----	37.2	----
1.01	256	17.10	----	----	16.6	----
1.01	305	5.87	0.784	1.42	6.74	2.64
2.94	305	5.17	0.709	2.16	6.79	5.17
1.01	354	4.51	0.346	0.798	4.76	0.756
2.94	354	4.18	0.239	1.06	4.69	1.17
1.01	403	4.14	0.204	0.527	4.12	0.320
2.94	403	3.95	0.158	0.576	3.98	0.357
1.01	501	3.97	0.143	0.345	3.77	0.140
2.94	501	3.91	0.134	0.349	3.71	0.140
1.01	574	3.90	0.134	0.299	3.65	0.108
2.94	574	3.86	0.130	0.305	3.62	0.110
1.01	745	3.87	0.124	0.265	3.59	0.086
2.94	745	3.82	0.126	0.260	3.53	0.084
1.01	989	3.89	0.123	0.258	3.60	0.082
2.94	989	3.88	0.125	0.259	3.59	0.083

APPENDIX C.XI: EXPERIMENTAL DATA FOR ISOCRATIC ELUTION OF β-LACTOGLOBULIN B ON CERAMIC Q-HYPERD F

For the experiments where no σ_{Gauss} and τ values are given the peaks could not be fitted due to the shape of the peaks. The retention volumes are therefore determined as the volume at the peak maximum.

The peaks are fitted with the EMG function. The retention volumes and the variances are calculated as:

$V_R = V_{R,Gauss} + \tau - V_{dead}$

$\sigma^2 = \sigma^2_{Gauss} + \tau^2$

Where $V_{dead} = V_{empty10,\ incl.\ filters} + V_{ID,\ pos.1}$ = 0.237 ml + 0.31 ml = 0.547 ml

Column position: 1
Load: 100 µl

Q [ml/min]	c_s [mM]	$V_{R,Gauss}$ [ml]	pH 6 σ_{Gauss} [ml]	τ [ml]	V_R [ml]	σ^2 [ml^2]
1.01	120	34.13	----	----	33.6	----
2.94	155	5.90	0.865	10.8	16.1	117
5.93	155	5.39	0.896	9.03	13.9	82.4
2.94	155	5.80	0.909	13.5	18.7	182
2.94	184	4.72	0.363	4.17	8.34	17.6
5.93	184	4.58	0.318	3.15	7.18	10.0
2.94	184	4.68	0.379	4.15	8.28	17.3
2.94	232	4.16	0.164	1.10	4.71	1.24
5.93	232	4.20	0.163	0.861	4.52	0.767
2.94	232	4.17	0.166	1.08	4.70	1.19
2.94	280	3.97	0.131	0.518	3.94	0.285
5.93	280	4.10	0.137	0.445	4.00	0.216
2.94	280	4.00	0.132	0.511	3.96	0.279
2.94	330	3.88	0.126	0.354	3.68	0.141
5.93	330	3.88	0.132	0.329	3.67	0.126
2.94	330	3.91	0.126	0.356	3.72	0.142
2.94	379	3.86	0.124	0.312	3.62	0.112
5.93	379	3.88	0.130	0.294	3.62	0.104
2.94	379	3.89	0.123	0.312	3.65	0.112
2.94	524	3.89	0.124	0.288	3.63	0.099
5.93	524	3.99	0.130	0.270	3.72	0.090
2.94	524	3.88	0.125	0.289	3.63	0.099
2.94	1010	3.88	0.126	0.260	3.60	0.084
5.93	1010	3.96	0.131	0.249	3.66	0.079
2.94	1010	3.86	0.127	0.261	3.57	0.084

Q [ml/min]	c_s [mM]	$V_{R,Gauss}$ [ml]	pH 7 σ_{Gauss} [ml]	τ [ml]	V_R [ml]	σ^2 [ml^2]
1.01	154	55.91	----	----	55.4	----
2.94	154	51.36	----	----	50.8	----
2.94	185	18.60	----	----	18.1	----
5.93	185	18.45	----	----	17.9	----
2.94	185	18.22	----	----	17.7	----
2.94	225	6.45	1.45	5.77	11.7	35.4
5.93	225	5.67	0.973	6.62	11.7	44.8
2.94	225	6.70	1.64	5.60	11.7	34.1
2.94	249	5.12	0.660	3.31	7.88	11.4
5.93	249	4.67	0.420	3.11	7.24	9.87
2.94	249	5.03	0.625	3.22	7.70	10.8
2.94	273	4.44	0.294	1.85	5.74	3.50
5.93	273	4.35	0.221	1.50	5.30	2.30
2.94	273	4.43	0.282	1.82	5.71	3.39
2.94	322	4.05	0.150	0.776	4.28	0.625
5.93	322	4.07	0.148	0.614	4.14	0.398
2.94	322	4.04	0.150	0.762	4.25	0.602
2.94	371	3.92	0.131	0.455	3.83	0.224
5.93	371	3.98	0.132	0.390	3.82	0.169
2.94	371	3.95	0.131	0.455	3.86	0.224
2.94	516	3.87	0.127	0.320	3.64	0.118
5.93	516	3.90	0.133	0.292	3.65	0.103
2.94	516	3.89	0.126	0.323	3.67	0.120
2.94	1001	3.86	0.128	0.268	3.59	0.088
5.93	1001	3.92	0.134	0.250	3.62	0.080
2.94	1001	3.83	0.128	0.267	3.55	0.088

pH 8

Q [ml/min]	c_s [mM]	$V_{R,Gauss}$ [ml]	σ_{Gauss} [ml]	τ [ml]	V_R [ml]	σ^2 [ml^2]
1.01	191	34.51	----	----	34.0	----
2.94	191	33.58	----	----	33.0	----
1.01	240	10.44	----	----	9.89	----
2.94	240	11.04	----	----	10.5	----
1.01	289	5.68	0.788	1.67	6.81	3.42
2.94	289	4.94	0.603	2.46	6.85	6.41
1.01	362	4.20	0.220	0.761	4.41	0.628
2.94	362	4.04	0.160	0.747	4.24	0.583
1.01	411	4.01	0.156	0.537	4.00	0.313
2.94	411	3.92	0.136	0.492	3.87	0.261
2.94	264	6.59	1.42	3.54	9.58	14.5
5.93	264	5.75	1.12	4.57	9.77	22.1
2.94	264	6.63	1.40	3.40	9.49	13.6
2.94	313	4.46	0.362	1.58	5.49	2.63
5.93	313	4.23	0.252	1.57	5.25	2.53
2.94	313	4.42	0.357	1.59	5.46	2.66
2.94	508	3.85	0.134	0.335	3.64	0.130
5.93	508	3.86	0.134	0.310	3.62	0.114
2.94	508	3.87	0.133	0.337	3.66	0.131
2.94	996	3.81	0.128	0.258	3.53	0.083
5.93	996	3.90	0.130	0.253	3.60	0.081
2.94	996	3.83	0.127	0.259	3.54	0.083

pH 9

Q [ml/min]	c_s [mM]	$V_{R,Gauss}$ [ml]	σ_{Gauss} [ml]	τ [ml]	V_R [ml]	σ^2 [ml^2]
1.01	183	95.96	----	----	95.4	----
1.01	208	37.96	----	----	37.4	----
1.01	208	35.51	5.82	3.34	38.3	45.0
2.94	208	32.29	6.61	5.67	37.4	75.9
1.01	232	20.14	----	----	19.6	----
2.94	232	19.27	----	----	18.7	----
1.01	256	11.30	----	----	10.7	----
2.94	256	11.01	----	----	10.5	----
1.01	305	5.87	0.784	1.42	6.74	2.64
2.94	305	5.17	0.709	2.16	6.79	5.17
1.01	354	4.51	0.346	0.798	4.76	0.756
2.94	354	4.18	0.239	1.06	4.69	1.17
1.01	403	4.14	0.204	0.527	4.12	0.320
2.94	403	3.95	0.158	0.576	3.98	0.357
1.01	501	3.97	0.143	0.345	3.77	0.140
2.94	501	3.91	0.134	0.349	3.71	0.140
1.01	574	3.90	0.134	0.299	3.65	0.108
2.94	574	3.86	0.130	0.305	3.62	0.110
1.01	745	3.87	0.124	0.265	3.59	0.086
2.94	745	3.82	0.126	0.260	3.53	0.084
1.01	989	3.89	0.123	0.258	3.60	0.082
2.94	989	3.88	0.125	0.259	3.59	0.083

APPENDIX C.XII: EXPERIMENTAL DATA FOR ISOCRATIC ELUTION OF BSA ON FRACTOGEL EMD TMAE 650(S)

For the experiments where no σ_{Gauss} and τ values are given the peaks could not be fitted due to the shape of the peaks. The retention volumes are therefore determined as the volume at the peak maximum.

The peaks are fitted with the EMG function. The retention volumes and the variances are calculated as:

$V_R = V_{R,Gauss} + \tau - V_{dead}$

$\sigma^2 = \sigma^2_{Gauss} + \tau^2$

Where $V_{dead} = V_{empty10,\ incl.\ filters} + V_{ID,\ pos.1}$ = 0.237 ml + 0.31 ml = 0.690 ml

Column position: 2
Load: 100 µl

pH 6

Q [ml/min]	c_s [mM]	$V_{R,Gauss}$ [ml]	σ_{gauss} [ml]	τ [ml]	V_R [ml]	σ^2 [ml^2]
2.94	71	15.80	3.07	7.25	22.4	61.9
5.93	71	15.35	4.06	7.15	21.8	67.7
2.94	71	16.19	3.30	6.24	21.7	49.9
2.94	76	12.80	2.62	5.45	17.6	36.5
5.93	76	12.29	2.99	6.61	18.2	52.6
2.94	76	12.89	2.46	5.27	17.5	33.9
2.94	87	9.49	2.03	2.84	11.6	12.2
5.93	87	9.35	2.30	2.73	11.4	12.8
2.94	87	9.27	1.79	2.32	10.9	8.59
2.94	98	5.53	1.06	1.21	6.05	2.59
5.93	98	5.17	1.18	1.70	6.18	4.27
2.94	98	5.50	1.04	1.24	6.05	2.64
2.94	108	4.62	0.770	1.21	5.14	2.04
5.93	108	4.37	0.865	1.60	5.28	3.30
2.94	108	4.59	0.753	1.22	5.11	2.05
2.94	111	5.06	1.00	0.937	5.30	1.88
5.93	111	4.75	1.15	1.31	5.37	3.04
2.94	111	4.94	0.962	0.973	5.23	1.87
2.94	120	4.27	0.660	1.16	4.74	1.77
5.93	120	4.11	0.762	1.52	4.94	2.89
2.94	120	4.30	0.646	1.16	4.77	1.77
2.94	126	4.25	0.681	0.810	4.37	1.12
5.93	126	4.07	0.824	1.11	4.49	1.92
2.94	126	4.21	0.664	0.836	4.35	1.14
2.94	139	3.69	0.481	0.775	3.77	0.832
5.93	139	3.55	0.561	1.03	3.89	1.38
2.94	139	3.67	0.469	0.776	3.76	0.822
2.94	157	3.33	0.416	0.556	3.20	0.483
5.93	157	3.30	0.489	0.770	3.38	0.832
2.94	157	3.33	0.408	0.566	3.21	0.487
2.94	185	3.24	0.457	0.291	2.84	0.294
5.93	185	3.11	0.551	0.471	2.89	0.526
2.94	185	3.20	0.446	0.309	2.82	0.294

pH 6

Q [ml/min]	c_s [mM]	$V_{R,Gauss}$ [ml]	σ_{gauss} [ml]	τ [ml]	V_R [ml]	σ^2 [ml^2]
2.94	196	3.05	0.381	0.311	2.67	0.242
5.93	196	2.98	0.435	0.507	2.80	0.446
2.94	196	3.02	0.374	0.319	2.64	0.242
2.94	215	2.98	0.373	0.285	2.57	0.221
5.93	215	2.90	0.423	0.482	2.69	0.411
2.94	215	2.96	0.366	0.295	2.57	0.221
2.94	236	2.85	0.350	0.261	2.42	0.191
5.93	236	2.76	0.393	0.448	2.52	0.355
2.94	236	2.86	0.343	0.267	2.43	0.189
2.94	333	2.73	0.323	0.241	2.28	0.162
5.93	333	2.61	0.356	0.416	2.34	0.300
2.94	333	2.70	0.316	0.248	2.25	0.161
2.94	527	2.63	0.307	0.241	2.18	0.152
5.93	527	2.63	0.337	0.408	2.34	0.280
2.94	527	2.65	0.301	0.247	2.20	0.151
2.94	1010	2.63	0.318	0.229	2.17	0.153
5.93	1010	2.53	0.339	0.409	2.25	0.282
2.94	1010	2.64	0.311	0.237	2.19	0.153

pH 7

Q [ml/min]	c_s [mM]	$V_{R,Gauss}$ [ml]	σ_{gauss} [ml]	τ [ml]	V_R [ml]	σ^2 [ml^2]
2.94	88	81.04	5.80	12.63	93.0	193
5.93	88	76.90	7.00	13.02	89.2	218
2.94	88	83.66	6.64	3.59	86.6	57.0
2.94	112	11.28	3.07	5.59	16.2	40.6
5.93	112	10.55	3.50	6.23	16.1	51.0
2.94	112	10.81	2.71	5.49	15.6	37.5
2.94	131	6.73	1.54	2.12	8.17	6.88
5.93	131	6.35	1.86	2.42	8.08	9.33
2.94	131	6.61	1.50	2.23	8.15	7.21
2.94	151	5.09	1.13	0.851	5.25	1.99
5.93	151	4.66	1.24	1.32	5.30	3.29
2.94	151	4.92	1.05	0.962	5.19	2.03
2.94	180	3.70	0.640	0.742	3.75	0.960
5.93	180	3.52	0.763	0.976	3.81	1.54
2.94	180	3.63	0.600	0.770	3.71	0.953
2.94	209	3.34	0.537	0.442	3.09	0.484
5.93	209	3.24	0.644	0.648	3.20	0.835
2.94	209	3.31	0.507	0.471	3.09	0.479
2.94	229	3.19	0.449	0.326	2.83	0.307
5.93	229	3.01	0.537	0.529	2.85	0.568
2.94	229	3.15	0.441	0.343	2.80	0.312
2.94	325	2.99	0.465	0.044	2.34	0.218
5.93	325	2.74	0.487	0.360	2.41	0.367
2.94	325	2.94	0.443	0.073	2.33	0.202
2.94	521	2.88	0.439	0.017	2.21	0.193
5.93	521	2.57	0.464	0.339	2.21	0.330
2.94	521	2.88	0.432	0.004	2.19	0.187
2.94	1007	2.84	0.441	0.018	2.17	0.195
5.93	1007	2.60	0.468	0.333	2.24	0.331
2.94	1007	2.85	0.442	0.005	2.17	0.196

pH 8

Q [ml/min]	c_s [mM]	$V_{R,Gauss}$ [ml]	σ_{gauss} [ml]	τ [ml]	V_R [ml]	σ^2 [ml^2]
2.94	140	33.85	7.06	4.74	37.9	72
5.93	140	31.73	9.87	8.25	39.3	165
2.94	140	33.91	6.99	4.83	38.1	72.2
2.94	162	11.52	3.15	3.04	13.9	19.1
5.93	162	10.72	3.87	3.44	13.5	26.8
2.94	162	11.19	3.08	2.77	13.3	17.1
2.94	172	9.11	2.67	1.54	9.96	9.47
5.93	172	8.29	2.94	2.31	9.91	14.0
2.94	172	8.74	2.39	1.71	9.76	8.65
2.94	198	5.87	1.27	0.010	5.19	1.62
5.93	198	4.77	1.27	1.01	5.09	2.64
2.94	198	5.62	1.19	0.019	4.95	1.41
2.94	218	4.05	0.733	0.682	4.04	1.00
5.93	218	3.76	0.802	1.07	4.14	1.79
2.94	218	4.00	0.690	0.689	4.00	0.951
2.94	236	3.58	0.558	0.592	3.48	0.662
5.93	236	3.40	0.678	0.795	3.51	1.09
2.94	236	3.53	0.535	0.596	3.43	0.641
2.94	256	3.37	0.514	0.403	3.09	0.427
5.93	256	3.21	0.615	0.611	3.13	0.752
2.94	256	3.33	0.493	0.425	3.07	0.424
2.94	316	3.24	0.484	0.004	2.55	0.234
5.93	316	2.93	0.529	0.376	2.61	0.421
2.94	316	3.08	0.459	0.143	2.53	0.232
2.94	511	2.93	0.443	0.016	2.26	0.197
5.93	511	2.67	0.474	0.332	2.32	0.335
2.94	511	2.91	0.438	0.004	2.23	0.192
2.94	996	2.92	0.450	0.003	2.24	0.203
5.93	996	2.67	0.483	0.326	2.30	0.339
2.94	996	2.86	0.444	0.004	2.17	0.197

			pH 9			
Q	c_s	$V_{R,Gauss}$	σ_{gauss}	τ	V_R	σ^2
[ml/min]	[mM]	[ml]	[ml]	[ml]	[ml]	[ml^2]
2.94	172	30.28	6.32	6.38	36.0	80.6
5.93	172	31.02	7.88	2.24	32.6	67.1
2.94	172	30.44	6.56	2.51	32.3	49.4
2.94	187	14.31	3.11	1.92	15.5	13.4
5.93	187	14.34	4.17	1.54	15.2	19.8
2.94	187	14.23	3.15	1.42	15.0	11.9
2.94	211	7.65	1.71	0.067	7.03	2.91
5.93	211	6.67	1.97	0.970	6.95	4.84
2.94	211	7.56	1.64	0.025	6.89	2.70
2.94	259	3.68	0.609	0.609	3.60	0.742
5.93	259	3.43	0.698	0.903	3.64	1.30
2.94	259	3.62	0.591	0.644	3.58	0.763
2.94	308	3.18	0.479	0.225	2.71	0.280
5.93	308	2.96	0.557	0.445	2.71	0.509
2.94	308	3.11	0.461	0.259	2.68	0.279
2.94	356	3.11	0.478	0.022	2.44	0.229
5.93	356	2.77	0.520	0.351	2.43	0.394
2.94	356	3.08	0.472	0.007	2.40	0.223
2.94	503	2.90	0.446	0.019	2.23	0.200
5.93	503	2.64	0.476	0.323	2.27	0.331
2.94	503	2.92	0.443	0.004	2.24	0.196
2.94	990	2.83	0.449	0.017	2.15	0.202
5.93	990	2.56	0.476	0.323	2.19	0.331
2.94	990	2.90	0.446	0.004	2.21	0.199

APPENDIX C.XIII: EXPERIMENTAL DATA FOR ISOCRATIC ELUTION OF α-LACTALBUMIN ON FRACTOGEL EMD TMAE 650(S)

For the experiments where no σ_{Gauss} and τ values are given the peaks could not be fitted due to the shape of the peaks. The retention volumes are therefore determined as the volume at the peak maximum.

The peaks are fitted with the EMG function. The retention volumes and the variances are calculated as:

$V_R = V_{R,Gauss} + \tau - V_{dead}$

$\sigma^2 = \sigma^2_{Gauss} + \tau^2$

Where $V_{dead} = V_{empty10,\ incl.\ filters} + V_{ID,\ pos.1}$ = 0.237 ml + 0.31 ml = 0.690 ml

Column position: 2
Load: 100 µl

Q [ml/min]	c_s [mM]	$V_{R,Gauss}$ [ml]	pH 6 σ_{Gauss} [ml]	τ [ml]	V_R [ml]	σ^2 [ml^2]
5.93	38	19.00	----	----	18.3	----
1.01	43	19.17	----	----	18.5	----
2.94	43	17.69	----	----	17.0	----
5.93	43	16.18	3.34	0.024	15.5	11.2
1.01	48	12.80	----	----	12.1	----
2.94	48	12.33	----	----	11.6	----
5.93	48	12.32	----	----	11.6	----
1.01	57	8.96	----	----	8.27	----
2.94	57	8.80	----	----	8.11	----
5.93	57	8.73	----	----	8.04	----
1.01	77	6.08	----	----	5.39	----
2.94	77	6.03	----	----	5.34	----
5.93	77	6.01	----	----	5.32	----
1.01	87	4.77	0.346	0.657	4.74	0.551
2.94	87	4.51	0.682	0.949	4.77	1.37
5.93	87	4.65	0.517	0.835	4.79	0.963
1.01	111	4.17	0.306	0.269	3.75	0.166
2.94	111	4.05	0.420	0.373	3.73	0.315
5.93	111	4.02	0.554	0.485	3.82	0.542
1.01	136	3.86	0.275	0.181	3.35	0.109
2.94	136	3.79	0.375	0.255	3.35	0.206
5.93	136	3.79	0.492	0.347	3.45	0.363
1.01	185	3.50	0.261	0.122	2.93	0.083
2.94	185	3.44	0.349	0.170	2.92	0.150
5.93	185	3.44	0.452	0.242	2.99	0.263
1.01	233	3.41	0.264	0.084	2.81	0.077
2.94	233	3.37	0.337	0.140	2.82	0.133
5.93	233	3.38	0.424	0.218	2.91	0.227
1.01	330	3.30	0.263	0.068	2.68	0.074
2.94	330	3.22	0.326	0.133	2.66	0.124
5.93	330	3.20	0.408	0.204	2.71	0.208
1.01	524	3.21	0.257	0.071	2.60	0.071
2.94	524	3.17	0.318	0.127	2.61	0.117
5.93	524	3.19	0.398	0.192	2.69	0.195
1.01	1011	3.27	0.283	0.002	2.59	0.080
2.94	1011	3.15	0.339	0.091	2.55	0.123
5.93	1011	3.16	0.437	0.134	2.60	0.209

Q [ml/min]	c_s [mM]	$V_{R,Gauss}$ [ml]	pH 7 σ_{Gauss} [ml]	τ [ml]	V_R [ml]	σ^2 [ml^2]
2.94	53	57.96	7.99	0.068	57.3	63.9
5.93	53	56.53	9.32	0.078	55.9	86.8
2.94	53	57.38	7.95	0.056	56.7	63.3
2.94	68	34.09	10.40	0.074	33.5	108
5.93	68	30.96	10.27	0.070	30.3	106
2.94	68	32.98	10.33	0.561	32.9	107
2.94	79	23.00	----	----	22.3	----
5.93	79	21.75	----	----	21.1	----
2.94	79	22.80	----	----	22.1	----
2.94	102	6.78	0.724	1.08	7.18	1.70
5.93	102	6.59	0.974	1.33	7.22	2.71
2.94	102	6.74	0.724	1.10	7.15	1.73
2.94	127	5.30	0.533	0.322	4.93	0.387
5.93	127	5.10	0.693	0.498	4.91	0.728
2.94	127	5.24	0.531	0.322	4.87	0.386
2.94	147	4.64	0.492	0.186	4.14	0.277
5.93	147	4.49	0.625	0.307	4.10	0.485
2.94	147	4.58	0.488	0.195	4.09	0.276
2.94	176	4.00	0.420	0.180	3.49	0.209
5.93	176	3.98	0.541	0.253	3.54	0.357
2.94	176	3.95	0.417	0.185	3.45	0.208
2.94	225	3.51	0.343	0.192	3.01	0.155
5.93	225	3.48	0.440	0.261	3.05	0.262
2.94	225	3.51	0.345	0.185	3.01	0.153
2.94	322	3.24	0.315	0.151	2.70	0.122
5.93	322	3.41	0.447	0.003	2.73	0.200
2.94	322	3.23	0.313	0.154	2.70	0.122
2.94	517	3.09	0.298	0.148	2.55	0.111
5.93	517	3.02	0.369	0.223	2.56	0.186
2.94	517	3.07	0.295	0.153	2.53	0.110
2.94	1005	3.08	0.297	0.145	2.54	0.109
5.93	1005	3.04	0.368	0.219	2.57	0.183
2.94	1005	3.06	0.296	0.149	2.52	0.110
2.94	1005	3.16	0.345	0.005	2.47	0.119

pH 8

Q [ml/min]	c_s [mM]	$V_{R,Gauss}$ [ml]	σ_{Gauss} [ml]	τ [ml]	V_R [ml]	σ^2 [ml^2]
1.01	94	14.59	0.953	1.03	14.9	1.98
2.94	94	14.09	1.42	1.50	14.9	4.28
5.93	94	13.86	1.97	1.99	15.2	7.82
1.01	120	8.21	0.596	0.430	7.95	0.540
2.94	120	8.01	0.912	0.502	7.82	1.09
5.93	120	8.05	1.25	0.516	7.88	1.83
1.01	147	5.63	0.425	0.330	5.27	0.289
2.94	147	5.55	0.626	0.412	5.27	0.561
5.93	147	5.46	0.831	0.533	5.30	0.974
1.01	168	4.83	0.354	0.229	4.36	0.178
2.94	168	4.72	0.511	0.293	4.32	0.347
5.93	168	4.65	0.677	0.368	4.33	0.593
1.01	193	4.18	0.301	0.186	3.68	0.125
2.94	193	4.08	0.430	0.227	3.62	0.236
5.93	193	3.99	0.557	0.297	3.60	0.398
1.01	218	3.79	0.274	0.183	3.28	0.109
2.94	218	3.68	0.376	0.242	3.23	0.200
5.93	218	3.66	0.481	0.314	3.28	0.330
1.01	266	3.66	0.288	0.002	2.97	0.083
2.94	266	3.43	0.340	0.162	2.91	0.142
5.93	266	3.36	0.433	0.230	2.90	0.240
1.01	315	3.35	0.232	0.125	2.78	0.069
2.94	315	3.25	0.316	0.160	2.72	0.125
5.93	315	3.19	0.396	0.231	2.73	0.210
1.01	510	3.14	0.218	0.122	2.57	0.062
2.94	510	3.08	0.291	0.156	2.55	0.109
5.93	510	2.97	0.364	0.218	2.50	0.180
1.01	997	3.09	0.214	0.122	2.53	0.061
2.94	997	3.00	0.285	0.154	2.47	0.105
5.93	997	2.97	0.359	0.213	2.49	0.174

pH 9

Q [ml/min]	c_s [mM]	$V_{R,Gauss}$ [ml]	σ_{Gauss} [ml]	τ [ml]	V_R [ml]	σ^2 [ml^2]
1.01	81	85.73	9.02	0.068	85.1	81.4
2.94	81	80.13	10.47	0.128	79.6	110
5.93	81	78.93	12.87	0.208	78.4	166
1.01	110	18.98	1.36	1.18	19.5	3.24
2.94	110	19.02	2.16	1.14	19.5	5.97
5.93	110	20.20	3.25	0.043	19.6	10.6
1.01	135	9.34	0.814	0.316	8.97	0.762
2.94	135	9.19	1.29	0.162	8.66	1.68
5.93	135	9.07	1.70	0.252	8.63	2.96
1.01	160	6.60	0.617	0.005	5.91	0.380
2.94	160	6.14	0.818	0.347	5.80	0.789
5.93	160	6.07	1.06	0.515	5.90	1.39
1.01	184	5.13	0.434	0.207	4.65	0.231
2.94	184	4.95	0.604	0.299	4.56	0.455
5.93	184	4.92	0.806	0.381	4.61	0.794
1.01	208	4.34	0.360	0.174	3.82	0.160
2.94	208	4.27	0.516	0.236	3.82	0.322
5.93	208	4.25	0.630	0.375	3.94	0.538
1.01	257	3.72	0.281	0.153	3.18	0.102
2.94	257	3.65	0.381	0.199	3.16	0.185
5.93	257	3.54	0.502	0.265	3.11	0.322
1.01	305	3.45	0.243	0.145	2.91	0.080
2.94	305	3.40	0.334	0.186	2.90	0.146
5.93	305	3.34	0.425	0.261	2.91	0.249
1.01	404	3.27	0.246	0.118	2.70	0.074
2.94	404	3.22	0.324	0.155	2.68	0.129
5.93	404	3.22	0.422	0.212	2.74	0.223
1.01	501	3.18	0.223	0.127	2.62	0.066
2.94	501	3.11	0.299	0.164	2.59	0.116
5.93	501	3.12	0.377	0.229	2.66	0.195
1.01	990	3.11	0.223	0.120	2.54	0.064
2.94	990	3.08	0.295	0.154	2.54	0.111
5.93	990	3.11	0.377	0.212	2.63	0.187

APPENDIX C.XIV: EXPERIMENTAL DATA FOR ISOCRATIC ELUTION OF β-LACTOGLOBULIN A ON FRACTOGEL EMD TMAE 650(S)

For the experiments where no σ_{Gauss} and τ values are given the peaks could not be fitted due to the shape of the peaks. The retention volumes are therefore determined as the volume at the peak maximum.

The peaks are fitted with the EMG function. The retention volumes and the variances are calculated as:

$V_R = V_{R,Gauss} + \tau - V_{dead}$

$\sigma^2 = \sigma^2_{Gauss} + \tau^2$

Where $V_{dead} = V_{empty10,\ incl.\ filters} + V_{ID,\ pos.1} = 0.237$ ml + 0.31 ml = 0.690 ml

Column position: 2
Load: 100 µl

pH 6

Q [ml/min]	c_s [mM]	$V_{R,Gauss}$ [ml]	σ_{Gauss} [ml]	τ [ml]	V_R [ml]	σ^2 [ml^2]
2.94	96	63.26	----	----	62.6	----
5.93	96	60.35	----	----	59.7	----
2.94	96	63.28	----	----	62.6	----
2.94	116	29.05	----	----	28.4	----
5.93	116	28.04	----	----	27.4	----
2.94	116	28.72	----	----	28.0	----
2.94	136	14.88	----	----	14.2	----
2.94	136	15.01	----	----	14.3	----
1.01	154	11.40	----	----	10.7	----
1.01	184	6.34	----	----	5.65	----
2.94	232	3.37	0.398	0.413	3.09	0.329
5.93	232	3.23	0.461	0.572	3.12	0.540
2.94	232	3.37	0.407	0.397	3.08	0.323
2.94	280	3.06	0.327	0.291	2.66	0.192
5.93	280	2.98	0.382	0.442	2.73	0.342
2.94	280	3.07	0.325	0.291	2.67	0.190
2.94	330	2.94	0.297	0.267	2.52	0.159
5.93	330	2.89	0.350	0.399	2.60	0.282
2.94	330	2.94	0.294	0.270	2.52	0.160
2.94	379	2.89	0.283	0.260	2.46	0.148
5.93	379	2.88	0.333	0.383	2.57	0.258
2.94	379	2.89	0.279	0.263	2.46	0.148
2.94	524	2.74	0.288	0.263	2.31	0.152
5.93	524	2.68	0.315	0.384	2.37	0.247
2.94	524	2.75	0.266	0.264	2.32	0.140
2.94	1010	2.69	0.263	0.263	2.26	0.138
5.93	1010	2.64	0.308	0.386	2.34	0.243
2.94	1010	2.71	0.261	0.263	2.28	0.137

pH 7

Q [ml/min]	c_s [mM]	$V_{R,Gauss}$ [ml]	σ_{Gauss} [ml]	τ [ml]	V_R [ml]	σ^2 [ml^2]
2.94	147	34.68	----	----	34.0	----
2.94	147	34.10	----	----	33.4	----
2.94	159	23.39	----	----	22.7	----
2.94	159	23.59	----	----	22.9	----
1.01	179	13.04	----	----	12.4	----
1.01	179	13.08	----	----	12.4	----
2.94	225	4.66	0.955	0.491	4.46	1.15
5.93	225	4.28	0.946	0.977	4.57	1.85
2.94	225	4.74	0.957	0.522	4.57	1.19
2.94	249	3.96	0.605	0.427	3.69	0.548
2.94	249	3.95	0.601	0.426	3.69	0.542
2.94	249	3.56	0.458	0.337	3.20	0.323
5.93	273	3.32	0.511	0.539	3.17	0.551
2.94	273	3.50	0.453	0.341	3.15	0.321
2.94	322	3.14	0.351	0.278	2.72	0.201
5.93	322	3.12	0.406	0.427	2.86	0.347
2.94	322	3.16	0.348	0.282	2.75	0.201
2.94	371	2.93	0.298	0.282	2.52	0.169
5.93	371	2.85	0.353	0.417	2.57	0.298
2.94	371	2.93	0.298	0.285	2.53	0.170
2.94	516	2.81	0.277	0.270	2.39	0.150
5.93	516	2.76	0.325	0.387	2.46	0.255
2.94	516	2.78	0.274	0.270	2.36	0.148
2.94	1001	2.70	0.267	0.267	2.28	0.142
5.93	1001	2.71	0.310	0.385	2.40	0.245
2.94	1001	2.72	0.264	0.269	2.30	0.142

pH 8

Q [ml/min]	c_s [mM]	$V_{R,Gauss}$ [ml]	σ_{Gauss} [ml]	τ [ml]	V_R [ml]	σ^2 [ml^2]
1.01	142	67.02	----	----	66.3	----
2.94	142	61.36	----	----	60.7	----
1.01	166	26.16	----	----	25.5	----
2.94	166	25.20	----	----	24.5	----
1.01	191	9.50	----	----	8.81	----
2.94	191	10.10	----	----	9.41	----
1.01	240	5.63	----	----	4.94	----
2.94	240	5.49	----	----	4.80	----
2.94	264	4.21	0.637	0.118	3.64	0.420
5.93	264	3.93	0.655	0.507	3.75	0.686
2.94	264	4.30	0.646	0.088	3.70	0.426
2.94	313	3.44	0.384	0.224	2.97	0.198
5.93	313	3.33	0.438	0.388	3.03	0.342
2.94	313	3.42	0.378	0.230	2.96	0.196
2.94	508	2.88	0.268	0.250	2.44	0.134
5.93	508	2.83	0.320	0.355	2.49	0.228
2.94	508	2.84	0.266	0.249	2.40	0.133
2.94	996	2.78	0.256	0.255	2.34	0.130
5.93	996	2.69	0.301	0.360	2.36	0.220
2.94	996	2.75	0.253	0.255	2.32	0.129

pH 9

Q [ml/min]	c_s [mM]	$V_{R,Gauss}$ [ml]	σ_{Gauss} [ml]	τ [ml]	V_R [ml]	σ^2 [ml^2]
1.01	158	50.11	----	----	49.4	----
2.94	158	48.56	----	----	47.9	----
1.01	183	19.84	----	----	19.1	----
2.94	183	18.84	----	----	18.1	----
1.01	208	10.34	----	----	9.65	----
1.01	232	6.73	----	----	6.04	----
2.94	232	6.47	----	----	5.78	----
1.01	256	4.91	0.703	0.005	4.22	0.494
2.94	256	4.81	0.810	0.006	4.12	0.657
1.01	305	3.87	0.379	0.003	3.18	0.143
2.94	305	3.68	0.455	0.181	3.17	0.240
1.01	354	3.49	0.359	0.003	2.81	0.129
2.94	354	3.33	0.384	0.159	2.80	0.173
1.01	403	3.31	0.300	0.002	2.62	0.090
2.94	403	3.14	0.350	0.170	2.62	0.151
1.01	501	3.17	0.299	0.002	2.48	0.089
2.94	501	2.99	0.346	0.189	2.48	0.156
1.01	745	3.06	0.340	0.003	2.37	0.116
2.94	745	2.90	0.355	0.173	2.39	0.156
1.01	989	3.03	0.355	0.002	2.35	0.126
2.94	989	2.91	0.352	0.186	2.40	0.159

APPENDIX C.XV: EXPERIMENTAL DATA FOR ISOCRATIC ELUTION OF β-LACTOGLOBULIN B ON FRACTOGEL EMD TMAE 650(S)

For the experiments where no σ_{Gauss} and τ values are given the peaks could not be fitted due to the shape of the peaks. The retention volumes are therefore determined as the volume at the peak maximum.

The peaks are fitted with the EMG function. The retention volumes and the variances are calculated as:

$V_R = V_{R,Gauss} + \tau - V_{dead}$

$\sigma^2 = \sigma^2_{Gauss} + \tau^2$

Where $V_{dead} = V_{empty10,\ incl.\ filters} + V_{ID,\ pos.1}$ = 0.237 ml + 0.31 ml = 0.690 ml

Column position: 2
Load: 100 µl

pH 6

Q [ml/min]	c_s [mM]	$V_{R,Gauss}$ [ml]	σ_{Gauss} [ml]	τ [ml]	V_R [ml]	σ^2 [ml^2]
2.94	85	42.80	----	----	42.1	----
5.93	85	40.56	----	----	39.9	----
2.94	85	42.79	----	----	42.1	----
2.94	96	26.76	----	----	26.1	----
5.93	96	26.15	----	----	25.5	----
2.94	96	26.76	----	----	26.1	----
2.94	116	14.22	----	----	13.5	----
5.93	116	14.40	----	----	13.7	----
2.94	116	13.89	----	----	13.2	----
2.94	136	8.95	----	----	8.26	----
5.93	136	9.34	----	----	8.65	----
2.94	136	8.83	----	----	8.14	----
2.94	155	6.49	----	----	5.80	----
5.93	155	6.71	----	----	6.02	----
2.94	155	6.50	----	----	5.81	----
1.01	154	6.80	----	----	6.11	----
2.94	184	4.33	0.806	0.870	4.51	1.41
5.93	184	4.20	0.842	1.10	4.60	1.91
2.94	184	4.36	0.807	0.881	4.55	1.43
1.01	184	4.50	----	----	3.81	----
2.94	232	3.37	0.398	0.413	3.09	0.329
5.93	232	3.23	0.461	0.572	3.12	0.540
2.94	232	3.37	0.407	0.397	3.08	0.323
2.94	280	3.06	0.327	0.291	2.66	0.192
5.93	280	2.98	0.382	0.442	2.73	0.342
2.94	280	3.07	0.325	0.291	2.67	0.190
2.94	330	2.94	0.297	0.267	2.52	0.159
5.93	330	2.89	0.350	0.399	2.60	0.282
2.94	330	2.94	0.294	0.270	2.52	0.160
2.94	379	2.89	0.283	0.260	2.46	0.148
5.93	379	2.88	0.333	0.383	2.57	0.258
2.94	379	2.89	0.279	0.263	2.46	0.148

pH 6

Q [ml/min]	c_s [mM]	$V_{R,Gauss}$ [ml]	σ_{Gauss} [ml]	τ [ml]	V_R [ml]	σ^2 [ml^2]
2.94	524	2.74	0.288	0.263	2.31	0.152
5.93	524	2.68	0.315	0.384	2.37	0.247
2.94	524	2.75	0.266	0.264	2.32	0.140
2.94	1010	2.69	0.263	0.263	2.26	0.138
5.93	1010	2.64	0.308	0.386	2.34	0.243
2.94	1010	2.71	0.261	0.263	2.28	0.137

pH 7

Q [ml/min]	c_s [mM]	$V_{R,Gauss}$ [ml]	σ_{Gauss} [ml]	τ [ml]	V_R [ml]	σ^2 [ml^2]
2.94	117	51.39	----	----	50.7	----
2.94	117	50.54	----	----	49.9	----
2.94	128	33.90	----	----	33.2	----
2.94	128	34.93	----	----	34.2	----
2.94	147	18.35	----	----	17.7	----
2.94	147	18.06	----	----	17.4	----
2.94	159	14.05	----	----	13.4	----
5.93	159	14.43	----	----	13.7	----
2.94	159	14.12	----	----	13.4	----
1.01	179	8.59	----	----	7.90	----
1.01	179	8.60	----	----	7.91	----
2.94	185	9.17	----	----	8.48	----
5.93	185	9.30	----	----	8.61	----
2.94	185	9.27	----	----	8.58	----
2.94	225	4.66	0.955	0.491	4.46	1.15
5.93	225	4.28	0.946	0.977	4.57	1.85
2.94	225	4.74	0.957	0.522	4.57	1.19
2.94	249	3.96	0.605	0.427	3.69	0.548
2.94	249	3.95	0.601	0.426	3.69	0.542
2.94	273	3.56	0.458	0.337	3.20	0.323
5.93	273	3.32	0.511	0.539	3.17	0.551
2.94	273	3.50	0.453	0.341	3.15	0.321
2.94	322	3.14	0.351	0.278	2.72	0.201
5.93	322	3.12	0.406	0.427	2.86	0.347
2.94	322	3.16	0.348	0.282	2.75	0.201
2.94	371	2.93	0.298	0.282	2.52	0.169
5.93	371	2.85	0.353	0.417	2.57	0.298
2.94	371	2.93	0.298	0.285	2.53	0.170
2.94	516	2.81	0.277	0.270	2.39	0.150
5.93	516	2.76	0.325	0.387	2.46	0.255
2.94	516	2.78	0.274	0.270	2.36	0.148
2.94	1001	2.70	0.267	0.267	2.28	0.142
5.93	1001	2.71	0.310	0.385	2.40	0.245
2.94	1001	2.72	0.264	0.269	2.30	0.142

pH 8

Q [ml/min]	c_s [mM]	$V_{R,Gauss}$ [ml]	σ_{Gauss} [ml]	τ [ml]	V_R [ml]	σ^2 [ml^2]
1.01	142	33.98	----	----	33.3	----
2.94	142	33.06	----	----	32.4	----
1.01	166	16.11	----	----	15.4	----
2.94	166	15.00	----	----	14.3	----
1.01	191	9.50	----	----	8.81	----
2.94	191	10.10	----	----	9.41	----
1.01	240	5.63	----	----	4.94	----
2.94	240	5.49	----	----	4.80	----
1.01	264	4.33	0.655	0.121	3.76	0.444
5.93	264	3.93	0.655	0.507	3.75	0.686
2.94	264	4.30	0.646	0.088	3.70	0.426
2.94	313	3.44	0.384	0.224	2.97	0.198
5.93	313	3.33	0.438	0.388	3.03	0.342
2.94	313	3.42	0.378	0.230	2.96	0.196
2.94	508	2.88	0.268	0.250	2.44	0.134
5.93	508	2.83	0.320	0.355	2.49	0.228
2.94	508	2.84	0.266	0.249	2.40	0.133
2.94	996	2.78	0.256	0.255	2.34	0.130
5.93	996	2.69	0.301	0.360	2.36	0.220
2.94	996	2.75	0.253	0.255	2.32	0.129

pH 9

Q [ml/min]	c_s [mM]	$V_{R,Gauss}$ [ml]	σ_{Gauss} [ml]	τ [ml]	V_R [ml]	σ^2 [ml^2]
1.01	139	56.98	----	----	56.3	----
2.94	139	55.42	----	----	54.7	----
1.01	158	27.87	----	----	27.2	----
2.94	158	26.75	----	----	26.1	----
1.01	183	12.59	----	----	11.9	----
2.94	183	12.07	----	----	11.4	----
1.01	208	7.76	----	----	7.07	----
1.01	232	6.73	----	----	6.04	----
2.94	232	6.47	----	----	5.78	----
1.01	256	4.91	0.703	0.005	4.22	0.494
2.94	256	4.81	0.810	0.006	4.12	0.657
1.01	305	3.87	0.379	0.003	3.18	0.143
2.94	305	3.68	0.455	0.181	3.17	0.240
1.01	354	3.49	0.359	0.003	2.81	0.129
2.94	354	3.33	0.384	0.159	2.80	0.173
1.01	403	3.31	0.300	0.002	2.62	0.090
2.94	403	3.14	0.350	0.170	2.62	0.151
1.01	501	3.17	0.299	0.002	2.48	0.089
2.94	501	2.99	0.346	0.189	2.48	0.156
1.01	745	3.06	0.340	0.003	2.37	0.116
2.94	745	2.90	0.355	0.173	2.39	0.156
1.01	989	3.03	0.355	0.002	2.35	0.126
2.94	989	2.91	0.352	0.186	2.40	0.159

APPENDIX C.XVI: THE INFLUENCE ON THE FITTED PARAMETERS WHEN ε IS INCREASED OR DECREASED

Source 30Q:

ε = 0.35: $\Delta G^0_{ads,s}/RT = 0.440$

ε = 0.45: $\Delta G^0_{ads,s}/RT = 0.202$

		Source 30Q							
		BSA		α-lactalbumin		β-lactoglobulin A		β-lactoglobulin B	
	ε	0.35	0.45	0.35	0.45	0.35	0.45	0.35	0.45
	$K_{d,p}$	0.664	0.550	0.773	0.695	0.738	0.649	0.738	0.649
	$\Delta G^0_{ads,p}/RT$	4.755	4.615	5.122	4.972	3.470	3.427	3.761	3.662
pH 6	ν	4.19	4.25	3.63	3.65	5.01	5.09	4.26	4.31
pH 7	ν	6.18	6.18	4.74	4.74	6.20	6.24	5.49	5.51
pH 8	ν	7.98	7.88	5.35	5.32	7.23	7.21	6.58	6.55
pH9	ν	9.94	9.69	6.35	6.28	8.01	7.94	7.35	7.27

Q-Sepharose XL:

ε = 0.25: $\Delta G^0_{ads,s}/RT = 0.471$

ε = 0.35: $\Delta G^0_{ads,s}/RT = 0.345$

		Q-Sepharose XL							
		BSA		α-lactalbumin		β-lactoglobulin A		β-lactoglobulin B	
	ε	0.25	0.35	0.25	0.35	0.25	0.35	0.25	0.35
	$K_{d,p}$	0.176	0.035	0.496	0.410	0.314	0.197	0.176	0.035
	$\Delta G^0_{ads,p}/RT$	4.382	2.951	2.782	2.576	2.006	1.718	4.382	2.951
pH 6	ν	5.05	5.16	2.77	2.80	3.64	3.79	5.05	5.16
pH 7	ν	6.62	6.72	3.69	3.71	4.88	5.05	6.62	6.72
pH 8	ν	7.96	8.03	4.12	4.12	5.14	5.31	7.96	8.03
pH9	ν	8.76	8.81	4.71	4.70	5.42	5.57	8.76	8.81

Ceramic Q-HyperD F:

$\varepsilon = 0.35$: $\Delta G^0_{ads,s} / RT = -0.199$

$\varepsilon = 0.45$: $\Delta G^0_{ads,s} / RT = -0.320$

		Ceramic Q-HyperD F							
		BSA		α-lactalbumin		β-lactoglobulin A		β-lactoglobulin B	
	ε	0.35	0.45	0.35	0.45	0.35	0.45	0.35	0.45
	$K_{d,p}$	0.256	0.048	0.289	0.090	0.271	0.068	0.271	0.068
	$\Delta G^0_{ads,p} / RT$	8.780	8.084	3.221	2.341	5.058	4.357	3.658	2.790
pH 6	ν	6.02	6.24	2.94	3.01	6.10	6.21	4.64	4.76
pH 7	ν	7.74	7.89	4.11	4.12	7.60	7.59	5.85	5.87
pH 8	ν	10.38	10.33	4.77	4.73	8.55	8.44	6.57	6.53
pH9	ν	12.20	11.93	5.49	5.38	9.56	9.33	7.28	7.16

Fractogel EMD TMAE 650(s):

$\varepsilon = 0.35$: $\Delta G^0_{ads,s} / RT = 1.576$

$\varepsilon = 0.45$: $\Delta G^0_{ads,s} / RT = 1.350$

		Fractogel EMD TMAE 650(s)							
		BSA		α-lactalbumin		β-lactoglobulin A		β-lactoglobulin B	
	ε	0.35	0.45	0.35	0.45	0.35	0.45	0.35	0.45
	$K_{d,p}$	0.520	0.359	0.866	0.821	0.615	0.486	0.615	0.486
	$\Delta G^0_{ads,p} / RT$	4.250	3.843	2.564	2.502	1.714	1.624	1.609	1.483
pH 6	ν	4.73	4.70	2.29	2.36	4.55	4.67	3.77	3.89
pH 7	ν	6.52	6.40	3.36	3.39	6.09	6.15	5.11	5.17
pH 8	ν	8.92	8.59	3.66	3.70	6.59	6.61	5.70	5.74
pH9	ν	11.33	10.71	4.56	4.55	7.13	7.11	6.17	6.18

APPENDIX D.I: EXPERIMENTAL DATA FOR LINEAR GRADIENT ELUTION ON SOURCE 30Q

For all the linear gradient elutions on Source 30Q a flow rate of 5.93 ml/min and a load of 100 µl were used.

			BSA			
pH	$c_{s,A}$ [M]	$c_{s,0}$ [M]	$c_{s,1}$ [M]	V_g [ml]	G [M/l]	V_{Rg} [ml]
6	0.038	0.059	0.233	16.00	10.9	17.9
				32.00	5.44	21.5
				64.00	2.72	26.5
				128.0	1.36	32.7
				256.0	0.679	42.2
7	0.027	0.048	0.224	16.00	11.0	23.3
				32.00	5.49	32.2
				64.00	2.75	48.0
				128.0	1.37	74.5
				256.0	0.686	128.5
8	0.019	0.045	0.263	16.00	13.6	25.2
				32.00	6.80	36.2
				64.00	3.40	56.4
				128.0	1.70	94.0
				256.0	0.850	163.2
9	0.011	0.043	0.304	16.00	16.3	25.0
				32.00	8.17	36.1
				64.00	4.08	57.1
				128.0	2.04	133.5
				256.0	1.02	169.7

α-lactalbumin						
pH	$c_{s,A}$ [M]	$c_{s,0}$ [M]	$c_{s,1}$ [M]	V_g [ml]	G [M/l]	V_{Rg} [ml]
6	0.038	0.049	0.136	16.00	5.46	21.6
				32.00	2.73	26.3
				64.00	1.37	31.8
				128.0	0.68	37.6
				256.0	0.341	42.9
7	0.028	0.060	0.322	16.00	16.4	19.2
				32.00	8.20	24.0
				64.00	4.10	31.5
				128.0	2.05	42.4
				256.0	1.02	58.2
8	0.022	0.054	0.315	16.00	16.3	21.1
				32.00	8.17	27.6
				64.00	4.08	38.5
				128.0	2.04	56.2
				256.0	1.02	84.7
9	0.010	0.042	0.305	16.00	16.4	23.0
				32.00	8.22	31.4
				64.00	4.11	45.9
				128.0	2.06	71.1
				256.0	1.03	115.8

β-lactoglobulin A						
pH	$c_{s,A}$ [M]	$c_{s,0}$ [M]	$c_{s,1}$ [M]	V_g [ml]	G [M/l]	V_{Rg} [ml]
6	0.037	0.063	0.280	16.00	13.5	21.6
				32.00	6.77	29.1
				64.00	3.39	40.3
				128.0	1.69	59.0
				256.0	0.847	86.7
7	0.029	0.061	0.323	16.00	16.4	22.7
				32.00	8.20	31.3
				64.00	4.10	46.2
				64.00	4.10	46.3
				128.0	2.05	71.3
				256.0	1.02	113.9
8	0.019	0.051	0.313	16.00	16.4	24.7
				32.00	8.20	35.0
				64.00	4.10	53.6
				128.0	2.05	86.4
				256.0	1.02	144.3
9	0.010	0.042	0.305	16.00	16.4	26.2
				32.00	8.22	37.8
				64.00	4.11	59.5
				128.0	2.06	98.7
				256.0	1.03	170.0

β-lactoglobulin B						
pH	$c_{s,A}$ [M]	$c_{s,0}$ [M]	$c_{s,1}$ [M]	V_g [ml]	G [M/l]	V_{Rg} [ml]
6	0.037	0.063	0.280	16.00	13.5	19.8
				32.00	6.77	24.3
				64.00	3.39	31.4
				128.0	1.69	38.8
				256.0	0.847	56.7
7	0.029	0.061	0.323	16.00	16.4	22.3
				32.00	8.20	28.7
				64.00	4.10	39.9
				64.00	4.10	39.8
				128.0	2.05	58.7
				256.0	1.02	89.5
8	0.019	0.051	0.313	16.00	16.4	24.7
				32.00	8.20	32.5
				64.00	4.10	48.2
				128.0	2.05	76.4
				256.0	1.02	125.3
9	0.010	0.042	0.305	16.00	16.4	24.9
				32.00	8.22	35.3
				64.00	4.11	54.4
				128.0	2.06	88.7
				256.0	1.03	150.0

APPENDIX D.II: EXPERIMENTAL DATA FOR LINEAR GRADIENT ELUTION ON Q-SEPHAROSE XL

The linear gradient elutions on Q-Sepharose XL are run at two flow rates. All the elutions with β-lactoglobulin A and B and the elutions with BSA at a pH of 7, 8 and 9 are run at Q = 15.1 ml/min. All the elutions with α-lactalbumin and the elutions with BSA at a pH of 6 are run at Q = 5.93 ml/min.
For all the gradient elutions a load of 100 µl was used.

			BSA			
pH	$c_{s,A}$ [M]	$c_{s,0}$ [M]	$c_{s,1}$ [M]	V_g [ml]	G [M/l]	V_{Rg} [ml]
6	0.037	0.058	0.232	16.00	10.9	24.7
				32.00	5.44	34.6
				64.00	2.72	51.4
				128.0	1.36	79.3
				256.0	0.679	125.9
7	0.027	0.048	0.224	16.00	11.0	30.0
				32.00	5.49	44.3
				64.00	2.75	74.4
				128.0	1.37	129.8
				256.0	0.686	221.2
8	0.019	0.045	0.263	16.00	13.6	32.0
				32.00	6.80	46.0
				64.00	3.40	76.0
				128.0	1.70	135.0
				256.0	0.850	242.0
9	0.011	0.043	0.304	16.00	16.3	30.7
				32.00	8.17	44.7
				64.00	4.08	74.9
				128.0	2.04	133.2
				256.0	1.02	241.5

α-lactalbumin						
pH	$c_{s,A}$ [M]	$c_{s,0}$ [M]	$c_{s,1}$ [M]	V_g [ml]	G [M/l]	V_{Rg} [ml]
6	0.038	0.070	0.330	16.00	16.3	21.8
				32.00	8.14	27.3
				32.00	8.14	27.3
				64.00	4.07	35.4
				128.0	2.03	46.3
				256.0	1.02	60.4
7	0.028	0.060	0.322	16.00	16.4	26.0
				16.00	16.4	26.0
				16.00	16.4	25.8
				32.00	8.20	35.3
				32.00	8.20	35.3
				64.00	4.10	50.8
				128.0	2.05	75.7
				256.0	1.02	116.4
8	0.022	0.054	0.315	16.00	16.3	28.0
				32.00	8.17	39.5
				32.00	8.17	39.5
				64.00	4.08	58.9
				128.0	2.04	91.2
				256.0	1.02	147.5
9	0.010	0.042	0.305	16.00	16.4	31.1
				32.00	8.22	43.9
				32.00	8.22	43.9
				64.00	4.11	68.2
				128.0	2.06	110.5
				256.0	1.03	185.1

β-lactoglobulin B						
pH	$c_{s,A}$ [M]	$c_{s,0}$ [M]	$c_{s,1}$ [M]	V_g [ml]	G [M/l]	V_{Rg} [ml]
6	0.037	0.063	0.280	16.00	13.5	26.9
				32.00	6.77	38.7
				64.00	3.39	57.8
				128.0	1.69	89.7
				256.0	0.847	140.5
7	0.029	0.061	0.323	16.00	16.4	28.4
				32.00	8.20	41.9
				64.00	4.10	65.3
				128.0	2.05	105.5
				256.0	1.02	176.0
8	0.019	0.051	0.313	16.00	16.4	35.4
				32.00	8.20	43.6
				64.00	4.10	66.8
				128.0	2.05	118.2
				256.0	1.02	209.7
9	0.010	0.042	0.305	16.00	16.4	39.3
				32.00	8.22	52.2
				64.00	4.11	79.0
				128.0	2.06	128.7
				256.0	1.03	222.2

APPENDIX D.III: EXPERIMENTAL DATA FOR LINEAR GRADIENT ELUTION ON CERAMIC Q-HYPERD F

For all the linear gradient elutions on Cermaic Q-HyperD F a flow rate of 5.93 ml/min and a load of 100 µl were used.

			BSA			
pH	$c_{s,A}$ [M]	$c_{s,0}$ [M]	$c_{s,1}$ [M]	V_g [ml]	G [M/l]	V_{Rg} [ml]
6	0.038	0.059	0.233	16.00	10.9	16.5
				32.00	5.44	20.2
				64.00	2.72	25.6
				128.0	1.36	31.9
				256.0	0.679	46.0
7	0.032	0.064	0.325	16.00	16.3	17.5
				32.00	8.17	23.0
				64.00	4.08	32.8
				128.0	2.04	50.7
				256.0	1.02	82.5
8	0.026	0.057	0.316	16.00	16.3	21.4
				32.00	8.17	30.2
				64.00	4.08	47.4
				128.0	2.04	79.6
				256.0	1.02	141.1
9	0.011	0.048	0.356	16.00	19.2	22.1
				32.00	9.62	32.0
				64.00	4.81	51.6
				128.0	2.40	88.8
				256.0	1.20	160.0

α-lactalbumin						
pH	$c_{s,A}$ [M]	$c_{s,0}$ [M]	$c_{s,1}$ [M]	V_g [ml]	G [M/l]	V_{Rg} [ml]
6	0.038	0.070	0.330	16.00	16.3	16.0
				32.00	8.14	18.6
				64.00	4.07	21.4
				128.0	2.03	24.2
				256.0	1.017	27.3
7	0.028	0.060	0.322	16.00	16.4	20.0
				32.00	8.20	26.8
				64.00	4.10	38.0
				128.0	2.05	55.9
				256.0	1.02	84.7
8	0.022	0.054	0.315	16.00	16.3	22.0
				32.00	8.17	30.9
				64.00	4.08	46.5
				128.0	2.04	72.7
				256.0	1.02	118.5
9	0.010	0.042	0.305	16.00	16.4	24.7
				32.00	8.22	36.0
				64.00	4.11	56.5
				128.0	2.06	93.0
				256.0	1.03	159.2

β-lactoglobulin A						
pH	$c_{s,A}$ [M]	$c_{s,0}$ [M]	$c_{s,1}$ [M]	V_g [ml]	G [M/l]	V_{Rg} [ml]
6	0.037	0.063	0.280	16.00	13.5	21.4
				32.00	6.77	29.5
				64.00	3.39	42.5
				128.00	1.69	64.3
				256.0	0.847	101.3
7	0.029	0.061	0.323	16.00	16.4	23.3
				32.00	8.20	33.3
				64.00	4.10	51.4
				128.00	2.05	84.0
				256.0	1.02	143.3
8	0.019	0.051	0.313	16.00	16.4	25.3
				32.00	8.20	37.7
				64.00	4.10	60.1
				128.00	2.05	101.3
				256.0	1.02	177.4
9	0.010	0.042	0.305	16.00	16.4	26.8
				32.00	8.22	40.7
				64.00	4.11	66.8
				128.00	2.06	114.8
				256.0	1.03	204.1

β-lactoglobulin B						
pH	$c_{s,A}$ [M]	$c_{s,0}$ [M]	$c_{s,1}$ [M]	V_g [ml]	G [M/l]	V_{Rg} [ml]
6	0.037	0.063	0.280	16.00	13.5	21.4
				32.00	6.77	29.5
				64.00	3.39	36.4
				128.0	1.69	50.4
				256.0	0.847	71.3
7	0.029	0.061	0.323	16.00	16.4	23.3
				32.00	8.20	33.3
				64.00	4.10	47.7
				128.0	2.05	75.5
				256.0	1.02	119.6
8	0.019	0.051	0.313	16.00	16.4	25.3
				32.00	8.20	37.7
				64.00	4.10	56.1
				128.0	2.05	91.1
				256.0	1.02	155.1
9	0.010	0.042	0.305	16.00	16.4	26.8
				32.00	8.22	39.0
				64.00	4.11	61.9
				128.0	2.06	104.8
				256.0	1.03	182.3

APPENDIX D.IV: EXPERIMENTAL DATA FOR LINEAR GRADIENT ELUTION ON FRACTOGEL EMD TMAE 650 (S)

For all the linear gradient elutions on Fractogel EMD TMAE 650(s) a flow rate of 5.93 ml/min and a load of 100 μl were used.

			BSA			
pH	$c_{s,A}$ [M]	$c_{s,0}$ [M]	$c_{s,1}$ [M]	V_g [ml]	G [M/l]	V_{Rg} [ml]
6	0.038	0.059	0.233	16.00	10.9	14.8
				32.00	5.44	17.5
				64.00	2.72	21.1
				128.0	1.36	26.2
				256.0	0.679	32.0
7	0.032	0.064	0.325	16.00	16.3	16.1
				32.00	8.17	20.5
				64.00	4.08	28.3
				128.0	2.04	40.5
				256.0	1.02	58.7
8	0.026	0.057	0.316	16.00	16.2	19.6
				32.00	8.08	27.1
				64.00	4.04	41.3
				128.0	2.02	66.6
				256.0	1.01	113.2
9	0.011	0.048	0.356	16.00	19.2	19.9
				32.00	9.62	28.4
				64.00	4.81	44.7
				128.0	2.40	74.5
				256.0	1.20	130.6

α-lactalbumin						
pH	$c_{s,A}$ [M]	$c_{s,0}$ [M]	$c_{s,1}$ [M]	V_g [ml]	G [M/l]	V_{Rg} [ml]
6	0.038	0.049	0.136	16.00	5.46	14.3
				32.00	2.73	15.8
				64.00	1.37	17.1
				128.0	0.683	18.2
				256.0	0.341	19.4
7	0.028	0.060	0.322	16.00	16.4	15.2
				16.00	16.4	15.2
				32.00	8.20	18.9
				32.00	8.20	18.8
				64.00	4.10	24.2
				64.00	4.10	24.2
				128.0	2.05	31.3
				128.0	2.05	31.3
				256.0	1.02	40.8
				256.0	1.02	40.8
8	0.022	0.054	0.315	16.00	16.3	15.8
				32.00	8.17	20.0
				64.00	4.08	31.5
				128.0	2.04	45.1
				256.0	1.02	65.1
9	0.010	0.042	0.305	16.00	16.4	18.1
				32.00	8.22	24.4
				64.00	4.11	35.3
				128.0	2.06	55.3
				256.0	1.03	89.9

β-lactoglobulin A						
pH	$c_{s,A}$ [M]	$c_{s,0}$ [M]	$c_{s,1}$ [M]	V_g [ml]	G [M/l]	V_{Rg} [ml]
6	0.037	0.063	0.280	16.00	13.5	17.6
				32.00	6.77	23.7
				64.00	3.39	33.7
				128.00	1.69	48.8
				256.0	0.847	70.6
7	0.029	0.061	0.323	16.00	16.4	19.4
				32.00	8.20	27.5
				64.00	4.10	41.4
				128.00	2.05	64.7
				256.0	1.02	103.5
8	0.019	0.051	0.313	16.00	16.4	20.7
				32.00	8.20	29.6
				64.00	4.10	45.4
				128.00	2.05	73.8
				256.0	1.02	122.4
9	0.010	0.042	0.305	16.00	16.4	21.7
				32.00	8.22	31.9
				64.00	4.11	50.0
				128.00	2.06	82.4
				256.0	1.03	139.6

β-lactoglobulin B						
pH	$c_{s,A}$ [M]	$c_{s,0}$ [M]	$c_{s,1}$ [M]	V_g [ml]	G [M/l]	V_{Rg} [ml]
6	0.037	0.063	0.280	16.00	13.5	17.6
				32.00	6.77	23.7
				64.00	3.39	29.3
				128.0	1.69	37.7
				256.0	0.847	49.7
7	0.029	0.061	0.323	16.00	16.4	19.4
				32.00	8.20	27.5
				64.00	4.10	36.7
				128.0	2.05	55.0
				256.0	1.02	84.5
8	0.019	0.051	0.313	16.00	16.4	20.7
				32.00	8.20	29.6
				64.00	4.10	42.1
				128.0	2.05	65.8
				256.0	1.02	107.3
9	0.010	0.042	0.305	16.00	16.4	21.7
				32.00	8.22	30.2
				64.00	4.11	46.3
				128.0	2.06	75.4
				256.0	1.03	128.3

APPENDIX D.V: EXPERIMENTAL DATA FOR LINEAR GRADIENT ELUTION OF α-LACTALBUMIN WITH THE NEW CALIBRATION OF THE MIXER

Source 30Q						
pH	$c_{s,A}$ [M]	$c_{s,0}$ [M]	$c_{s,1}$ [M]	V_g [ml]	G [M/l]	V_{Rg} [ml]
6	0.038	0.042	0.136	16.00	5.89	21.6
				32.00	2.94	26.3
				64.00	1.47	31.8
				128.0	0.736	37.6
				256.0	0.368	42.9
7	0.028	0.039	0.322	16.00	17.7	19.2
				32.00	8.83	24.0
				64.00	4.42	31.5
				128.0	2.21	42.4
				256.0	1.10	58.2
8	0.022	0.033	0.315	16.00	17.6	21.1
				32.00	8.80	27.6
				64.00	4.40	38.5
				128.0	2.20	56.2
				256.0	1.10	84.7
9	0.010	0.021	0.305	16.00	17.7	23.0
				32.00	8.86	31.4
				64.00	4.43	45.9
				128.0	2.22	71.1
				256.0	1.11	115.8

Q-Sepharose XL						
pH	$c_{s,A}$ [M]	$c_{s,0}$ [M]	$c_{s,1}$ [M]	V_g [ml]	G [M/l]	V_{Rg} [ml]
6	0.038	0.049	0.330	16.00	17.5	21.8
				32.00	8.77	27.3
				64.00	4.39	35.4
				128.0	2.19	46.3
				256.0	1.10	60.4
7	0.028	0.039	0.322	16.00	17.7	26.0
				16.00	17.7	26.0
				16.00	17.7	25.8
				32.00	8.83	35.3
				32.00	8.83	35.3
				64.00	4.42	50.8
				128.0	2.21	75.7
				256.0	1.10	116.4
8	0.022	0.033	0.315	16.00	17.6	28.0
				32.00	8.80	39.5
				64.00	4.40	58.9
				128.0	2.20	91.2
				256.0	1.10	147.5
9	0.010	0.021	0.305	16.00	17.7	31.1
				32.00	8.86	43.9
				64.00	4.43	68.2
				128.0	2.22	110.5
				256.0	1.11	185.1

Ceramic Q-HyperD F						
pH	$c_{s,A}$ [M]	$c_{s,0}$ [M]	$c_{s,1}$ [M]	V_g [ml]	G [M/l]	V_{Rg} [ml]
6	0.038	0.049	0.330	16.00	17.5	16.0
				32.00	8.77	18.6
				64.00	4.39	21.4
				128.0	2.19	24.2
				256.0	1.10	27.3
7	0.028	0.039	0.322	16.00	17.7	20.0
				32.00	8.83	26.8
				64.00	4.42	38.0
				128.0	2.21	55.9
				256.0	1.10	84.7
8	0.022	0.033	0.315	16.00	17.6	22.0
				32.00	8.80	30.9
				64.00	4.40	46.5
				128.0	2.20	72.7
				256.0	1.10	118.5
9	0.010	0.021	0.305	16.00	17.7	24.7
				32.00	8.86	36.0
				64.00	4.43	56.5
				128.0	2.22	93.0
				256.0	1.11	159.2

Fractogel EMD TMAE 650(s)						
pH	$c_{s,A}$ [M]	$c_{s,0}$ [M]	$c_{s,1}$ [M]	V_g [ml]	G [M/l]	V_{Rg} [ml]
6	0.038	0.042	0.136	16.00	5.89	14.3
				32.00	2.94	15.8
				64.00	1.47	17.1
				128.0	0.736	18.2
				256.0	0.368	19.4
7	0.028	0.039	0.322	16.00	17.7	15.2
				16.00	17.7	15.2
				32.00	8.83	18.9
				32.00	8.83	18.8
				64.00	4.42	24.2
				64.00	4.42	24.2
				128.0	2.21	31.3
				128.0	2.21	31.3
				256.0	1.10	40.8
				256.0	1.10	40.8
8	0.022	0.033	0.315	16.00	17.6	15.8
				32.00	8.80	20.0
				64.00	4.40	31.5
				128.0	2.20	45.1
				256.0	1.10	65.1
9	0.010	0.021	0.305	16.00	17.7	18.1
				32.00	8.86	24.4
				64.00	4.43	35.3
				128.0	2.22	55.3
				256.0	1.11	89.9

APPENDIX E.I: THE Cl^--CONCENTRATIONS AT THE BEGINNING AND THE END OF THE LINEAR GRADIENTS

Source 30Q:

pH	c_{s0} [M]	c_{s1} [M]
6	0.060	0.200
7	0.060	0.320
8	0.050	0.310
9	0.042	0.305

Q-Sepharose XL:

pH	c_{s0} [M]	c_{s1} [M]
6	0.064	0.280
7	0.055	0.270
8	0.050	0.290
9	0.042	0.305

Ceramic Q-HyperD F:

pH	c_{s0} [M]	c_{s1} [M]
6	0.065	0.280
7	0.061	0.323
8	0.054	0.315
9	0.042	0.305

Fractogel EMD TMAE 650(s):

pH	c_{s0} [M]	c_{s1} [M]
6	0.045	0.200
7	0.061	0.323
8	0.051	0.313
9	0.042	0.305

APPENDIX F.I: CAPACITY MEASUREMENTS WITH BSA ON SOURCE 30Q AT A pH OF 7

$Q_{eluting}$ = 4.94 ml/min.

				V_{col} = 1.35 ml		
c_{Cl-} [M]	c_{BSA} [g/l]	V_{load} [ml]	Q_{load} [ml/min]	A [Abs. 280 nm·s]	q_{BSA} [g/l CV]	q_{BSA} [mol/l ass. pore vol.]
0.037	0.562	300.0	4.94	175.75	29.63	2.16E-03
0.037	0.565	300.0	4.94	176.45	29.75	2.17E-03
0.037	1.078	150.0	4.94	185.36	31.25	2.28E-03
0.037	1.083	150.0	2.45	184.08	31.03	2.27E-03
0.037	2.116	75.0	4.94	192.16	32.40	2.37E-03
0.037	2.122	75.0	1.25	193.39	32.60	2.38E-03
0.037	3.126	50.0	4.94	196.16	33.07	2.42E-03
0.037	3.135	50.0	0.85	197.77	33.34	2.44E-03
0.037	4.093	37.5	0.64	200.68	33.83	2.47E-03
0.037	4.103	37.5	4.94	198.64	33.49	2.45E-03
0.037	5.046	30.0	0.53	203.97	34.39	2.51E-03
0.037	5.066	30.0	4.94	200.33	33.77	2.47E-03
0.077	0.556	300.0	4.94	86.50	14.58	1.07E-03
0.077	0.556	300.0	4.94	86.30	14.55	1.06E-03
0.077	1.055	150.0	4.94	95.74	16.14	1.18E-03
0.077	1.070	150.0	2.45	95.92	16.17	1.18E-03
0.077	2.065	75.0	4.94	106.36	17.93	1.31E-03
0.077	2.083	75.0	1.25	107.06	18.05	1.32E-03
0.077	3.050	50.0	4.94	112.81	19.02	1.39E-03
0.077	3.072	50.0	0.85	113.80	19.18	1.40E-03
0.077	3.999	37.5	4.94	116.73	19.68	1.44E-03
0.077	4.002	37.5	0.64	118.19	19.92	1.46E-03
0.077	4.919	30.0	0.53	122.29	20.62	1.51E-03
0.077	4.924	30.0	4.94	124.57	21.00	1.53E-03
0.117	0.555	300.0	4.94	26.04	4.39	3.21E-04
0.117	0.556	300.0	4.94	26.01	4.38	3.20E-04
0.117	1.064	150.0	4.94	33.40	5.63	4.11E-04
0.117	1.067	150.0	2.45	33.86	5.71	4.17E-04
0.117	2.063	75.0	4.94	42.51	7.17	5.23E-04
0.117	2.074	75.0	1.25	43.98	7.41	5.42E-04
0.117	3.060	50.0	4.94	48.95	8.25	6.03E-04
0.117	3.077	50.0	0.85	50.65	8.54	6.24E-04
0.117	3.990	37.5	0.64	55.73	9.39	6.86E-04
0.117	4.023	37.5	4.94	53.78	9.07	6.62E-04
0.117	4.921	30.0	4.94	57.67	9.72	7.10E-04
0.117	4.935	30.0	0.53	60.12	10.14	7.40E-04
0.157	5.015	30.0	0.53	23.98	4.04	2.95E-04
0.157	0.571	300.0	4.94	4.62	0.78	5.69E-05
0.157	0.574	300.0	4.94	4.64	0.78	5.71E-05
0.157	1.087	150.0	2.45	7.53	1.27	9.27E-05
0.157	1.092	150.0	4.94	7.47	1.26	9.20E-05
0.157	2.117	75.0	1.25	12.54	2.11	1.54E-04
0.157	3.119	50.0	4.94	16.24	2.74	2.00E-04
0.157	3.122	50.0	0.85	16.41	2.77	2.02E-04
0.157	4.082	37.5	0.64	20.03	3.38	2.47E-04
0.157	4.106	37.5	4.94	20.32	3.43	2.50E-04
0.157	5.023	30.0	4.94	23.21	3.91	2.86E-04

The data is obtained around 1 year before the data in the table above, and is not used in the fit for determination of σ.
Q_{load} = 1.01 ml/min
$Q_{eluting}$ = 1.01 ml/min

V_{col} = 1.35 ml (old data)					
c_{Cl^-} [M]	c_{BSA} [g/l]	V_{load} [ml]	A [Abs. 280 nm·s]	q_{BSA} [g/l CV]	q_{BSA} [mol/l ass. pore vol.]
0.037	0.249	400.0	886.1	30.4	2.22E-03
0.037	0.252	400.0	869.4	29.9	2.18E-03
0.037	0.512	200.0	913.0	31.4	2.29E-03
0.037	0.514	200.0	932.5	32.0	2.34E-03
0.037	1.503	66.7	968.0	33.2	2.43E-03
0.037	1.504	66.7	987.2	33.9	2.48E-03
0.037	3.435	28.6	1008.6	34.6	2.53E-03
0.037	3.448	28.6	1026.5	35.3	2.58E-03
0.037	4.835	20.0	1023.5	35.2	2.57E-03
0.037	4.842	20.0	1041.2	35.8	2.61E-03

The data is obtained around 1 year before the latest data from the column with V_{col} = 1.35 ml. The data is not used in the fit for determination of σ.
Q_{load} = 1.01 ml/min
$Q_{eluting}$ = 1.01 ml/min

V_{col} = 0.46 ml					
c_{Cl^-} [M]	c_{BSA} [g/l]	V_{load} [ml]	A [Abs. 280 nm·s]	q_{BSA} [g/l CV]	q_{BSA} [mol/l ass. pore vol.]
0.037	0.250	141.0	275.6	27.8	2.21E-03
0.037	0.513	70.5	290.4	29.3	2.33E-03
0.037	1.503	23.5	310.3	31.3	2.48E-03
0.037	3.441	10.1	330.1	33.3	2.64E-03
0.037	4.838	7.1	341.6	34.4	2.74E-03

APPENDIX F.II: CAPACITY MEASUREMENTS WITH BSA ON SOURCE 30Q AT A pH OF 8

$Q_{eluting}$ = 4.94 ml/min.

				V_{col} = 1.35 ml		
c_{Cl-} [M]	c_{BSA} [g/l]	V_{load} [ml]	Q_{load} [ml/min]	A [Abs. 280 nm·s]	q_{BSA} [g/l CV]	q_{BSA} [mol/l ass. pore vol.]
0.037	0.543	300.0	4.94	249.43	42.05	3.07E-03
0.037	0.543	300.0	4.94	233.70	39.40	2.88E-03
0.037	0.553	300.0	4.94	234.91	39.60	2.89E-03
0.037	0.554	300.0	4.94	239.26	40.33	2.95E-03
0.037	1.049	150.0	2.45	246.02	41.47	3.03E-03
0.037	1.052	150.0	2.45	252.41	42.55	3.11E-03
0.037	1.065	150.0	4.94	240.85	40.60	2.97E-03
0.037	1.065	150.0	4.94	243.35	41.02	3.00E-03
0.037	2.028	75.0	1.25	250.70	42.26	3.09E-03
0.037	2.044	75.0	1.25	255.59	43.09	3.15E-03
0.037	2.065	75.0	4.94	247.29	41.69	3.05E-03
0.037	2.078	75.0	4.94	243.76	41.09	3.00E-03
0.037	2.988	50.0	0.85	252.97	42.65	3.12E-03
0.037	3.020	50.0	0.85	256.18	43.19	3.15E-03
0.037	3.064	50.0	4.94	249.52	42.06	3.07E-03
0.037	3.082	50.0	4.94	245.02	41.31	3.02E-03
0.037	3.967	37.5	0.64	255.04	42.99	3.14E-03
0.037	3.971	37.5	0.64	256.40	43.22	3.16E-03
0.037	4.044	37.5	4.94	250.54	42.24	3.09E-03
0.037	4.058	37.5	4.94	255.75	43.11	3.15E-03
0.037	4.905	30.0	0.53	257.28	43.37	3.17E-03
0.037	4.909	30.0	0.53	261.16	44.03	3.22E-03
0.037	5.017	30.0	4.94	254.18	42.85	3.13E-03
0.037	5.036	30.0	4.94	246.75	41.60	3.04E-03
0.077	0.531	300.0	4.94	164.20	27.68	2.02E-03
0.077	0.539	300.0	4.94	153.85	25.94	1.89E-03
0.077	1.049	150.0	2.45	165.43	27.89	2.04E-03
0.077	1.050	150.0	2.45	161.47	27.22	1.99E-03
0.077	2.027	75.0	1.25	168.46	28.40	2.07E-03
0.077	2.054	75.0	1.25	172.71	29.12	2.13E-03
0.077	2.996	50.0	0.85	173.37	29.23	2.13E-03
0.077	3.004	50.0	0.85	176.02	29.67	2.17E-03
0.077	3.974	37.5	0.64	178.59	30.11	2.20E-03
0.077	3.975	37.5	0.64	177.62	29.94	2.19E-03
0.077	4.913	30.0	0.53	179.11	30.19	2.21E-03
0.077	4.920	30.0	0.53	180.86	30.49	2.23E-03
0.117	0.544	300.0	4.94	95.82	16.15	1.18E-03
0.117	0.555	300.0	4.94	93.47	15.76	1.15E-03
0.117	1.057	150.0	2.45	102.98	17.36	1.27E-03
0.117	1.066	150.0	2.45	100.89	17.01	1.24E-03
0.117	2.064	75.0	1.25	111.03	18.72	1.37E-03
0.117	2.070	75.0	1.25	109.32	18.43	1.35E-03
0.117	3.036	50.0	0.85	113.88	19.20	1.40E-03
0.117	3.045	50.0	0.85	114.01	19.22	1.40E-03
0.117	3.997	37.5	0.64	118.15	19.92	1.45E-03
0.117	4.004	37.5	0.64	118.89	20.04	1.46E-03
0.117	4.918	30.0	0.53	120.21	20.26	1.48E-03
0.117	4.918	30.0	0.53	121.40	20.47	1.49E-03

$Q_{eluting}$ = 4.94 ml/min

V_{col} = 1.35 ml						
c_{Cl^-} [M]	c_{BSA} [g/l]	V_{load} [ml]	Q_{load} [ml/min]	A [Abs. 280 nm·s]	q_{BSA} [g/l CV]	q_{BSA} [mol/l ass. pore vol.]
0.157	0.546	300.0	4.939	39.65	6.68	4.88E-04
0.157	1.059	150.0	2.454	46.00	7.75	5.66E-04
0.157	2.073	75.0	1.248	53.85	9.08	6.63E-04
0.157	2.074	75.0	1.248	55.10	9.29	6.78E-04
0.157	3.045	50.0	0.845	59.36	10.01	7.31E-04
0.157	3.055	50.0	0.845	60.44	10.19	7.44E-04
0.157	3.991	37.5	0.644	63.68	10.74	7.84E-04
0.157	4.001	37.5	0.644	64.11	10.81	7.90E-04
0.157	4.927	30.0	0.529	67.41	11.36	8.30E-04

The data is obtained around 1 year before the data from the column with V_{col} = 1.35 ml. The data is not used in the fit for determination of σ.
Q_{load} = 2.45 ml/min
$Q_{eluting}$ = 2.45 ml/min
V_{load} = 100.0 ml

V_{col} = 0.98 ml				
c_{Cl^-} [M]	c_{BSA} [g/l]	A [Abs. 280 nm·s]	q_{BSA} [g/l CV]	q_{BSA} [mol/l ass. pore vol.]
0.038	0.5	338.55	38.98	3.05E-03
0.038	0.5	336.71	38.77	3.03E-03
0.038	0.5	336.54	38.75	3.03E-03
0.038	1.5	375.10	43.19	3.38E-03
0.038	1.5	368.11	42.39	3.32E-03
0.038	3.0	371.33	42.76	3.34E-03
0.038	3.0	360.24	41.48	3.24E-03
0.078	0.5	203.37	23.42	1.83E-03
0.078	0.5	207.91	23.94	1.87E-03
0.078	1.5	256.74	29.56	2.31E-03
0.078	1.5	252.98	29.13	2.28E-03
0.078	3.0	248.38	28.60	2.24E-03
0.078	3.0	243.16	28.00	2.19E-03
0.117	0.5	104.20	12.00	9.38E-04
0.117	0.5	104.74	12.06	9.43E-04
0.117	1.5	167.78	19.32	1.51E-03
0.117	1.5	164.81	18.98	1.48E-03
0.117	3.0	164.19	18.91	1.48E-03
0.117	3.0	168.17	19.36	1.51E-03
0.157	0.5	41.33	4.76	3.72E-04
0.157	0.5	41.04	4.73	3.70E-04
0.157	1.5	76.71	8.83	6.91E-04
0.157	1.5	74.97	8.63	6.75E-04
0.157	3.0	82.95	9.55	7.47E-04
0.157	3.0	80.62	9.28	7.26E-04

The data is obtained around 1 year before the data from the column with V_{col} = 1.35 ml. The data is not used in the fit for determination of σ.

Q_{load} = 1.01 ml/min

$Q_{eluting}$ = 1.01 ml/min

V_{load} = 70.0 ml

V_{col} = 0.98 ml				
c_{Cl^-} [M]	c_{BSA} [g/l]	A [Abs. 280 nm·s]	q_{BSA} [g/l CV]	q_{BSA} [mol/l ass. pore vol.]
0.037	0.5	379.27	38.23	3.04E-03
0.037	0.5	376.07	37.91	3.01E-03
0.037	1.5	270.35	27.25	2.17E-03
0.037	1.5	400.14	40.34	3.20E-03
0.037	1.5	425.36	42.88	3.41E-03
0.037	3.0	200.36	20.20	1.60E-03
0.037	3.0	427.59	43.10	3.42E-03
0.037	3.0	413.04	41.64	3.31E-03
0.077	0.5	242.83	24.48	1.94E-03
0.077	0.5	198.46	20.01	1.59E-03
0.077	0.5	203.50	20.51	1.63E-03
0.077	1.5	275.78	27.80	2.21E-03
0.077	1.5	273.57	27.58	2.19E-03
0.077	3.0	303.39	30.58	2.43E-03
0.077	3.0	300.73	30.31	2.41E-03
0.117	0.5	123.94	12.49	9.93E-04
0.117	0.5	138.88	14.00	1.11E-03
0.117	0.5	139.11	14.02	1.11E-03
0.117	1.5	180.77	18.22	1.45E-03
0.117	1.5	178.30	17.97	1.43E-03
0.117	3.0	200.63	20.22	1.61E-03
0.117	3.0	196.37	19.79	1.57E-03
0.157	0.5	62.33	6.28	4.99E-04
0.157	0.5	61.51	6.20	4.93E-04
0.157	1.5	96.47	9.72	7.73E-04
0.157	1.5	95.51	9.63	7.65E-04
0.157	3.0	127.82	12.88	1.02E-03
0.157	3.0	127.05	12.81	1.02E-03

APPENDIX G.I: THE EXPERIMENTAL DATA EXCLUDED IN THE CORRELATION OF THE REDUCED PLATE HEIGHTS

In this appendix the data from the isocratic elutions, which have been excluded in the correlation of the reduced plate heights, is listed. The data is excluded due to ambiguous variances caused by impurities.

The excluded data for Source 30Q:

BSA: pH 6: c_{Cl^-} = 0.071, 0.076 and 0.087 M
pH 7: c_{Cl^-} = 0.125 and 0.145 M

α-lactalbumin: pH 7: c_{Cl^-} = 0.068, 0.079, 0.102, 0.127 and 0.147 M
pH 9: c_{Cl^-} = 0.110 and 0.135 M

The excluded data for Q-Sepharose XL:

The data obtained at Q = 15 ml/min is excluded in all the fits, because it seems as this flow rate has been to high and have resulted in indistinct variances.

β-lactoglobulin B: pH 8: c_{Cl^-} = 0.411 M

The excluded data for Ceramic Q-HyperD F:

BSA: pH 6: c_{Cl^-} = 0.071, 0.076 and 0.087 M
pH 7: c_{Cl^-} = 0.112 and 0.131 M

α-lactalbumin: pH 6: c_{Cl^-} = 0.057, 0.077, 0.087 and 0.111 M

β-lactoglobulin A: pH 6: c_{Cl^-} = 0.155 and 0.184 M
pH 7: c_{Cl^-} = 0.225 M

β-lactoglobulin B: pH 6: c_{Cl^-} = 0.155 M

The excluded data for Fractogel EMD TMAE 650(s):

BSA: pH 6: c_{Cl^-} = 0.071 and 0.076 M
pH 7: c_{Cl^-} = 0.088, 0.112 and 0.131 M
pH 8: c_{Cl^-} = 0.140, 0.162 and 0.172 M

α-lactalbumin: pH 6: c_{Cl^-} = 0.043, 0.087 and 0.111 M
pH 7: c_{Cl^-} = 0.053, 0.068, 0.102, 0.127 and 0.147 M

APPENDIX H.I: DEAD VOLUMES AND VARIANCES

Measured dead volumes

Determination of the dead volume in the system from injection to the UV detector without a column

Q [ml/min]	V_{sys} [ml]	σ^2_{sys} [ml^2]
5	2.03	0.20
5	2.12	0.31
5	2.15	0.32
Mean value:	2.10	0.28
Variance:	0.003	0.004
Standard Error:	0.03	0.04

Determination of the dead volume in the system from injection to the UV detector with an empty column

Q [ml/min]	$V_{sys+col}$ [ml]	$\sigma^2_{sys+col}$ [ml^2]
2	12.11	13.89
5	11.19	22.46
10	11.33	20.30
5	12.62	24.18
10	13.09	19.50
2	12.05	14.77
Mean value:	12.06	19.18
Variance:	0.53	16.92
Standard Error:	0.30	1.68

Volume of distributor

Weight of empty distributor: 0.0 g (the balance was reset)

Weight of water filled distributor in grams:

	2.05
	2.10
	2.10
	2.15
	2.10
Mean value:	2.10
Variance:	0.001
Standard Error:	0.02

$V_{distributor}$ = 2.10 ml (It is assumed that the density of water is 1.0 g/ml)

Determination of the dead volume from the injection to the column inlet (bottom) by direct connection to the UV-detector

Q [ml/min]	$V_{inj-col}$ [ml]	$\sigma^2_{inj-col}$ [ml^2]
1	1.67	0.22
1	1.74	0.29
1	1.74	0.27
1	1.68	0.23
2	1.74	0.29
4	1.68	0.29
1	1.64	0.19
1	1.65	0.20
1	1.72	0.29
1	1.67	0.21
2	1.72	0.25
4	1.67	0.28
1	1.65	0.19
1	1.68	0.22
Mean value:	1.69	0.24
Variance:	0.001	0.002
Standard Error:	0.01	0.01

Determination of the dead volume from the injection to the column inlet (bottom) by direct connection to the conductivity sensor

Q [ml/min]	$V_{inj-col*}$ [ml]	$\sigma^2_{inj-col*}$ [ml^2]
1	1.93	0.27
1	1.91	0.23
4	1.90	0.29
1	1.87	0.20
1	1.88	0.19
1	1.89	0.21
4	1.90	0.31
1	1.89	0.21
1	1.90	0.21
Mean value:	1.90	0.23
Variance:	0.0002	0.0019
Standard Error:	0.01	0.01

Calculated dead volumes

The volume of the empty column calculated from measurements and a drawing of the column

$V_{col,empty}$ = (0.40 cm/2)^2 π 47.96 cm + 2 $V_{distributor}$ = 6.03 ml + 4.2 ml = 10.23 ml

The volume of the top adaptor calculated from a drawing of the column

$V_{top\ adaptor}$ = (0.40 cm/2)^2 π 43.26 cm + $V_{distributor}$ = 5.44 ml + 2.1 ml = 7.54 ml

The volume of the bottom of the column

V_{bottom} = 10.23 ml - 7. 54 ml = 2.69 ml

The dead volume from the column outlet (top) to the UV detector

Length of tubes:
108.5 cm of tube with inner diameter 0.12 cm
20.0 cm of tube with inner diameter 0.075 cm

$V_{col\text{-}UV}$ = 20.0 cm (0.075 cm/2)^2 π + 108.5 cm (0.12 cm/2)^2 π = 1.32 ml

When injection is made at the top of the column the tubes connected to the column are switched. This means that the tube normally connected to the bottom of the column, is now connected to the top of the column.

The dead volume from the injection to the bed at the bottom of the column

$V_{inj\text{-}bed,bottom}$ = $V_{inj\text{-}col}$ + V_{bottom} = 1.69 ml + 2.69 ml = 4.38 ml

The dead volume from the injection to the bed at the top of the column

$V_{inj\text{-}bed,top}$ = $V_{inj\text{-}col}$ + V_{top} = 1.69 ml + 7.54 ml = 9.23 ml

The dead volume from the bed at the bottom of the column to the UV detector

$V_{bed,bottom-UV} = V_{col-UV} + V_{bottom} = 1.32\ ml + 2.69\ ml = 4.01\ ml$

The dead volume from the bed at the top of the column to the UV detector

$V_{bed,top-UV} = V_{col-UV} + V_{bottom} = 1.32\ ml + 7.54\ ml = 8.86\ ml$

APPENDIX H.II: DETERMINATION OF VOID VOLUME WITH LATEX BEADS ON THE PROTOTYPE MEDIA

Column no. 1, $P_{packing}$ = 14.1 bar (before the nitrate experiments)					
V_{elu} [ml]	$V_{inj.\ point}$ [ml]	V_R [ml]	$V_{R,cor}$ [ml]	σ^2 [ml^2]	σ^2_{cor} [ml^2]
181.16	0.93	180.23	168.17	26.23	7.05
434.31	253.22	181.09	169.03	28.14	8.96
1470.42	1286.00	184.42	172.36	23.96	4.78
3057.22	2872.60	184.62	172.56	22.86	3.68
4643.90	4459.21	184.70	172.64	26.19	7.01
	Mean value:	183.01	170.95	25.48	6.30
	Variance:	4.71	4.71	4.32	4.32
	Standard Error:	0.97	0.97	0.93	0.93

Column no. 1, $P_{packing}$ = 14.1 bar (after the nitrate experiments)					
V_{elu} [ml]	$V_{inj.\ point}$ [ml]	V_R [ml]	$V_{R,cor}$ [ml]	σ^2 [ml^2]	σ^2_{cor} [ml^2]
1467.56	1285.10	182.46	170.40	41.26	22.08
3053.30	2871.47	181.84	169.78	42.89	23.71
	Mean value:	182.15	170.09	42.08	22.90
	Variance:	0.19	0.19	1.33	1.33
	Standard Error:	0.31	0.31	0.81	0.81

Examples of calculations of V_R, $V_{R,cor}$ and σ^2_{cor}:

$V_R = V_{elu} - V_{inj.\ point}$ = 181.16 ml – 0.93 ml = 180.23 ml

$V_{R,cor} = V_R - V_{sys+col}$ = 180.23 ml – 12.06 ml = 168.17 ml

$\sigma^2_{cor} = \sigma^2 - \sigma^2_{sys+col}$ = 26.23 ml^2 – 19.18 ml^2 = 7.05 ml^2

Column no. 2, $P_{packing}$ = 7.2 bar (before the nitrate experiments)					
V_{elu} [ml]	$V_{inj.\ point}$ [ml]	V_R [ml]	$V_{R,cor}$ [ml]	σ^2 [ml^2]	σ^2_{cor} [ml^2]
393.52	200.90	192.62	180.56	37.69	18.51
592.29	400.26	192.03	179.97	30.98	11.80
793.91	600.79	193.12	181.06	39.88	20.70
191.63	0.53	191.10	179.04	29.60	10.42
1019.99	828.65	191.34	179.28	32.08	12.90
	Mean value:	192.04	179.98	34.04	14.86
	Variance:	0.72	0.72	20.08	20.08
	Standard Error:	0.38	0.38	2.00	2.00

Column no. 3, $P_{packing}$ = 7.2 bar (before the nitrate experiments)					
V_{elu} [ml]	$V_{inj.\ point}$ [ml]	V_R [ml]	$V_{R,cor}$ [ml]	σ^2 [ml^2]	σ^2_{cor} [ml^2]
196.74	0.55	196.19	184.13	68.24	49.06
398.49	199.58	198.91	186.85	63.05	43.87
598.99	399.43	199.56	187.50	67.04	47.86
798.52	599.42	199.10	187.04	72.71	53.53
740.95	543.74	197.22	185.16	63.43	44.25
740.58	543.61	196.98	184.92	75.79	56.61
	Mean value:	197.99	185.93	68.38	49.20
	Variance:	1.88	1.88	25.67	25.67
	Standard Error:	0.56	0.56	2.07	2.07

Column no. 3, $P_{packing}$ = 7.2 bar (after the nitrate experiments)					
V_{elu} [ml]	$V_{inj.\ point}$ [ml]	V_R [ml]	$V_{R,cor}$ [ml]	σ^2 [ml^2]	σ^2_{cor} [ml^2]
200.46	0.49	199.97	187.91	89.76	70.58
219.61	0.48	219.13	207.07	90.37	71.19
	Mean value:	209.55	197.49	90.07	70.89
	Variance:	183.55	183.55	0.19	0.19
	Standard Error:	9.58	9.58	0.31	0.31

Column no. 4, $P_{packing}$ = 21.2 bar (before the nitrate experiments)					
V_{elu} [ml]	$V_{inj.\ point}$ [ml]	V_R [ml]	$V_{R,cor}$ [ml]	σ^2 [ml^2]	σ^2_{cor} [ml^2]
366.80	249.36	117.44	105.38	61.16	41.98
616.59	499.47	117.12	105.06	62.91	43.73
865.99	749.31	116.68	104.62	59.70	40.52
1115.23	999.18	116.05	103.99	60.03	40.85
1364.71	1249.27	115.44	103.38	57.26	38.08
-134.66	-1.32	116.68	104.62	54.33	35.15
116.56	0.41	116.15	104.09	42.20	23.02
366.90	250.54	116.36	104.30	51.67	32.49
115.25	-1.25	116.50	104.44	66.93	47.75
	Mean value:	116.49	104.43	57.35	38.17
	Variance:	0.35	0.35	52.63	52.63
	Standard Error:	0.20	0.20	2.42	2.42

Column no. 4, $P_{packing}$ = 21.2 bar (after the nitrate experiments)					
V_{elu} [ml]	$V_{inj.\ point}$ [ml]	V_R [ml]	$V_{R,cor}$ [ml]	σ^2 [ml^2]	σ^2_{cor} [ml^2]
1014.58	877.71	136.87	124.81	41.43	22.25
1213.35	1077.49	135.86	123.80	43.84	24.66
1414.59	1277.63	136.97	124.91	45.65	26.47
	Mean value:	136.57	124.51	43.64	24.46
	Variance:	0.38	0.38	4.48	4.48
	Standard Error:	0.35	0.35	1.22	1.22

Column no. 5, $P_{packing}$ = 10.0 bar (before the nitrate experiments)					
V_{elu} [ml]	$V_{inj.\ point}$ [ml]	V_R [ml]	$V_{R,cor}$ [ml]	σ^2 [ml^2]	σ^2_{cor} [ml^2]
458.33	249.33	209.00	196.94	56.15	36.97
715.60	499.37	216.23	204.17	52.76	33.58
967.13	749.23	217.90	205.84	50.21	31.03
1216.77	999.21	217.57	205.51	55.69	36.51
216.62	0.51	216.11	204.05	51.61	32.43
706.29	499.60	206.69	194.63	55.63	36.45
214.13	0.45	213.68	201.62	58.78	39.60
513.45	299.98	213.47	201.41	62.84	43.66
815.78	599.32	216.47	204.41	57.33	38.15
1117.43	899.76	217.68	205.62	56.65	37.47
1416.89	1199.30	217.59	205.53	62.33	43.15
	Mean value:	214.76	202.70	56.36	37.18
	Variance:	14.22	14.22	15.89	15.89
	Standard Error:	1.14	1.14	1.20	1.20

Column no. 5, $P_{packing}$ = 10.0 bar (after the nitrate experiments)					
V_{elu} [ml]	$V_{inj.\ point}$ [ml]	V_R [ml]	$V_{R,cor}$ [ml]	σ^2 [ml^2]	σ^2_{cor} [ml^2]
221.48	1.50	219.98	207.92	66.91	47.73
514.08	300.50	213.58	201.52	64.50	45.32
217.12	2.50	214.62	202.56	111.27	92.09
493.13	300.50	192.63	180.57	102.12	82.94
309.91	2090.50	219.41	207.35	84.94	65.76
	Mean value:	212.04	199.98	85.95	66.77
	Variance:	100.63	100.63	345.24	345.24
	Standard Error:	4.10	4.10	7.59	7.59

Column no. 6, $P_{packing}$ = 9.8 bar (before the nitrate experiments)					
V_{elu} [ml]	$V_{inj.\ point}$ [ml]	V_R [ml]	$V_{R,cor}$ [ml]	σ^2 [ml^2]	σ^2_{cor} [ml^2]
-70.95	-249.00	178.05	165.99	52.84	33.66
-71.33	-250.00	178.67	166.61	70.88	51.70
-73.68	-250.00	176.32	164.26	75.26	56.08
-74.69	-250.00	175.31	163.25	75.85	56.67
1175.97	1000.50	175.47	163.41	90.35	71.17
3368.68	3185.50	183.18	171.12	82.57	63.39
2263.40	2080.50	182.90	170.84	65.00	45.82
-66.34	-249.00	182.66	170.60	63.22	44.04
-70.83	-250.00	179.17	167.11	75.95	56.77
-68.14	-250.00	181.86	169.80	90.71	71.53
933.00	750.50	182.50	170.44	71.15	51.97
	Mean value:	179.65	167.59	73.98	54.80
	Variance:	9.62	9.62	129.17	129.17
	Standard Error:	0.94	0.94	3.43	3.43

Column no. 6, $P_{packing}$ = 9.8 bar (after the nitrate experiments)					
V_{elu} [ml]	$V_{inj.\ point}$ [ml]	V_R [ml]	$V_{R,cor}$ [ml]	σ^2 [ml^2]	σ^2_{cor} [ml^2]
-50.37	-49.00	198.63	186.57	61.86	42.68
-54.87	-250.00	195.13	183.07	73.27	54.09
-53.37	-50.00	196.63	184.57	62.58	43.40
949.47	750.50	198.97	186.91	64.05	44.87
3104.69	2902.50	202.19	190.13	59.28	40.10
3395.01	3200.50	194.51	182.45	71.41	52.23
6851.24	6650.50	200.74	188.68	44.05	24.87
7127.24	6930.50	196.74	184.68	41.35	22.17
	Mean value:	197.94	185.88	59.73	40.55
	Variance:	7.18	7.18	133.55	133.55
	Standard Error:	0.95	0.95	4.09	4.09

Column no. 7, $P_{packing}$ = 16.9 bar (before the nitrate experiments)					
V_{elu} [ml]	$V_{inj.\ point}$ [ml]	V_R [ml]	$V_{R,cor}$ [ml]	σ^2 [ml^2]	σ^2_{cor} [ml^2]
-95.46	-248.50	153.04	140.98	49.61	30.43
-96.20	-249.50	153.30	141.24	48.46	29.28
-96.13	-49.50	153.37	141.31	49.47	30.29
906.99	750.50	156.49	144.43	48.72	29.54
2469.18	2302.50	166.68	154.62	37.52	18.34
2747.48	2585.50	161.98	149.92	40.99	21.81
5646.98	5480.50	166.48	154.42	39.93	20.75
-92.91	-248.50	155.59	143.53	38.21	19.03
-90.89	-249.50	158.61	146.55	38.02	18.84
-90.96	-249.50	158.54	146.48	37.06	17.88
-88.91	-249.50	160.59	148.53	45.40	26.22
-86.02	-249.50	163.48	151.42	39.56	20.38
1416.36	1250.50	165.86	153.80	47.22	28.04
-83.90	-248.50	164.60	152.54	45.57	26.39
-88.09	-249.50	161.41	149.35	39.00	19.82
-87.59	-249.50	161.91	149.85	47.66	28.48
914.66	750.50	164.16	152.10	43.14	23.96
	Mean value:	160.36	148.30	43.27	24.09
	Variance:	22.03	22.03	22.08	22.08
	Standard Error:	1.14	1.14	1.14	1.14

Column no. 7, $P_{packing}$ = 16.9 bar (after the nitrate experiments)					
V_{elu} [ml]	$V_{inj.\ point}$ [ml]	V_R [ml]	$V_{R,cor}$ [ml]	σ^2 [ml^2]	σ^2_{cor} [ml^2]
171.17	1.50	169.67	157.61	41.43	22.25
407.82	250.50	157.32	145.26	34.89	15.71
662.55	500.50	162.05	149.99	41.24	22.06
2447.71	2302.50	145.21	133.15	22.66	3.48
2729.68	2585.50	144.18	132.12	32.69	13.51
5366.52	5220.50	146.02	133.96	24.59	5.41
5625.97	5480.50	145.47	133.41	29.02	9.84
1353.71	1210.50	143.21	131.15	32.33	13.15
1583.94	1440.50	143.44	131.38	42.89	23.71
	Mean value:	150.73	138.67	33.53	14.35
	Variance:	95.40	95.40	53.98	53.98
	Standard Error:	3.26	3.26	2.45	2.45

Column no. 8, $P_{packing}$ = 14.1 bar (before the nitrate experiments)					
V_{elu} [ml]	$V_{inj.\ point}$ [ml]	V_R [ml]	$V_{R,cor}$ [ml]	σ^2 [ml^2]	σ^2_{cor} [ml^2]
-94.00	-49.00	155.00	142.94	31.49	12.31
405.87	250.50	155.37	143.31	28.49	9.31
	Mean value:	155.19	143.13	29.99	10.81
	Variance:	0.07	0.07	4.49	4.49
	Standard Error:	0.19	0.19	1.50	1.50

Column no. 8, $P_{packing}$ = 14.1 bar (after the nitrate experiments)					
V_{elu} [ml]	$V_{inj.\ point}$ [ml]	V_R [ml]	$V_{R,cor}$ [ml]	σ^2 [ml^2]	σ^2_{cor} [ml^2]
850.30	701.50	148.80	136.74	59.35	40.17
1070.36	920.50	149.86	137.80	58.70	39.52
	Mean value:	149.33	137.27	59.03	39.85
	Variance:	0.56	0.56	0.21	0.21
	Standard Error:	0.53	0.53	0.32	0.32

APPENDIX H.III: DETERMINATION OF LIQUID VOLUME WITH $NaNO_3$ ON THE PROTOTYPE MEDIA

Column no. 1, $P_{packing}$ = 14.1 bar					
V_{elu} [ml]	$V_{inj.\ point}$ [ml]	V_R [ml]	$V_{R,cor}$ [ml]	σ^2 [ml^2]	σ^2_{cor} [ml^2]
561.86	0.53	561.33	549.27	456.42	437.24
760.83	200.76	560.07	548.01	423.10	403.92
561.90	0.47	561.44	549.38	475.85	456.67
761.90	200.78	561.13	549.07	434.78	415.60
960.87	400.33	560.54	548.48	434.13	414.95
1160.44	600.75	559.69	547.63	413.04	393.86
	Mean value:	560.70	548.64	439.55	420.37
	Variance:	0.51	0.51	525.59	525.59
	Standard Error:	0.29	0.29	9.36	9.36

Examples of calculations of V_R, $V_{R,cor}$ and σ^2_{cor}:

$V_R = V_{elu} - V_{inj.\ Point}$ = 1160.44 ml – 600.75 ml = 559.69 ml

$V_{R,cor} = V_R - V_{sys+col}$ = 559.69 ml – 12.06 ml = 547.63 ml

$\sigma^2_{cor} = \sigma^2 - \sigma^2_{sys+col}$ = 413.04 ml^2 – 19.18 ml^2 = 393.86 ml^2

Column no. 3, $P_{packing}$ = 7.2 bar					
V_{elu} [ml]	$V_{inj.\ point}$ [ml]	V_R [ml]	$V_{R,cor}$ [ml]	σ^2 [ml^2]	σ^2_{cor} [ml^2]
901.85	300.38	601.48	589.42	271.62	252.44
1101.68	500.40	601.29	589.23	268.49	249.31
1401.52	800.38	601.14	589.08	269.92	250.74
1601.81	1000.41	601.40	589.34	269.10	249.92
	Mean value:	601.33	589.27	269.78	250.60
	Variance:	0.02	0.02	1.84	1.84
	Standard Error:	0.07	0.07	0.68	0.68

Column no. 4, $P_{packing}$ = 21.2 bar					
V_{elu} [ml]	$V_{inj.\ point}$ [ml]	V_R [ml]	$V_{R,cor}$ [ml]	σ^2 [ml^2]	σ^2_{cor} [ml^2]
464.96	0.58	464.38	452.32	138.95	119.77
665.05	199.46	465.59	453.53	136.44	117.26
865.57	399.45	466.12	454.06	136.63	117.45
1066.05	599.39	466.66	454.60	135.44	116.26
1266.09	799.39	466.70	454.64	134.36	115.18
467.53	0.53	467.00	454.94	139.53	120.35
	Mean value:	466.08	454.02	136.89	117.71
	Variance:	0.94	0.94	3.99	3.99
	Standard Error:	0.40	0.40	0.82	0.82

Column no. 5, $P_{packing}$ = 10.0 bar					
V_{elu} [ml]	$V_{inj.\ point}$ [ml]	V_R [ml]	$V_{R,cor}$ [ml]	σ^2 [ml^2]	σ^2_{cor} [ml^2]
1332.74	749.24	583.50	571.44	184.74	165.56
1582.70	999.27	583.43	571.37	181.51	162.33
584.11	0.52	583.59	571.53	184.17	164.99
832.96	249.38	583.58	571.52	180.85	161.67
1082.97	499.38	583.59	571.53	183.14	163.96
	Mean value:	583.54	571.48	182.88	163.70
	Variance:	0.01	0.01	2.80	2.80
	Standard Error:	0.03	0.03	0.75	0.75

Column no. 6, $P_{packing}$ = 9.8 bar					
V_{elu} [ml]	$V_{inj.\ point}$ [ml]	V_R [ml]	$V_{R,cor}$ [ml]	σ^2 [ml^2]	σ^2_{cor} [ml^2]
50.45	-499.00	549.45	537.39	119.13	99.95
48.87	-500.00	548.87	536.81	115.06	95.88
49.10	-500.00	549.10	537.04	115.23	96.05
49.05	-500.00	549.05	536.99	111.46	92.28
48.92	-500.00	548.92	536.86	112.08	92.90
3799.73	3250.50	549.23	537.17	111.55	92.37
4049.98	3500.50	549.48	537.42	112.85	93.67
4801.04	4250.50	550.54	538.48	118.30	99.12
50.52	-499.00	549.52	537.46	127.69	108.51 *
49.27	-500.00	549.27	537.21	127.88	108.70 *
1549.76	1000.50	549.26	537.20	129.29	110.11 *
1799.89	1250.50	549.39	537.33	127.20	108.02 *
5.62	-499.00	544.62	532.56	129.43	110.25 *
98.27	250.50	547.77	535.71	120.84	101.66 *
1049.52	500.50	549.02	536.96	123.48	104.30 *
51.26	-499.00	550.26	538.20	128.17	108.99 *
50.04	-500.00	550.04	537.98	126.01	106.83 *
1550.79	1000.50	550.29	538.23	127.73	108.55 *
	Mean value:	549.33	537.27	114.46	95.28
	Variance:	0.29	0.29	9.05	9.05
	Standard Error:	0.19	0.19	1.06	1.06

The ten rows marked with * are not included in calculation of the mean value and the variance.

These ten determinations were made after a second round of latex experiments.

Column no. 7, $P_{packing}$ = 16.9 bar					
V_{elu} [ml]	$V_{inj.\ point}$ [ml]	V_R [ml]	$V_{R,cor}$ [ml]	σ^2 [ml^2]	σ^2_{cor} [ml^2]
2509.26	2001.50	507.76	495.70	246.58	227.40
3058.35	2550.50	507.85	495.79	241.65	222.47
3608.58	3100.50	508.08	496.02	248.09	228.91
4158.39	3650.50	507.89	495.83	245.26	226.08
1608.96	1100.50	508.46	496.40	246.03	226.85
	Mean value:	508.01	495.95	245.52	226.34
	Variance:	0.08	0.08	5.77	5.77
	Standard Error:	0.12	0.12	1.07	1.07

Column no. 8, $P_{packing}$ = 14.1 bar					
V_{elu} [ml]	$V_{inj.\ point}$ [ml]	V_R [ml]	$V_{R,cor}$ [ml]	σ^2 [ml^2]	σ^2_{cor} [ml^2]
-11.55	-548.50	536.95	524.89	191.82	172.64
-12.48	-549.50	537.02	524.96	185.52	166.34
1638.05	1100.50	537.55	525.49	185.84	166.66
	Mean value:	537.17	525.11	187.73	168.55
	Variance:	0.11	0.11	2.05	2.05
	Standard Error:	0.19	0.19	12.59	12.59

APPENDIX H.IV: REVERSED FLOW EXPERIMENTS WITH LATEX BEADS ON THE PROTOTYPE MEDIA

Column no. 1, $P_{packing}$ = 14.1 bar (before nitrate experiments)

V_{elu} [ml]	$V_{inj.\ point}$ [ml]	$V_{forward}$ [ml]	V_R [ml]	$V_{R,mean}$ [ml]	$V_{R,cor}$ [ml]	σ^2 [ml^2]	σ^2_{mean} [ml^2]
43.63	0.56	16.23	43.07			4.86	
43.02	0.53	16.23	42.50	42.18	33.79	4.98	5.00
1627.69	1585.99	16.23	41.71			4.95	
3213.82	3172.36	16.23	41.46			5.22	
44.26	1.00	16.82	43.26			5.54	
44.03	0.98	16.82	43.05	43.05	34.66	5.10	5.30
1630.51	1587.56	16.82	42.95			5.16	
3216.97	3174.05	16.82	42.92			5.39	
212.02	101.56	49.87	110.46			7.39	
211.56	101.78	49.87	109.78	109.64	101.25	9.67	7.29
1796.28	1687.02	49.87	109.26			5.95	
3382.21	3273.15	49.87	109.06			6.15	
257.44	146.98	50.46	110.46			6.10	
212.44	102.26	50.46	110.18	110.32	101.93	6.29	6.24
1798.58	1688.29	50.46	110.29			6.22	
3385.45	3275.09	50.46	110.36			6.35	
430.66	252.61	83.51	178.05			11.26	
429.55	252.73	83.51	176.82	177.02	168.63	12.74	10.04
2014.38	1837.95	83.51	176.43			8.05	
3600.68	3423.91	83.51	176.77			8.11	
430.84	253.17	84.10	177.68			7.73	
2016.68	1839.21	84.10	177.48	177.49	169.10	7.29	7.42
3603.76	3426.44	84.10	177.32			7.22	
773.76	528.66	117.14	245.10			12.04	
772.24	528.36	117.14	243.88	244.31	235.92	10.00	10.23
2357.74	2113.80	117.14	243.94			8.65	
773.85	529.20	117.73	244.66			8.94	
2360.54	2115.37	117.73	245.18	244.94	236.55	9.17	9.06
3947.35	3702.35	117.73	245.00			9.06	
1186.37	874.84	150.78	311.53			17.89	
1184.85	873.88	150.78	310.97	311.14	302.75	11.55	13.04
2770.88	2459.96	150.78	310.92			9.69	
1187.46	875.30	151.37	312.16			9.90	
2773.37	2461.60	151.37	311.78	311.96	303.57	9.94	9.87
4360.25	4048.31	151.37	311.94			9.77	

Column no. 1, $P_{packing}$ = 14.1 bar (after nitrate experiments)

V_{elu} [ml]	$V_{inj.\ point}$ [ml]	$V_{forward}$ [ml]	V_R [ml]	$V_{R,cor}$ [ml]	σ^2 [ml^2]
345.76	301.37	16.23	44.40	36.01	3.69
514.00	402.29	49.87	111.71	103.32	4.42
732.12	553.04	83.51	179.08	170.69	5.19
1074.67	828.99	117.14	245.68	237.29	6.14
1487.42	1174.53	150.78	312.90	304.51	7.32

Column no. 2, $P_{packing}$ = 7.2 (before nitrate experiments)

V_{elu} [ml]	$V_{inj.\ point}$ [ml]	$V_{forward}$ [ml]	V_R [ml]	$V_{R,mean}$ [ml]	$V_{R,cor}$ [ml]	σ^2 [ml^2]	σ^2_{mean} [ml^2]
46.71	0.47	18.00	46.24	45.87	37.48	3.48	3.77
45.95	0.45	18.00	45.50			4.05	
349.93	301.31	19.00	48.62	48.62	40.23	3.55	3.55
219.48	101.36	53.99	118.12	118.19	109.80	4.47	4.78
219.98	101.72	53.99	118.26			5.10	
526.99	402.42	57.00	124.57	124.57	116.18	4.90	4.90
467.62	277.29	89.98	190.33	190.45	182.06	6.96	6.35
467.90	277.34	89.98	190.56			5.75	
778.86	578.05	95.00	200.82	200.82	192.43	5.37	5.37
790.10	528.02	125.98	262.08	262.37	253.98	6.88	6.80
791.06	528.40	125.98	262.66			6.73	
1406.48	1129.48	133.00	277.01	277.01	268.62	5.92	5.92
1188.04	853.91	161.97	334.13	334.13	325.74	7.38	7.38
1808.11	1455.32	171.00	352.80	352.80	344.41	6.92	6.92

Column no. 3, $P_{packing}$ = 7.2 (before nitrate experiments)

V_{elu} [ml]	$V_{inj.\ point}$ [ml]	$V_{forward}$ [ml]	V_R [ml]	$V_{R,mean}$ [ml]	$V_{R,cor}$ [ml]	σ^2 [ml^2]	σ^2_{mean} [ml^2]
47.43	0.51	18.71	46.92	47.22	38.83	4.72	4.59
324.09	276.33	18.71	47.76			4.34	
47.43	0.45	18.71	46.98			4.72	
223.81	101.66	56.14	122.15	122.18	113.79	5.37	5.40
273.89	151.68	56.14	122.22			5.45	
689.99	567.60	56.14	122.40			5.70	
362.58	240.64	56.14	121.94			5.09	
479.74	282.72	93.57	197.02	197.15	188.76	6.32	6.18
479.95	282.64	93.57	197.31			6.16	
599.92	402.77	93.57	197.15			6.47	
1125.82	928.51	93.57	197.32			5.91	
674.72	477.78	93.57	196.94			6.04	
1091.51	819.67	130.99	271.84	271.81	263.42	6.68	6.89
1091.58	819.54	130.99	272.04			7.11	
1035.62	763.55	130.99	272.07			7.22	
271.96	0.53	130.99	271.42			6.85	
1209.27	937.61	130.99	271.67			6.62	
1497.21	1150.79	168.42	346.42	346.48	338.09	7.94	7.70
1581.01	1234.63	168.42	346.38			8.10	
347.25	0.53	168.42	346.72			7.42	
1651.00	1304.61	168.42	346.39			7.33	

Column no. 3, $P_{packing}$ = 7.2 (after nitrate experiments)

V_{elu} [ml]	$V_{inj.\ point}$ [ml]	$V_{forward}$ [ml]	V_R [ml]	$V_{R,cor}$ [ml]	σ^2 [ml^2]
471.08	424.41	18.71	46.68	38.29	11.52
786.30	665.24	56.14	121.07	112.68	10.26
1118.84	922.37	93.57	196.48	188.09	10.79
1533.66	1262.54	130.99	271.12	262.73	11.35
1974.42	1629.26	168.42	345.16	336.77	12.03

Column no. 4, $P_{packing}$ = 21.2 (before nitrate experiments)

V_{elu} [ml]	$V_{inj.\ point}$ [ml]	$V_{forward}$ [ml]	V_R [ml]	$V_{R,mean}$ [ml]	$V_{R,cor}$ [ml]	σ^2 [ml^2]	σ^2_{mean} [ml^2]
30.82	0.54	10.44	30.29			2.51	
31.08	0.50	10.44	30.57	30.40	22.01	6.73	4.48
754.58	724.30	10.44	30.28			4.57	
756.16	725.71	10.44	30.46			4.10	
41.06	0.50	15.66	40.56			4.29	
41.17	0.58	15.66	40.59	40.77	32.38	4.37	4.10
41.23	0.55	15.66	40.67			3.98	
211.55	170.31	15.66	41.24			3.76	
51.66	0.49	20.89	51.18			4.63	
51.47	0.47	20.89	51.00	51.14	42.75	4.69	4.69
1405.28	1354.04	20.89	51.24			4.75	
226.40	154.47	31.33	71.93			4.67	
231.13	159.50	31.33	71.63			3.86	
251.88	179.63	31.33	72.25	71.92	63.53	4.97	4.61
251.12	179.24	31.33	71.88			5.13	
1605.98	1534.07	31.33	71.91			4.43	
467.25	374.37	41.77	92.88			5.37	
1817.00	1724.14	41.77	92.86	92.89	84.50	4.92	4.97
93.40	0.49	41.77	92.91			4.62	
458.71	345.04	52.22	113.68			5.36	
459.06	345.36	52.22	113.70	113.62	105.23	5.53	5.42
478.95	365.13	52.22	113.82			5.38	
688.15	574.87	52.22	113.28			5.42	
318.79	184.09	62.66	134.71	134.71	126.32	4.95	4.95
705.58	549.90	73.10	155.68			5.69	
725.33	569.67	73.10	155.66	155.68	147.29	6.14	5.72
924.98	769.28	73.10	155.70			5.33	
570.48	394.01	83.55	176.47	176.47	168.08	5.76	5.76
981.99	784.63	93.99	197.36			6.13	
1001.81	804.40	93.99	197.41	197.26	188.87	6.86	6.28
1201.46	1004.45	93.99	197.01			5.85	

Column no. 4, $P_{packing}$ = 21.2 (after nitrate experiments)

V_{elu} [ml]	$V_{inj.\ point}$ [ml]	$V_{forward}$ [ml]	V_R [ml]	$V_{R,mean}$ [ml]	$V_{R,cor}$ [ml]	σ^2 [ml^2]	σ^2_{mean} [ml^2]
0.46	40.85	15.66	32.46	32.46	24.07	4.00	4.00
0.48	52.72	20.89	44.33	43.71	35.32	4.51	4.42
0.55	51.49	20.89	43.10			4.33	
0.47	72.33	31.33	63.94	63.96	55.57	5.47	5.53
1058.75	72.37	31.33	63.98			5.60	
169.45	94.30	41.77	85.91	85.28	76.89	6.47	6.42
169.79	93.05	41.77	84.66			6.38	
1238.65	114.33	52.22	105.94	105.65	97.26	7.07	6.59
179.26	113.75	52.22	105.36			6.11	
359.45	135.84	62.66	127.45	126.79	118.40	7.39	7.73
359.61	134.53	62.66	126.14			8.08	
1438.77	155.49	73.10	147.10	147.15	138.76	8.00	8.30
379.11	155.59	73.10	147.20			8.61	
569.87	177.25	83.55	168.86	168.42	160.03	8.31	8.37
570.12	176.37	83.55	167.98			8.43	
1668.71	196.75	93.99	188.36	188.28	179.89	10.12	9.46
608.94	196.60	93.99	188.21			8.81	

Column no. 5, $P_{packing}$ = 10.0 bar (before nitrate experiments)

V_{elu} [ml]	$V_{inj.\ point}$ [ml]	$V_{forward}$ [ml]	V_R [ml]	$V_{R,mean}$ [ml]	$V_{R,cor}$ [ml]	σ^2 [ml^2]	σ^2_{mean} [ml^2]
42.24	0.46	15.60	41.78	41.78	33.39	11.38	11.38
1312.38	1263.81	19.50	48.57	48.57	40.18	9.61	9.61
1673.80	1623.31	20.38	50.49	50.49	42.10	9.69	9.69
295.62	244.47	20.80	51.15	51.15	42.76	10.10	10.10
71.38	0.48	29.25	70.91	70.91	62.52	11.49	11.49
71.17	0.45	30.57	70.72	70.71	62.32	11.16	11.08
71.25	0.54	30.57	70.70			10.99	
375.59	284.12	40.77	91.47	91.35	82.96	12.92	13.22
375.39	284.16	40.77	91.23			13.53	
562.09	469.34	41.61	92.76	92.76	84.37	11.75	11.75
132.66	0.45	61.15	132.22	132.22	123.83	14.56	14.56
834.05	699.38	62.41	134.67	134.67	126.28	13.48	13.48
722.15	549.14	81.53	173.01	173.03	164.64	15.51	15.83
722.41	549.35	81.53	173.06			16.15	
1115.62	939.54	83.22	176.08	176.08	167.69	14.81	14.81
498.08	284.04	101.91	214.04	214.04	205.65	16.10	16.10
1113.97	859.36	122.30	254.61	254.52	246.13	16.38	17.38
1113.91	859.47	122.30	254.44			18.38	
909.65	613.91	142.68	295.75	295.75	287.36	18.41	18.41
1375.50	998.78	183.45	376.72	376.72	368.33	21.49	21.49

Column no. 5, $P_{packing}$ = 10.0 (after nitrate experiments)

V_{elu} [ml]	$V_{inj.\ point}$ [ml]	$V_{forward}$ [ml]	V_R [ml]	$V_{R,mean}$ [ml]	$V_{R,cor}$ [ml]	σ^2 [ml^2]	σ^2_{mean} [ml^2]
653.92	602.50	20.38	51.42	51.42	43.03	13.53	13.53
964.83	871.50	40.77	93.33	92.35	83.96	11.35	13.04
962.88	871.50	40.77	91.38			14.74	
1295.00	1161.50	61.15	133.50	132.91	124.52	13.06	14.33
1293.83	1161.50	61.15	132.33			15.59	
1646.07	1471.50	81.53	174.57	173.66	165.27	16.82	17.07
1644.26	1471.50	81.53	172.76			17.32	
2017.30	1801.50	101.91	215.80	214.79	206.40	17.13	17.44
245.29	31.50	101.91	213.79			17.74	
2408.61	2151.50	122.30	257.11	256.17	247.78	16.66	17.99
636.73	381.50	122.30	255.23			19.32	
2829.51	2531.50	142.68	298.01	296.82	288.43	17.37	18.59
1057.13	761.50	142.68	295.63			19.82	
3270.62	931.50	163.06	339.12	337.87	329.48	19.38	20.36
1498.11	161.50	163.06	336.61			21.35	
3731.12	351.50	183.45	379.62	378.33	369.94	21.23	21.72
1958.54	581.50	183.45	377.04			22.21	

Column no. 6, $P_{packing}$ = 9.8 bar (before nitrate experiments)

V_{elu} [ml]	$V_{inj.\ point}$ [ml]	$V_{forward}$ [ml]	V_R [ml]	$V_{R,mean}$ [ml]	$V_{R,cor}$ [ml]	σ^2 [ml^2]	σ^2_{mean} [ml^2]
45.41	2.50	16.40	42.91	44.00	35.61	11.44	10.87
3632.58	3587.50	16.40	45.08			10.29	
2998.18	2936.50	24.60	61.68	61.68	53.29	10.09	10.09
332.99	256.50	32.80	76.49			10.90	
3919.91	3841.50	32.80	78.41	77.76	69.37	10.61	10.53
2719.88	2641.50	32.80	78.38			10.10	
635.51	526.50	49.20	109.01			12.52	
4227.43	4116.50	49.20	110.93	110.22	101.83	11.33	12.05
2432.21	2321.50	49.20	110.71			12.30	
959.05	816.50	65.60	142.55			12.44	
4550.53	4406.50	65.60	144.03	143.29	134.90	11.62	12.61
2124.79	1981.50	65.60	143.29			13.76	
1301.90	1126.50	82.00	175.40			13.33	
4893.56	4716.50	82.00	177.06	176.02	167.63	12.53	13.66
1797.11	1621.50	82.00	175.61			15.10	
1660.08	1451.50	98.40	208.58			13.31	
408.46	201.50	98.40	206.96	208.04	199.65	12.70	13.99
1450.07	1241.50	98.40	208.57			15.94	
2038.55	1796.50	114.80	242.05	241.32	232.93	15.36	15.22
787.08	546.50	114.80	240.58			15.08	
2436.57	2161.50	131.20	275.07	274.63	266.24	16.65	16.53
1190.69	916.50	131.20	274.19			16.40	
2849.83	2541.50	147.60	308.33	307.18	298.79	16.99	17.94
308.53	2.50	147.60	306.03			18.89	

Column no. 6, $P_{packing}$ = 9.8 (after nitrate experiments)

V_{elu} [ml]	$V_{inj.\ point}$ [ml]	$V_{forward}$ [ml]	V_R [ml]	$V_{R,mean}$ [ml]	$V_{R,cor}$ [ml]	σ^2 [ml^2]	σ^2_{mean} [ml^2]
6599.93	6536.50	24.60	63.43	63.43	55.04	5.38	5.38
348.41	271.50	32.80	76.91	78.29	69.90	6.53	6.83
6321.17	6241.50	32.80	79.67			7.13	
651.02	541.50	49.20	109.52	111.03	102.64	7.53	7.18
6034.04	5921.50	49.20	112.54			6.84	
973.79	831.50	65.60	142.29	143.41	135.02	7.86	8.16
5726.03	5581.50	65.60	144.53			8.46	
1316.99	1141.50	82.00	175.49	176.46	168.07	8.75	8.60
5398.93	5221.50	82.00	177.43			8.44	
1675.54	1466.50	98.40	209.04	209.91	201.52	10.08	10.09
5052.27	4841.50	98.40	210.77			10.11	
2053.39	1811.50	114.80	241.89	242.58	234.19	11.37	11.48
4689.78	4446.50	114.80	243.28			11.59	
2451.52	2176.50	131.20	275.02	275.68	267.29	12.63	12.55
4312.85	4036.50	131.20	276.35			12.46	
2864.42	2556.50	147.60	307.92	307.78	299.39	13.96	13.07
3910.15	3602.50	147.60	307.65			12.17	

Column no. 7, $P_{packing}$ = 16.9 bar (before nitrate experiments)

V_{elu} [ml]	$V_{inj.\ point}$ [ml]	$V_{forward}$ [ml]	V_R [ml]	$V_{R,mean}$ [ml]	$V_{R,cor}$ [ml]	σ^2 [ml^2]	σ^2_{mean} [ml^2]
2928.43	2890.00	14.15	38.43	38.43	30.04	14.25	14.25
269.25	216.50	21.23	52.75			11.71	
194.29	141.50	21.23	52.79	52.78	44.39	17.58	14.62
309.31	256.50	21.23	52.81			14.57	
263.57	196.50	28.30	67.07			16.76	
3150.78	3084.00	28.30	66.78	67.00	58.61	17.12	18.15
278.66	211.50	28.30	67.16			20.58	
496.98	401.50	42.45	95.48			17.02	
3389.42	3294.00	42.45	95.42	95.41	87.02	21.05	19.18
526.83	431.50	42.45	95.33			19.48	
750.48	626.50	56.60	123.98			24.86	
3643.45	3519.00	56.60	124.45	124.09	115.70	24.12	24.11
795.35	671.50	56.60	123.85			23.36	
1023.87	871.50	70.75	152.37			18.76	
3916.97	3764.00	70.75	152.97	152.81	144.42	23.48	21.33
1084.60	931.50	70.75	153.10			21.75	
1307.57	1126.50	84.90	181.07			24.13	
4205.08	4024.00	84.90	181.08	181.31	172.92	22.68	24.69
1383.29	1201.50	84.90	181.79			27.26	
1611.44	1401.50	99.05	209.94			29.09	
4514.29	4304.00	99.05	210.29	210.06	201.67	26.11	28.85
1701.47	1491.50	99.05	209.97			31.36	
1929.49	1691.50	113.20	237.99			24.71	
4837.40	4599.00	113.20	238.40	238.41	230.02	25.30	26.62
2035.36	1796.50	113.20	238.86			29.86	
2262.63	1996.50	127.35	266.13			22.57	
5176.12	4909.00	127.35	267.12	266.70	258.31	23.90	25.42
2383.36	2116.50	127.35	266.86			29.79	

Column no. 8, $P_{packing}$ = 14.1 bar (before nitrate experiments)

V_{elu} [ml]	$V_{inj.\ point}$ [ml]	$V_{forward}$ [ml]	V_R [ml]	$V_{R,mean}$ [ml]	$V_{R,cor}$ [ml]	σ^2 [ml^2]	σ^2_{mean} [ml^2]
41.16	2.50	14.25	38.66	38.66	30.27	16.05	16.05
274.44	206.50	28.49	67.94	67.77	59.38	14.32	17.14
274.10	206.50	28.49	67.60			19.95	
518.17	421.50	42.74	96.67	96.38	87.99	16.21	17.25
517.59	421.50	42.74	96.09			18.28	
782.11	656.50	56.98	125.61	125.30	116.91	15.53	18.41
781.49	656.50	56.98	124.99			21.28	
1070.77	916.50	71.23	154.27	154.15	145.76	19.18	20.37
1070.52	916.50	71.23	154.02			21.57	
1364.33	1181.50	85.47	182.83	182.78	174.39	19.54	19.66
1364.23	1181.50	85.47	182.73			19.78	
1677.63	1466.50	99.72	211.13	211.07	202.68	21.09	23.48
1677.51	1466.50	99.72	211.01			25.87	
2006.37	1766.50	113.96	239.87	239.88	231.49	21.09	22.55
2006.40	1766.50	113.96	239.90			24.01	
2354.77	2086.50	128.21	268.27	268.47	260.08	21.06	23.98
2355.16	2086.50	128.21	268.66			26.91	

APPENDIX H.V: REVERSED FLOW EXPERIMENTS WITH $NaNO_3$ ON THE PROTOTYPE MEDIA

Column no. 1, $P_{packing}$ = 14.1 bar

V_{elu} [ml]	$V_{inj.\ point}$ [ml]	$V_{forward}$ [ml]	V_R [ml]	$V_{R,mean}$ [ml]	$V_{R,cor}$ [ml]	σ^2 [ml^2]	σ^2_{mean} [ml^2]
121.02	0.55	54.82	120.47	120.21	111.82	16.38	16.94
120.51	0.57	54.82	119.94			17.51	
541.73	201.71	164.47	340.02	339.78	331.39	38.47	40.28
541.21	201.66	164.47	339.55			42.08	
1182.18	623.00	274.12	559.19	558.99	550.60	59.76	62.31
1180.96	622.17	274.12	558.79			64.87	
2042.26	1263.88	383.76	778.39	778.16	769.77	89.84	87.97
2041.06	1263.13	383.76	777.93			86.10	
3122.63	2124.71	493.41	997.93	997.75	989.36	116.41	117.06
3121.13	2123.55	493.41	997.58			117.71	

Column no. 3, $P_{packing}$ = 7.2

V_{elu} [ml]	$V_{inj.\ point}$ [ml]	$V_{forward}$ [ml]	V_R [ml]	$V_{R,mean}$ [ml]	$V_{R,cor}$ [ml]	σ^2 [ml^2]	σ^2_{mean} [ml^2]
128.02	0.44	58.57	127.58			35.34	
128.24	0.53	58.57	127.71	127.83	119.44	32.74	33.26
128.89	0.52	58.57	128.38			33.52	
2908.81	2781.14	58.57	127.67			31.45	
563.88	201.76	175.71	362.12			67.63	
983.01	621.32	175.71	361.69	361.95	353.56	72.37	69.51
983.53	621.50	175.71	362.03			68.55	
1239.94	642.50	292.86	597.44			112.17	
1967.60	1372.01	292.86	595.59	596.21	587.82	96.07	99.91
1968.27	1372.68	292.86	595.59			91.47	
2144.62	1313.39	410.00	831.23			115.82	
830.28	0.47	410.00	829.81	830.00	821.61	139.04	123.80
829.75	0.52	410.00	829.23			123.51	
2161.08	1331.36	410.00	829.72			116.83	
2045.25	981.19	527.14	1064.06			143.73	
2045.09	981.16	527.14	1063.94	1063.94	1055.55	148.01	143.99
1064.32	0.50	527.14	1063.82			140.22	

Column no. 4, $P_{packing}$ = 21.2

V_{elu} [ml]	$V_{inj.\ point}$ [ml]	$V_{forward}$ [ml]	V_R [ml]	$V_{R,mean}$ [ml]	$V_{R,cor}$ [ml]	σ^2 [ml^2]	σ^2_{mean} [ml^2]
100.84	0.51	45.38	100.33			17.58	
651.78	551.01	45.38	100.77	100.61	92.22	25.11	22.40
842.18	741.45	45.38	100.73			24.52	
282.44	0.50	136.14	281.94			34.23	
1294.05	1011.83	136.14	282.22	282.08	273.69	43.58	40.53
282.58	0.51	136.14	282.07			43.78	
995.19	531.63	226.90	463.56			50.74	
463.93	0.51	226.90	463.42	463.64	455.25	53.56	56.52
464.35	0.52	226.90	463.82			60.44	
464.30	0.53	226.90	463.77			61.32	
1196.47	551.36	317.66	645.11	644.98	636.59	70.43	70.35
1295.29	650.43	317.66	644.86			70.28	
2148.94	1322.52	408.42	826.43	826.26	817.87	88.85	89.60
2237.42	1411.33	408.42	826.10			90.36	

Column no. 5, $P_{packing}$ = 10.0 bar

V_{elu} [ml]	$V_{inj.\ point}$ [ml]	$V_{forward}$ [ml]	V_R [ml]	$V_{R,mean}$ [ml]	$V_{R,cor}$ [ml]	σ^2 [ml^2]	σ^2_{mean} [ml^2]
124.58	0.51	57.08	124.08			47.72	
2706.29	2582.00	57.08	124.29	125.16	116.77	47.03	48.10
128.01	2.00	57.11	126.01			48.93	
1128.24	1002.00	57.11	126.24			48.73	
926.50	687.00	114.21	239.50			73.80	
3270.62	3032.00	114.21	238.62	239.20	230.81	72.00	70.96
1926.49	1687.00	114.21	239.49			67.06	
937.53	585.55	171.24	351.99			78.17	
3524.19	3172.00	171.24	352.19	352.84	344.45	81.72	84.46
1785.88	1432.00	171.32	353.88			89.02	
2785.29	2432.00	171.32	353.29			88.92	
1154.14	687.00	228.43	467.14			98.18	
2699.80	2232.00	228.43	467.80	467.37	458.98	100.98	97.66
3699.17	3232.00	228.43	467.17			93.82	
1862.92	1282.53	285.40	580.39			99.54	
4462.28	3882.00	285.40	580.28			99.61	
3668.49	3087.00	285.53	581.49	580.81	572.42	116.38	105.41
922.73	342.00	285.53	580.73			105.44	
4668.17	4087.00	285.53	581.17			106.09	
2177.37	1482.00	342.64	695.37			115.25	
4697.87	4002.00	342.64	695.87	695.43	687.04	120.14	116.35
5697.07	5002.00	342.64	695.07			113.65	
810.63	2.00	399.56	808.63			128.73	
5791.90	4982.00	399.75	809.90	809.41	801.02	137.95	131.23
6791.70	5982.00	399.75	809.70			127.03	
3330.75	2407.00	456.85	923.75			131.23	
1245.55	322.00	456.85	923.55	923.66	915.27	133.38	136.18
2070.80	1147.00	456.85	923.80			141.17	
7945.55	7022.00	456.85	923.55			138.94	
1984.05	947.00	513.72	1037.05			144.08	
2459.56	1422.00	513.96	1037.56	1037.40	1029.01	151.96	144.74
9159.59	8122.00	513.96	1037.59			138.18	

Column no. 6, $P_{packing}$ = 9.8 bar

V_{elu} [ml]	$V_{inj.\ point}$ [ml]	$V_{forward}$ [ml]	V_R [ml]	$V_{R,mean}$ [ml]	$V_{R,cor}$ [ml]	σ^2 [ml^2]	σ^2_{mean} [ml^2]
122.22	2.50	53.68	119.72			62.75	
3674.42	3556.50	53.68	117.92			47.73	
119.42	0.00	53.68	119.42	118.38	109.99	54.52	49.70
119.94	2.50	53.68	117.44			40.04	
634.89	517.50	53.68	117.39			43.45	
846.87	621.50	107.37	225.37			61.11	
4396.66	4171.50	107.37	225.16	225.37	216.98	62.19	58.98
847.06	621.50	107.37	225.56			53.64	
1624.48	1291.50	161.05	332.98			73.53	
5174.40	4841.50	161.05	332.90	332.96	324.57	68.94	68.19
1624.62	1291.50	161.05	333.12			64.77	
1414.36	1081.50	161.05	332.86			65.54	
2466.78	2026.50	214.74	440.28			86.05	
6016.51	5576.50	214.74	440.01	440.40	432.01	78.79	79.70
2467.40	2026.50	214.74	440.90			74.26	
3364.03	2816.50	268.42	547.53			93.42	
6913.94	6366.50	268.42	547.44	547.67	539.28	88.25	88.52
3364.72	2816.50	268.42	548.22			86.64	
2308.98	1761.50	268.42	547.48			85.74	
4316.85	3661.50	322.10	655.35			103.67	
7866.32	7211.50	322.10	654.82	655.01	646.62	98.09	99.01
857.37	202.50	322.10	654.87			95.26	
764.34	2.50	375.79	761.84			105.30	
8878.54	8116.50	375.79	762.04	762.35	753.96	108.61	106.20
1869.11	1106.50	375.79	762.61			105.21	
3319.41	2556.50	375.79	762.91			105.67	
1835.82	966.50	429.47	869.32			117.59	
9945.71	9076.50	429.47	869.21	869.46	861.07	118.42	116.67
2936.35	2066.50	429.47	869.85			113.99	
2973.32	1996.50	483.16	976.82			127.81	
11082.38	10106.50	483.16	975.88	977.36	968.97	126.77	130.13
805.29	-173.98	483.16	979.27			139.74	
4443.97	3466.50	483.16	977.47			126.21	

Column no. 7, $P_{packing}$ = 16.9 bar

V_{elu} [ml]	$V_{inj.\ point}$ [ml]	$V_{forward}$ [ml]	V_R [ml]	$V_{R,mean}$ [ml]	$V_{R,cor}$ [ml]	σ^2 [ml^2]	σ^2_{mean} [ml^2]
4223.33	4201.50	4.21	21.83	22.34	13.95	14.14	14.10
4894.34	4871.50	4.21	22.84			14.07	
33.02	2.50	10.00	30.52	30.52	22.13	17.89	17.89
4333.52	4291.50	14.21	42.02	42.50	34.11	21.23	21.58
5004.48	4961.50	14.21	42.98			21.92	
172.02	121.50	20.00	50.52	50.52	42.13	24.78	24.78
4463.35	4401.50	24.21	61.85	62.61	54.22	26.67	26.41
5134.87	5071.50	24.21	63.37			26.15	
332.15	261.50	30.00	70.65	70.65	62.26	31.06	31.06
4613.54	4531.50	34.21	82.04	82.75	74.36	30.68	30.58
5284.95	5201.50	34.21	83.45			30.48	
512.55	421.50	40.00	91.05	91.05	82.66	35.41	35.41
4793.99	4691.50	44.21	102.49	103.18	94.79	34.71	34.80
5465.37	5361.50	44.21	103.87			34.89	
112.11	2.50	49.55	109.61	109.85	101.46	39.51	40.50
6516.58	6406.50	49.55	110.08			41.49	
515.30	306.50	99.11	208.80	209.18	200.79	51.01	51.92
6921.05	6711.50	99.11	209.55			52.83	
1024.47	716.50	148.66	307.97	308.35	299.96	61.22	62.52
7430.23	7121.50	148.66	308.73			63.82	
1638.65	1231.50	198.22	407.15	407.51	399.12	71.10	71.98
8044.36	7636.50	198.22	407.86			72.85	
2352.69	1846.50	247.77	506.19	506.74	498.35	81.21	82.08
8758.79	8251.50	247.77	507.29			82.94	
3166.98	2561.56	297.32	605.42	605.67	597.28	91.67	91.40
9572.42	8966.50	297.32	605.92			91.13	
4091.13	3386.50	346.88	704.63	705.09	696.70	101.28	101.47
10497.05	9791.50	346.88	705.55			101.65	
5090.36	4286.50	396.43	803.86	804.20	795.81	112.35	112.59
11496.04	10691.50	396.43	804.54			112.82	
6164.38	5261.50	445.99	902.88	903.39	895.00	124.37	124.80
12570.39	11666.50	445.99	903.89			125.23	
951.58	2.50	470.76	949.08	949.25	940.86	134.49	135.56
2020.93	1071.50	470.76	949.43			136.64	

Column no. 8, $P_{packing}$ = 14.1 bar							
V_{elu} [ml]	$V_{inj.\ point}$ [ml]	$V_{forward}$ [ml]	V_R [ml]	$V_{R,mean}$ [ml]	$V_{R,cor}$ [ml]	σ^2 [ml^2]	σ^2_{mean} [ml^2]
1133.20	1102.50	10.00	30.70	31.67	23.28	13.63	13.47
2930.14	2897.50	10.00	32.64			13.31	
1272.86	1221.50	20.00	51.36	52.07	43.68	18.17	18.02
3069.27	3016.50	20.00	52.77			17.87	
1432.98	1361.50	30.00	71.48	72.28	63.89	21.50	21.59
3229.57	3156.50	30.00	73.07			21.69	
1613.53	1521.50	40.00	92.03	92.43	84.04	24.54	24.60
3409.33	3316.50	40.00	92.83			24.66	
117.85	2.50	52.51	115.35	115.33	106.94	28.09	28.14
816.80	701.50	52.51	115.30			28.20	
541.68	321.50	105.02	220.18	220.38	211.99	38.19	38.57
1242.08	1021.50	105.02	220.58			38.95	
1076.94	751.50	157.53	325.44	325.31	316.92	48.79	48.55
356.68	31.50	157.53	325.18			48.32	
1716.67	1286.50	210.04	430.17	430.40	422.01	57.82	57.67
997.13	566.50	210.04	430.63			57.53	
2461.80	1926.50	262.56	535.30	535.60	527.21	67.54	67.27
1742.39	1206.50	262.56	535.89			66.99	
3311.71	2671.50	315.07	640.21	640.63	632.24	77.28	77.76
2592.55	1951.50	315.07	641.05			78.25	
4276.53	3531.50	367.58	745.03	745.71	737.32	87.87	88.12
3557.88	2811.50	367.58	746.38			88.37	
5321.25	4471.50	420.09	849.75	850.43	842.04	97.84	97.86
4602.61	3751.50	420.09	851.11			97.89	
2778.03	1821.50	472.60	956.53	956.53	948.14	108.96	108.96

APPENDIX H.VI: DETERMINATION OF VOID VOLUME WITH DEXTRAN ON SUPERDEX 30PG

Injection at the bottom					
V_{elu} [ml]	$V_{inj.\ point}$ [ml]	V_R [ml]	$V_{R,cor}$ [ml]	σ^2 [ml^2]	σ^2_{cor} [ml^2]
3132.2	2961.5	170.7	158.6	140.0	120.8
171.4	1.5	169.9	157.8	116.6	97.4
416.1	245.5	170.6	158.5	132.0	112.8
470.1	300.5	169.6	157.5	123.5	104.3
771.1	600.5	170.6	158.6	138.9	119.7
4059.6	3885.5	174.1	162.1	173.8	154.6
4329.5	4155.5	174.0	162.0	165.5	146.3
4599.4	4425.5	173.9	161.8	153.7	134.5
	Mean value:	171.7	159.6	143.0	123.8
	Variance:	3.9	3.9	398.1	398.1
	Standard Error:	0.7	0.7	7.1	7.1

Injection at the top					
V_{elu} [ml]	$V_{inj.\ point}$ [ml]	V_R [ml]	$V_{R,cor}$ [ml]	σ^2 [ml^2]	σ^2_{cor} [ml^2]
169.7	1.5	168.2	156.2	71.9	52.7
468.9	300.5	168.4	156.3	71.0	51.8
769.0	600.5	168.5	156.5	73.1	53.9
3495.4	3325.5	169.9	157.8	72.5	53.3
3775.6	3605.5	170.1	158.1	73.0	53.8
	Mean value:	169.0	157.0	72.3	53.1
	Variance:	0.8	0.8	0.7	0.7
	Standard Error:	0.4	0.4	0.4	0.4

Examples of calculations of V_R, $V_{R,cor}$ and σ^2_{cor}:

$V_R = V_{elu} - V_{inj.\ point} = 3132.2\ ml - 2961.5\ ml = 170.7\ ml$

$V_{R,cor} = V_R - V_{sys+col} = 170.7\ ml - 12.06\ ml = 158.6\ ml$

$\sigma^2_{cor} = \sigma^2 - \sigma^2_{sys+col} = 140.0\ ml^2 - 19.18\ ml^2 = 123.8\ ml^2$

APPENDIX H.VII: DETERMINATION OF LIQUID VOLUME WITH NaCl ON SUPERDEX 30PG

Injection at the bottom					
V_{elu} [ml]	$V_{inj.\ point}$ [ml]	V_R [ml]	$V_{R,cor}$ [ml]	σ^2 [ml^2]	σ^2_{cor} [ml^2]
522.9	1.5	521.4	509.4	167.7	148.5
1152.0	630.5	521.5	509.5	170.3	151.1
1782.3	1260.5	521.8	509.7	168.1	148.9
2414.3	1895.5	518.8	506.7	165.6	146.4
3044.6	2525.5	519.1	507.1	170.4	151.2
3674.1	3155.5	518.6	506.5	170.5	151.3
5179.4	4660.5	518.9	506.9	173.6	154.4
5809.3	5290.5	518.8	506.8	182.0	162.8
6439.8	5920.5	519.3	507.2	181.9	162.7
	Mean value:	519.8	507.7	172.2	153.0
	Variance:	1.8	1.8	35.4	35.4
	Standard Error:	0.4	0.4	2.0	2.0

Injection at the top					
V_{elu} [ml]	$V_{inj.\ point}$ [ml]	V_R [ml]	$V_{R,cor}$ [ml]	σ^2 [ml^2]	σ^2_{cor} [ml^2]
517.6	1.5	516.1	504.0	111.7	92.5
1146.1	630.5	515.6	503.6	119.4	100.2
1776.2	1260.5	515.7	503.7	120.7	101.5
	Mean value:	515.8	503.8	117.2	98.0
	Variance:	0.1	0.1	23.8	23.8
	Standard Error:	0.1	0.1	2.8	2.8

Examples of calculations of V_R, $V_{R,cor}$ and σ^2_{cor}:

$V_R = V_{elu} - V_{inj.\ Point} = 517.6\ ml - 1.5\ ml = 516.1\ ml$

$V_{R,cor} = V_R - V_{sys+col} = 516.1\ ml - 12.06\ ml = 504.0\ ml$

$\sigma^2_{cor} = \sigma^2 - \sigma^2_{sys+col} = 111.7\ ml^2 - 19.18\ ml^2 = 92.5\ ml^2$

APPENDIX H.VIII: REVERSED FLOW EXPERIMENTS WITH DEXTRAN ON SUPERDEX 30PG

Injection at the bottom

V_{elu} [ml]	$V_{inj.\ point}$ [ml]	$V_{forward}$ [ml]	V_R [ml]	$V_{R,mean}$ [ml]	$V_{R,cor}$ [ml]	σ^2 [ml^2]	σ^2_{mean} [ml^2]
532.9	491.5	15.7	41.4	41.4	33.1	12.4	12.5
44.0	2.5	15.7	41.5			12.7	
784.4	711.5	31.4	72.9	73.0	64.6	14.9	14.3
294.6	221.5	31.4	73.1			13.8	
1070.7	966.5	47.2	104.2	104.3	95.9	16.1	15.7
580.9	476.5	47.2	104.4			15.4	
896.6	761.5	62.9	135.1	135.7	127.3	18.4	18.1
1387.4	1251.5	62.9	135.9			17.8	
897.6	761.5	62.9	136.1			18.1	
1248.3	1081.5	78.7	166.8	167.4	159.0	21.3	21.1
1249.5	1081.5	78.7	168.0			20.9	
1634.8	1436.5	94.4	198.3	198.7	190.4	24.2	23.6
1635.7	1436.5	94.4	199.2			23.0	
2056.3	1826.5	110.2	229.8	230.1	221.8	26.5	26.5
2056.9	1826.5	110.2	230.4			26.5	
2482.5	2221.5	125.9	261.0	261.5	253.1	27.2	27.2
2483.5	2221.5	125.9	262.0			27.2	
2913.5	2621.5	141.7	292.0	292.6	284.3	34.3	34.8
2914.8	2621.5	141.7	293.3			35.3	

Injection at the top

V_{elu} [ml]	$V_{inj.\ point}$ [ml]	$V_{forward}$ [ml]	V_R [ml]	$V_{R,cor}$ [ml]	σ^2 [ml^2]
54.0	2.5	15.7	51.5	33.4	11.7
315.1	231.5	31.4	83.6	65.5	12.9
611.3	496.5	47.2	114.8	96.7	16.4
937.6	791.5	62.9	146.1	128.0	20.3
1299.4	1121.5	78.7	177.9	159.8	24.5
1695.6	1486.5	94.4	209.1	191.0	27.5
2126.7	1886.5	110.2	240.2	222.1	30.8
2562.9	2291.5	125.9	271.4	253.3	34.8
3009.7	2706.5	141.7	303.2	285.2	40.3

Examples of calculations of V_R and $V_{R,cor}$:

$V_R = V_{elu} - V_{inj.\ Point} = 54.0\ ml - 2.5\ ml = 51.5\ ml$

Injection at the bottom of the column:

$V_{R,cor} = V_{R,mean} - V_{inj\text{-}bed,bottom} - V_{bed,bottom\text{-}UV} = 41.4\ ml - 4.38\ ml - 4.01\ ml = 33.1\ ml$

Injection at the top of the column:

$V_{R,cor} = V_R - V_{inj\text{-}bed,top} - V_{bed,top\text{-}UV} = 51.5\ ml - 9.23\ ml - 8.86\ ml = 33.4\ ml$

APPENDIX H.IX: REVERSED FLOW EXPERIMENTS WITH NaCl ON SUPERDEX 30PG

Injection at the bottom							
V_{elu} [ml]	$V_{inj.\ point}$ [ml]	$V_{forward}$ [ml]	V_R [ml]	$V_{R,mean}$ [ml]	$V_{R,cor}$ [ml]	σ^2 [ml^2]	σ^2_{mean} [ml^2]
113.6	2.5	50.8	111.1	111.2	102.8	26.4	25.9
113.8	2.5	101.8	111.3			25.5	
514.7	301.5	152.7	213.2	213.3	204.9	40.7	40.6
514.8	301.5	203.6	213.3			40.5	
1021.5	706.5	254.6	315.0	315.0	306.6	56.2	56.2
1021.5	706.5	305.5	315.0			56.2	
1637.8	1221.5	356.4	416.3	416.7	408.3	69.4	69.5
1638.7	1221.5	407.4	417.2			69.6	
720.1	201.5	458.3	518.6	518.6	510.2	87.2	87.2
1552.0	931.5	50.8	620.5	620.5	612.1	102.5	102.5
2483.5	1761.5	101.8	722.0	722.0	713.7	118.8	118.8
3490.2	2666.5	152.7	823.7	823.7	815.3	133.7	133.7
4587.4	3661.5	203.6	925.9	925.9	917.5	146.4	146.4

Injection at the top					
V_{elu} [ml]	$V_{inj.\ point}$ [ml]	$V_{forward}$ [ml]	V_R [ml]	$V_{R,cor}$ [ml]	σ^2 [ml^2]
125.0	2.5	50.8	122.5	104.4	31.0
541.4	316.5	101.8	224.9	206.8	50.0
1058.0	731.5	152.7	326.5	308.4	65.5
1685.1	1256.5	203.6	428.6	410.5	82.0
2416.7	1886.5	254.6	530.2	512.1	96.6
733.2	101.5	305.5	631.7	613.6	112.5
1680.1	946.5	356.4	733.6	715.5	125.2
2702.1	1866.5	407.4	835.6	817.5	140.5
3838.8	2901.5	458.3	937.3	919.2	159.0

Examples of calculations of V_R and $V_{R,cor}$:

$V_R = V_{elu} - V_{inj.\ Point}$ = 113.6 ml – 2.5 ml = 111.1 ml

Injection at the bottom of the column:

$V_{R,cor} = V_{R,mean} - V_{inj\text{-}bed,bottom} - V_{bed,bottom\text{-}UV}$ = 111.2 ml – 4.38 ml – 4.01 ml
= 102.8 ml

$V_{R,cor} = V_R - V_{inj\text{-}bed,bottom} - V_{bed,bottom\text{-}UV}$ = 518.6 ml – 4.38 ml – 4.01 ml = 510.2 ml

Injection at the top of the column:

$V_{R,cor} = V_R - V_{inj\text{-}bed,top} - V_{bed,top\text{-}UV}$ = 122.5 ml – 9.23 ml – 8.86 ml = 104.4 ml